Mitochondrial stress communication in mammalian cells

Author:
Barbour, Jayne

Publication Date:
2017

DOI:
https://doi.org/10.26190/unsworks/20561

MITOCHONDRIAL STRESS COMMUNICATION IN MAMMALIAN CELLS

Jayne Barbour

A thesis in fulfilment of the requirements for the degree of Doctor of Philosophy

School of Medical Sciences,

Faculty of Medicine

2017

PLEASE TYPE

THE UNIVERSITY OF NEW SOUTH WALES
Thesis/Dissertation Sheet

Surname or Family name: Barbour

First name: Jayne Other name/s: Alexandra

Abbreviation for degree as given in the University calendar:
PhD

School: Medical Sciences Faculty: Medicine

Title: Mitochondrial Stress Communication in Mammalian Cells

Abstract 350 words maximum: (PLEASE TYPE)

Mitochondria are crucial organelles in energy transduction, with an emerging role in cell signaling beginning to be appreciated. Due to the endosymbiotic nature of mitochondria and as a by-product of energy transduction via the electron transport chain (ETC), mitochondria are inherently exposed to many stresses (e.g. reactive oxygen species, genomic damage and proteotoxic stress). We postulated that there would be active intracellular and extracellular pathways of mitochondrial communication engaged to maintain cellular fitness, however this has not been well studied in mammalian cells.
The overarching aim of this thesis was to explore how mammalian cells communicate mitochondrial stress. More specifically, to characterise intracellular signaling adaptations to mitochondrial stress and to investigate cell non-autonomous communication of mitochondrial stress through secreted proteins.
To address the first aim, a xeno-cybrid model was employed where cells had mismatch between nuclear and mitochondrial genomes resulting in an impairment of ETC function. Compared with controls, cells with ETC dysfunction had substantial oxidative defects, but were viable and maintained cellular ATP. This 'rescue' of cell survival appeared to be driven by upregulation of glycolysis and pro-survival Akt and AMPK signaling. To interrogate a potential upstream mediator, ATM kinase was explored, and it was found that a number of adaptations were reversed by a selective ATM kinase inhibitor. These results therefore support a role for ATM kinase as an important adaptation promoting survival of mammalian cells in response to mitochondrial stress.
To address cell non-autonomous communication, HEK293 cells, and primary murine hepatocytes and adipocytes were incubated with ETC inhibitors (rotenone or antimycin A) or an oxidative phosphorylation uncoupler (Dinitrophenol), and secreted proteins were analysed by LC-MS/MS to map the mitochondrial stress-sensitive secretome. Significant alterations in secreted proteins were observed for HEK293 cells and adipocytes with ETC complex I and III inhibition and in hepatocytes treated with DNP.
Collectively, the work presented in this thesis sheds new light on the pathways employed by mammalian mitochondria to signal and respond to stress.

FOR OFFICE USE ONLY Date of completion of requirements for Award:

THIS SHEET IS TO BE GLUED TO THE INSIDE FRONT COVER OF THE THESIS

ORIGINALITY STATEMENT

‘I hereby declare that this submission is my own work and to the best of my knowledge it contains no materials previously published or written by another person, or substantial proportions of material which have been accepted for the award of any other degree or diploma at UNSW or any other educational institution, except where due acknowledgement is made in the thesis. Any contribution made to the research by others, with whom I have worked at UNSW or elsewhere, is explicitly acknowledged in the thesis. I also declare that the intellectual content of this thesis is the product of my own work, except to the extent that assistance from others in the project's design and conception or in style, presentation and linguistic expression is acknowledged.’

Signed ……....

Date … …….....

TABLE OF CONTENTS

THESIS ABSTRACT

Mitochondria are crucial organelles in energy transduction, with an emerging role in cell signaling beginning to be appreciated. Due to the endosymbiotic nature of mitochondria and as a by-product of energy transduction via the electron transport chain (ETC), mitochondria are inherently exposed to many stresses (e.g. reactive oxygen species, genomic damage and proteotoxic stress). We postulated that there would be active intracellular and extracellular pathways of mitochondrial communication engaged to maintain cellular fitness, however this has not been well studied in mammalian cells.

The overarching aim of this thesis was to explore how mammalian cells communicate mitochondrial stress. More specifically, to characterise intracellular signaling adaptations to mitochondrial stress and to investigate cell non-autonomous communication of mitochondrial stress through secreted proteins.

To address the first aim, a xeno-cybrid model was employed where cells had mismatch between nuclear and mitochondrial genomes resulting in an impairment of ETC function. Compared with controls, cells with ETC dysfunction had substantial oxidative defects, but were viable and maintained cellular ATP. This 'rescue' of cell survival appeared to be driven by upregulation of glycolysis and pro-survival Akt and AMPK signaling. To interrogate a potential upstream mediator, ATM kinase was explored, and it was found that a number of adaptations were reversed by a selective ATM kinase inhibitor. These results therefore support a role for ATM kinase as an important adaptation promoting survival of mammalian cells in response to mitochondrial stress.

To address cell non-autonomous communication, HEK293 cells, and primary murine hepatocytes and adipocytes were incubated with ETC inhibitors (rotenone or antimycin A) or an oxidative phosphorylation uncoupler (DNP), and secreted proteins secreted were analysed by LC-MS/MS to map the mitochondrial stress-sensitive secretome. Significant alterations in secreted proteins were observed for HEK293 cells and adipocytes with ETC complex I and III inhibition and in hepatocytes treated with DNP.

Collectively, the work presented in this thesis sheds new light on the pathways employed by mammalian mitochondria to signal and respond to stress.

ACKNOWLEDGEMENTS

First and foremost I would like to express gratitude to my supervisor Associate Professor Nigel Turner for his ongoing guidance and support throughout my thesis. He has not only been a great source of intellectual insight but has also an encouraging supervisor. I also acknowledge the input of my co-supervisor Kyle Hoehn. He has been offered advice and guidance throughout my thesis and help with seahorse assays.

I graciously acknowledge Ian Trounce for kindly gifting xeno-cybrid cells produced and characterised by him and Matthew McKenzie. I acknowledge Valerie Wasingner at the UNSW Bioanalytical Mass Spectrometry Facility for assistance with mass spectrometry and Darren Saunders and Jessie McKenna (UNSW) for proteomics data analysis R scripts. I also want to thank Brenna Osborne for her isolation of primary hepatocytes and dissection of adipose tissue for chapters 5 and 6 and Brendan Wilkins for assistance culturing cells.

Funding is acknowledged including my Australian Postgraduate Award Scholarship, ARC and NHMRC grants. Additionally, PRSS award and SOMS travel Scholarship enabled presentation of the work at conferences.

I also wish to acknowledge the School of Medical Sciences and Department of Pharmacology at UNSW for allowing me to undertake my PhD here along with the continuous efforts of affiliated research support staff. Importantly, I would like to thank the other members of the Mitochondrial Bioenergetics lab for making my time here enjoyable.

Papers and presentations arising from this thesis

Paper

Barbour JA & **Turner N**. (2014). Mitochondrial Stress Signaling Promotes Cellular Adaptations. *Int J Cell Biol* 2014:156020.

Oral presentations

Jayne Barbour, Ian Trounce, Kyle Hoehn, Nigel Turner. Anabolic metabolism and pro-survival signaling are engaged to rescue the phenotype of electron transport chain dysfunction in a cybrid cell model. 2015 Australian Physiological Society Annual Meeting, Hobart.

Jayne Barbour, Ian Trounce, Kyle Hoehn, Nigel Turner. Electron Transport Chain Stress Signals Activation of ATM Kinase to Promote Pro-Survival Signaling and Metabolic Adaptations by a ROS Dependent Mechanism. 2016 AussieMit Meeting, Sydney

Poster presentations

EuroMit
AussieMit 2014
NSW Cell Dev Biol
Cancer Metabolism meeting
EMBL PhD symposium
AussieMit 2016

LIST OF FIGURES

LIST OF TABLES

CHAPTER 1: INTRODUCTION

1.1 Mitochondria: From Origins to Function

1.1.1 The Endosymbiotic Origins of Mitochondria

Up until ~2-3 billion years ago, life on earth consisted of two kingdoms of single-celled, simple organisms, prokaryotes and archaea. By a 'fateful encounter' a prokaryote entered an archaea and rather than being degraded or infective, these two cells coexisted and ultimately formed a symbiotic relationship leading to formation of what is now the 'mitochondrion' of modern cells. This theory was first articulated by Mereschowsky in 1910 and sequencing data confirms that mitochondria arose from an α-proteobacterial ancestor (Gray, Burger, & Lang, 2001; D. Yang, Oyaizu, Oyaizu, Olsen, & Woese, 1985).

Energy is required to maintain the highly ordered state of the cell which is entropically unfavourable. Hence it has been postulated that the bioenergetic advantage formed by this symbiosis drove evolution of complexity in life and lead to the development of eukaryotic cells as we know them today (Lane, 2014). For example, mitochondria energetically allowed for great expansion of the genome in terms of number of genes which could theoretically assist development of genomic complexity (Lane & Martin, 2010). Acquirement of mitochondria was also likely necessary for development of multicellular organisms and eukaryotic sex (Garg & Martin, 2016). Despite the elegance of this symbiosis, complex coordination of two genomes is required for the functioning of the whole system. Further, there are imperfections in mitochondrial processes such as mitochondrial DNA (mtDNA) replication and incomplete reduction of oxygen which ultimately leads to mitochondrial stress.

Accordingly, mitochondria are stress prone organelles and must have evolved systems of communication of mitochondrial function and in particular of mitochondrial stress to engage appropriate cellular responses to support this symbiotic relationship (Barbour & Turner, 2014; Quiros, Mottis, & Auwerx, 2016; Searcy, 2003) . Literature examination suggests that inadequate cellular adaptations to mitochondrial stress or 'mitochondrial miscommunication' may lead to or exacerbate disease (Barbour & Turner, 2014;

Searcy, 2003). Hence it is important to understand these molecular mechanisms to shed light on these diseases. ***This thesis explores mitochondrial stress communication supporting the symbiotic relationship between mitochondria and its host cell as a critical system involved in supporting healthy cellular function. The overall aim is to understand some of the molecular mechanisms mediating this in mammalian cells.***

1.1.2 Mitochondrial Structure and Dynamics

Mitochondria are intracellular, double membrane bound organelles that exist as dynamic, reticular networks within the cell. Here I will briefly describe the anatomical organisation of mitochondria and their structural interactions with other cellular components. These physical interactions are important for transduction of information from mitochondria to other components of the cell i.e. mitochondrial communication, which is a central theme of the thesis and discussed later in this chapter.

Mitochondrial Ultrastructure –

Mitochondrial ultrastructure was first resolved by electron microscopy (EM) in the 1950s which enabled an insight into the structural morphology of mitochondria (Palade, 1953; Sjostrand, 1953). Mitochondria have 2 membranes, the outer membrane which spatially separates the organelle from the cytosol and the inner membrane. The space between the outer and inner membranes is the intermembrane space and enclosed by the inner membrane is the mitochondrial matrix where numerous metabolic enzymes are located. The inner membrane has 2 regions, the inner boundary membrane which lies adjacent (and within) the outer membrane and the cristae membrane which are folds of inner membrane projecting into the matrix. It is across the cristae membrane that ETC supercomplexes are assembled and a proton gradient is formed energetically, powering ATP synthesis.

Following these pioneering images, EM images of mitochondria from different tissues and physiological conditions revealed that mitochondrial ultrastructure is dramatically varied amongst different cell types and under healthy and pathological conditions. This has led to the idea that mitochondrial ultrastructure has a large impact on the bioenergetic function of mitochondria and changes in mitochondrial ultrastructure couple tightly with the bioenergetic necessities of the cell. Mitochondrial cristae can be

tubular or lamellar to adapt to the bioenergetic needs of the cell (Cogliati, Enriquez, & Scorrano, 2016). For example, fast twitch and slow twitch skeletal muscle fibres possess mitochondria of different morphology as they have different oxidative demands (Mishra, Varuzhanyan, Pham, & Chan, 2015). This also demonstrates how cell identity, which is a product of gene expression, affects mitochondrial morphology and vice versa implicating mitochondrial morphology and function in cellular communication. Further, cristae can undergo dynamic remodelling in response to cellular cues including cellular actions and development (Pernas & Scorrano, 2016). The deeper implications of this are that mitochondrial morphology has plasticity in response to cellular communication.

Mitochondrial Dynamics –

Mitochondria were previously thought to be static organelles placed in the cytosol but it is now appreciated that they exist in reticular networks associated with the cytoskeleton (Anesti & Scorrano, 2006; Ball & Singer, 1982; Palmer, Osellame, Stojanovski, & Ryan, 2011). Mitochondria interact with molecular motor proteins like dynein and kinesins by Rho like GTPases miro (Morlino et al., 2014) and milton (Glater, Megeath, Stowers, & Schwarz, 2006) respectively. This enables mitochondria to move along microtubular networks hence making them dynamic (Glater et al., 2006; Koutsopoulos et al., 2010). This direct interaction with the cytoskeleton enables communication with the cell.

Other processes underlying mitochondrial dynamics are the processes of fusion and fission which occurs by a group of dynamin proteins which are also GTPases (van der Bliek, Shen, & Kawajiri, 2013). In fusion, multiple mitochondria form one elongated mitochondrion, whereas in fission, a mitochondrion generates small, fragmented mitochondria (van der Bliek et al., 2013). Fusion and fission are constantly occurring to meet bioenergetic demands in response to different cellular cues (Westermann, 2012) and stress (Youle & van der Bliek, 2012).

The protein OPA1is a protein located in the cristae and it mediates mitochondrial inner membrane fusion (Cipolat, Martins de Brito, Dal Zilio, & Scorrano, 2004). Mitofusin protein located on the outer membrane and mediates outer membrane fusion (Z. Song, Ghochani, McCaffery, Frey, & Chan, 2009). Fission occurs when the protein

Drp1translocates from the cytosol to the outer membrane of mitochondria to form a fission complex which induces fission powered by GTP hydrolysis (Otera, Ishihara, & Mihara, 2013).

Endoplasmic Reticulum (ER) Tethering –

As well as being networked with each other and the cytoskeleton, mitochondria are tethered to the endoplasmic reticulum (ER) which is a membranous extension of the nuclear envelope. The ER is the cell's major store of free calcium (Ca^{2+}) which is an important cell signaling molecule (Clapham, 2007). Early EM images revealed the close association between mitochondria and ER but more recently the biochemical basis of mitochondria-ER tethering has been elucidated. The major molecular mediators of mitochondria-ER tethering are the proteins mitofusin-2 (Mfn2) and Dnm1/Drp1 (Friedman et al., 2011).

The ER Mitochondrial Associated Membrane (MAM) is enriched in proteins involved in lipid synthesis and transfer (Rusinol, Cui, Chen, & Vance, 1994; Stone et al., 2009; Vance, 1990, 2008) and Ca^{2+} transfer (Garcia-Perez, Hajnoczky, & Csordas, 2008; Mao et al., 1996; Szabadkai et al., 2006). The physical coupling of mitochondria and ER allows for crosstalk between the two organelles mediated by Ca^{2+} which is an important second messenger signaling molecule, the functional importance of mitochondrial-ER tethering beyond Ca^{2+} handling is cell signaling which is discussed later in this review.

Mitochondrial Membranes and Transport –

Transport of molecules into and out of the mitochondria is effectively what mediates communication between mitochondria and the cell so understanding mitochondrial membrane permeability and transporters is crucial for understanding mitochondrial communication. The mitochondrial outer membrane (MOM) is a phospholipid bilayer and hence permeable to small molecules and contains integral membrane proteins or porins to regulate entry of small metabolites and ions.

In contrast to the MOM, the mitochondrial inner membrane (MIM) does not contain porins and has a high protein-to-phospholipid ratio with the major phospholipid being

cardiolipin which has four fatty acids rather than 2 (Ardail et al., 1990). These factors make the inner mitochondrial membrane highly impermeable to most molecules and so specific transport proteins are required to allow entry of molecules to and from the mitochondrial matrix to the intermembrane space.

Import and Processing of Mitochondrial Proteins –

Over 99% of mitochondrial proteins are nuclear encoded and so mitochondrial protein import and folding is essential for proper coordination of both nuclear and mitochondrial genomes and maintenance of mitochondrial function (Schmidt, Pfanner, & Meisinger, 2010; Wiedemann, Frazier, & Pfanner, 2004). Most mitochondrially targeted matrix proteins have an amphithatic helix targeting sequence on the N-terminus which interacts with the outer mitochondrial membrane translocase of the outer membrane (TOM) complex, which allows proteins into the intermembrane space (Dudek, Rehling, & van der Laan, 2013). From the intermembrane space, proteins can undergo different pathways depending on their unique chemistry. Proteins which are destined for either the outer or the inner membranes are first carried by small translocase of inner membrane (Tims), which are chaperones located in the intermembrane space (Schmidt et al., 2010). For β-barrel proteins that are located in the MOM, the small Tims carry them to sorting and assembly machinery (SAM) complex which is embedded in the OM whereas carrier proteins of the IM are carried to the Tim22 complex in the IM (Dudek et al., 2013). Proteins with cysteine rich signals are imported through the mitochondrial intermembrane space import and assembly (MIA) pathway (Stojanovski et al., 2008). Pre-sequence containing proteins are able to enter the mitochondrial matrix by the translocase of inner membrane 23 (Tim23) complex which is associated with pre-sequence associated import motor (PAM) complex (Stojanovski et al., 2008). There the pre-sequence is cleaved by the mitochondrial processing peptidase (MPP) enzyme and proteins are folded by chaperones (Gakh, Cavadini, & Isaya, 2002). Protein import across in the inner membrane is dependent upon the mitochondrial membrane potential and requires ATP hydrolysis (Agarraberes & Dice, 2001). Hence healthy bioenergetic function is required for mitochondrial proteostasis and vice versa. Maintenance of mitochondrial proteostasis is discussed in detail below.

1.1.3 The Mitochondrial Genome

Mitochondria contain their own genome retained from its endosymbiotic ancestor. Homologous recombination does not occur and mtDNA is exclusively inherited down the maternal line. Structurally, the genomic information is stored as circular, double stranded DNA and organised onto nucleoids. mtDNA contains a regulatory D-loop region and encodes 22 tRNAs, 12S rRNA, 16S rRNA and 11 protein encoding genes which include subunits of complex I, III, IV and V of the ETC (Taanman, 1999). mtDNA also encodes long non coding RNA molecules (lncRNAs) (Mercer et al., 2011; Rackham et al., 2011) and potentially small peptides (C. Lee, Yen, & Cohen, 2013). The regulation of mitochondrial genomics is a major source of information that can be communicated to the rest of the cell.

Architecture of the Mitochondrial Genome –

The mitochondrial genome is packaged into nucleoids which are non-membrane bound regions of DNA used to package prokaryotic DNA. The main mtDNA packageing protein is TFAM (T. I. Alam et al., 2003) which similar to the bacterial HU protein (Ngo, Kaiser, & Chan, 2011) and a major component of mammalian nucleoids (Kukat et al., 2015). Mammalian nucleoids are of uniform size and frequently contain a single copy of mtDNA (Kukat et al., 2011). Cross strand binding of TFAM to single mtDNA molecules is necessary for mitochondrial nucleoid formation (Kukat et al., 2015). Mammalian mitochondrial nucleoids also contain mitochondrial transcription termination protein MTERF2 (Pellegrini et al., 2009) and mitochondrial translation machinery (He et al., 2012) which enables mitochondrial gene expression and translation within nucleoids.

In the context of nuclear DNA, post translational modification of histones (the main DNA packaging proteins) causes chromatin remodelling which is important for regulation of gene expression. Similarly, nucleoid remodelling occurs under select conditions to regulate flow of mitochondrial genetic material but less is known about the biochemistry of TFAM post-translational modifications and how that affects nucleoid function (Kucej, Kucejova, Subramanian, Chen, & Butow, 2008). Phosphorylation of the DNA binding site of TFAM occurs by a cAMP dependent

mitochondrial kinase which prevents mtDNA binding (B. Lu et al., 2013). Lysine acetylation of TFAM has been reported in rodents (Dinardo et al., 2003; Hebert et al., 2013) but is not yet linked with functional consequences on mtDNA binding.

Nucleoid remodelling occurs under conditions of fission and fusion mediated by mitochondrial membrane dynamics proteins (Ban-Ishihara, Ishihara, Sasaki, Mihara, & Ishihara, 2013). This enables coupling of mitochondrial morphology and mitochondrial genome regulation. At a functional level, nucleoid remodelling occurs in response to metabolic cues including glucose and amino acid starvation (Kucej et al., 2008) which may have implications in mitochondrial signalling.

mtDNA Replication –

Mitochondria contain machinery to replicate their genome which is relatively simple involving nuclear encoded proteins. As mtDNA is one circular chromosome, it has a displacement loop (D-loop) which is a structure where two strands of dsDNA are separated by third strand of DNA (Taanman, 1999). This is the start site of mtDNA replication. Of the two strands of DNA, one contains relatively more purine nucleotides hence being the 'heavy strand' (H strand) while the complementary strand contains relatively more pyramidines hence being the 'light strand' (L strand) (Taanman, 1999).

Replication is performed by the mitochondrial DNA polymerase complex which is composed of the catalytic DNA polymerase subunit γ gene (POLG) and two accessory subunits proteins DNA polymerase subunit gamma-2 (POLG2). POLG possess 3'-5' exonuclease proofreading activity (Longley, Ropp, Lim, & Copeland, 1998) , DNA polymerase activity (Kaguni, 2004) and 5′-deoxyribose phosphate lyase activity (Longley, Prasad, Srivastava, Wilson, & Copeland, 1998) catalytic activity while POLG2 enhances DNA binding to promote DNA polymerisation (S. E. Lim, Longley, & Copeland, 1999). Mitochondrial single strand binding proteins also help maintain the replicative activity of POLG (Ciesielski et al., 2015). The process is initiated at the D-loop upon replisome formation which involved the DNA helicase TWINKLE unwinding short stretches of dsDNA in the 5' to 3' direction with mitochondrial single stranded binding proteins to prevent reannealing (Jemt et al., 2011). DNA synthesis continues on both the L strand and H strand (Robberson, Kasamatsu, & Vinograd,

1972) and ligation occurs by POLG (Macao et al., 2015). Since mtDNA replication requires nuclear encoded components, mtDNA regulation is dependent on coordination of nuclear and mitochondrial genomes.

mtDNA Transcription and Translation –

mtDNA encodes tRNAs and proteins including ETC subunits hence mitochondrial gene expression is required for functional oxidative phosphorylation (OXPHOS). Transcription of mtDNA occurs when the transcription factors, Mitochondrial transcription factor A (TFAM) and Mitochondrial transcription factor B (TFB2M), bind transcriptional start sites and recruit the single subunit mitochondrial RNA polymerase (POLRMT) (Asin-Cayuela & Gustafsson, 2007; Shoubridge, 2002). There are two major transcriptional start sites in the D-loop with a critical promoter element that surrounds the transcriptional start sites (Bhat, Avdalovic, & Avadhani, 1989; Bogenhagen, Yoza, & Cairns, 1986).

Once transcription has been initiated, RNA is transcribed as a single polycistronic precursor mRNA encoding all the genetic material of that strand (Gelfand & Attardi, 1981). Following this process, mRNA processing is critical for maturation of RNAs. This process is relatively simple compared with nuclear mRNA processing because there are no introns and minimal intergenic regions and no alternative splicing. All mitochondrial rRNAs and most protein coding genes are flanked or 'punctuated' by mitochondrial tRNAs (Ojala, Montoya, & Attardi, 1981). Mitochondrial tRNAs are excised by endonucleolytic enzymes which yielding other mitochondrial RNA species (Sanchez et al., 2011). After transcription, mitochondrial RNAs are processed in RNA granules and then directed to mitochondrial ribosomes (mitoribosomes) for translation (Antonicka & Shoubridge, 2015; Jourdain et al., 2013).

1.1.4 Mitochondrial Biogenesis

Mitochondrial biogenesis is the synthesis of new mitochondria. This requires replication and transcription of mtDNA, transcription and translation of nuclear encoded mitochondrial proteins and electron transport chain (ETC) subunits, mitochondrial protein import and folding and ETC complex assembly.

These processes are under control of various transcription factors described in the table below.

Table 1.1.1 Transcription Factors that are Involved in Mitochondrial Biogenesis

Transcription Factor	Role in Promoting Mitochondrial Biogenesis
Nuclear Respiratory Factor 1 (NRF-1)	Controls expression of many ETC subunits and TFAM (Virbasius & Scarpulla, 1994) NRF-1 controls expression of TFAM and TFBs (Gleyzer, Vercauteren, & Scarpulla, 2005)
GA binding protein (GABP) also known as nuclear respiratory factor 2 (NRF-2) not to be confused with Nuclear factor (erythroid-derived 2)-like 2, also known as NFE2L2 or *Nrf2*	GABPα (DNA binding subunit of GABP transcriptional complex) is essential for expression of TFBM protein Tfb1m (Z. F. Yang, Drumea, Mott, Wang, & Rosmarin, 2014) TFAM are regulated by GABP (Virbasius & Scarpulla, 1994) TFBs by GABP (Gleyzer et al., 2005)
Peroxisome Proliferator Activated Receptors (PPARs including PPARα, PPARγ, PPARδ)	PPARα drives expression of genes involved in mitochondrial fatty acid oxidation (Gulick, Cresci, Caira, Moore, & Kelly, 1994) PPARγ causes mitochondrial biogenesis in white adipose tissue (Wilson-Fritch et al., 2004)
Thyroid Hormone Receptors (THR)	Directly drive expression of nuclear encoded mitochondrial genes (Dominy & Puigserver, 2013) THR activation indirectly drive mitochondrial biogenesis through up-regulation of NRF-1 (Rodriguez-Pena, Escriva, Handler, & Vallejo, 2002; Weitzel, Radtke, & Seitz, 2001) and GABP (Irrcher, Adhihetty, Sheehan, Joseph, & Hood, 2003).
cAMP activated transcription factor	CREB controls transcription of complex IV subunits and enzymes in mitochondrial β-oxidation (Gopalakrishnan & Scarpulla, 1994)

(CREB)	
Estrogen Related Receptors (ERRs including ERR-α and ERR-γ)	ERRs are orphaned receptors as their endogenous ligand is unknown (Horard & Vanacker, 2003) ERR-α activates transcription of genes for OXPHOS, mitochondrial beta oxidation, mitochondrial fusion and fission (Dufour et al., 2007; Schreiber et al., 2004) ERR- γ regulates expression of nuclear encoded mitochondrial genes (Alaynick et al., 2007; Dufour et al., 2007)
Yin and Yang 1 (YY1)	Regulates expression of OXPHOS genes (Cunningham et al., 2007)
Glucocorticoid receptor (GR)	Glucocorticoid hormone increases mtDNA transcription and complex IV activity by a glucocorticoid receptor dependent mechanism only in skeletal muscle (K. Weber et al., 2002)
Specificity protein 1 (Sp1)	Sp1 controls transcription of all cytochrome C oxidase subunits (Dhar, Johar, & Wong-Riley, 2013)

One thing all of these transcription factors have in common is that their activity can be modulated by the transcriptional coactivator PGC-1α (PPAR (peroxisome proliferator-activated receptor)-γ coactivator-1α) and so PGC1α is often referred to as the master regulator of mitochondrial biogenesis.

By definition, a transcriptional coregulator increases the transcriptional activity of the transcription factors it operates with. This means it may not be necessary for any transcriptional activity but is required for enhanced transcriptional activity. In line with this, evidence from transgenic PGC1 depleted mouse models suggests that PGC1α is dispensable for basal mitochondrial biogenesis (Adhihetty et al., 2009; Arany et al., 2008) but required to increase mitochondrial biogenesis in response to catabolic stress

(Arany et al., 2008; Arany et al., 2005). This has implications in anterograde signaling discussed at a later section of the introduction.

1.1.5 Mitochondrial Oxidative Phosphorylation

Oxidative phosphorylation (OXPHOS) is the process by which oxidation of fuel substrate is coupled with formation of chemiosmotic gradient which is harnessed for adenosine triphosphate (ATP) synthesis. OXPHOS is widely considered to be the major function of mitochondria, producing up to 90% of cellular ATP in the heart (Harris & Das, 1991; Rolfe & Brown, 1997).

Nucleoside triphosphates work as effective molecules for energy exchange in the cell because they are stable and do not spontaneously hydrolyse under physiological conditions and also because phosphate groups which has a lot of free energy with a G value close to -31 KJ/mole so they can meet the energetic demands of the cell in a regulated fashion. ATP is the primary nucleoside triphosphate used under most conditions because hydrolysis is fast.

Oxidation of Fuel Substrates and the Tricarboxylic Acid Cycle –

The tricarboxylic acid (TCA) is the series of chemical reactions which occur in the inner mitochondrial matrix whereby the 2 carbon compound acetyl, in the form of acetyl-CoA, is completely oxidised to yield 2 x CO_2 molecules. Acetyl-CoA is primarily derived from oxidation of fuel substrates glucose, lipids and amino acids. When glucose is converted to pyruvate in glycolysis, pyruvate can either be converted to lactate outside of the mitochondria or it can be transported into the mitochondria where it is converted to acetyl-CoA. Long chain fatty acids are unable to diffuse across the mitochondrial membranes but are transported across the outer membrane by carnitine palmitoyltransferase I and subsequently across the inner membrane by carnitine palmitoyltransferase II. In contrast, short chain and medium chain fatty acids enter the mitochondria by non-carnitine dependent mechanisms. Once in the mitochondria, fatty acids undergo beta oxidation to yield acetyl CoA, the reduced forms of flavin adenine dinucleotide ($FADH_2$) and nicotinamide adenine dinucleotide (NADH). While amino acids are often associated with anabolic metabolism, they can also be deaminated or

oxidatively deaminated in the mitochondria producing molecules that can enter the TCA cycle.

Utilisation of Electrons for ATP production: The Electron Transport Chain –

Intermediates from the TCA cycle carry electrons to enzyme complexes located in the inner mitochondrial membrane. Electron transport is coupled with the pumping of protons across the inner mitochondrial membrane which forms a proton gradient that contains a proton motive force to power the final complex to produce ATP in a process known as the electron transport chain (ETC). At NADH dehydrogenase (complex I), two electrons are transferred from NADH to ubiquione producing ubiquinolol and NAD^+. Complex I electron transport is mostly associated with pyruvate and glutamate oxidation. Succinate dehydrogenase (complex II) catalyses reduction of succinate to fumarate which is accompanied by electrons being transferred to ubiquione. Complex III then transfers electrons from ubiquione to cytochrome C which is oxidised at Cytochrome C oxidase (complex IV), producing water by reducing oxygen. Electron transport is coupled with formation of a proton gradient which is finally harnessed by the ATP synthase (complex V) to produce ATP. Here, a highly sophisticated molecular motor utilises the proton gradient at the F_0 subunit to cause the F_1 subunit to spin around to generate ATP from ADP and inorganic phosphate.

ETC Supercomplexes –

The textbook model of ETC or the 'fluid model' describes electron complexes as separate entities with electron carriers moving in between. In 2008, evidence for the supercomplex model was presented in human cells (Acin-Perez, Fernandez-Silva, Peleato, Perez-Martos, & Enriquez, 2008). Respirasomes measured by blue native page (BN-PAGE) occur in range of rodent tissues (Mourier, Matic, Ruzzenente, Larsson, & Milenkovic, 2014; Reifschneider et al., 2006), human cells (Acin-Perez et al., 2008), bovine heart (Schafer, Dencher, Vonck, & Parcej, 2007) and *C.elegans* (Suthammarak, Somerlot, Opheim, Sedensky, & Morgan, 2013). Additionally, respirasomes have been reported in plants (Schafer et al., 2007) and fungi including mould (Marques, Dencher, Videira, & Krause, 2007) and yeast (Braun, Sunderhaus, Boekema, & Kouril, 2009) suggesting they are evolutionarily conserved across kingdoms. The functional

significance is only beginning to be appreciated with recent research indicating that supercomplex assembly has a large impact on the utilisation of electrons (Hornig-Do et al., 2012), enabling electron flux (Lapuente-Brun et al., 2013). Mitochondrial cristae morphology has an impact on supercomplex assembly and efficiency (Cogliati et al., 2013) which is relevant as mitochondrial cristae can dynamically change with communication of various cellular and metabolic cues.

1.1.6 Mitochondria and Apoptosis

Besides their metabolic functions that are required for maintenance of life, mitochondria are the cellular site of programmed cell death or apoptosis. Apoptosis is a stand-alone topic, too large to be reviewed here. For the purpose of this thesis, it is important to note that mitochondria are the cellular sites of apoptosis and can occur in response to bioenergetic stress (Kroemer, Dallaporta, & Resche-Rigon, 1998). Both intrinsic and extrinsic apoptosis pathways converge on the mitochondrial release of cytochrome C (Goldstein et al., 2005) which triggers apoptosome formation and activation of caspase-9 (H. E. Kim, Du, Fang, & Wang, 2005) which triggers a signaling cascade for cell death (Riedl & Salvesen, 2007). Mitochondrial cytochrome c release is also associated with a large drop in mitochondrial membrane potential and a large burst of mitochondrial ROS which can occur in response to a large bioenergetic stressor

1.2 Mitochondria are Inherently Stressful Organelles

Because of their endosymbiotic origin, their requirement to coordinate two genomes and as a consequence of their functions highlighted above, mitochondria are inherently stress prone organelles. Below I outline the various forms of stress encountered by mitochondria.

1.2.1 Oxidative Stress

When dimolecular oxygen (O_2) is reduced by a single electron it becomes highly reactive as it has unpaired valence electrons (Hayyan, Hashim, & AlNashef, 2016). Molecules containing this type of oxygen are known as reactive oxygen species (ROS) (Hayyan et al., 2016), which in the biological system can cause damage to biomolecules including lipids, membranes, proteins and DNA if not detoxified correctly (Schieber & Chandel, 2014). Accumulation of these damaged biomolecules is referred to as a state of 'oxidative stress'. By one estimate, 1-2% of oxygen consumed by the cell is reduced to ROS in the mitochondria (Chance, Sies, & Boveris, 1979). Mitochondria are major producers of ROS, notably at ETC complex I and III but also at other sites of the mitochondria. Here I will briefly describe how mitochondria produce ROS and how ROS production is increased with bioenergetic stress.

Electron Transfer in the Mitochondria and Superoxide Production –

ETC function requires electron donation from TCA substrates to ETC complexes. Under normal conditions, electron carriers like NADH, $CoQH_2$ and glutathione do not readily react with oxygen during healthy ETC function when unbound to proteins (Murphy, 2009). However, superoxide is formed when electron carriers are bound to redox-sensitive protein prosthetic groups such as metal groups (Murphy, 2009). It is noteworthy that a significant proportion of the mitochondrial proteome contains redox-sensitive proteins and hence even when ETC function is healthy there will be background production of ROS as a by-product of the electron transport function of mitochondria.

Complex I Mediated Superoxide Production –

The flavin mononucleotide (FMN) prosthetic group of complex I has strong oxidising capacity during electron transfer and it is estimated that this is the major site complex I mediated superoxide production (Kussmaul & Hirst, 2006). The rate of superoxide production by FMN at complex I is accelerated when NADH/NAD^+ ratio is high (Kussmaul & Hirst, 2006). This can occur when the NAD^+ pool is reduced back to NADH which will happen when ETC function is disturbed (Adam-Vizi & Chinopoulos, 2006) or complex I is inhibited (Kudin, Bimpong-Buta, Vielhaber, Elger, & Kunz, 2004) meaning that OXPHOS stress increases complex I mediated ROS production. Another mechanism of complex I superoxide production also occurs during reverse electron transport chain electrons are transported from $CoQH_2$ into complex I (Votyakova & Reynolds, 2001). This occurs when the inner mitochondrial membrane is hyperpolarised such as with inhibition of the ATP synthase by oligomycin (Votyakova & Reynolds, 2001) but can also occur in mitochondria that are actively using succinate as the main substrate (Murphy, 2009).

Complex III Mediated Superoxide Production –

Complex III transports electrons from CoQ to cytochrome C and can reduce O_2 to superoxide (Adam-Vizi & Chinopoulos, 2006). Ubisemiquione is the electron donor that enables complex III mediated superoxide production (Turrens, Alexandre, & Lehninger, 1985). Superoxide is also generated by electron transfer from succinate to cytochrome c (L. Zhang, Yu, & Yu, 1998). However, complex III produces very little ROS when not inhibited by antimycin A (Forman & Azzi, 1997). Complex III produces negligible ROS compared with complex I under physiologically relevant conditions (Murphy, 2009).

Other Sites of Mitochondrial ROS Production –

ROS can also be produced at sites besides complex I and III in the mitochondrion. Recent evidence suggests that ROS can be produced at complex II (Quinlan et al., 2012). ROS are also produced in the mitochondria when α-ketoglutartate from TCA cycle is used as an ETC substrate as the mitochondrial α-ketoglutarate dehydrogenase complex generates ROS (Starkov et al., 2004; Tretter & Adam-Vizi, 2004). Further,

there is an additive effect of reduced NADH pool contributing to complex I mediated superoxide when α-ketoglutartate is used as a substrate (Murphy, 2009).

In addition to ETC related ROS production, mitochondrial ROS can be produced by substrate oxidation including fatty acids, 2-oxoacid and proline. Mitochondrial ROS production is increased palmitoyl-CoA oxidation causes H_2O_2 production (Murphy, 2009) long chain fatty acyl-CoA oxidation causes succinate mediated H_2O_2 release (Bortolami, Comelato, Zoccarato, Alexandre, & Cavallini, 2008). 2-oxoacid dehydrogenase complexes (Quinlan et al., 2014) and mitochondrial proline oxidation (R. L. Goncalves et al., 2014) can also cause generation of ROS.

1.2.2 Genomic Stress

Genomic stressors are endogenous and exogenous insults that increase the risk of genomic instability or loss of genomic integrity. mtDNA is particularly susceptible to genomic stress because for a number of reasons. It has a higher mutation rate during replication, higher rate of deletions, susceptibility to DNA damage and more basic DNA repair machinery than nuclear DNA (Pinto & Moraes, 2015; Szczepanowska & Trifunovic, 2015).

mtDNA mutations and deletions by spontaneous error –

A number of factors make mtDNA more vulnerable to mutations and deletions by spontaneous error than nDNA. mtDNA is more susceptible to sequence variations than nDNA (Marcelino & Thilly, 1999). One reason for this may be the high error rate of DNA polymerase gamma (W. Zheng, Khrapko, Coller, Thilly, & Copeland, 2006). Another reason for incorrect nucleotide incorporation into mtDNA is the dependency on correctly balanced nucleotide pools (Lopez et al., 2009). mtDNA is particularly susceptible to deletions because the L strand can get displaced from the H strand during replication mtDNA repair (Krishnan et al., 2008). Further, oxidative damage can stall the mtDNA replication machinery (Stojkovic et al., 2016) which may increase the risk of errors during replication. It is important to note that there may be a high physiological significance of spontaneous mtDNA mutations. Because mtDNA is small and without substantial intergenic regions, mtDNA mutations are statistically much more likely to hit a region that will directly affect protein function (Tuppen, Blakely,

Turnbull, & Taylor, 2010) making mitochondria genomic stress particularly detrimental to mitochondrial function.

mtDNA damage and (lack of) repair –

Extensive evidence suggests that mtDNA is more vulnerable to DNA damage than nuclear DNA (Cline, 2012). For example, mtDNA oh8dG lesions occur at roughly 16 times the rate that they occur in nDNA in rat liver mitochondria (Richter, Park, & Ames, 1988). This can lead to functional consequences on the mitochondria and potentially lead to a vicious cycle as mtDNA damage has been experimentally demonstrated to affect OXPHOS function and elevate ROS production (Indo et al., 2007). Another reason often cited that mtDNA is more vulnerable to DNA damage is that it is not packaged with protective histones.

In addition to being more vulnerable to DNA damage, mitochondria also contain less sophisticated DNA repair mechanisms than the nucleus. Mitochondria do not have a pyrimidine dimer repair system and thus cannot repair their genome in face of UV damage (Clayton, Doda, & Friedberg, 1974). Further, bulky adduct cannot be removed from mtDNA (LeDoux et al., 1992; Pettepher, LeDoux, Bohr, & Wilson, 1991). Mammalian mitochondria are thought not to have efficient double stranded break repair although there is some evidence to challenge this (Lakshmipathy & Campbell, 1999). POLG has base excision repair activity (Longley, Prasad, et al., 1998). Having one enzyme complex for both DNA replication and repair could lead to more errors.

At a functional level, direct comparison of mtDNA and nDNA damage and repair in response to the same stress reveals that mtDNA damage is not repaired in response chronic ROS exposure unlike that of the nucleus (Yakes & Van Houten, 1997). The D-loop is more vulnerable to oxidative stress (Rothfuss, Gasser, & Patenge, 2010) than other parts of the mitochondrial genome. Since this is the control region, oxidative damage to this region may destabilise genomic regulation.

Hence it is clear that mitochondria are particularly vulnerable to genomic stress and that can have functional consequences on OXPHOS.

1.2.3 Proteotoxic Stress

Cellular proteostasis encompasses the cellular processes required for synthesis, folding, trafficking, assembly and degradation of proteins at the correct time and place in the cell, and is obviously important for healthy cellular function as proteins are the molecular effectors of many cellular processes (Bustamante, Kaiser, Maillard, Goldman, & Wilson, 2014). Proteotoxic stress is a state of a large load of damaged and/or misfolded proteins which could lead to reduced cellular function or build-up of aggregated proteins which are toxic (Shibata & Morimoto, 2014). Several factors make the mitochondria more vulnerable to proteotoxic stress including aggregation or damaged or aggregated proteins, the protein folding load and the requirement to coordinate proteins of both nuclear and mitochondrial genomes.

Mitochondria are vulnerable to accumulating damaged and aggregated proteins. The positive charge and amphiphilic properties of the mitochondrial pre-sequence makes mitochondrial pre-proteins vulnerable to aggregating (Endo, Mitsui, & Roise, 1995). Further, there is evidence that aggregated proteins are shuttled into the mitochondrion (Chang & Chang, 2015). Mitochondrial free radicals including ROS can also modify and damage existing mitochondrial proteins (Bulteau, Szweda, & Friguet, 2006).

As most mitochondrial proteins are nuclear-encoded and have to be imported into the mitochondrion and in an unfolded state, mitochondria have a heavy protein folding load (Wiedemann et al., 2004). Overexpression of wild type mitochondrially located proteins partially induces a mitochondrial stress response (Q. Zhao et al., 2002) suggesting that a high mitochondrial protein import load itself causes a mitochondrial protein stress. As mitochondrial protein import is coupled with polarized mitochondrial membrane potential, ATP dependent mitochondrial proteostasis may be disturbed in response to even a mild bioenergetic stress (Wiedemann et al., 2004). Also, mitochondrial matrix pH is roughly 7.8 and intermembrane space is 6.8 (Santo-Domingo & Demaurex, 2012) which may affect protein folding as protein conformation is pH dependent. As ETC complexes, especially complex I, have a large number of subunits and these have to be assembled into supercomplexes it is conceivable that a small problem with mitochondrial protein conformation could have a large impact on mitochondrial proteostasis and ETC function (Mimaki, Wang, McKenzie, Thorburn, & Ryan, 2012).

Coordination of nuclear and mitochondrial genomes is required for healthy mitochondrial proteostasis and a breakdown of this process leads to mitochondrial protein stress (Houtkooper et al., 2013). Mismatch between nuclear and mitochondrially encoded ETC complex subunits causes misassembly (McKenzie, Chiotis, Pinkert, & Trounce, 2003; I. A. Trounce, Crouch, Carey, & McKenzie, 2013). Further, incompatibility between mitochondrial tRNAs and the nuclear-encoded, mitochondrial tRNA synthetase results in perturbed mitochondrial proteostasis and function (Holmbeck, Donner, Villa-Cuesta, & Rand, 2015; Meiklejohn et al., 2013).

In summary, a number of factors render mitochondria vulnerable to proteotoxic stress.

1.2.4 Mitochondrial Vulnerability to Exogenous Stress

In addition to being intrinsically stress prone, a number of features of mitochondria make them particularly vulnerable to exogenous stresses such as toxins, drugs and environmental pollutions.

Firstly, there is a tendency for toxins to accumulate in mitochondria. The mitochondrial inner membrane is very lipid rich and the elevated matrix pH both attract accumulation of lipophilic and amphiphilic compounds which may be toxic (Modica-Napolitano & Aprille, 2001; Pereira et al., 2011). Heavy metals can enter mitochondria through mitochondrial calcium transporters by molecular mimicry (Meyer et al., 2013). Cadium (Sokolova, Ringwood, & Johnson, 2005), lead (Castellino & Aloj, 1969), manganese (Gavin, Gunter, & Gunter, 1992) and mercury (Bucio et al., 1999) have all been demonstrated to accumulate in mitochondria which leads to mitochondrial dysfunction. Carcinogens also accumulate in mitochondria (Backer & Weinstein, 1982; Wunderlich, Tetzlaff, & Graffi, 1972).

Once these toxins accumulate in mitochondria, they can cause mitochondrial dysfunction because many toxins chemically interact with mitochondrial biomolecules including ETC complexes, mtDNA and mitochondrial enzymes hence interfering with mitochondrial function. Environmental toxins interact with a range of mitochondrial proteins. For example, many pesticides directly interact with ETC components with rotenone, antimycin A and azides inhibiting complex I, III and IV respectively (Pardini, Heidker, Baker, & Payne, 1980). Fluorochemicals can interact with mitochondrial

proteins interfering with mitochondrial metabolism (Starkov & Wallace, 2002). Carcinogens can interact with mtDNA more strongly than they do for nuclear DNA (Backer & Weinstein, 1982; Wunderlich et al., 1972). Additionally, because of the endosymbiotic origin of mitochondria, tetracycline antibiotics target mitochondrial protein synthesis machinery such as (Moullan et al., 2015). These metals can bind mitochondrial enzymes with higher affinity than cofactors impeding metabolic function (Meyer et al., 2013).

In summary, mitochondria are vulnerable to environmental pollutants and drug induced toxicity due to a tendency for toxins to accumulate in the mitochondria where they can directly interact with mitochondrial enzymes, mtDNA and ETC complexes causing mitochondrial stress.

1.3 Mitochondrial Stress Communication and Quality Control is required for Maintenance of Symbiotic Relationship between Mitochondria and the Cell

Thus far, it is established that mitochondria are critically important but paradoxically stress prone organelles. A major theme of this thesis is that cellular communication to and from the mitochondrion to the rest of the cell is required to maintain the symbiotic relationship of the mitochondria and adapt to mitochondrial stress. Here I will discuss communication to the mitochondrion (anterograde signaling); from the mitochondrion (retrograde signaling); and the possibility of cell-to-cell mitochondrial stress communication.

1.3.1 Anterograde Communication

Anterograde communication is the process by which the nucleus controls mitochondrial number and function. Basic mechanisms of mitochondrial morphology and nuclear control of mitochondrial biogenesis were described in section 1.1.4. Here, I will discuss some upstream cell signaling events illustrating nuclear control of mitochondrial biogenesis and mitochondrial function.

Catabolic Stress Signals Alterations in Mitochondrial Density and Function –

Catabolic stress including exercise can signal alterations in mitochondrial biogenesis and function through AMP, Ca^{2+} and mitochondrial fission and fusion machinery (Quiros et al., 2016). The beneficial effects exercise on mitochondrial biogenesis are well known (Hood, 2009; Irrcher, Adhihetty, Joseph, Ljubicic, & Hood, 2003) and more recently on mitochondrial quality control (Ding, Zhang, Zhang, & Zhang, 2013). A major mechanism by which exercise signals mitochondrial biogenesis is by adenosine mononucleotide phosphate (AMP) activation of AMP kinase (AMPK) (Kemp et al., 1999). Another anterograde signaling pathway of by which exercise signaling mitochondrial biogenesis is through Ca^{2+} activation of calcium/calmodulin-dependent protein kinase IV (CaMKIV) activation of PGC1α (H. Wu et al., 2002). calcium/calmodulin-dependent protein kinase kinase (CaMKK) signaling occurs upstream of AMPK (Woods et al., 2005) suggesting that it is also an important anterograde signaling pathway.

Exercise promotes expression of mitochondrial fission proteins (Kitaoka, Nakazato, & Ogasawara, 2016) and changes in mitochondrial ultrastructure (Hambrecht et al., 1997; Tarnopolsky et al., 2007). However, the mechanisms by which exercise controls mitochondrial morphology dynamics are still unclear. Mitophagy is also activated by exercise by PGC1α (Vainshtein, Tryon, Pauly, & Hood, 2015). A kinase which plays an important role in mitophagy ULK1 is also activated by exercise (Moller et al., 2015).

Caloric Intake Signals Mitochondria by Sirtuins –

Nicotinamide adenine dinucleotide (NAD^+) is a coenzyme that is increased by calorie restriction and stimulates mitochondrial biogenesis making it an anterograde signaling molecule. Sirtuin (Sirts) are a class of NAD^+ dependent deacetylase enzymes which can modulate cell function through removal of an acetyl group from lysine residues. Sirt1, Sirt6 and Sirt7 are localised to the nucleus and have reported roles in controlling mitochondrial biogenesis. Sirt6 has not been reported to be closely related to mitochondrial function but Sirt1(B. L. Tang, 2016) and Sirt7 (Ryu et al., 2014) have.

Sirt1 has a body of literature too extensive to review here but the main mechanism by which Sirt1 is thought to control mitochondrial biogenesis is through deacetylation of PGC1α (Gerhart-Hines et al., 2007; Nemoto, Fergusson, & Finkel, 2005) which was noted in section 1.1.4 as the master regulator of mitochondrial biogenesis by its action as a transcriptional coactivator for a number of important transcription factors which appears to be tissue specific (B. L. Tang, 2016) Sirt7 knockout mice display significantly reduced number and function of mitochondria through deacetylation of 3 critical lysine residues of GABPβ which promotes stabilisation of the GABPα/GABPβ complex (Ryu et al., 2014). The fact that there is a strong, multi-systemic mitochondrial disease phenotype associated with Sirt7 knockout mice suggests that without additional NAD^+ or fasted conditions suggests that this process may be constitutively active (Ryu et al., 2014). Increasing NAD^+ levels using different pharmacological treatments stimulates mitochondrial biogenesis in a number of different mouse models (Canto et al., 2012; Cerutti et al., 2014; Khan et al., 2014; Pirinen et al., 2014). This suggest that any additional improvement in mitochondrial function from NAD^+ may be Sirt1 or non-Sirt mediated. Sirt1 is important for improvements in mitochondrial biogenesis with

NAD^+ (Cerutti et al., 2014) but whether there are non-Sirt1 mediated effects of NAD^+ on mitochondrial biogenesis is not studied in mammals. Further, the effect of NAD^+ supplementation in PGC1 null mice has not been studied so it is not clear if Sirt1is acting by PGC1 or through other histone changes. In summary, NAD^+ is a robust anterograde signaling molecule but the molecular mechanisms are not well elucidated.

Cell Non-Autonomous Anterograde Communication –

It was noted in the earlier section 1.1.4 on mitochondrial biogenesis that many endocrine receptors regulate mitochondrial biogenesis including thyroid receptors, glucocorticoid receptor and estrogen receptor related receptors. As such, changes in circulating hormones in theory could elicit anterograde signaling in distal tissues. Thyroid hormone has been demonstrated to increase mitochondrial biogenesis in skin (Vidali et al., 2016) and mitophagy (Lesmana et al., 2016). Glucocorticoids stimulate mitochondrial biogenesis specifically in muscle (K. Weber et al., 2002)

Estrogen-related receptors have not yet been deorphanized (Horard & Vanacker, 2003) but activation by exogenous ligands could promote mitochondrial biogenesis. It has recently just been shown that the 5-HT2 serotonin receptor can regulate mitochondrial biogenesis (Harmon et al., 2016) but whether physiologically relevant cell non-autonomous anterograde communication can occur via this receptor is unknown. Although it is an interesting observation because in *C.elegans*, serotonin is important for cell non-autonomous induction of mitochondrial unfolded protein response (mtUPR) (Berendzen et al., 2016).

1.3.2 Retrograde Communication

It is established that mitochondria are vulnerable to stress and are major sensors of environmental stress. Mitochondria signal stress in a number of ways, namely membrane depolarization, alterations in adenine nucleotide levels, ROS production, Ca^{2+} fluxes, permeability transition pore opening, and perhaps secretion of proteins/peptides. Here I will discuss how these stress signals promote the development of mitochondrial quality control pathways through retrograde signalling from the

mitochondria to the nucleus, post-translational modifications or activation of proteins and other mechanisms represented in Figure 1.1.

Retrograde communication in the process by which mitochondrial function is relayed out of the mitochondria to communicate to the rest of the cell and nucleus. Retrograde communication was first described in yeast by retrograde signaling proteins RTG1 and RTG2 (X. Liao & Butow, 1993). These proteins are not conserved in the mammalian system and mechanisms by which mammalian cells communicate mitochondrial stress are beginning to be elucidated, although still not well understood (Arnould, Michel, & Renard, 2015). In contrast to anterograde signaling, retrograde signaling in mammalian cells is less well studied and thus is a major focus of this thesis.

Mitochondrial ROS Initiates Diverse Signaling Cascades

ROS produced in the electron transport chain can readily exit mitochondria and elicit cellular responses, making them active signaling molecules. Major mechanisms by which ROS causes signaling cascades include activation of redox sensitive proteins including kinases, transcription factors and enzymes (Indo et al., 2017).

There are other examples where ROS induces cellular adaptations to clear ROS or improve mitochondrial function, which may be thought of as negative feedback mechanisms. One major mechanism that switches on antioxidant defences in the cell is the activation of antioxidant response element (ARE). ARE is a *cis*-acting enhancer sequence that controls expression of a variety of antioxidant enzymes. A ROS-mediated signaling cascade that results in activation of this enhancer has been identified which provides evidence for cellular adaptation in response to ROS signals where NRF2 activates the ARE enhancer to switch on an anti-oxidant gene program (Nguyen, Nioi, & Pickett, 2009). Oxidation of lipids, especially membrane lipids is one of the mechanisms proposed in the free radical theory of ageing but products of lipid oxidation may actually function in cell signaling to cause adaptations. For instance, the oxidised lipid metabolite 4-hydroxynonenal promotes NRF2 activation of the ARE inducing expression of antioxidant genes (Y. Huang, Li, & Kong, 2012). Furthermore, activation of this pathway appears to be chemoprotective which implies that dysregulation of this adaptation may potentiate disease. Further, ROS activates the transcription factor

FOXO3a (Bonello et al., 2007) which induces expression of MnSOD (Kops et al., 2002) catalase (W.-Q. Tan, Wang, Lv, & Li, 2008) and PrxIII (Jeong et al., 2011) which have antioxidant functions in the mitochondria. These responses are actually protective against damage suggesting that low grade ROS might actually be beneficial against a major insult later.

Much of the literature surrounding ROS induced damage have incubated cultured cells in supraphysiological concentrations of exogenous hydrogen peroxide or have used high doses of pharmacological inhibitors of complex I and III for short periods of time (Leuner et al., 2012; Tyurina et al., 2013; Yen et al., 2011). These are major chemical insults that induce extensive cell damage and apoptosis and do not model endogenous, physiologically normal levels of mitochondrial ROS production during chronic mitochondrial stress. For instance, when OXPHOS dysfunction was modelled by DNA gamma polymerase mutation, resulting in complex I and III defects and an accompanying increase in ROS production, there was no decrease in cell survival because the cells were rescued by ZNF143 induction of GSH and GPX (W. Lu et al., 2012). Another example is the role of low grade ROS insults in inducing PKC epsilon translocation, which is involved in neuroprotective ischemic preconditioning, whereas larger insults cause PKC delta which causes apoptosis and neurodegeneration (Perez-Pinzon, Dave, & Raval, 2005). Mitochondrial ROS also have preconditioning roles in cardiomyocytes (Vanden Hoek, Becker, Shao, Li, & Schumacker, 1998).

ROS not only induces antioxidant responses in a negative feedback type mechanism but also stimulates cellular adaptations that improve mitochondrial capacity in general. ROS can increase mitochondrial biogenesis and mitochondrial DNA content (H.-C. Lee, Yin, Chi, & Wei, 2002; H. C. Lee, Yin, Lu, Chi, & Wei, 2000). Hydrogen peroxide treatment increases PGC1α promoter activity and expression, as well as expression of multiple antioxidant defences in a PGC1α dependent manner (St-Pierre et al., 2006). In addition to inducing mitochondrial biogenesis and metabolism, PGC1α also stimulates antioxidant defences (Valle, Alvarez-Barrientos, Arza, Lamas, & Monsalve, 2005) reinforcing the idea that ROS stimulates antioxidant capacity in a negative feedback like fashion. Nuclear respiratory factor 1 (NRF1) is a transcription factor associated with mitochondrial biogenesis and was found to be activated and subsequently activate

mitochondrial transcription factor A (TFAM) in a redox dependent pathway (Piantadosi & Suliman, 2006), which suggests that ROS may improve mitochondrial function. Additionally, the autophagy gene family Atg14 are regulated by ROS (Scherz-Shouval et al., 2007) and hence there may even be a role of mitochondrial ROS in stimulating mitophagy.

ROS is also involved in signaling mtDNA repair. Interestingly, many of the cellular adaptations to OXPHOS stress also lead to increased expression of mtDNA repair enzyme 8-Oxoguanine glycosylase (OGG1). For example the NRF2, part of the ROS induced antioxidant adaptation, can bind to the OGG1 promoter region to induce OGG1 expression (B. Singh, Chatterjee, Ronghe, Bhat, & Bhat, 2013), reinforcing the notion that in response to mitochondrial stress, multiple cellular repair and adaptive responses are induced. The antioxidant enzyme MnSOD can also interact with DNA polymerase gamma to promote repair of mtDNA lesions (Bakthavatchalu et al., 2012), further linking antioxidant defences with mtDNA repair.. Mitochondrial OGG1 activity is also increased by exercise (Radak et al., 2009) which tends to up-regulates other mitochondrial quality control processes.

Mitochondrial AMP Initiates Cell Signaling

OXPHOS is a multi-step process that effectively results in ATP production from fuel substrates. The ratio of AMP to ATP is a signal of energy charge and hence OXPHOS function or energy supply. During conditions of compromised mitochondrial function there are shifts in the ratio of adenine nucleotides and the best characterised cellular adaptation of an increased AMP/ATP ratio and also ADP/ATP ratio (Oakhill et al., 2011), resulting from defective OXPHOS, is activation the enzyme AMP-activated protein kinase (AMPK). This is a key energy-sensing kinase that reprograms cellular metabolism through phosphorylation by alterations of phosphoproteomic networks.

AMPK activation generally stimulates a shift to catabolic metabolism and increases mitochondrial biogenesis and oxidative capacity. Activation of AMPK increases expression of PGC1α and metabolic enzymes in skeletal muscle (Fillmore, Jacobs, Mills, Winder, & Hancock, 2010; W. J. Lee et al., 2006) with increased fatty acid oxidation (W. J. Lee et al., 2006; Vitzel et al., 2013) and glycogen synthesis (Vitzel et

al., 2013). Consistent with an important role for AMPK in energy transduction, oxidative capacity is reduced in myocardial tissue when AMPK activity is lost (Stride et al., 2012).

Metformin treatment activates AMPK activity in conjunction with inducing PGC1α and mitofusin protein 2 (Mfn2) protein expression in myocardial tissue (Whittington et al., 2013). A gain of function AMPK mutation in skeletal muscle increases expression of mitochondrial fusion/fission proteins, Mfn2, optic atrophy 1 (OPA1) and dynamin related protein 1 (Drp1) (Garcia-Roves, Osler, Holmström, & Zierath, 2008) which implicates AMPK in the regulation of mitochondrial dynamics as well as content. Activation of AMPK functionally prevents high-glucose induced mitochondrial fission in endothelial cells (Bhatt, Lim, Kim, & Ha, 2013), highlighting that AMPK activity promotes mitochondrial quality control processes, as well as stimulating mitochondrial metabolism. In line with this, AMPK may function in the regulation of mitophagy through phosphorylation of an autophagy gene (Egan et al., 2011) and AMPK can affect mitochondrial fission in response to ETC inhibition (Toyama et al., 2016).

Collectively, metabolic reprogramming by AMPK activation enables the cell to adapt to bioenergetic stress through pro-survival processes and enhanced mitochondrial function and quality control.

Mitochondrial NAD^+ and Cell Signaling

During oxidative phosphorylation, electrons are stripped out of fuel substrates and carried on NAD^+. NAD dehydrogenase (ETC complex I) reduces NADH to NAD^+. NAD^+ is an important signaling molecule due to its capacity to activate PARP enzymes which are involved in DNA repair and SIRTs. In this way, NAD^+ may be considered retrograde signaling molecules. However, the mitochondrial membrane is impermeable to NAD^+ and NADH and so question of whether NAD^+ from the mitochondria can exit needs to be answered in order to evaluate its role in retrograde signaling. However, development of fluorescent probes may assist with compartmental measurements of NAD^+ in the future.

In addition to mitochondrial NAD^+ being synthesised through reduction of NADH at Complex I, the mitochondrion also possesses enzymes for NAD^+ biosynthesis though through the *de novo* pathway or the salvage pathway from tryptophan (Stein & Imai, 2012). Nicotinamide phosphoribosyltransferase (Nampt) inhibition decreases cytosolic but not mitochondrial NAD (Pittelli et al., 2010) and Nmnat3 knockout mice maintain mitochondrial NAD^+ *in vivo* (Yamamoto et al., 2016) which may suggest that tryptophan pathway is the main supplier of the mitochondrial pool. Addressing the issue of NAD+ movement from the mitochondria, a mitochondrial NAD^+ transporter exists in yeast (Todisco, Agrimi, Castegna, & Palmieri, 2006) and plants (Palmieri et al., 2009). Overexpressing the closest mammalian homologues to yeast and plant NAD^+ transporters have no effect on mitochondrial NAD+ whereas overexpressing the yeast and plant NAD^+ transporters into human cells does (VanLinden et al., 2015). This suggests that there most likely is not a mammalian NAD+ transporter. Additionally, the fact that the mitochondrial pool of NAD^+ is at a higher concentration than the cytosolic/ nuclear pool suggest that the two pools are not equilibrated and so increasing mitochondrial NAD^+ is unlikely to increase the cytosolic/ nuclear pool.

In summary, it is possible but unlikely that mitochondrial NAD^+ leaves the mitochondria to engage retrograde signaling with exception of PTP opening during apoptosis. However, mitochondrial NAD^+ may initiate signaling within the mitochondrion through activation of NAD^+ dependent enzymes such as Sirt3, Sirt4 and Sirt5 (Osborne, Cooney, & Turner, 2014) and mitochondrial PARPs (Rossi et al., 2009) which could alter mitochondrial function in ways that could initiate retrograde signaling. However, the physiological relevance of increased mitochondrial NAD^+ through these enzymes is unclear because the dissociation constants for NAD^+ activation of Sirt3, Sirt4, and Sirt5 suggests that mitochondrial NAD^+ concentrations are high enough to be operating at near maximal capacity. Further, presence of Sirt3 reduces lysine acetylation under non-fasted conditions suggesting physiological mitochondrial NAD^+ levels are sufficient for sirt3 mediated deacetylation.

However, anaerobic glycolysis that occurs to compensate for a lack of ETC function can result in generation of NAD^+ in the cytoplasm. In this way, loss of OXPHOS function may promote NAD^+ dependent signaling in the cytoplasm leading to changes in the

nucleus through histone modification. Further, AMPK activation can also increase NAD^+ levels and Sirt1 activity (Canto et al., 2009) which is another mechanism by which mitochondrial function can control NAD^+-sirtuin signaling.

Mitochondrial Membrane Depolarization Can Signal 'Mitophagy'

Autophagy of mitochondria, or mitophagy, is a quality control process by which lysosomes form autolysosomes from defective mitochondria to mediate a self-eating process. The term mitophagy was first coined in a perspective paper (Lemasters, 2005) to describe a process in yeast where autophagy of mitochondria was distinct from general cellular autophagic flux (Kissova, Deffieu, Manon, & Camougrand, 2004).

The best characterised mitophagy pathway occurs in response to mitochondrial membrane depolarization and is largely mediated by the ubiquitin kinase PTEN induced kinase 1 (PINK1) and the ligase parkin. Seminal studies on this pathway showed that PINK1 is cleaved and stabilised on depolarized mitochondria to signal recruitment of the protease parkin recruitment in (Matsuda et al., 2010; Narendra et al., 2010; Vives-Bauza et al., 2010) which degrades mitofusins for proteosomal degradation and autophagosomal degradation to allow mitophagy (A. Tanaka et al., 2010). Constitutively, PINK1is degraded in the cytosol but upon mitochondrial depolarization, it is imported into the mitochondria and cleaved by mitochondrial protease PARL (Meissner, Lorenz, Weihofen, Selkoe, & Lemberg, 2011; Yamano & Youle, 2013). PINK1 phosphorylates parkin (Shiba-Fukushima et al., 2012) and binds to the TOM complex (Lazarou, Jin, Kane, & Youle, 2012) to allow efficient translocation of parkin to the mitochondria where it mediates rupture of the outer mitochondrial membrane by a proteasome dependent mechanism (Yoshii, Kishi, Ishihara, & Mizushima, 2011). The outer mitochondrial membrane protein VDAC is strongly ubiquinitylated by parkin (Geisler et al., 2010) in response to mitochondrial depolarization and required for the full process of PINK1/parkin mitophagy pathway (Yu Sun, Vashisht, Tchieu, Wohlschlegel, & Dreier, 2012).

General cellular autophagy proteins are then linked to the mitochondria. Autophagy related proteins are recruited to depolarized mitochondria by parkin (Itakura, Kishi-Itakura, Koyama-Honda, & Mizushima, 2012). PINK1 also links mitochondria with

general cellular macroautophagy player, LC3 (Kawajiri et al., 2010) and recruiting autophagy receptors (Lazarou et al., 2015).

Most of these studies have utilised overexpressed, tagged parkin in response to a chemical mitochondrial uncoupler so it is difficult to discern the physiological relevance of mitophagy as a mitochondrial stress response in response to a physiologically relevant drop in mitochondrial membrane potential that would be seen with bioenergetic stress. However, it has been demonstrated to occur in response to nutrient deprivation (I. Kim & Lemasters, 2011), accumulation of misfolded proteins (Jin & Youle, 2013) and iron depletion (Allen, Toth, James, & Ganley, 2013) suggesting that mitophagy is active in response to a range of physiologically relevant stressors. Further, there is some evidence for parkin independent mitophagy (Allen et al., 2013; Kageyama et al., 2014; Roy, Kageyama, Iijima, & Sesaki, 2015; Strappazzon et al., 2015).

The Mitochondrial Unfolded Protein Response (mtUPR)

Like the endoplasmic reticulum, the mitochondrion has an unfolded protein response (mtUPR) to counter proteotoxic stress. The mtUPR was first identified in 1996, whereby mitochondrial chaperones were induced in mtDNA depleted cells (Martinus et al., 1996). Later, it was shown in a model where a primate immortalized cell line induced by overexpression of a mutant version of OTC which does not fold properly (Quan Zhao et al., 2002). The mtUPR response in this model resulted in increased expression of mitochondrial import proteins, folding chaperones and heat shock proteins and the ATP-dependent mitochondrial protease ClpP (Quan Zhao et al., 2002). Up-regulation of these genes during mtUPR induction was found to occur via activation of the CHOP, MURE1 and MURE2 elements that induces transcription of a number of proteins including mitochondrial heat shock proteins and other mitochondrial quality control proteins (Aldridge, Horibe, & Hoogenraad, 2007), but the mechanisms that lead to activation of the CHOP, MURE1, MURE2 remained elusive. Activation of this pathway in human cell lines HeLa and MCF-7 occurs in rho0 and doxycycline treated cells and requires eIF2α/ATF4 (Michel, Canonne, Arnould, & Renard, 2015).

The topic was approached in a simpler model organism, *C.elegans*, which facilitated some further characterisation of steps involved in this pathway. Transcriptional

activation of mitochondrial folding chaperones is dependent on nuclear translocation of the ubiquitin-like protein 5 (ubl-5) (Benedetti, Haynes, Yang, Harding, & Ron, 2006), a bZip transcription factor and homeodomain containing transcription factor, DVE (Cole M. Haynes, Yun Yang, Steven P. Blais, Thomas A. Neubert, & David Ron, 2010; C. M. Haynes, Y. Yang, S. P. Blais, T. A. Neubert, & D. Ron, 2010). mtUPR activation was demonstrated to be dependent on the activity of ATP-dependent mitochondrial protease ClpP (Haynes, Petrova, Benedetti, Yang, & Ron, 2007) suggesting a role for mitochondrial protein degradation and export of mitochondrial peptides in the process. Following this, a mitochondrial peptide transporter HAF-1 was found to be required for (transcription factor) hence ClpP digests to make peptides which are exported from the mitochondria to activate transcription of mitochondrial heat shock proteins (Cole M. Haynes et al., 2010). In mammalian cells, ClpX, the catalytic subunit of ClpPX is required for mtUPR initiation (Al-Furoukh et al., 2015).

Although HAF-1 is homologous to mammalian ATP binding cassette proteins, mitochondrially located ATP binding cassette proteins have roles in heme transport, whereas ATP binding cassette proteins with peptide efflux roles are located elsewhere in the cell (Dean, Hamon, & Chimini, 2001), so thus far mitochondrial peptide export has not been confirmed in mammalian systems. During mtUPR activation, the import efficiency of Activating transcription factor associated with stress-1 (ATFS-1) is reduced which allows more to enter the nucleus and activate transcription of mitochondrial quality control proteins (Amrita M. Nargund, Pellegrino, Fiorese, Baker, & Haynes, 2012). ATFS-1 also binds to promoter elements for OXPHOS complex assembly and iron sulfur biogenesis leading to a functional increase in oxidative capacity (A. M. Nargund, Fiorese, Pellegrino, Deng, & Haynes, 2015).

Although mtUPR has been reported in primate cells including human cells (Kohler, Muller-Rischart, Conradt, & Rolland, 2015; Michel et al., 2015) , *C.elegans*, rodents, drosophila (Baqri et al., 2014) and yeast, it does not seem to be a conserved pathway making it unclear what the definition mtUPR actually means. A blast search for CHOP, MURE1, MURE2 promoter elements reveals that they are only present in primates and not conserved in lower organisms or even other mammals. LRPPRC gene is required for mtUPR in human cells and *C.elegans*, suggesting that part of the pathway is

conserved (Kohler et al., 2015). Another point of consideration is that in *C.elegans,* mtUPR is typically assayed as hsp-6 promoter activity which is different to mammalian mtUPR promoter elements. So it seems that mtUPR is conserved at a functional level across species but perhaps the molecular machinery is not.

Mitochondrial Calcium Fluxes in Cell Signaling –

Free calcium (Ca^{2+}) can bind to proteins altering their local electrostatic field which modulates their charge and thus conformation (Clapham, 2007). This can lead to allosteric modification of enzymes including kinases and activation of ion channels making Ca^{2+} an important cellular signal transduction molecule (Clapham, 2007). Early observations that mitochondria sequester cellular Ca^{2+} lead to the recognition of mitochondria as a player in cellular Ca^{2+} handling. More recently, it is becoming appreciated that modulation of mitochondrial Ca^{2+} handling can cause alterations in cellular Ca^{2+} signaling. In this way, mitochondrial Ca^{2+} acts as a chemical signal by which information about mitochondrial function is decoded by the cell and hence it can be considered a retrograde signaling mechanism.

Firstly, energised mitochondria take up Ca^{2+} and mitochondrial Ca^{2+} is required for normal bioenergetic function. Mitochondrial Ca^{2+} uptake can be explained on the basis of the Nernst equation, as the mitochondrial proton gradient is an electrochemical driving force for calcium accumulation into mitochondria (Rizzuto, De Stefani, Raffaello, & Mammucari, 2012). It is estimated that the mitochondrial matrix concentration of energised mitochondria is maintained at concentrations Ca^{2+} is ~10-100 fold higher than the cytosol. This is important for bioenergetic function because Ca^{2+} is required for activity of many mitochondrially localised metabolic enzymes including mitochondrial dehydrogenases involved in the TCA cycle (Nichols & Denton, 1995; Williams, Boyman, & Lederer, 2015). This process of energised mitochondria taking up Ca^{2+} may be decoded as a reflection of mitochondrial function behaving as a retrograde signaling pathway. Hence the process of energised mitochondria taking up Ca^{2+} is not only important for their normal physiological function but also transduces a message to the cell.

Under mitochondrial stress, mitochondrial Ca^{2+} is perturbed which affects cellular Ca^{2+} signaling and subsequently cellular events. Cytosolic calcium is kept low (~ 100 nM) by calcium efflux into the extracellular space (Clapham, 2007) and so mitochondrial calcium handling may not affect cytosolic Ca^{2+} concentrations. However, cellular Ca^{2+} travels in oscillatory waves and so perturbations to mitochondrial Ca^{2+} can drive oscillations which may ultimately affecting cell signaling. For example, mitochondrial potential affects Ca^{2+} uptake which has downstream implications on cytosolic Ca^{2+} signaling and proliferation (Valero, Senovilla, Nunez, & Villalobos, 2008). In this way, mitochondrial Ca^{2+} fluxes links mitochondrial dysfunction with the cellular signal not to proliferate. Further, mitochondrial calcium accumulation modulates nuclear calcium level (Faulk et al., 1995) and plasma membrane function (Demaurex, Poburko, & Frieden, 2009). Mitochondrial quality control is also engaged when mitochondrial Ca^{2+} is perturbed. Mitofusin-1 is upregulated when mitochondrial calcium homeostasis is perturbed (Choudhary, Kaddour-Djebbar, Alaisami, Kumar, & Bollag, 2014).

Under normal mitochondrial function and during stress, mitochondrial Ca^{2+} fluxes are decoded by the cell hence playing an active signaling role.

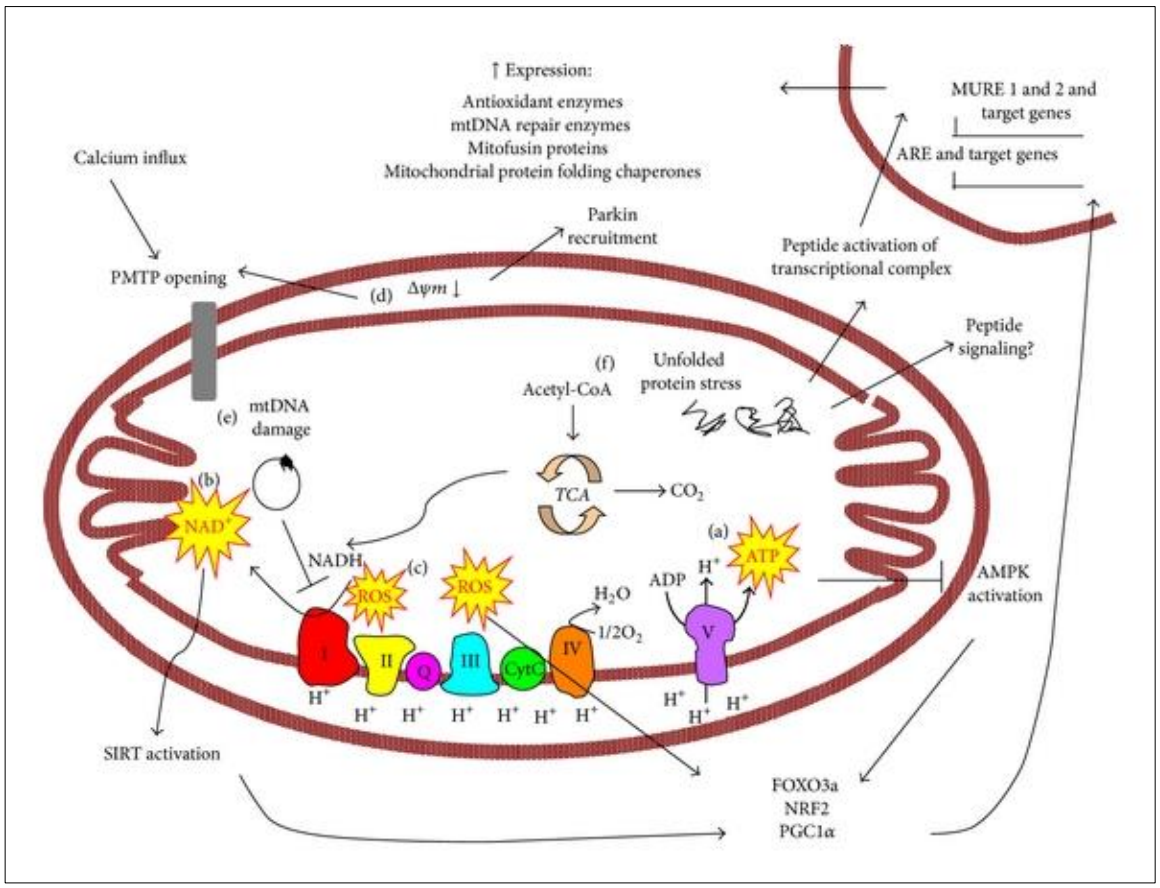

Figure 1.1 Retrograde Signaling Pathways in Mammalian Cells

Schematic summary of mitochondrial stress signaling and cellular adaptations. ATP (a), NAD+ (b), and ROS (c) are outputs of the electron transport chain and oxidative phosphorylation that may function as stress signals. NAD+ can activate sirtuins (SIRT) and increased AMP/ATP ration can activate AMPK, which activate transcription of antioxidant defences, mitochondrial DNA repair enzymes, and other target genes important in mitochondrial biogenesis and metabolism through transcription factors FOXO3a, NRF2, and the transcriptional coactivator PGC1α. ROS can also directly activate these transcriptional regulators. Mitochondrial DNA (mtDNA) damage can potentiate OXPHOS dysfunction (e) and hence lead to the above responses. Loss of innermitochondrial membrane potential (d) can lead to PMTP opening or parkin recruitment and hence mitophagy. Through peptide export, unfolded protein stress (f) can activate a transcriptional complex which acts on the MURE1, MURE2, and CHOP elements to induce the transcription of mitochondrial protein folding chaperones.

Mitohormesis –

To summarise, mitochondrial stress can relay retrograde signaling cascades to elicit quality control responses that help the cell adapt to mitochondrial stress through retrograde signaling (Figure 1.1). Taking this one step further, Ristow and colleagues have observed that low grade mitochondrial stress can actually have beneficial effects on healthspan through heightened mitochondrial quality control mechanisms. This concept was termed 'mitochondrial hormesis' or 'mitohormesis' published as medical hypothesis (Tapia, 2006) and a review (Ristow & Zarse, 2010).

This may explain increased life span in *C.elegans* in response to low-grade arsenic exposure (Schmeisser, Schmeisser, et al., 2013), low glucose availability (Schulz et al., 2007) and londamine (Schmeisser, Zarse, & Ristow, 2011). Low-grade mitochondrial stressors protect neuronal cells against a secondary large stress by maintaining mitochondrial membrane potential (Daiva Bironaite, Johan Anders Westberg, Leif Christer Andersson, & Algirdas Venalis, 2013) and low dose complex I inhibition improves mitochondrial capacity and antioxidant defences in neuronal cells (Yuyun et al., 2013) implicating mitohormesis in neuroprotection. Although mitohormesis has been demonstrated to improve life-span in *C.elegans* and functioning in mammalian cell culture, *in vivo* mammalian studies are lacking. Alterations in AMP, NAD+ and ROS will all occur simultaneously with mitochondrial stress. To elucidate the importance of any particular signaling pathway, complex I inhibition mediated mitohormesis still occurred in worm strains with neurons deficient in sirt1 and ampk but not with worms deficient in redox protein (Schmeisser, Priebe, et al., 2013) suggesting that at least in *C.elegans*, neuronal mitohormesis pathway is indeed mediated by ROS. However, lifespan extension has also been reported by PPARα dependent mechanisms occurs in worms (Brandstadt, Schmeisser, Zarse, & Ristow, 2013). Muscle mitohormesis suppresses insulin signaling in *C.elegans* which is known to extend lifespan (Owusu-Ansah, Song, & Perrimon, 2013). Further, impaired insulin signaling extends lifespan through increased ROS (Zarse et al., 2012). In *C.elegans* metformin induces mitohormesis through PRDX signaling (De Haes et al., 2014). However, a more comprehensive analysis of mtUPR in *C.elegans* reveals that mtUPR is probably not associated with longevity under most circumstances (Bennett et al., 2014)

Protective effects of low grade mitochondrial stress have been recapitulated in mammalian cell culture systems. In a mammalian glioma cell line, low doses of rotenone, an ETC complex I inhibitor induces SIRT1, PGC1alpha promoting beneficial effects (Yuyun et al., 2013). Mild stresses induces preconditioning and mitohormesis in neural crest derived cells (D. Bironaite, J. A. Westberg, L. C. Andersson, & A. Venalis, 2013). The stress induced protein sestrin-2 promotes beneficial effects in brown adipose tissue and the authors proposed this is mitohormesis (Ro, Semple, Ho, Park, & Lee, 2015). Metabolites from metabolic reprogramming associated with mitochondrial dysfunction may promote survival. For example, L-lactate itself may initiate mitohormesis (Zelenka, Dvorak, & Alan, 2015). A small number of mammalian *in vivo* studies on mitohormesis exist. In a transgenic mouse model overexpressing UCP in muscle as a means of low grade mitochondrial stress, increased rates of serine catabolism rescues the phenotype and authors posit that this is a mitohormetic pathway (Ost et al., 2015). In human, antioxidant supplementation attenuates the beneficial effects of exercise (Ristow et al., 2009) suggesting that exercise causes mitohormesis.

In brief, there is convincing evidence in worms for healthspan extending effects of low grade mitochondrial stress which appears to be ROS specific. In mammalian cells, there are many pathways that signal low grade mitochondrial stress but there may be more mechanisms than the one ROS dependent pathway.

Cell Non-Autonomous Retrograde Signaling –

The observation that ETC dysfunction in neurons of *C.elegans* engages a mitochondrial quality control response in gut lead to the idea that mitochondrial stress may be controlled in a cell non-autonomous manner (Durieux, Wolff, & Dillin, 2011). The authors concluded that there is a chemical signal from the mitochondria which could be protein, peptide, nucleic acid or metabolite in nature and termed it a ‘mitokine’. Since then, a number of reviews have been published speculating a role for cell- to-cell or extracellular communication of mitochondrial stress. The term ‘mitokine’ is not specifically defined in the literature and many potential mechanisms of how extracellular signaling may occur in response to mitochondrial stress are possible at the protein, peptide, nucleic acid or metabolite level.

With retrograde signaling in mind, it is possible that mitochondrial stress is communicated to the nucleus which alters translation of nuclear encoded proteins which may be secreted. An example of this is fibroblast growth factor 21 (FGF21) which has been termed a 'mitokine' in a mouse model of mitochondrial dysfunction (K. H. Kim et al., 2013) and has also been identified as a blood biomarker for human mitochondrial disease (Davis et al., 2013). Serum growth and differentiation factor 15 (GDF-15) also predicts mitochondrial disease (Yatsuga et al., 2015). Severe mitochondrial stress has also been implicated with a senescence associated secreted phenotype (SASP) (Nakamura, Ohsawa, & Igaki, 2014) which could link retrograde signaling at the protein level with cell non-autonomous potentiation of disease.

There is evidence for extracellular signaling via mitochondrial derived peptides. The earliest discovered example is humanin, a peptide that aligns with a small open reading frame. Another extracellular peptide that aligns with a small open reading frame of the 16S rRNA is (mitochondrial open reading frame of the 12S rRNA-c) (MOTS-C) (C. Lee et al., 2015).When administered to mice, MOTS-C played a role in obesity and insulin resistance suggesting that mitochondrially encoded whole body energy homeostasis (C. Lee et al., 2015). However, the peptide was administered exogenously at 10 μM in cell culture experiments and mice were intraperitoneally injected at 5 mg/kg/day (25738459). These levels may be supra-physiological as abundance of MOTS-C and humanin in plasma both under physiological conditions and conditions of mitochondrial stress has not been performed. Further, little is known about the stability or pharmacokinetics of these peptides in plasma. As such, it is difficult to speculate the physiological significance of these mitochondrially derived peptides in light of existing research and there are further gaps in the literature with respect to how mitochondrially derived peptides are actually secreted. Neither humanin nor MOTS-C contains the classical protein secretion signal peptide so it is unlikely that they are classically secreted via the golgi. Though 2 peptides have been discovered that are encoded by mtDNA, it remains possible that mitochondrial peptides are generated by mitochondrial protein cleavage. This is a signaling mechanism that occurs to produce peptides that are exported into the cytosol to activate transcription factors for mtUPR (Haynes et al., 2007; C. M. Haynes et al., 2010) as discussed above. Proteolysis and efflux of mitochondrial derived peptides was also identified in yeast (Augustin et al., 2005).

Although an extracellular export of these peptides has not been identified, it cannot be precluded. One group has reported mitochondrial peptides from protein cleavage, termed ‘mitocryptides’ (Hokari et al., 2012; Mukai et al., 2008; Mukai et al., 2009; Seki, Fukamizu, Kiso, & Mukai, 2011), and showed that they are N-formylated and can activate formyl-peptide receptor like 1 (Marutani et al., 2015; Seki et al., 2011) suggesting that peptides derived from cleavage of mitochondrial proteins could participate in cell non-autonomous communication.

There is some evidence supporting the idea of nucleic acid based cell-to-cell communication. mtDNA has been amplified in exosomes of stressed cells (Guescini, Genedani, Stocchi, & Agnati, 2010; Guescini, Guidolin, et al., 2010; B. Zhang, Asadi, Weng, Sismanopoulos, & Theoharides, 2012) and xeno-grafted Rho0 tumours acquire the mtDNA of the host highlighting a role for ‘horizontal transfer’ of mtDNA *in vivo* (A. S. Tan et al., 2015). Hence mtDNA can be secreted and taken up in a cell-to-cell manner making it a possible extracellular signaling mechanism.

Metabolites associated with the metabolic reprogramming that occurs with mitochondrial dysfunction may also participate in cell non-autonomous signaling. Metabolites that may be elevated with mitochondrial dysfunction that have extracellular signaling functions include lactate and ketone bodies (Arnold, Wagner-Ecker, Ansorge, & Langer, 2006).

1.4 Mitochondria and Disease: A Role for Mitochondrial Stress and Communication?

Given the critical importance of mitochondria in producing energy for life and being the site of programmed cell death, it is not surprising that mitochondrial stress is associated with disease. Mitochondrial dysfunction is undoubtedly associated with disease being causally implicated in mitochondrial disease and being associated with complex disease, ageing and cancer. The fundamental reason that we wish to characterise molecular mechanisms of mitochondrial stress communication in mammalian cells is to enrich our understanding of disease processes that involve mitochondria but also because mitochondrial quality control pathways may be therapeutically attractive. We postulate that perhaps a 'miscommunication' of mitochondrial stress may potentiate diseases with a mitochondrial component.

1.4.1 Mitochondrial Disease

Mitochondrial disease describes the large, heterogeneous set of conditions that are caused by mutations in either the mitochondrial DNA or nuclear encoded mitochondrial proteins (Gorman et al., 2016). Mitochondrial dysfunction is a primary and causative feature of these diseases (Gorman et al., 2016) unlike complex diseases of ageing where mitochondrial dysfunction is involved but whether it is cause or consequence is contentious (will be discussed in 1.4.2). A pathogenic mtDNA mutation may be present in up to 1 in 200 people and 1 in 2000 people of the population will acquire serious illness (Cree, Samuels, & Chinnery, 2009). Mitochondrial disease is exceptionally heterogeneous because one mutation can result in a number of different clinical phenotypes and conversely the one clinical phenotype can be caused by different mutations (Khan, Govindaraj, Meena, & Thangaraj, 2015).

The lack of genotype-phenotype correlation described above suggests that there is a role of environment in the pathology of the disease. Hence it is plausible that mitochondrial quality control and stress responses may also be an important factor I mitochondrial disease pathology. Here, I explore the (limited) published literature that analyses a connection between mitochondrial quality control or stress signaling and mitochondrial disease. It is possible that mitochondrial stress signaling may be deleterious by enabling

replication of mutant mitochondrial genomes or protective by mitigating mitochondrial stress.

Elevated mitophagy and mitochondrial biogenesis (Garrido-Maraver et al., 2015) and ROS dependent autophagy (Cotan et al., 2011) have been demonstrated in the mitochondrial disease Mitochondrial Encephalopathy, Lactic Acidosis, and Stroke-like episodes (MELAS) patient cybrid cells which suggests that it is a compensatory mechanism that is engaged in MELAS cells. Cybrid cells of MELAS from patients of different severity (in terms of heteroplasmy and clinical manifestation) revealed that AMPK activation and mitochondrial biogenesis were activated in less severe cases and exogenous activation of these pathways rescued the more severe cybrids (Garrido-Maraver et al., 2015). This suggests that mitochondrial quality control may alleviate phenotype in MELAS fibroblasts. In another cybrid model of MELAS, mitophagy prevented cell death (Cotan et al., 2011) indicating that mitophagy may be important for survival in MELAS. Increased mitochondrial degradation and turnover in cells with carrying MELAS or MERRF mutations (James, Wei, Pang, & Murphy, 1996). Comparison of Rho0 cells with MELAS cells showed that Rho0 cells induced mitochondrial proteostasis quality control whereas MELAS did not suggesting that quality control may be highly specific to particular mutations (Joseph, Rungi, Robinson, & Hood, 2004).

Aberrant stress responses may also be involved in mitochondrial disease pathology. Hsp60 deficiency occurs in mitochondrial encephalomyopathy (Huckriede & Agsteribbe, 1994) suggesting that perhaps mitochondrial proteostasis quality control is important for maintaining health in mitochondrial disease. Inactivation of the LRPPRC gene, the gene causing French Canadian Leigh Syndrome induces an mtUPR to restore proteostasis transiently (Kohler et al., 2015). Therefore it is also possible that mtUPR is engaged at first and over time actually decreases indicating a breakdown of mitochondrial stress signaling. Excessive mitophagy and mitochondrial fragmentation occurs in OPA1 deficient cells (C. Liao et al., 2017) highlighting an example where induction of mtiochonrdial stress responses is aberrant. In a study comparing carriers with affected individual LHON mutation cybrids from Leber's hereditary optic neuropathy (Giordano et al., 2014), carriers had more efficient mitochondrial biogenesis

which mitochondrial biogenesis has a role in limiting proliferation of abberant mtDNA mutations. Similarly, mtUPR can promote propagation of deleterious mtDNA mutations (Lin et al., 2016) hence suggesting that mtDNA quality control may be enables propagation of the diseased genome.

Overall, the above literature highlights that often mitochondrial stress signaling and quality control is engaged in mitochondrial disease cells. Whether this helps cell survival or deleterious may be highly context specific once which further emphasizes how heterogeneous these diseases are.

1.4.2 Mitochondrial Function and Communication in the Aetiology of Complex Diseases of Ageing

Concomitant observations of mitochondrial dysfunction and complex disease are well established, but whether the link between mitochondrial dysfunction and disease is cause, consequence or both remains a point of controversy. Here I will discuss the links between mitochondrial stress and disease and also explore literature linking mitochondrial communication with disease.

Alzheimer's and Sporadic Parkinson's disease –

Dementia is overtaking heart disease as a leading cause of morbidity and mortality in Australia due to our ageing population. The brain accounts for only 2% of body weight but 20% of whole body oxygen consumption (Raichle & Gusnard, 2002). This high energy turnover is largely due to the energy required to maintain ion gradients across membranes in the firing of action potentials in excitatory signaling (Attwell & Laughlin, 2001). Age related neurodegeneration in particular dementias, Alzheimer's disease (AD) and Parkinson's disease (PD), are associated with reduced mitochondrial function (Beal, 2004) and indeed mitochondrial targeted drugs ameliorate the phenotype of PD in mouse models (Ghosh et al., 2016; Mena et al., 2015). As the demand on mitochondria is exceptionally high to maintain brain function and mitochondria are the site of apoptosis, mitochondrial dysfunction could tip the balance in favour of cell death.

Hypotheses implicating a role for mitochondrial dysfunction in neurodegeneration are founded on observations of complex I and complex IV deficiency in PD and AD

respectively. Complex I deficiency is observed in post mortem PD brain tissue (Mizuno et al., 1989; Schapira et al., 1990) and pharmacological inhibition of complex I produces a PD phenotype when administered to mice suggesting an active role complex I dysfunction plays an active role in the aetiology of PD (Greenamyre, Sherer, Betarbet, & Panov, 2001). However, it is still controversial as it has been suggested that the rotenone model of PD does not reflect reality *in vivo* (Fukui & Moraes, 2008) and rotenone directly interacts with α-synuclein, a major player in PD pathology (B. A. Silva, Einarsdottir, Fink, & Uversky, 2013). Complex IV deficiency is present in AD and may trigger pathogenic events in disease progression by the mitochondrial cascade hypothesis of AD (Swerdlow & Khan, 2004). Mitochondrial dysfunction in AD/PD is also systemic ETC defects is present in blood of drug naïve sporadic PD patients (Calligaris et al., 2015). In addition to ETC defects described above, literature implicates a role for oxidative stress and mitochondrial genotoxic and proteotoxic stress in these disorders which I will discuss below.

There is considerable evidence implicating oxidative stress with AD and PD from post mortem brain samples (Z. I. Alam et al., 1997; Ansari & Scheff, 2010; Dexter et al., 1989; Floor & Wetzel, 1998; Raukas et al., 2012; Yoritaka et al., 1996); AD and PD patient blood and cerebrospinal fluid (Buhmann et al., 2004; Di Domenico et al., 2016; Namioka et al., 2016; Prigione et al., 2006) as well as mouse models (Belkacemi & Ramassamy, 2012; Casadei et al., 2016; Sanders & Greenamyre, 2013; Yao et al., 2004). This may be from increased ROS production but also from reduced capacity to respond to oxidative stress. Nrf2 signaling is protective in PD (Burton, Kensler, & Guilarte, 2006) and AD (Kanninen et al., 2008) suggesting that oxidative stress signaling mitigates neurodegenerative phenotype. DJ-1 and α-synuclein both have antioxidant roles and are both dysfunctional in PD and thus inadequate capacity to respond to ROS may be part of the pathology. DJ-1 stabilises Nrf2 (Clements, McNally, Conti, Mak, & Ting, 2006). Another study found that a brain specific mitochondrial stress response transcriptional program including mtUPR and antioxidant responses can occur early and protect against further neurodegeneration (Moisoi et al., 2009) which suggests that breakdown of mitochondrial stress signaling may be a component of neurodegenerative diseases. Upregulation of Nrf2 in *drosophila* rescues PD phenotype (Barone, Sykiotis, & Bohmann, 2011) suggesting that this pathway is protective in PD.

MnSOD, the key mitochondrial antioxidant enzyme is unchanged in any brain region unlike cytosolic antioxidant responses (Aksenov et al., 1998).

There is also evidence for a role of mitochondrial genomic and proteotoxic stress in age related neurodegeneration. Both a loss of mtDNA (Grunewald et al., 2016) and increased rates of somatic mtDNA mutations (Coxhead et al., 2016) occurs in PD post mortem brain tissue. Proteotoxic stress is a major component of both AD and PD. AD is associated with amyloid aggregation and PD with α-synuclein aggregation. In addition to disrupted cellular proteostasis, recent evidence also suggests a role for disrupted mitochondrial proteostasis (Beck, Mufson, & Counts, 2016).

Defective mitophagy coincides with cell models of neurological diseases like AD (Khandelwal, Herman, Hoe, Rebeck, & Moussa, 2011) and PD (Batlevi & La Spada, 2011). In fibroblasts derived from human patients, a mutation in PD associated protein DJ-1 has been reported to be important for mitophagy and mitochondrial dynamics (Krebiehl et al., 2010) suggesting that a role of this protein is to ensure mitochondrial quality control. Further investigation of basal mitophagy *in vivo* in mammalian disease models would greatly facilitate insight into the role of defective mitophagy in disease development. In addition to healthy mitophagy, mitochondrial morphology transitions may be an important mitochondrial stress pathway to protect from neurodegernation as a mutation in OPA1, the a pro-fusion mitochondrial dynamin-related GTPase, a mitochondrial dynamin-related GTPase involved in mitochondrial fusion promotes neurodegeneration (Sarzi et al., 2012)

In summary, there is strong evidence for a role of ETC dysfunction and oxidative stress in AD and PD. A concept emerging from the literature is that other parameters of mitochondrial stress play a role in PD and AD and healthy mitochondrial stress signaling may protect against these disorders.

Cardiomyopathies –

The heart has an extraordinary bioenergetic task pumping 10 tonnes of blood around the body and turning over 20-30 times its weight in ATP each day. Per gram of tissue, the heart uses the most energy of any tissue in the body, roughly 4 x more glucose and fatty

acids than brain and 8 x more glucose than quadriceps per gram of tissue (Furler et al., 2000; Hegarty, Cooney, Kraegen, & Furler, 2002; Manini et al., 2011; Rolfe & Brown, 1997; Smith, Young, & Cawthorne, 1986). Hence it is not surprising that bioenergetic dysfunction is strongly linked with heart failure (Hunter, Kelly, McGarrah, Kraus, & Shah, 2016; Sabbah, 2016). Heart failure is a debilitating and fatal condition of weakened myocardium resulting in the inability for the heart is unable to pump blood at the rate the body requires it. It can be caused by ageing, diabetes and chemotherapy. Since heart failure is so closely linked with mitochondrial dysfunction, it is plausible that mitochondrial stress responses are important. Ablation of mitochondrial stress induced OPA1 processing causes heart failure in mice (Wai et al., 2015) suggesting a role for mitochondrial quality control in protection against heart failure. Further, mitochondrial DNA repair can improve heart failure (Marin-Garcia, 2016). Defective mitophagy has also been implicated in cardiomyopathy and heart failure (Gottlieb, Mentzer, & Linton, 2011; Tong & Sadoshima, 2016). These findings collectively reveal that mitochondrial stress responses are important for healthy heart function.

Insulin Resistance/ Metabolic Syndrome –

Excess caloric intake, especially from lipid, is a major trigger of insulin resistance which is a pathological condition that can lead to Type 2 Diabetes Mellitus (T2DM). Metabolic syndrome is marked by insulin resistance and lipid abnormalities with hyperinsulinemia as a mechanism to offset loss of responsiveness to insulin resistance (Lusis, Attie, & Reue, 2008). Early observations that skeletal muscle of human diabetic subjects have lower mitochondrial function in particular fatty acid oxidative capacity than healthy subjects lead to the hypothesis that mitochondrial dysfunction is involved in skeletal muscle insulin resistance (Kelley, Goodpaster, Wing, & Simoneau, 1999; Simoneau, Veerkamp, Turcotte, & Kelley, 1999).

In rodent studies, HFD is also associated with reduced mitochondrial content (Ciapaite et al., 2011) mRNA transcript levels for OXPHOS genes and PGC1alpha are decreased on short term calorie matched HFD (Sparks et al., 2005) which suggests that it may be that lipid oversupply rather than excess energy intake causes results in changes in mitochondrial biogenesis. Collectively, these findings suggest that a reduction in

mitochondrial function and content occurs secondary to chronic lipid oversupply. In line with this, insulin sensitizing drugs thiazolidinediones increase mitochondrial biogenesis (Bolten et al., 2007; Fujisawa et al., 2009). Thus increasing mitochondrial content may partially offset lipid oversupply through increased mitochondrial metabolism hence ameliorating the effect of a HFD to some extent.

However, there is evidence that directly perturbing mitochondrial function through ETC inhibitors in cell culture rapidly causes loss of insulin signaling (Abu Bakar, Cheng, Sarmidi, Yaakob, & Huri, 2015; Al-Lahham, Deford, & Papaconstantinou, 2016; Y. C. Chen, Wu, & Wei, 2015) indicating that mitochondrial stress is sufficient to drive insulin resistance. Nrf2 null mice are more susceptible to metabolic abnormalities when challenged with a high fat diet (Meakin et al., 2014) suggesting that mitochondrial oxidative stress signaling is important for preventing insulin resistance. Loss of mitophagy also promotes a metabolic disease phenotype (Seillier et al., 2015; L. Wang et al., 2015) and exercise, which ameliorates these diseases, promotes mitophagy and mitochondrial quality control (I. O. Goncalves et al., 2016). Exercise also promotes mitochondrial morphology transitions (Fealy, Mulya, Lai, & Kirwan, 2014). Further, loss of mitochondrial quality control homeostatic mechanisms promotes insulin resistance in muscle (X. Wang et al., 2016) and liver (Jacobi et al., 2015). Recent evidence suggests that mtUPR may be associated with metabolic fitness (Latorre-Pellicer et al., 2016). Further, mitochondrial quality control, in particular PGC1α activation is dysregulated by obesogenic diets (Greene et al., 2015) suggesting that dysregulated mitochondrial stress signaling may be part of the pathology of metabolic disorders.

Pancreatic β-Cell Dysfunction in Type 2 Diabetes Mellitus –

Metabolic syndrome increases the risk of pancreatic failure causing a transition into T2DM (Lorenzo, Okoloise, Williams, Stern, & Haffner, 2003) a condition where the pancreas is no longer able to produce appropriate levels of insulin. This can lead to elevation of blood glucose and eventually complications such as kidney failure, peripheral neuropathy, amputation and blindness all of which are major contributors to disability and mortality in Australia (Huo et al., 2016).

The point mutations A3243G in mtDNA causes a type of diabetes associated with dysfunction in the pancreatic β-cells (van den Ouweland et al., 1992) indicating that mitochondrial stress promotes pathological states in β-cell. It has been suggested that pancreatic β-cells are thought to be especially sensitive to ROS and mitochondrial injury as a result of their glucose sensing role (Li, Frigerio, & Maechler, 2008). Mitochondrial ROS reduces β-cells insulin secretion (Sakai et al., 2003) suggesting that mitochondrial oxidative stress has a deleterious impact on healthy β-cell function. It is not possible to study ETC complex linked respiration biopsies of live human pancreatic β-cells in the way it is with skeletal muscle in insulin resistance, however, some access to human islets from islet transplant patients has enabled studies into the mitochondrial function of T2DM β-cells (Anello et al., 2005). Mitochondrial morphology and function is decreased in diabetic islets compared with control islets (Anello et al., 2005) which highlights some involvement of mitochondrial function in the pancreatic failure, although this could of course be a consequence of the disease. Further, mouse models where mitochondrial genes are specifically deleted from pancreas display a glucose intolerant phenotype (Robson-Doucette et al., 2011; J. P. Silva et al., 2000; Z. Zhang et al., 2011). The above literature suggests a role for mitochondrial dysfunction in pancreatic β-cell dysfunction. New literature suggests that there may also be a role for a breakdown in mitochondrial stress signaling as well. For example, defective mitophagy in pancreatic β-cell dysfunction (Mitchell et al., 2013) and dysfunction of mitochondrial morphology transitions and mitophagy are associated with reduced insulin secretion (Lo et al., 2015)

Analysing literature on various complex diseases highlights that mitochondrial dysfunction most likely plays a role in potentiating the progression of degenerative processes. While mitochondrial dysfunction may not be an active initiator of disease, the common themes across different complex diseases mitochondrial stress and breakdown of mitochondrial stress signaling promotes disease phenotype and that enhancing mitochondrial activity and homeostasis at least partially ameliorates conditions.

1.4.3 Mitochondrial Stress, Quality Control and Ageing

Like the complex diseases of ageing, the ageing process itself has been implicated with reduced mitochondrial function, however, whether it is a cause or consequence of ageing remains elusive.

A seminal study in 1989 found inverse correlations between age and state III respiration in skeletal muscle of human subjects which was linked with ultrastructural changes (I. Trounce, Byrne, & Marzuki, 1989). This was measured relative to mitochondrial protein suggesting that there is a decline in the functional quality of mitochondria with age. Similar findings were recapitulated (Cooper, Mann, & Schapira, 1992) where it was linked with mtDNA deletions. In contrast with these findings, there are no differences between young and old skeletal muscle oxidative capacity when subjects are matched for physical activity level (Kent-Braun & Ng, 2000; Rasmussen, Krustrup, Kjaer, & Rasmussen, 2003). Hence it is possible that sedentary behaviour associated with ageing may reduce mitochondrial quality as well as mitochondrial content. Studies that have looked at rates of mitochondrial ATP production have failed to find a difference in oxidative capacity with ageing (Lanza, Befroy, & Kent-Braun, 2005; Rasmussen et al., 2003) which is intriguing because it suggests that mitochondrial deficits with ageing may be more closely linked with mitochondrial stress parameters e.g. ROS rather than bioenergetics per se. The recent observation that decreased mitochondrial activity in skeletal muscle with age occurs exclusively in slow twitch fibres (Picard, Ritchie, Thomas, Wright, & Hepple, 2011) may explain conflicting results based on the fibre type composition of the muscle type analysed. However it is also important to note that there are endocrine associated changes with ageing such as thyroid hormone level that can also impact on mitochondrial content (Bratic & Larsson, 2013).

The above studies in humans are suggestive of a relationship but conflicting. However, evidence for a direct relationship between mtDNA mutations and ageing has been demonstrated in the DNA mutator mouse (Trifunovic et al., 2004; Vermulst et al., 2008). Mitochondrial germline mutations also likely play an important role linking mitochondrial mutagenesis with ageing (Ross et al., 2013). This suggests that mitochondrial genomic stress and ROS may indeed accelerate the ageing process.

As discussed in the section on mitohormesis, mitochondrial quality control and mitochondrial stress signaling are linked with longevity in lower organisms. Whether or not breakdown of mitochondrial stress signaling and quality control promotes the ageing process in mammals is currently unknown. It has been suggested that defective mitophagy may be a component of human ageing (Diot, Morten, & Poulton, 2016). However, in skeletal muscle from human samples, expression of fission and fusion and autophagy proteins were not associated with age (Distefano et al., 2016).

1.5 Project Aims and Hypotheses

Although controversy surrounding the precise definition of the term 'mitohormesis' exists and whether or not a true relationship exists between mitochondrial content and healthspan remains debatable, the concept that undoubtedly emerges through analysis of literature is that ***there is a crucial role for mitochondrial quality control and stress signaling in healthspan extension***. It is an apparent recent literature trend that enhanced mitochondrial function through metabolic flexibility and homeostatic mechanisms to offset stress supports healthy function and may have a beneficial impact on healthspan extension, rather than simply increasing mitochondrial content.

Much of the work above has mostly been performed in lower organisms such as flies and worms and there is limited literature available interrogating the basic molecular mechanisms of mitochondrial stress signaling in mammalian cells and hence it is an important gap to be filled in understanding these complex diseases. Also since mitochondria are vulnerable to exogenous stresses, understanding these stress responses is important in understanding drug induced cytotoxicity and responses to environmental poisons. Hence the purpose of this thesis is to address the gaps in the literature surrounding communication from the mitochondrial to the rest of the cell in mammalian cells.

The overarching hypothesis is that ***mitochondrial stress communication between mitochondria is critical for maintaining the symbiotic relationship which is paramount for healthy cell functioning.*** Specific aims for the project include:

Explore intracellular responses to ETC stress in a model of mismatch between nuclear and mitochondrial genomes
Analyse the secreted proteome from HEK293 cells, primary murine hepatocytes and primary murine adipocytes in response to ETC toxins

CHAPTER 2: MATERIALS AND METHODS

Materials

2.1.1 Reagents

Reagent	Supplier and Catalogue Number
2% Bis	Bio-Rad, 161-0142
2-deoxy-glucose	Sigma-Aldrich, D8375
3H-2-deoxy-glucose	Perkin Elmer, NET549001MC
40% Acrylamide	Bio-Rad, 161-0144
Acetone, for HPLC	Sigma, 34850-1L
alamarBlue	Life Technologies, DAL1025
Antimycin A	Sigma-Aldrich, A8674
Ammonium Persulfate	Sigma-Aldrich, A3678
ATPlite Kit	Perkin Elmer, 6016941
BCA kit	Pierce, 23225
Bio-Rad Protein Assay	Bio-Rad, 500-0006
BSA	Sigma, A7030
U-C14-Glucose	Perkin Elmer, NEC042A001MC
CaCl2	Ajax FineChem, 127
Coomassie Blue G	Sigma-Aldrich, 27815
Cytochalasin B	Sigma-Aldrich, C6762
Dinitrophenol	Sigma-Aldrich, D198501
Dithiothreitol	Sigma, D0632
DMEM glucose free, pyruvate free	Life Technologies, 11966025
DMEM high glucose	Life Technologies, 11965-092
DMEM high glucose, phenol red free	Life Technologies, 11965-092
DMEM low glucose	Life Technologies, 11885-084
DMEM low glucose, phenol red free	Life Technologies, 11054020
Ethylene glycol-bis(2-aminoethylether)-N,N,N′,N′-tetraacetic acid	Sigma-Aldrich, 03779
Foetal bovine serum	Life Technologies, 26140-079
FCCP	Sigma-Aldrich, C2920
Galactose	Sigma-Aldrich , G7134
HEPES	Sigma-Aldrich, H3375
JC-1	Sigma-Aldrich, T4069
KCl	Ajax FineChem, 383
KH2P04	Ajax FineChem, 391
L-ascorbic acid	Sigma-Aldrich, A7631
MgCl2.6H2O	Ajax FineChem, 296
MgSO4	Ajax FineChem, 302
Mitosox Red	Life Technologies, M36008

NaCl	Ajax FineChem, 465
Oligomycin A	Sigma-Aldrich, 75351
Phenol red free Trypsin-EDTA	Life Technologies, 15400054
Rotenone	Sigma-Aldrich, R8875
Sequencing grade tryspin	Promega, V5111
Sucrose	Sigma-Aldrich, S0389
TEMED	Sigma-Aldrich, T9281
Trichloroacetic acid	Sigma-Aldrich, T0699
Tricine	Sigma-Aldrich, T0377
Tris(hydroxymethyl) aminomethane	Merck-Chemicals 1.08383.0500
Triton X 100	Sigma-Aldrich, X100
Trizma HCl	Sigma-Aldrich, T594
Tryspin-EDTA	Sigma-Aldrich, 59429C
Ultima Gold XR Scintillation Fluid	Perkin Elmer, 6013111
Uridine	Sigma-Aldrich, U3003
Western Lighting Plus-ECl, Enhanced Chemiluminescent Subtrate	Perkin Elmer, NEL104001EA
β-Mercaptoethanol	Sigma-Aldrich, M6250

2.1.2 Buffer Compositions

Buffer	Composition
Krebs-Ringer	140mM NaCl, 20mM HEPES, 5mM KCl, 2.5mM MgSO4, 1.2mM $CaCl_2$, pH7.4.
Phosphate Buffered Saline	135 mM NaCl, 2.7 mM KCl, 10 mM Na_2HPO_4, 1.8 mM KH_2PO_4, pH 7.4
RIPA Buffer	20 mM Tris-HCl (pH 7.5) 150 mM NaCl, 1 mM Na2EDTA 1 mM EGTA 1% NP-40 1% sodium deoxycholate 2.5 mM sodium pyrophosphate, 1 mM b-glycerophosphate
Laemli Buffer	2% SDS, 10% glycerol, 5% 2-mercaptoethanol, 0.002% bromphenol blue, 0.0625 M Tris HCl pH 6.8
Western Transfer Buffer	(Made in Stores) 0.3 Tris(hydroxymethyl) aminomethane, 1.44 % Glycine, 1%
Tris-glycine Running Buffer	0.3 Tris(hydroxymethyl) aminomethane, 1.44 % Glycine, 1%, 0.1% (w/v) SDS
Tris-tricine Running Buffer	100 mM Tris, 100 mM Tricine, 0.1% SDS, pH 8.3 following dilution to 1x with water
Tris Buffered Saline (TBS)	(Made in Stores) 0.12 % Tris base (v/v), 0.87% NaCl (w/v) pH 7.5
Tris Buffered Saline + Tween 20 (TBS-T)	TBS + 0.05% (v/v) tween20

2.1.3 Antibodies

Primary –

Target Protein(s)	Developed in	Dilution	Supplier and Catalogue Number
ACC	Rabbit	1 in 1000	Cell Signaling Technology, 3662
Akt	Rabbit	1 in 1000	Cell Signaling Technology, 9271
AMPKα	Rabbit	1 in 1000	Cell Signaling Technology, 2532
ATM	Rabbit	1 in 1000	Cell Signaling Technology, 13050
ClpP	Rabbit	1 in 1000	Abcam, ab124822
GSK3β	Rabbit	1 in 1000	Cell Signaling Technology, 9315
Hsp10	Rabbit	1 in 1000	Abcam, ab108611
Hsp60	Rabbit	1 in 1000	Cell Signaling Technology, 4870
MitoProfile Total OXPHOS	Mouse	1 in 1000	Mitosciences, M5601
MnSOD	Rabbit	1 in 1000	Santa Cruz Biotechnology, sc-30080
mTOR	Mouse	1 in 1000	Cell Signaling Technology, 4517
p70 S6 Kinase	Rabbit	1 in 1000	Millipore, 14-486
Pan 14-3-3 (K-19)	Rabbit	1 in 1000	Santa Cruz Biotechnology, sc-629
Phopsho mTOR (ser 2448)	Rabbit	1 in 1000	Cell Signaling Technology, 2971
Phospho ACC (ser 79)	Rabbit	1 in 1000	Cell Signaling Technology, 3661
Phospho ATM	Mouse	1 in 1000	Cell Signaling Technology, 4526
Phospho-Akt (ser 473)	Rabbit	1 in 1000	Cell Signaling Technology, 4691
Phospho-AMPKα	Rabbit	1 in 1000	Cell Signaling Technology, 2535
Phospho-GSK3α/β (ser 21/9)	Rabbit	1 in 1000	Cell Signaling Technology, 9331
Phospho p70 S6 Kinase (thr 412)	Rabbit	1 in 1000	Millipore, 07-018
VDAC	Rabbit	1 in 1000	Cell Signaling Technology, 4866

Secondary –

Target	Developed in	Dilution	Supplier and Catalogue Number
Anti-Mouse IgG	Sheep	1:10 000	Sigma-Aldrich, A6782
Anti-Rabbit IgG	Goat	1:10 000	Sigma-Aldrich, A6154

2.2 Methods

2.2.1 Cell Culture

Xeno-mitochondrial Cytoplasmic Hybrid Cells (Cybrid Cells)

Cybrid cells were a gift from A/Prof Ian Trounce, Centre for Eye Research Australia, Melbourne, Australia. These cells were generated by fusion of *Mus musculus* Rho0 LMEB3 clone, derived from ethidum bromide treatment of LMTK parent cell line, with enucleated primary fibroblasts of *Mus musculus*, *Mus dunni*, *Mus dahari*, *Rattus norvegicus* The resulting cybrid cells include a control (both genomes Mm) and then increasing evolutionary divergence between nuclear and mitochondrial genomes respectively (McKenzie et al., 2003). The cells were incubated at 37°C, 5% CO_2 cultured in a 1:1 high glucose: low glucose DMEM supplemented with 10% FBS and Rn cells were additionally supplemented with 2.5 µg/mL uridine. Upon receipt, cells were expanded and a confluent T75 flask was trypsinised and pelleted and divided into 5 aliquots which were frozen in 300 µL of freezing medium (10% DMSO, 20% FBS, 70% high glucose DMEM) with the temperature reduced by 1 degree per minute by placing in isopropanol jacketed Mr Frosty in a -80°C freezer. These were transferred to liquid nitrogen vapour phase tanks for long term storage. For revivial, an aliquot was thawed completely at 37°C and 1 mL of warmed culture media was added drop wise over 60 seconds with gentle swirling before being diluted in 12 mL of culture media and transferred to a T25 flask.

Hek293

Hek293 cells were propagated in low glucose DMEM supplemented with 10% FBS, incubated at 37°C, 5% CO_2. Cells were passaged at ~80% confluence by detaching with Trypsin-EDTA and seeding at ~25% in flasks or at a specific cell density in plates or dishes for experiments. For freezing down $1x10^6$ cells were suspended in 300 µL of freezing media (10% DMSO, 10% FBS, 80% low glucose DMEM) and the temperature reduced by 1 degree per minute by placing in isopropanol jacketed Mr Frosty in a -80°C freezer. These were transferred to liquid nitrogen vapour phase tanks for long term storage. For revival, cells were thawed at 37°C, diluted in 10 mL culture media and

pelleted at 200 g for 5 minutes. Cell pellets were resuspended in fresh culture medium which was free of DMSO.

Isolation and Culture of Primary Murine Hepatocytes

Isolation and culture of primary murine hepatocytes was performed as described (Montgomery et al., 2015). Ketamine/xylazine anaesthetised 6-8 week old C57/Bl6J mice were opened and liver was perfused at 4-5 ml/min first in an EGTA wash buffer for 10-15 minutes to chelate Ca^{2+}, then in $CaCl_2$/collagenase buffer to digest the liver*. The liver was then excised and the outer membrane of the liver lobes were torn allowing hepatocytes to be released. Hepatocytes were then strained using a 100 µm cell strainer. Hepatocytes were washed in cold $CaCl_2$ buffer and pelleted by spinning at 50 g for 3 minutes twice and then washed once more in cold M199 media. Cells were then counted and plated onto type A collagen coated culture plates/ dishes in adherence media and 4 hours later changed to maintenance culture media.

* Liver perfusion surgery was performed by Dr. Brenna Osborne

Isolation and Culture of Primary Murine Adipocytes

From the same mice that were used for hepatocytes isolation, before liver perfusion, inguinal fat pads were dissected for primary adipocyte isolation. Fat pads were minced and digested in a 37°C shaking water bath for 30-45 minutes in isolation buffer[3] composed of Dulbecco's phosphate buffered saline (0.901 mM CaCl2, 0.493 mM MgCl2.6H2O) and Roche 0.75 U/mL collagenase D and 2.4 / mL dispase II.

After digestion, SV medium (low glucose DMEM/F12 1:1, penicillin/streptomycin, 10% foetal bovine serum) was added to the suspensions (5:1) and then the final suspension was sieved through a 100 µm cell strainer. Cells were then centrifuged at 600 x g for 5 mins, pelleting the stromal vascular fraction (SVF) which was then resuspended in SVF culture medium before being sieved through a 40 µm cell strainer. Cells were counted on a haematocytometer, mixed with trypan blue (1:1) to determine viability and seeded in culture plates or flasks at 25 000 cells/ cm_2.

Preadipocytes were then grown to 80 % confluence in SV culture medium after which an adipogenic cocktail medium (low glucose DMEM/F12 1:1, penicillin/streptomycin, 5% foetal bovine serum, 1 µM dexamethasone, 5 µg/ mL insulin, 0.5 mM isobutylmethylxanthine, 1 µM rosiglitazone) was added to initiate differentiation. After 48 hours, the medium was changed to an insulin containing media (DMEM/F12 1:1 + glutamax, penicillin/streptomycin, 5% foetal bovine serum, 5 µg/ mL insulin) which they were maintained on with/without drug treatments for 7 days before use.

Galactose Conditions

A feature of immortalised cells lines is that they readily use glucose for glycolysis and don't exclusively rely on mitochondrial metabolism (Marroquin, Hynes, Dykens, Jamieson, & Will, 2007). In experiments where it was necessary to challenge cells to rely on mitochondrial energy production, cells were cultured in a media composed of: glucose free, pyruvate free DMEM, 10% FBS, 10 mM L-galactose as published (Marroquin et al., 2007).

Total Protein Concentration Determination of Cell Lysates

Total protein concentration of cell lysates was frequently used to normalise *in vitro* assay results or for western blotting. This was performed by colorimetric assay using either BioRad Protein Assay dye or pierce BCA kit following manufacturer's directions. The BioRad method was generally used when cells were lysed in 1 M NaOH at completion of an assay for normalisation. The BCA was used for sample preparation for western blotting as unlike the BioRad method, it is detergent compatible. For the BioRad Protein assay dye method, the stock was diluted 1 in 5 in H_2O. 10 µL of either BSA concentration range of 0 – 1000 µg/mL for a standard curve or sample diluted appropriately such that the signal was within the standard curve range were pipetted into wells of a 96 well microtiter plate. 200 µL of working solution was added to the wells and the microtiter plate was read immediately at 595 nm uisng an iMark bioRad plate reader. Bovine serum albumin (BSA) standards were made using the kit stock and diluted according to kit instructions resulting a standard curve with a BSA concentration range of 0 – 1000 µg/mL. BCA working solution was prepared by mixing reagent A and reagent B 50:1. 25 µL of standard and 25 µL of lysate appropriately diluted to give a

signal within the standard curve range (~1 in 10 dilution was used for most western blot experiments) were pipetted into wells of a 96 well microtiter plate. 200 µL of reagent working solution was added to the wells and the microtiter plate was incubated at 37°C for 30 minutes. Absorbance was then measured on an iMark bioRad plate reader at 570 nm.

2.2.2 Characterisation of Whole Cell Metabolism and Function

Oxygen Consumption Rate by Clark-type Electrode

Cells cultured to ~90% confluence in 10 cm dishes (55 cm^2 area) were trypsinised and pelleted before being resuspended in 1.5 mL of their media which was added to a chamber of a dissolved oxygen electrode (Rank-brothers). Basal oxygen consumption was monitored at 37°C and after approximately 20% of the oxygen in the chamber was consumed. An ATP synthase inhibitor, oligomycin was then added at 2 ug/mL to inhibit ATP dependent oxygen consumption. To obtain maximal respiration, 3 µM FCCP, an inner membrane ionophore that uncouples oxidative phosphorylation from ATP synthesis was used and to completely shut down the electron transport chain, a maximal dose (10 µM) of antimycin A was added and hence non-mitochondrial oxidative metabolism could be obtained. The average slope was taken to obtain % oxygen per second and this was converted to nmole oxygen per minute using constant 100 % air-saturated water = 409 nmol oxygen/mL at 37°C. Cell suspension from the chamber was collected at the end of the run, pelleted and PBS washed 2 times before being lysed in 1 M NaOH. Protein of the lysate was determined using Bio-Rad protein assay (described above) and this was used to normalise oxygen consumption data.

Oxygen Consumption Rate by Seahorse Bioanalyser XF-96

Oxygen consumption rate (OCR) was measured using the Seahorse Bioanalyser XF-96 following the manufacturers protocol. The system uses fluorescent oxygen sensitive probes to measure OCR. Cells were changed to unbuffered DMEM and then 6 baseline measures were taken followed by 4 measures after injection of different drugs. The measurement cycle consisted of a 2 minute mix, 3 minute wait and 2 minute measure.

ATP Levels

Cellular ATP was determined using an ATPlite kit (Perkin Elmer) following manufacturer's protocol. This kit is based on a bioluminescence reaction whereby ATP reacts with D-luciferin, catalysed by luciferase which emits light which is proporational to ATP content. Briefly, cells cultured to 80-90% confluence in a well of a 12 well plate were washed with PBS and then scraped into a 96 well plate well with 50 µL of PBS. Fifty µL of "ATP lysis solution" was added and the plate was shaken at 700 rpm for 5 minutes before adding 50 µL of "ATP substrate solution" and repeating the shake. The plate was dark adapted for 10 minutes and then luminescence was analysed using an omega plate reader at 590 nm emission against a standard curve of ATP (0-50 pmole per well). Some was taken for protein determination using Bio-Rad Protein Assay.

Glucose Uptake

2-Deoxy-Glucose (2-DG) is an analogue of glucose that is taken up by cell the same way as glucose but is not metabolised substantially once it is phosphorylated and is also trapped inside the cell. Hence tracing its uptake into the cell is indicative of glucose uptake. Cells were washed in PBS and incubated in a Krebs-Ringer Buffer for 8 minutes containing 10 µM 2-DG + 0.5µCi/ml ^{3}H 2-DG. At the conclusion of the assay the cells were rapidly washed 3 times in cold PBS and then lysed in 100 µL of 1 M NaOH. Eighty µL of which was added to a scintillation vial containing 6 mL scintillation fluid and counted (Beckman Coulter Tri-Carb) and the remaining 20 µL was used for protein determination using a Bio-Rad protein assay. To correct for background, a well for each sample was performed as above with addition of a glucose transporter inhibitor 20 µM cytochalasin B.

Lactate Determination

Lactate from conditioned cell medium was determined colorimetrically. An L-Lacate standard curve (0 – 5 mM) or appropriately diluted conditioned medium to allow absorbance to fall in the standard curve (note that medium from Rn cells needed to be diluted more than the other samples) was added to 96 wells with a final concentration of 0.4M Hydrazine hydrate pH 9.0, 10mM EDTA, 0.5mM NAD^{+}, 10 µU Lactate

Dehydrogenase (LDH). The increase in absorbance at 340 nm, representing the generation of NADH resulting from the conversion of lactate to pyruvate, was measured until it plateaued, with this timepoint taken as representing complete conversion of lactate. A well containing no sample was used to calculate the background absorbance change and lactate concentration was calculated from the standard curve that was concurrently run.

Fuel Oxidation

Glucose – A solution of low glucose DMEM + 10% FBS and 2 µCi/mL ^{14}C-glucose was added to cells (1 mL to 1 well of a 6 well plate) for 60 minutes to determine the amount of glucose oxidised to CO_2. At the conclusion of the assay 800 µL of media was added 10% perchloric acid in a sealed 20 ml glass scintillation vial. The perchloric acid acidifies the media to release CO_2 and within the vial was a tube with 100 uL of 1M NaOH to sequester CO_2 over a 2 hour period. The solution from the NaOH tube was added to a scintillation vial containing 6 mL scintillation fluid and counted on a beta-counter (Tri-Carb). Cells were PBS washed three times and lysed in 1M NaOH and protein was determined using Bio-Rad protein dye to correct values to protein.

Glutamine – A solution of low glucose DMEM + 10% FBS and 0.75 µCi/mL ^{14}C-glutamine was added to cells (1 mL to 1 well of a 6 well plate) for 60 minutes to determine the amount of glutamine oxidised to CO_2. The amount of labelled CO_2 in the media was determined as described above for glucose. Cells were PBS washed three times and lysed in 1M NaOH and protein was determined using Bio-Rad protein dye to correct values to protein.

Fatty Acids – 1-^{14}C palmitate (0.5 µCi/mL) and cold palmitate (0.5 mM) was conjugated to 2% BSA by incubation for 2 hours at 55°C in DMEM + 10% FBS. The media was cooled to 37°C and then 1 mL was added to wells of a 6 well plate for 60 minutes and then the amount oxidised to CO_2 was measured as described above for glucose. Cells were PBS washed three times and lysed in 1M NaOH and protein was determined using Bio-Rad protein dye to correct values to protein.

Cell Viability

Cell Viability was assessed by multiple methods including AlamarBlue which is a marker of metabolically active cells, crystal violet, a DNA stain which marks cells and propidium iodide, a DNA stain that only penertrates permeable membrane and hence is a marker for dead cells.

AlamarBlue (Resazurin) is a non-fluorescent dye which is converted to the fluorescent product, resorufin, by reduction reactions of metabolically active cells. The amount of resorufin produced is proportional to the number of viable cells which when corrected for cell number gives an indication of cell viability. Cells were cultured in black-walled, low fluorescence 96 well plates. On the day of the assay, cells were given 100 µL fresh media and 10 µL of Alamar blue stain. This was incubated at 37°C, 5 % CO_2 for 4 hours and fluorescence was read at excitation 570-10 nm, emission 590 nm. In chapter 3, cells were PBS washed twice and lysed in 1 M NaOH and the lysate was assayed for protein content using the Bio-Rad assay to correct for cell number.

A crystal violet stain may be advantageous over an AlamarBlue stain when mitochondrial activity is perturbed and could potentially confound resazurin reduction. Cells in 96 well plates were washed gently with 37 °C PBS. 50 uL of 0.5% w/v crystal violet in 50% methanol was added to each well and incubated for 10 minutes at room temperature. Plates were washed by immersion in a large beaker of distilled water. One hundred uL of 1% SDS was added to solubilise the stain and plates were agitated on an orbital shaker until color was uniform with no areas of dense coloration in bottom of wells. Absorbence of each well was determined at 570 nm.

Cells in 96 well plates were incubate in 30 uM propidium iodide at 37°C in a cell culture incubator, in phenol red free medium for 1 hour. Fluorescence was measured at 570 nm excitation and 585 nm emission with signal correlating with dead cells. To obtain a measure of cell death as a percentage of total cells in the well, after the first reading, cells were incubated in 600 uM digitonin at 37°C for 30 minutes and the plate read again. Digitonin is a detergent that permeabilises the plasma membrane hence allowing propidium iodide to enter cells that were alive.

Cell proliferation was assessed using a Roche BrDU incorporation ELISA assay following manufactures instructions. Briefly, cells of 96 well plates were labelled for 2 hours with BrDU which gets incorporated into the DNA of proliferating cells. Cells were then fixed and permeabilised and incubated with anti-BrDU-peroxidase antibody was incubated for 1 hour, washed and substrate solution was added to give colorimetric signal which was read at 370 nm using a spectramax plate reader.

2.2.3 Characterisation of Mitochondrial Stress

Mitochondrial Membrane Potential

JC-1 is a dye that is selectively targeted to the mitochondrial membrane and exists as a monomer which fluoresces green when the membrane is depolarised or an aggregate that fluoresces red when the membrane is polarised and as such, counting cells that fluoresce red or green can be used as an indicator of mitochondrial membrane potential. Cells of a 12 well plate were incubated in 2 µM JC-1 for 10 minutes and rapidly trypsinised in phenol red free trypsin and suspended in phenol red free 10 % FBS DMEM and transferred to a 96 well microtiter plate to be read using a spectramax plate reader. Dual fluorescent readings of were performed at 535/595 and 485/535 excitation/ emission and a ratio of the 2 readings was calculated.

Mitochondrial Superoxide Levels

Mitochondrial superoxide can be detected using the probe mitoSOX Red which is a derivative of *dihydroethidium.* The probe is selectively targeted to the mitochondria and when oxidised by superoxide to 2-OH-MitoE^+, intercalates with DNA to produce red fluorescence, fluorescing maximally at 580 nm. . Cells of a 12 well plate were washed 3 times in FBS free DMEM and then incubated for 45 minutes in a solution of 5µM mitoSOX Red (stock prepared in argon bubbled DMSO) in FBS free DMEM. The probe was washed off in phenol red free DMEM and then phenol red free trypsin-EDTA was added. Cells were suspended in 10% FBS, phenol red free DMEM and transferred to a 96 well microtiter plate and fluorescence was measured at 510/580 nm excitation/emission using a spectramax platereader. Unstained cells were used to measure background autofluorescence and cells incubated with 10 µM antimycin A to

induce mitochondrial superoxide production were used as a positive control. A caveat of using mitoSOX fluorescence as an indicator of mitochondrial superoxide is that with reactions with hydride acceptors, mitoSOX can form a Mito-E^+ which has a similar emission spectrum. These two products can only be distinguished by HPLC (Zielonka, Hardy, & Kalyanaraman, 2009) which was not possible in the following study.

2.2.4 Western Blotting

Sample Preparation

Cells were placed on ice, rapidly washed 3 times in ice cold PBS and lysed in RIPA with protease and phosphatase inhibitors 20 mM NaF, 100 mM activated Na Orthovanadate, 100 µM leupeptin, aprotinin, 1 mM PMSF. At 4°C, lysates were scraped and collected and then sonicated to lyse cells and shear chromosomal DNA on ice. This was performed on ice at 35 H_z, sonicating for 5 seconds, then incubating on ice 15 seconds 3 times. Lysate were spun at 12, 000 g for 12 minutes to pellet debris and sheared DNA. The supernatant was collected and protein determination was performed using a pierce BCA kit (described above) and then samples were prepared in laemli buffer and denatured at 65°C for 15 minutes

SDS- Polyacrylamide Gel Electrophoresis (SDS-PAGE)

For most experiments, samples were run on 10% SDS-PAGE tris-glycine gels in a tris-glycine-SDS at 200 V for ~ 40 minutes. For ATM and phospho-ATM blots, biorad tris-acetate 3-8% gradient gels were electrophoresed in tris-tricine-SDS buffer at 200 V for 60 minutes at room temperature then a further 30-45 minutes at 4 °C.

Transfer, Antibody Probing and Imaging

For most experiments, wet transfer was performed at 4°C with an ice brick for 70 minutes at 100 V onto PVDF membrane in a tris-glycine transfer buffer. For ATM/ phosphor-ATM experiments, transfer was performed at 90 V for 90 minutes at 4°C with an ice brick for 70 minutes at 100 V in a tris-glycine transfer buffer

Membranes were blocked in a solution of 5% (w/v) skim milk powder in TBS for 10 minutes and then incubated in primary antibody solution overnight at 4°C, washed twice in TBS-T and once in TBS and then incubated in a solution containing horseradish peroxidase conjugated secondary antibody for 90 minutes at room temperature. Membranes were washed twice in TBS-T and once in TBS and then incubated in enhanced chemiluminescence reagents and chemiluminescence was imaged using LAS4000 gel doc.

2.2.5 Statistical Analysis

In chapter 3, Md, Mp and Rn were statistically compared with the control (Mm) by one way ANOVA followed by Dunnetts test in order to perform multiple comparisons to the mean without increasing the chance of type 1 errors which can occur with multiple t-tests. All data are presented as mean with error bars representing the standard error of the mean (SEM

2.3 HPLC-MS/MS Based Shotgun Proteomics on Conditioned Media

2.3.1 Characterising the Secretome

Classical protein secretion occurs in specific proteins that have a secretion signal peptide on the N-terminus. These are N-glycosylated in the golgi body and then translocated to the plasma membrane where it fuses and exits (Lord, Ferro-Novick, & Miller, 2013). Previous attempts at characterising secreted proteins have often enriched for N-glycosylated proteins or even performed expression analysis (L. E. Wu et al., 2014). However, it is now known that a substantial amount of proteins can leave the cell through non-classical pathways (Rabouille, 2016). Rather than secretion being regulated by initiation of transcription, translation and subsequent export, proteins secreted through non classical pathways may be functioning in the cell and export can be initiated by cellular stress (Rabouille, 2016). Hence I decided to perform a shotgun, label-free proteomics experiments on all proteins obtained from conditioned medium using the method described below. The workflow is illustrated in Figure 2.2.1.

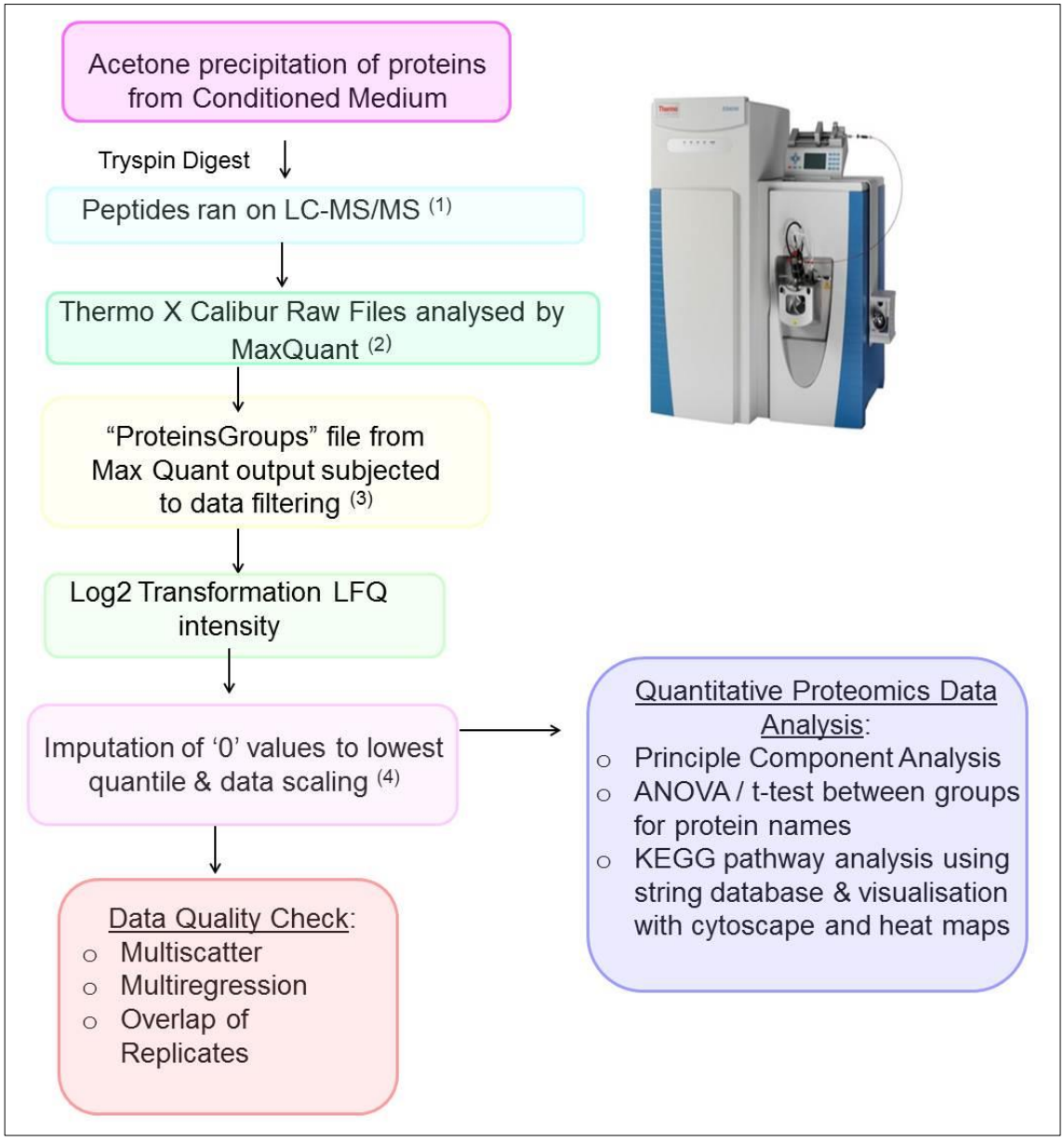

Figure 2.3.0.1 Workflow for Proteomics Experiments (detailed description of steps in subsequent sections)

Acetone precipitation of proteins and subsequent trypsin digest was performed according to section 2.3.2. Peptides were separated by HPLC then their mass analysed using LTQ Orbitrap Velos ETD (Thermo Scientific, US) [(2)]. Raw files were analysed by MaxQuant for interpretation of peptide retention time and mass spectra data and protein identification by FASTA database search [(3)]. ProteinGroups file was read in R and filtered for contaminants, for reverse identification, for modification identification, for proteins only identified by 1 unique peptide and finally for proteins where less than 2 out of 3 or 3 out of 4 replicates were '0' [(3)]. Proteins were $\log_2$ transformed and the lowest quantile of the normal distribution of a sample was used to randomly assign values to those proteins where MaxQuant would otherwise have given a 0 value. In order to calculate a value of the lowest quantile to replace 0 values with, when there

were 2 conditions, the mean of the other condition was used to replace it. When there were 3 conditions, the value was replaced by average of other 2 variables [4]. Data quality was assessed and data was statistically and biologically analysed.

2.3.2 Sample Preparation

To prepare conditioned medium, cells were stringently washed (5 times in PBS then 2 times in serum free medium) then incubated with ETC toxins at the respective doses in serum free medium. Twenty four hours later, conditioned medium was collected and spun at 1,000 g for 10 minutes to pellet any potential cell debris and filtered through a 0.22 µm filter. Samples were snap frozen and stored at -80 C°.

Four volumes of -20°C, HPLC grade acetone was added to conditioned medium, vortexed and incubated at -20°C for 60 mins. The protein pellet was spun down for 10 min at 13,000 g. The supernatant was removed without delay and protein pellets air dried. Protein pellets were suspended in 50mM ammonium bicarbonate pH 8. BCA assay was determined for determination of protein concentration. One hundred µg protein was resuspend in additional 50mM ammonium bicarbonate pH 8.0, along with a final concentration of 2 mM DTT, 6 M guanidine HCl (pH 8.0) and incubated for 45 minutes at 65°C to denature proteins.

Samples were cooled on ice after denaturation and 6 volumes of 50mM ammonium bicarbonate pH 8.0were added to dilute DTT and guanidine HCl. Then 1µg of promega sequencing grade trypsin was added and samples were incubated at 37°C for 16 hours for digestion. Peptides were air-dried using a speed vac concentrator. Samples were stage tipped to remove salt using Thermo C18 stage tips and then suspended in 0.1% formic acid for MS analysis.

2.3.3 Mass Spectrometry

Relative quantitative analysis LC-MS/MS analysis was performed on peptide samples prepared as above using the LTQ Orbitrap Velos ETD (Thermo Scientific, US). Glufib was used as a standard with at least 4 standards being run to clean column before analysis commenced. Blanks and standards were run throughout the mass spec run to monitor performance. These were run on a 30 minute HPLC gradient. Samples were all run on a 90 minute HPLC gradient.

Protein Identification using MaxQuant -

For each individual experiment, Raw thermos files were subjected to MaxQuant to extract peptide masses and retention time and identify proteins using database search proteins. The following MaxQuant parameters were selected under each category:

Modifications and labels:

Trypsin with “up to 2 missed cleavages” were selected for digest conditions

Main search ppm = 6

“Individual mass peptide tolerances was selected”

Maximum number of modifications per peptide = 5

Maximum charge = 7

MS & Sequences:
FTMS mass analyzer = 20 ppm Mass Tolerance with 10 / Top peaks per 100 Da
ITMS mass analyzer = 0.5 Da Mass Tolerance with 6 / Top peaks per 100 Da
TOF mass analyzer = 0.1 Da Mass Tolerance with 10 / Top peaks per 100 Da
Unknown mass analyzer = 0.5 Da Mass Tolerance with 6 / Top peaks per 100 Da
FASTA human or mouse for HEK293 and adipocytes/hepatocytes respectively used for protein identification of sequences

Identification and Quantification
Peptide FDR = 0.01 (false discovery rate = 1%)
Protein FDR = 0.01 (false discovery rate = 1%)
Site FDR = 0.01 (false discovery rate = 1%) and “apply site FDR separately” was selected
Minimum peptides = 1
Minimum razor + unique peptides = 1
Minimum unique peptides = 0 , “second peptides” selected

“use only unmodified peptides” was selected
“discard unmodified counterpart peptides” was selected
Minimum ratio count = 2
Site quantification → “mode” = Use least modified peptides and “Use for occupancies” = Normalized ratios

Miscellaneous
“Re-quantify” selected with “Keep low-scoring versions of identified peptides” unselected
“Label Free Quantification” was selected with “LFQ min. ratio count” = 2 and “Fast LFQ” selected
Match between runs was selected

2.3.3 Data Analysis

"Perseus" is a software package developed for shotgun proteomics data analysis with MaxQuant as companion software. I independently performed data analysis in the R programming language using R studio as an integrated development environment writing and using an original script that was developed by Jessica McKenna (UNSW) which translated Perseus into R. Codes that I used are available in the appendix. ProteinGroups.txt files from MaxQuant output was converted to a csv file and read in R.

Data Filtering –

Firstly, data was filtered for the MaxQuant parameters "only identified by site", "contaminants", "reverse" to ensure data quality. "Contaminants" is assigned to a particular peptide that was found to be part of a commonly occurring contaminant and thus needs to be removed. "Reverse" means that this particular protein group contains no protein, made up of at least 50% of the peptides of the leading protein, with a peptide derived from the reversed part of the decoy database. "Only identified by site" means a particular protein group was identified only by a modification site making it unreliable hence desirable to remove from data. Data was then filtered to remove proteins only identified by 1 unique peptide. This is a common cut off used in label free analysis as having 2 unique peptides to identify a protein increases confidence that a protein is genuinely present. A final filtering step was performed to remove proteins where less than 2 out of 3 or 3 out of 4 replicates were '0'.

Data Transformation –

After filtering, LFQ Intensity values were Log_2 transformed to get LFQ intensity values in a workable format. Since the log of 0 is an undefined number with R output being 'infinity' at this stage of the analysis, the infinity values were marked with 'NA'. The next step of data processing involves imputing '0' values, whereby 'NA' values are replaced with a value obtained from the lowest quantile. The rationale behind this is based upon the understanding that mass spectrometry works on a threshold basis and so when a "top 10" is run (see MaxQuant parameters), it means that only the top 10 peptides are analysed at a time. Hence any peptide not in the top 10 will be assigned a value of 0. Therefore a value of 0 doesn't mean that the peptide is not present but rather

that it is not in the top 10. Therefore, the lowest quantile of the normal distribution was used as a value to randomly assign values to these proteins where MaxQuant would otherwise have given a 0 value. In order to calculate a value of the lowest quantile to replace 0 values with, for 3 conditions. In order to calculate a value of the lowest quantile to replace 0 values with, for analyses with 3 conditions, the mean of the other 2 conditions was used to scale a condition. When there were 2 conditions the mean of the other condition was used to scale that condition.

Checking LFQ Intensity Data Quality –

After data transformation above, data quality was assessed by plotting transformed LFQ Intensity values against each other as a multiscatter graph and calculating Pearson's correlation coefficient to assess how tightly samples were correlated within an experiment. Frequency distribution of transformed LFQ Intensity values for individual replicates were graphed and merged to analyse how well they superimposed for replicate reproducibility. Additionally replicate reproducibility was assessed by overlap analysis of protein IDs detected in replicates of each experimental group.

Proteomics Analysis –

ANOVA was used for 3 variable analyses (vehicle, low dose and high dose) to obtain pvalue or a two-sided unpaired t-test assuming unequal variances were used for 2 variable analysis to obtain pvalue. A Benjamini-Hochberg correction analysis used to obtain false discovery rate (FDR) values. For visualisation, principle component analysis (PCA) and abundance heat maps were used. For biological interpretation, Protein IDs were exported to string database (www.string-db.org) using "high confidence (0.7) for the minimum required interaction score and only selecting experiments and databases parameters for active interaction sources. From here string networks were exported and KEGG pathway enrichment analysis was performed.

CHAPTER 3: INVESTIGATION OF INTRACELLULAR COMMUNICATION AND ADAPTATIONS TO ELECTRON TRANSPORT CHAIN STRESS REVEALS A ROLE FOR ATM KINASE AS A MITOCHONDRIAL STRESS RESPONSE

3.1 Introduction

Mitochondria are major energy producing organelles of eukaryotic cells and mitochondrial stress is associated with pathological states such as neurodegeneration (Golpich et al., 2017; Hu & Wang, 2016), cardiometabolic diseases (Ashrafian, Frenneaux, & Opie, 2007; Befroy et al., 2007; Brownlee, 2005) and ageing (Castro Mdel et al., 2012; Chaudhary, El-Sikhry, & Seubert, 2011; J. H. Huang & Hood, 2009). As highlighted in section 1.2, organelle stress in the mitochondrion includes reactive oxygen species (ROS), genotoxic stress and proteotoxic stress which may occur through free radical leak as a by-product of ETC function, mtDNA damage and mutations and perturbed mitochondrial proteostasis. Given that mitochondria have an extremely important function and are inherently stress prone, we hypothesise that there must be homeostatic mechanisms in place to mitigate this stress (Barbour & Turner, 2014; Chandel, 2015; Quiros et al., 2016). There has been some recent research attention towards mitochondrial quality control and retrograde signaling, but much of the work has been performed on lower organisms and there has been relatively little work in mammalian cells.

To date, major chemical signals which participate in retrograde signaling events include reactive oxygen species (ROS), adenosine monophosphate (AMP), nicotinamide adenine dinucleotide (NAD^+) and calcium fluxes. These initiate cell signaling events including mitochondrial biogenesis, antioxidant defences, mitochondrial unfolded protein response (mtUPR), phosphorylation of AMP activated kinase (AMPK), sirtuin activation and mitophagy, which are all considered major ways in which cells may offset mitochondrial stress and maintain mitochondrial homeostasis and bioenergetic

function (Butow & Avadhani, 2004). Loss of these processes is linked with complex diseases and the ageing process as outlined in detail in secretion 1.4.

Importantly, there is evidence that sublethal mitochondrial stress, through initiation of some of these responses can promote resistance to further stress and increase healthspan (Ristow & Schmeisser, 2014). While exciting, these responses have mostly been demonstrated in *C.elegans* and *Drosophila*. It is currently unclear whether such mechanisms are physiologically important in mammalian cells and are induced by pharmacological treatments as well genetic approaches. Another issue in this area is that most of the literature looking at mammalian responses to mitochondrial stress have used acute, high doses of ETC inhibitors which would not accurately mimic the physiologically relevant stresses normally endured by mitochondria with ageing and in complex diseases.

The aim of the present study was to explore some of these adaptations in a mammalian model of chronic mitochondrial stress. Given that the overarching hypothesis of this thesis recognises that aberrant coordination of mitochondrial and nuclear genomes can induce mitochondrial stress, while appropriate coordination of the two genomes is essential for adaptation to mitochondrial stress, we employed a model whereby discordance between nuclear and mitochondrial genomes resulted in a progressive level of mitochondrial stress and dysfunction. Cytoplasmic hybrid cells (cybrid cells) are a model whereby mtDNA depleted cells (Rho0 cells) as a nuclear donor are fused with enucleated cells with intact mtDNA as mtDNA donor cells (Wilkins, Carl, & Swerdlow, 2014). The result is cells with a consistent nuclear genome and varied mitochondrial genomes (Wilkins et al., 2014). The cybrid models used in this chapter were first published in 2003 (McKenzie et al., 2003). They all have a Mus musculus nuclear background with mitochondrial genomes of Mus musculus (Mm), the slightly more divergent mouse strain Mus dunni (Md), more divergent mouse strain Mus parhari (Mp) and the rat strain Rattus norvetigus (Rn) (McKenzie et al., 2003). The Mm cells act as a control and with evolutionary divergence between the nuclear and mitochondrial genomes with more divergent rodent strains there is a mismatch of electron transport complex protein subunits and a corresponding ETC defect (McKenzie et al., 2003).

3.2 Results

3.2.1 – Characterisation of Oxidative Metabolism and Mitochondrial Stress with ETC Dysfunction

The cybrid cell models used in this chapter were previously characterised in terms of their ETC biochemistry (McKenzie et al., 2003). I first aimed to characterise the whole cell oxidative metabolism and other parameters of mitochondrial stress.

Basal OCR was decreased by 39%, 61% and 73% for Md, Mp and Rn respectively compared with Mm, indicative of a graded decrease in bioenergetic capacity (Fig 3.2.1). This indicates that the cells had reduced whole cell respiration with increased evolutionary mtDNA divergence (Figure 3.2.1). While respiration of both the Mm and Md cells were increased in response to FCCP, the Mp and Rn cells did not display an increase in OCR in response to FCCP (Figure 3.2.1), indicating limited spare respiratory capacity.

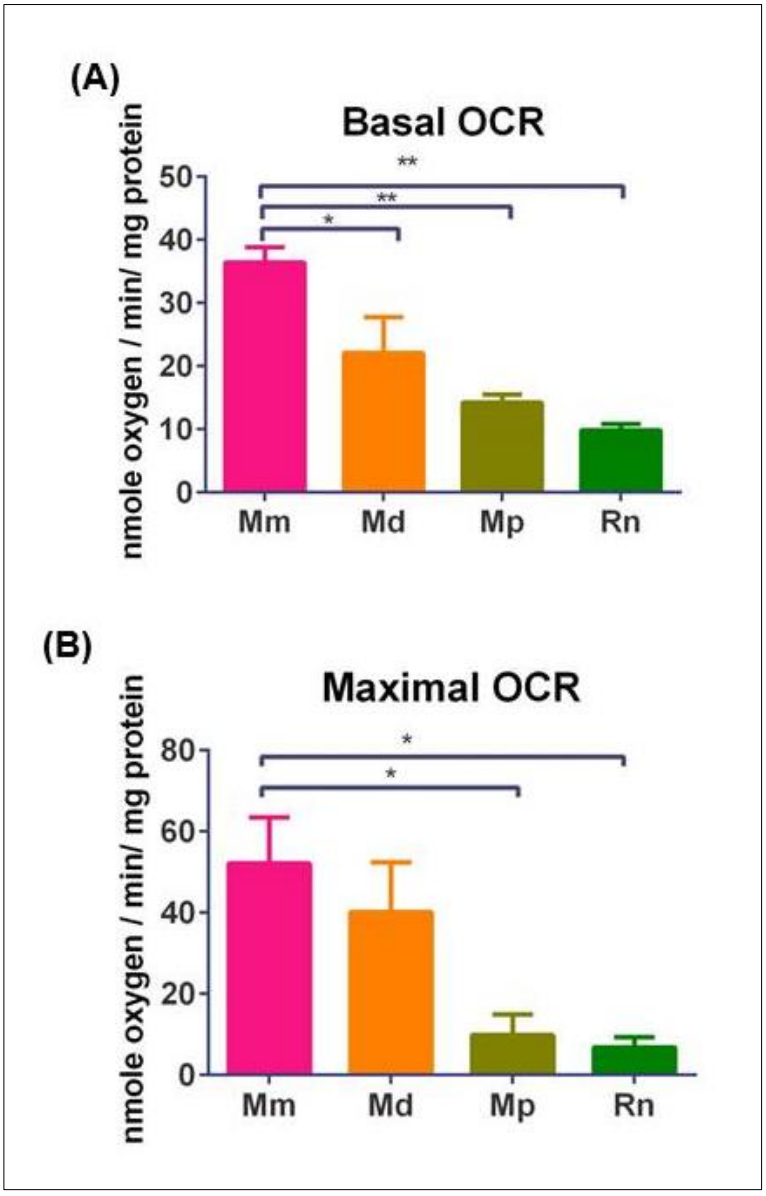

Figure 3.2.1 Characterisation of Whole Cell Respiration in Cybrid Cells

Oxygen Consumption Rate (OCR) was measured in a Clark-type electrode in the basal state (A) and stimulated with OXPHOS uncoupler 4µM FCCP to drive maximal respiration (B). A confluent 10 cm dish of cells were trypsinised and then resuspended in 2 mL of culture media and added to chamber of Rank-Brothers oxygen electrode. The experiment was performed 3 independent times and data is expressed as mean with error bars representing standard error of the mean (SEM). An ANOVA followed by Dunnett test for multiple comparisons to the mean was performed with * representing $p < 0.05$ and ** representing $p < 0.01$, n=3.

Radiotracer assays for oxidation of different fuels were then employed to look more specifically at metabolism of different substrates that are utilised for cellular respiration (Figure 3.2.2). All of the cells oxidised roughly twice as much glutamine as glucose (Figure 3.2.2), which suggests that the main fuel for respiration of these cells is glutamine. Rn cells had half the glutamine oxidation rate as the Mm cells (Figure 3.2.2) which is consistent with the strong OCR defect (Figure 3.2.1). Surprisingly, Rn cells showed no significant defect in glucose oxidation (Figure 3.2.1). Mp cells did not display reduced oxidation of exogenous fuel substrates (Figure 3.2.2), despite the strong OCR phenotype (Figure 3.2.1). Palmitate oxidation was also reduced by about half in Rn cells but not significantly changed in Mp or Md cells. The overall rate of palmitate oxidation to CO_2 was ~10% and ~5 % of the rate for glucose and glutamine respectively, indicating that fatty acids only contribute a minor proportion to cellular respiration in these cell lines.

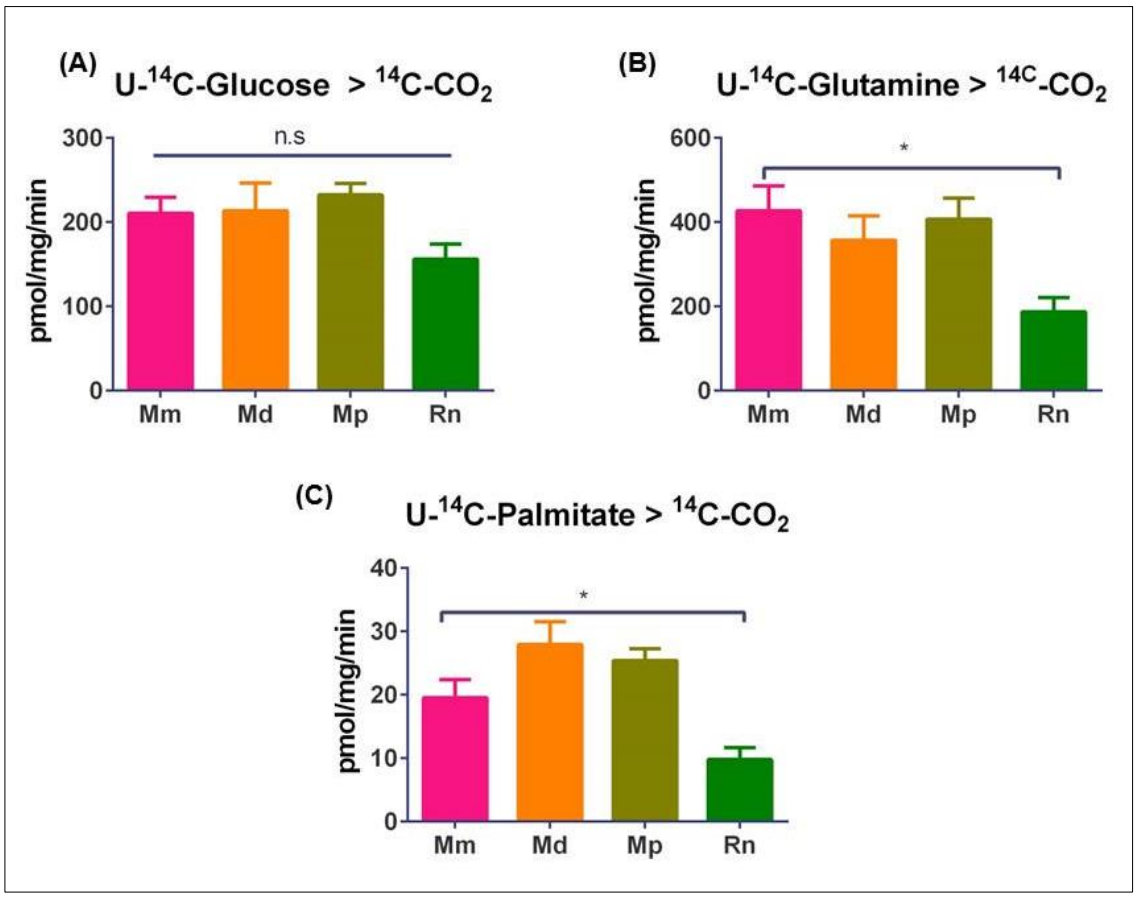

Figure 3.2.2 Fuel Utilisation in Cybrid Cells

Radiolabelled (U-^{14}C) glucose (A), (U-^{14}C) glutamine (B) and (1-^{14}C) palmitate (C) were traced into CO_2 production to measure fuel oxidation. $^{14}CO_2$ was measured using a Beckman Coulter β-counter following sequestration of CO_2. Data are presented as mean with +/- error bars representing standard error of the mean (SEM). An ANOVA followed by Dunnett test for multiple comparisons to the mean was performed with * representing $p < 0.05$ and ** representing $p < 0.01$, n =4.

It was apparent that the Mp and more particularly Rn cells displayed a strong defect in terms of whole cell oxidative capacity. I next characterised other parameters of mitochondrial stress and function, including ROS and mitochondrial membrane potential.

Mitochondrial membrane potential was measured using the stain JC-1 which accumulates in the inner mitochondrial membrane and has a different fluorescence pattern depending on whether it is an aggregate or monomer which depends on mitochondrial membrane potential. The OXPHOS uncoupler FCCP was used as a positive control as it depolarizes mitochondrial membrane. It is a caveat of JC-1 stain that it tends to accumulate more aggregate with time even in healthy cells and as a result it was difficult to distinguish between polarized and depolarized. There was however a trend towards more mitochondrial membrane depolarization with increased evolutionary divergence between mitochondrial and nuclear genomes. More importantly, Mp and Rn cells had similar levels to that of the FCCP positive control which indicates that they possess mitochondrial with low membrane potential. TMRM may have been a more useful stain to use. There was a trend for increased mitochondrial superoxide production with evolutionary divergence (Figure 3.2.3 B) but these levels were much lower than that seen with an acute, high dose treatment with complex III inhibitor, antimycin A which was used as a positive control.

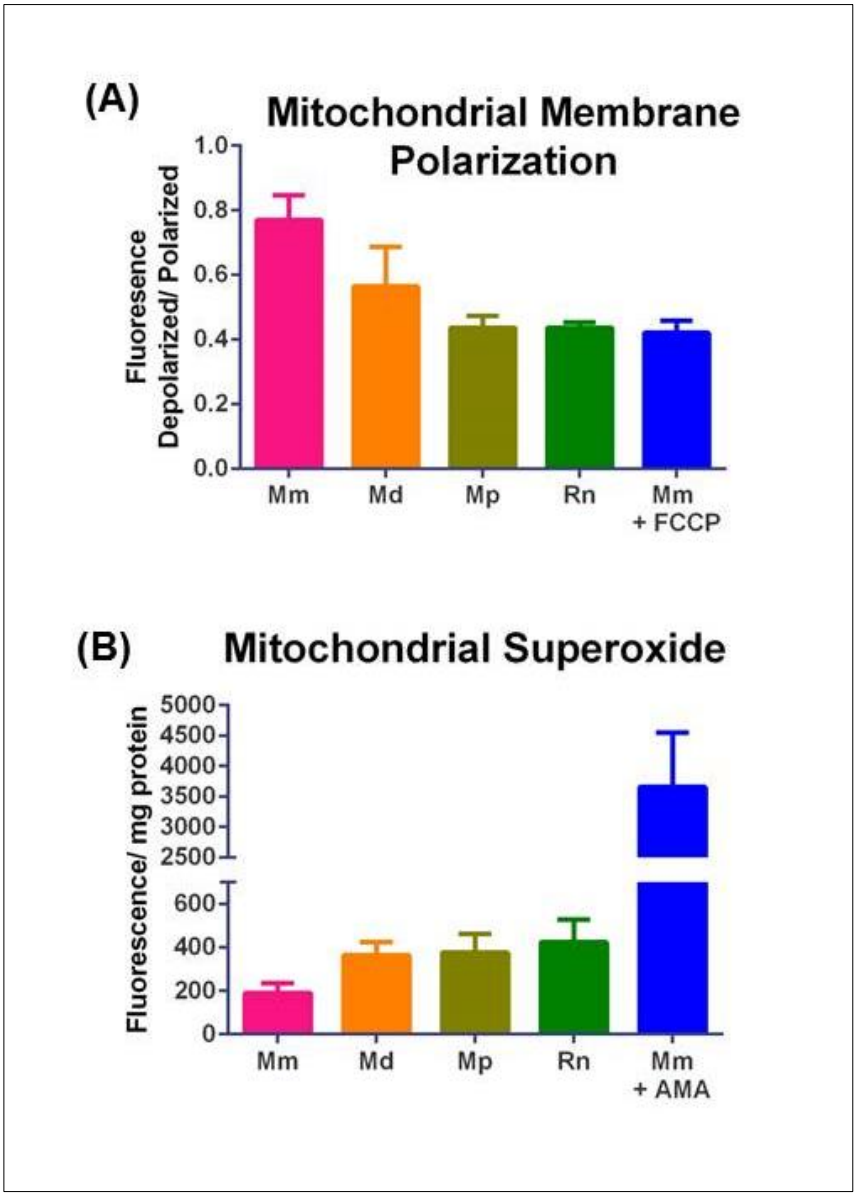

Figure 3.2.3 Non-ETC Parameters of Mitochondrial Stress

Mitochondrial membrane potential (A), Superoxide (B) were measured using fluorescent probes. Membrane potential (n=4) (A) was measured by incubating cells in 2 µM JC-1 for 10 minutes in phenol red-free, FBS-free DMEM. FCCP was used as a positive control. Cells were quickly washed, collected and transferred to black-walled 96 well plate. Fluorescence was measured using excitation and emission in a spectramax plate reader. Superoxide (n=3) (B) was measured by incubating cells in 5 µM MitoSox probe in phenol red-free, FBS-free DMEM, and then the cells were washed, collected and transferred to black-walled 96 well plate. Fluorescence was measured using excitation and emission in a spectramax plate reader. 10 µM antimycin A (AMA) was used as a positive control. Data are presented as mean with +/- error bars representing standard error of the mean (SEM).

Results from Figures 3.2.1 – 3.2.3 collectively highlight that Mp, and more strongly, Rn cells both had substantial metabolic defects and signs of mitochondrial stress. However, they visibly appeared healthy and proliferated normally. For this reason, I directly measured cell viability, proliferation and ATP and found no significant changes (Figure 3.2.4).

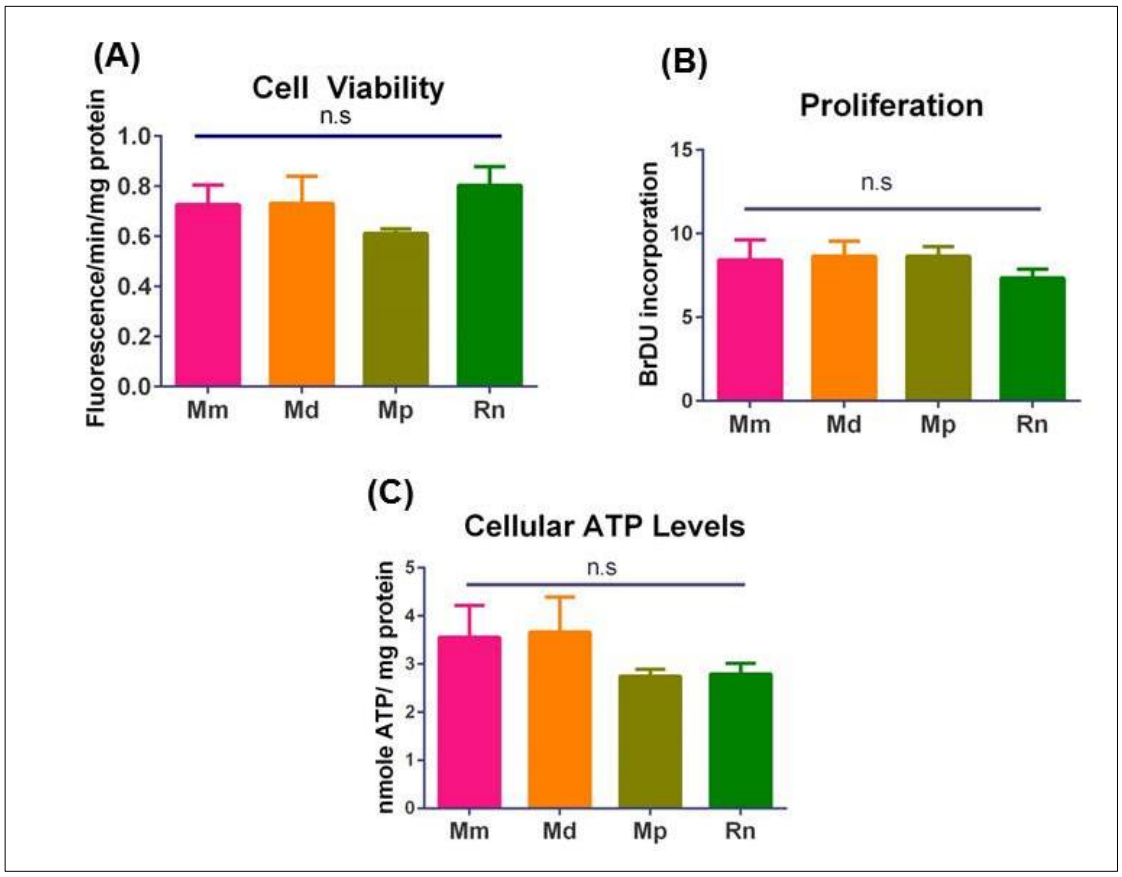

Figure 3.2.4 Viability of Cybrid Cells

Cell viability was measured by Alamar Blue (A), Proliferation measured by BrDU ELISA (B), ATP measured by luminescence based assay (PerkinElmer ATPlite) (C). Data are presented as mean with +/- error bars representing standard error of the mean (SEM). An ANOVA followed by Dunnett test for multiple comparisons to the mean was performed with n.s meaning non-significant

3.2.2 – Metabolic Reprogramming

The cells had a strong bioenergetic and mitochondrial stress phenotype but despite this, they maintained viability, proliferation and ATP (section 3.2.1). I hypothesised that anaerobic glycolysis was responsible for maintaining cellular fitness with the large metabolic defect. I measured glucose uptake and lactate accumulation in media which are indicators of anaerobic glycolysis (Figure 3.2.5).

The rate of glucose uptake was increased roughly 3 fold in Mp and Rn cells (Figure 3.2.5 A). Accumulation of lactate in the media conditioned from Mp and Rn cells was increased compared with that of Mm cells while there were no changes in Md cells (Figure 3.2.5 B). Collectively, these data suggest that Mp and Rn cells are mores glycolytic than Mm and Md cells.

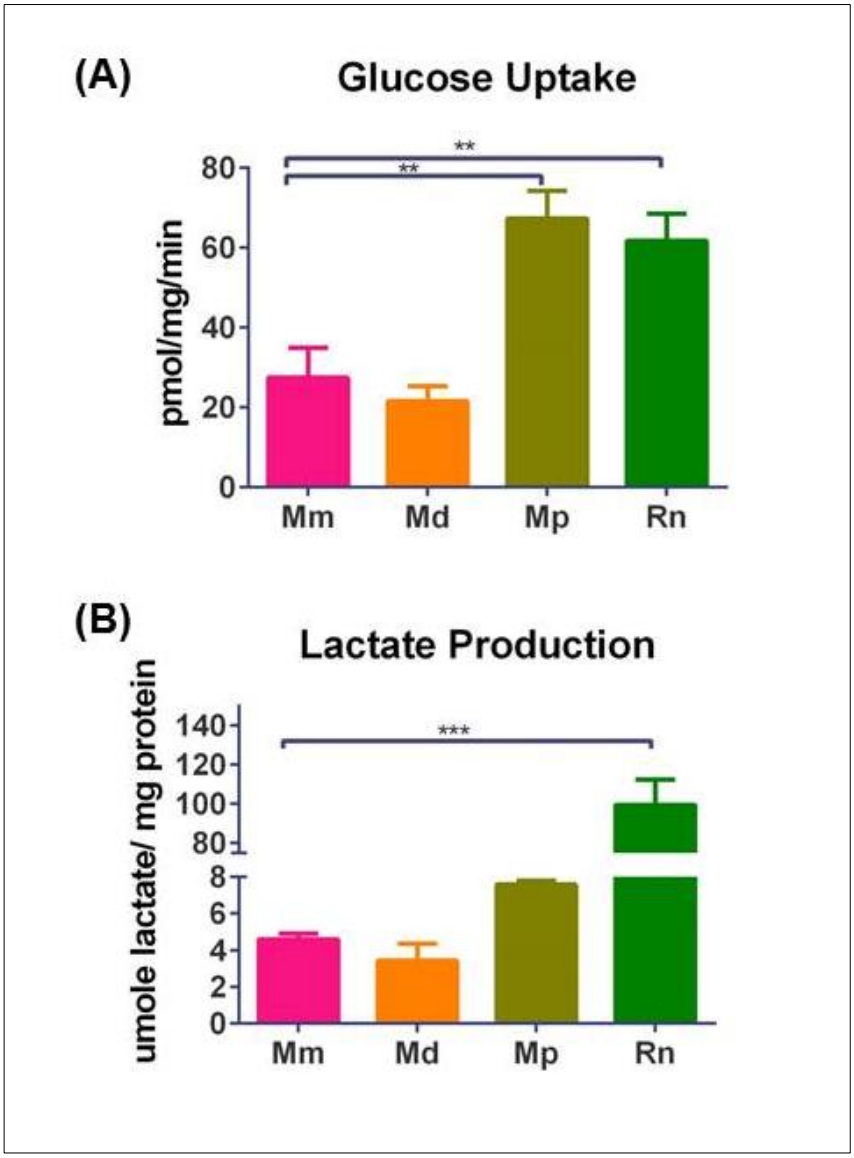

Figure 3.2.5 Markers of Glycolysis in Cybrid Cells

Glucose uptake was measured by tracing cellular uptake of ^{3}H-2-Deoxy-glucose (2DG) n = 4 (A). Lactate accumulation in culture media was measured by colorimetric assay (n=3) (B). Data are presented as mean with +/- error bars representing standard error of the mean (SEM). An ANOVA followed by Dunnett test for multiple comparisons to the mean was performed with * representing $p < 0.05$ and ** representing $p < 0.01$.

As noted earlier, Rn cells did not display reduced glucose oxidation, and glutamine was the main fuel used for oxidation (Figure 3.2.2). This led me to hypothesise that much of the glucose being oxidised by the cells may be being oxidised in the pentose phosphate pathway (PPP) rather than conversion to pyruvate for entry into mitochondria and oxidative phosphorylation (OXPHOS). This notion was supported by an increase in incorporation of glucose-derived carbons into nucleic acids and lipids, both endpoints of the PPP (Figure 3.2.6A&B)The glucose oxidation experiment in Figure 3.2.2 A was performed using uniformly labelled glucose. Carbon-1-glucose (C1-glucose) is oxidised by the PPP or TCA cycle, whereas carbon-6-glucose (C6-glucose) is exclusively oxidised in the TCA cycle. A pilot study with glucose tracers that were ^{14}C labelled at either C1 or C6 was used to investigate whether the glucose was being oxidised in the PPP or TCA cycle (Figure 3.2.6 C and 3.2.3 D). C1-glucose oxidation was higher in Rn cells than Mm cell (Figure 3.2.6 C) but C6-glucose oxidation was lower in Rn cells compared with Mm cells (Figure 3.2.6 D). From this data, I speculate that Rn cells have less glucose utilisation linked with OXPHOS but greater glucose utilisation linked with PPP flux compared with Mm cells, and this may explain why there is no obvious decrease in oxidation of uniformly labelled glucose. Unfortunately the experiment was not repeated due to unavailability of more tracers.

As an alternative measure, I used DHEA, an inhibitor of glucose-6-phosphate dehydrogenase (G6PD) which is the rate limiting enzymes of the PPP and performed a uniformly labelled glucose oxidation assay. Inhibition of G6PD by DHEA reduced glucose oxidation by roughly 40% (Figure 3.2.6 E). This indicates that almost half of the oxidised glucose is due to flux through the PPP in both Mm and Rn cells. I was unable to differentiate differences between Mm and Rn in the percentage of glucose oxidation with and without DHEA but this may be because it was a very crude way of assessing PPP linked glucose oxidation.

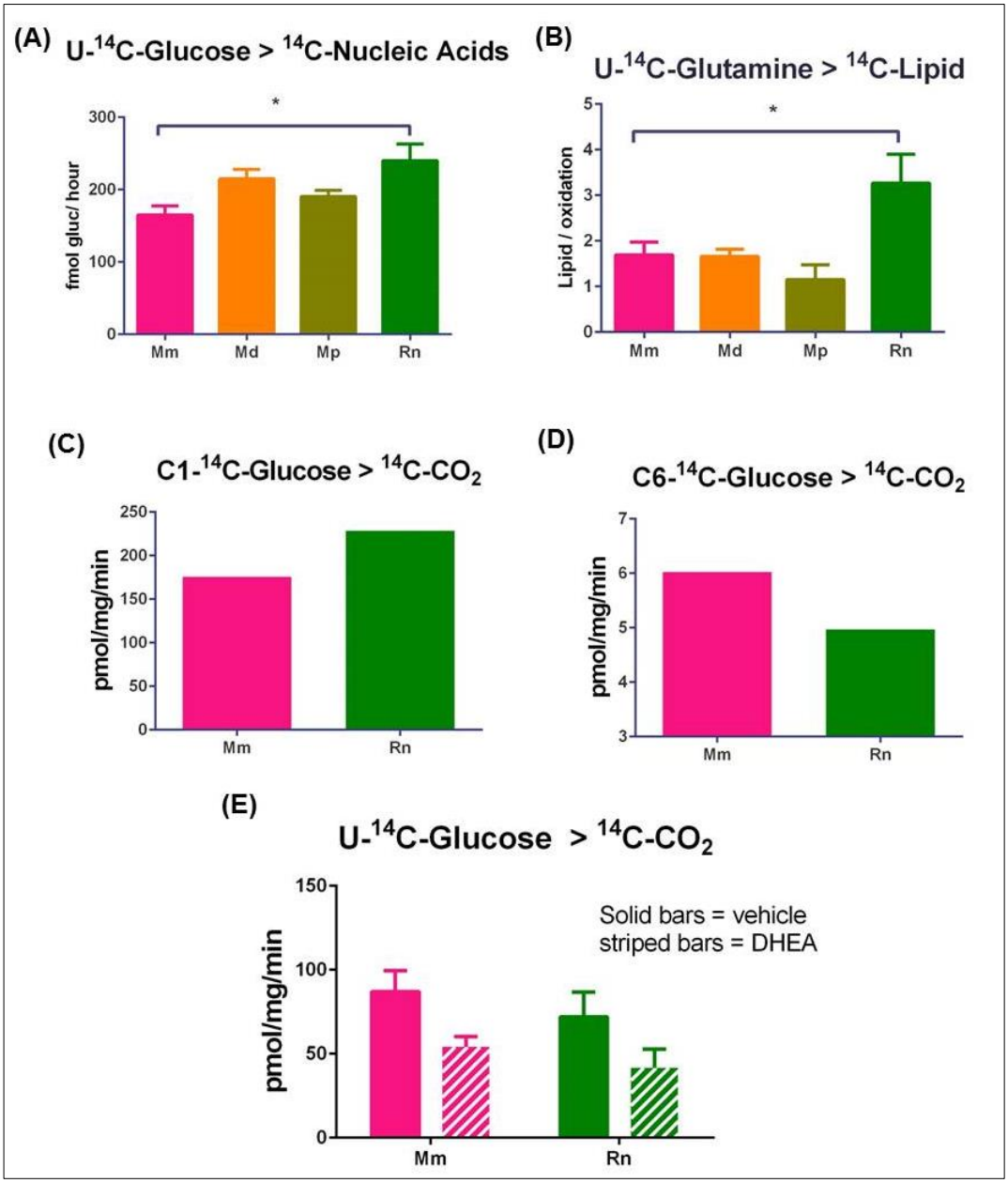

Figure 3.2.6 Metabolic Reprogramming in Cybrid Cells

Glucose incorporation into nucleic acids (A) and glutamine incoproation into lipid (B) determined by radiotracer methods n = 4 An ANOVA followed by Dunnett test for multiple comparisons to the mean was performed with * representing $p < 0.05$ and ** representing $p < 0.01$. (C) and (D) are glucose oxidation assays using carbon1 and crabon6 labelled radiotracers n=1. (E) Uniformly labelled glucose oxidation assay treated with vehicle or DHEA (n=4)

3.2.4 No Major Changes in Mitochondrial Unfolded Protein Response Proteins

Given that the mismatch of genomes may has resulted in ETC complex misassembly (McKenzie et al., 2003), I hypothesised that these cells may have engaged a mitochondrial unfolded protein response (mtUPR) to mitigate conformational protein stress. Accordingly, the protein expression of the heat shock protein Hsp60 and the protease ClpP, two documented markers of the mtUPR, were assessed. The levels of Hsp60 not significantly changed across the 4 groups although there was a tendency for the expression of ClpP to be higher in Mp cells.

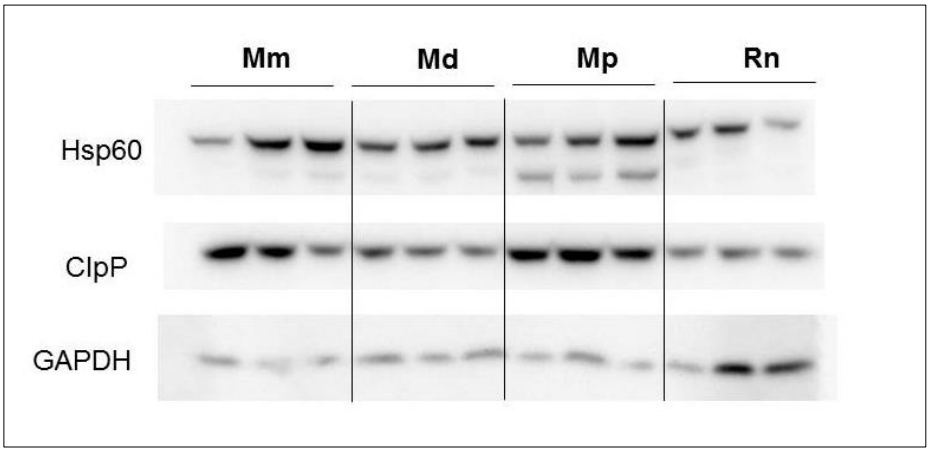

Figure 3.2.7 mtUPR markers in the cybrid

Mm, Md, Mp and Rn cells were seeded and cultured for 24 hours, lysates were collected and subjected to western blot being probed with the indicated primary antibody. Membranes were incubated in a horseradish peroxidase conjugated secondary antibody and subjected to chemiluminescence which was imaged using a LAS4000 gel doc. 14-3-3 used as a loading control. Pixel intensity was analysed in image J (n=4).

3.2.5 Galactose Culturing Conditions

Because of the limited changes in stress responses and the evidence of metabolic reprogramming (Figure 3.2.5 and Figure 3.2.6), it was plausible that mitochondrial stress was being 'masked' by the cell's ability to upregulate glycolysis, and this may explain why there were no changes in viability, proliferation, ATP and mtUPR. In an attempt to unmask a dysfunctional mitochondrial phenotype, I employed glucose and pyruvate free, galactose supplemented culture conditions (galactose conditions). This sugar produces no net ATP during its conversion to pyruvate, meaning that cells rely on mitochondrial oxidation for ATP (Marroquin et al., 2007). By manual cell counts, I found that the population doubling time of Mp and Rn cells were both roughly half when cultured in galactose rather than in glucose conditions. Following this observation, I performed side-by-side cell viability and ATP assays in cybrid cells cultured in either glucose and galactose conditions (Figure 3.2.8).

There was a trend for a slight improvement in cell viability galactose for Mm cells compared with glucose culturing conditions but not for Md, Mp or Rn cells. There was a trend for a decrease in cellular ATP levels in galactose compared with glucose culture conditions for Md and Rn cells (Figure 3.2.8) indicating that they do have reduced ATP levels when they cannot undergo glycolysis. Note that this is even after normalising for protein so the decrease in cell number was corrected for. By manual cell counts, proliferation of Mp and Rn cells were strongly compromised in galactose but there was interestingly a trend for proliferation to be slightly increased in galactose compared with glucose media in Mm and Md cells.

Collectively these data support the idea that glycolytic metabolism is an important adaptation to maintain proliferation, viability and ATP. I then aimed to investigate whether there were any signaling changes accompanying the ETC stress phenotype in glucose and galactose culturing conditions.

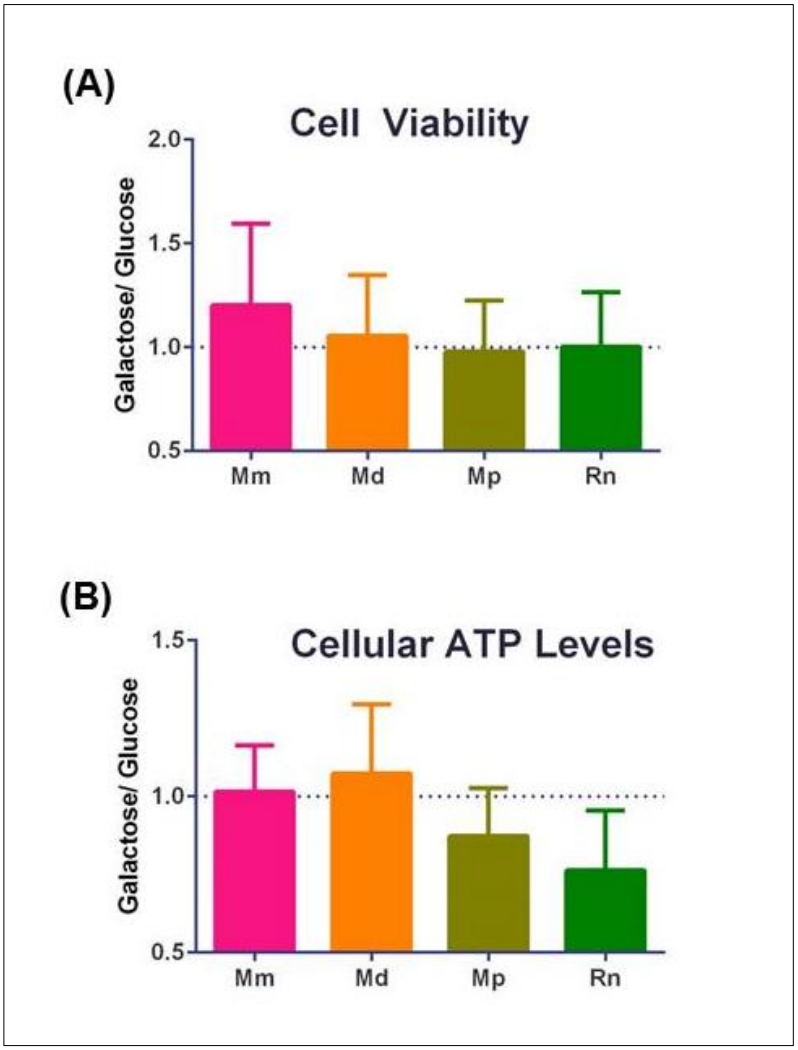

Figure 3.2.8 Cell Viability and ATP in Glucose and Galactose Culture Conditions

(A) cell viability using AlamarBlue (B) ATP using Perkin Elmer ATP lite kit.
Data are presented as mean with +/- error bars representing standard error of the mean (SEM).

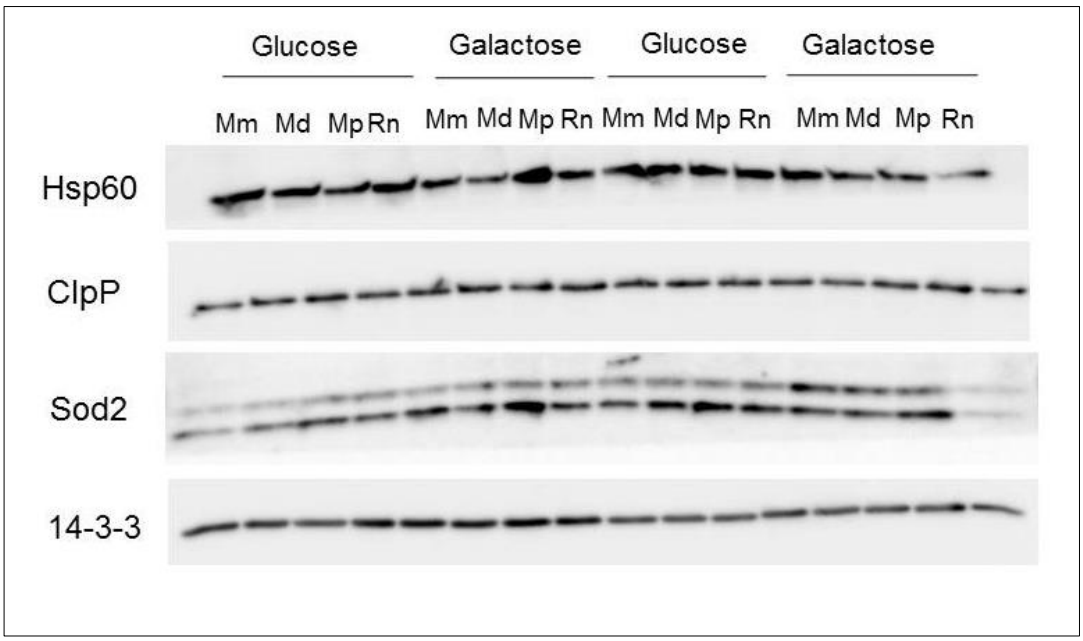

Figure 3.2.9 mtUPR signaling in glucose and galactose culturing conditions

Mm, Md, Mp and Rn cells were seeded and cultured in the appropriate media for 24 hours, lysates were collected and subjected to western blot being probed with the indicated primary antibody. Membranes were incubated in a horseradish peroxidase conjugated secondary antibody and subjected to chemiluminescence which was imaged using a LAS4000 gel doc. 14-3-3 used as a loading control. Pixel intensity was analysed in image J (n=6).

3.2.4 Investigation of Pro-Survival Kinase Signaling as a Mitochondrial Stress Response

After no significant changes in major mitochondrial mtUPR markers or the expression of a major mitochondrial antioxidant protein, I investigated other signaling events that may accompany the metabolic reprogramming to rescue the phenotype of these bioenergetically compromised cells. The results in section 3.2.5 indicate that metabolic reprogramming is a major way in which cells adapt to ETC defects to maintain proliferation and viability. Hence I wanted to explore signaling pathways that are known to be regulated metabolically. I first measured activation of AMP kinase (AMPK) signaling, expecting that alterations in adenine nucleotide levels may lead to phosphorylation of AMPK.

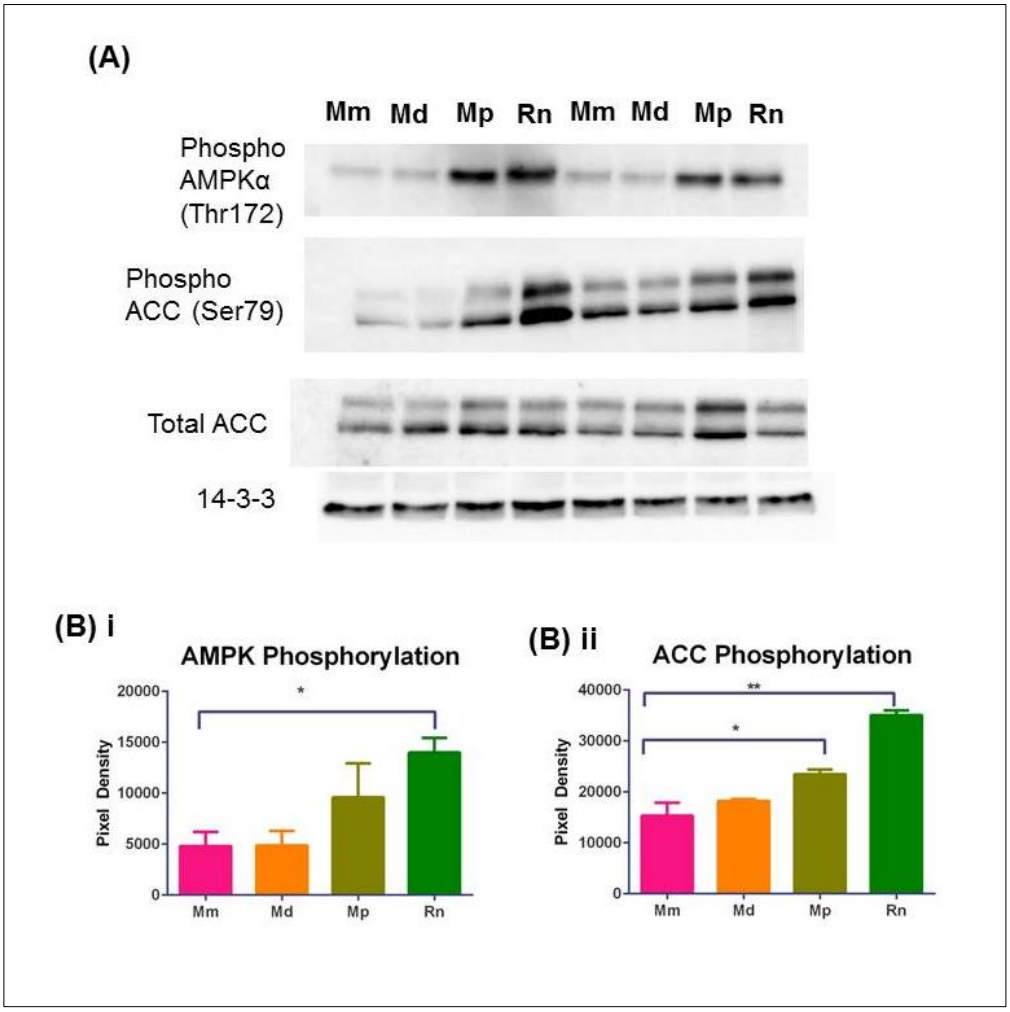

Figure 3.2.10 AMPK Signaling in Cybrid Cells

Mm, Md, Mp and Rn cells were seeded and 24 hours later, lysates were collected and subjected to western blot being probed with the indicated primary antibody. Membranes were incubated in a horseradish peroxidase conjugated secondary antibody and subjected to chemiluminescence which was imaged using a LAS4000 gel doc. 14-3-3 used as a loading control. Pixel density quantification (n=4) (B) of i AMPK phosphorylation and ii ACC phosphorylation. Densitometry data is expressed at mean +/- SEM and an ANOVA followed by Dunnett test for multiple comparisons to the mean was performed $p < 0.01$.

The phosphorylation of AMPKα at threonine 172 was markedly increased, indicating activation of this energy sensing kinase. Phosphorylation of its downstream target acetyl-CoA carboxylase (ACC) at serine 79 was also increased in both Mp and Rn cells. These phosphorylation results are indicative of active AMPK signaling cascades. In addition to phosphorylation of AMPK activation I wanted to explore Protein kinase B (Akt) activation. Akt is a critical pro-survival kinase and it was found that inhibition of both Complex I and the mitochondrial pyruvate carrier results in activation of Akt signaling (Trefely et al., 2015) which indicates mitochondrial signaling may be important for Akt activation. Further, Complex I inhibitor rotenone has been shown to activate Akt signaling (Connor et al., 2005). I explored Akt signaling by western blot of Akt phosphorylation along with that of downstream targets (Figure 3.2.11).

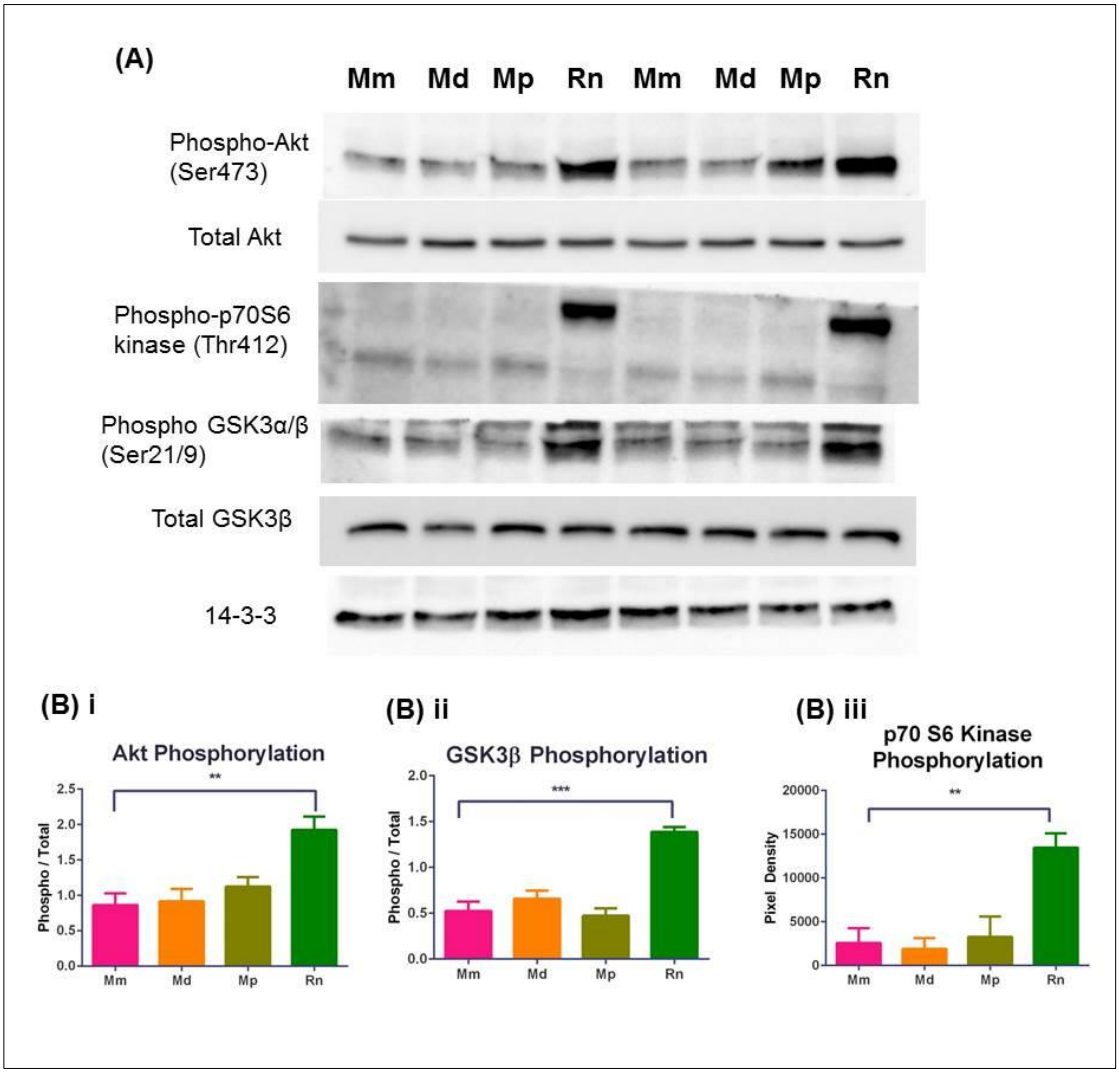

Figure 3.2.11 Akt Signaling in Cybrid Cells

Respresentative images (A) of Mm, Md, Mp and Rn cells were seeded and 24 hours later, lysates were collected and subjected to western blot being probed with the indicated primary antibody. Membranes were incubated in a horseradish peroxidase conjugated secondary antibody and subjected to chemiluminescence which was imaged using a LAS4000 gel doc. 14-3-3 was used as a loading control. Pixel density quantification (n=4). (B) of i Akt phosphorylation, ii GSK3B phosphorylation and iii p70 S6 Kinase phosphorylation. Densitometry data is expressed at mean +/- SEM and an ANOVA followed by Dunnett test for multiple comparisons to the mean was performed **P<0.01, ***P<0.001.

In contrast to AMPK signaling which was only activated in both Mp and Rn cells, Akt was phosphorylation only increased in Rn cells. Phosphorylation of downstream targets p70 S6 kinase and GSK3β was also selectively increased in Rn cells, confirming that Akt signaling is engaged with mitochondrial dysfunction in this cell line.

3.2.6 ATM Kinase Activity is required for Adaptations of Rn Cells

Ataxia Telangiectasia Mutated kinase (ATM) is a kinase that is known to phosphorylate both Akt (Halaby, Hibma, He, & Yang, 2008; Viniegra et al., 2005) and AMPK (Y. Sun, Connors, & Yang, 2007) and be activated by ROS (Z. Guo, Kozlov, Lavin, Person, & Paull, 2010), making it a plausible candidate to be upstream of Akt and AMPK in Rn cells. ATM is best known for its nuclear role in the DNA damage response (Awasthi, Foiani, & Kumar, 2015) but intriguingly there is a cytosolic pool that has functions in molecular metabolism including activation of glycolysis (T. Tanaka, Kurose, Halicka, Traganos, & Darzynkiewicz, 2006) and the PPP (Cosentino, Grieco, & Costanzo, 2011). Given that glycolysis was an important adaptation in Rn cell and Rn cells may have more flux through the PPP, there was motivation to explore ATM kinase as a potential adaptation to mitochondrial stress through AMPK and Akt signaling and metabolic reprogramming. Hence I employed the selective ATM inhibitor, KU-55933 to see if treatment with this compound ablated the cell signaling observed with ETC stress.

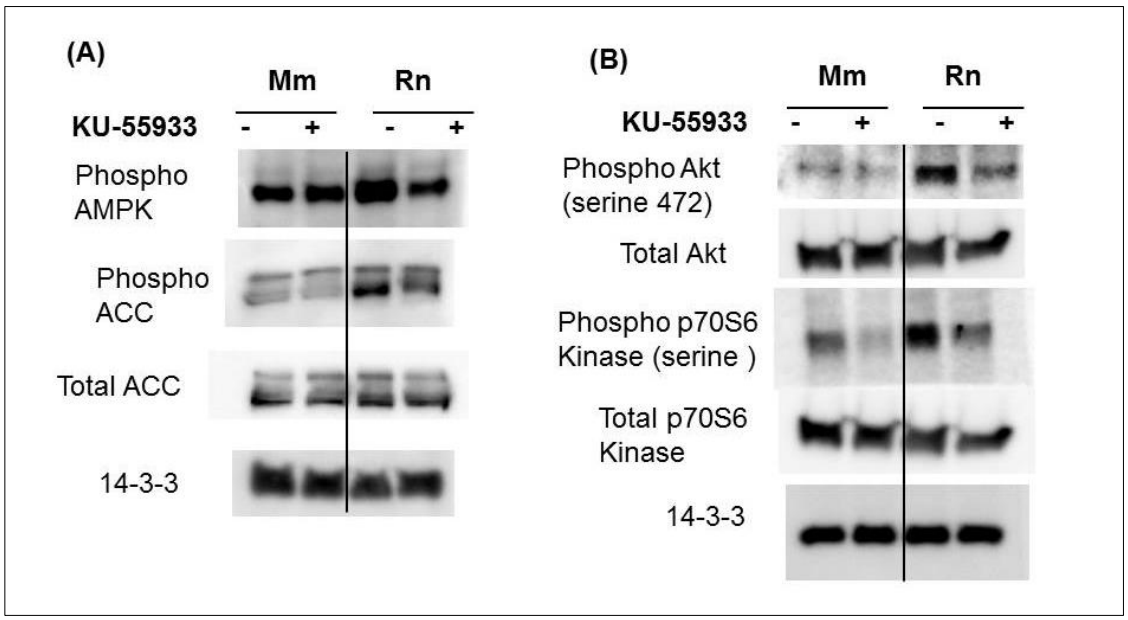

Figure 3.2.12 Effect of Selective ATM Inhibition on Signaling Adaptations

Mm and Rn cells were treated then 24 hours later, incubated with selective ATM inhibitor 1 µM KU-55933 or DMSO (vehicle) for 1 hour the lysates subjected to western blotting for AMPK and downstream targets (A); and Akt and downstream targets (B). Lysates were collected and subjected to western blot being probed with the indicated primary antibody. Membranes were incubated in a horseradish peroxidase conjugated secondary antibody and subjected to chemiluminescence which was imaged using a LAS4000 gel doc. Pixel intensity was measured using densitometry in image J (n=2)

Inhibition of ATM had little effect in Mm cells, but attenuated the increase in phosphorylation of AMPK and its downstream target ACC (Figure 3.2.6 A), as well as phosphorylation of Akt and its downstream target p70 S6 kinase (Figure 3.2.6 B) in the Rn cells. These results indicated that ATM may be activated in Rn cells and largely responsible for pro-survival signaling adaptations. While it would have been ideal to examine phosphorylation of ATM (particularly the cytosolic fraction that is thought to be responsible for metabolic actions), all commercially available antibodies for phosphorylated ATM are produced by immunising against a human peptide and the antibodies we tried did not cross react with mouse. However, to further assess the physiological significance of ATM-mediated signaling, I went on to see if treatment with the selective ATM inhibitor KU-55933 also reversed glucose uptake, as glycolysis appeared to be a major adaptation rescuing the phenotype of Rn cells (Figure 3.2.5).

Figure 3.2.13 Effect of Selective ATM on Glucose Uptake

Cells were treated with the selective ATM inhibitor (10 µM) for 24 hours. Following incubation, glucose uptake was measured by tracing uptake of ^{3}H-2-Deoxy-glucose (2DG) into cell lysate (n=4). Data are presented as mean with +/- error bars representing standard error of the mean (SEM).

Glucose uptake was decreased in the Rn cells but not the Mm cells in response to selective ATM inhibitor (Figure 3.2.13). This reveals that ATM kinase activation is likely to be responsible for the enhance glucose uptake phenotype of Rn cells that was shown in Figure 3.2.5.

3.2.9 Effect of Antioxidants on Signaling

ATM kinase is required for adaptations to ETC stress in Rn cells and I hypothesised that ATM was activated by ROS. To test that it was activated by ROS, I treated cells with antioxidants and measured signaling adaptations and glucose uptake. Most reported literature on ATM in response to H_2O_2 used N-acetyl cysteine as an antioxidant. As it has a lot of non-specific effects, I also used mito-TEMPO which is a mitochondrial targeted, superoxide scavenger. Mm and Rn cells were treated with these antioxidants and then subjected to western blot of signaling measured in Figures 3.2.10 – 3.2.12.

Contrary to reports in the literature for ATM (S. Tang et al., 2015), antioxidants did not reverse the enhanced AMPK and Akt signaling, suggesting that ROS is not driving these signaling adaptations. Alternatively, cells may need to be passaged with antioxidants long term to reverse the effects.

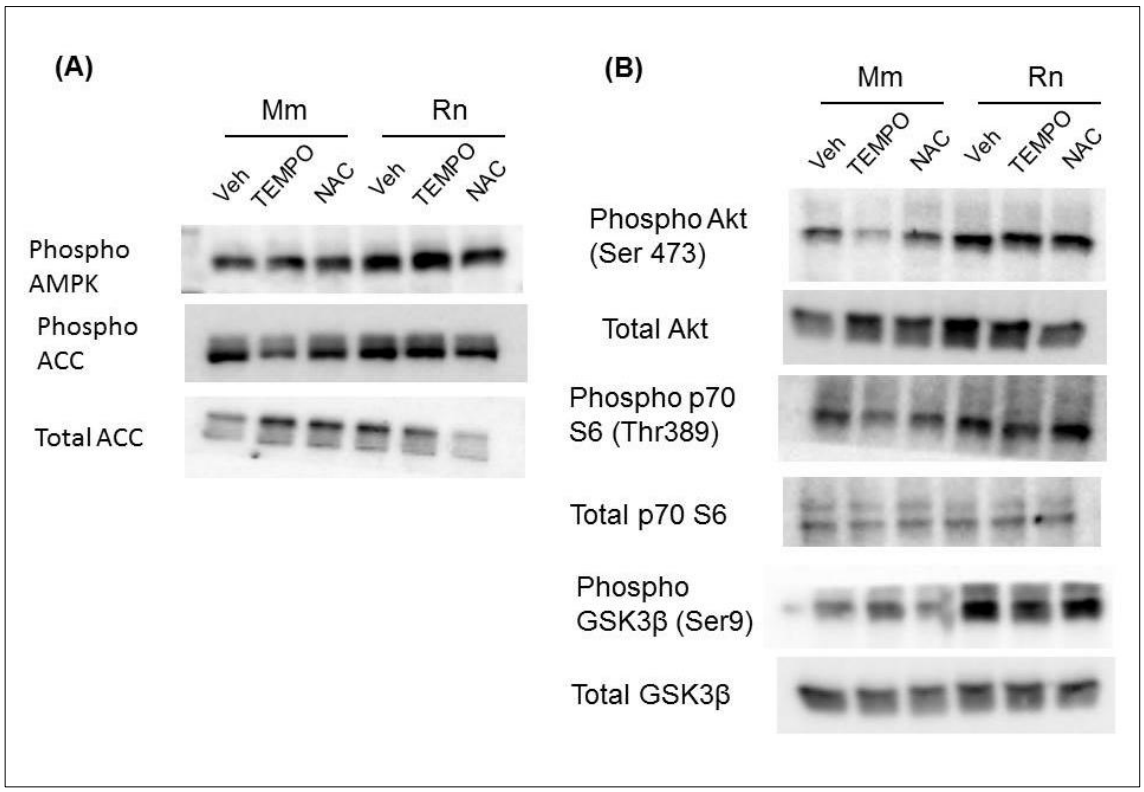

Figure 3.2.14 Effect of Antioxidants on Signaling Adaptations

Mm and Rn cells were seeded with vehicle, 10μM mito-TEMPO (TEMPO) or 1 mM N-acetyl-cysteine (NAC) overnight. The following morning, fresh antioxidants were added. Lysates were collected 24 hours after being seeded and subjected to western blot being probed with the indicated primary antibody. Membranes were incubated in a horseradish peroxidase conjugated secondary antibody and subjected to chemiluminescence which was imaged using a LAS4000 gel doc.

3.3 Discussion

Mitochondrial signaling is important in maintaining health of the cell in response to mitochondrial stress (Rose, Santoro, & Salvioli, 2016). The aim of this chapter was to interrogate intracellular adaptations to ETC stress that promote cell survival in a mammalian cell model. I found that despite a large bioenergetic defect with ETC stress, survival and proliferation were maintained. This phenotype was not associated with mtUPR activation but was associated with the ATM-Akt/AMPK signaling pathway.

Phenotype of Cells –

Characterisation of the cybrid cells revealed that large bioenergetic defects were offset by metabolic reprogramming to maintain cell viability. While metabolic effects were obvious, non-ETC related parameters of mitochondrial stress changed in a more subtle way. Oxidative metabolism phenotyping revealed a marked reduction in OCR in the more divergent Mp and Rn cells, which was partially recapitulated with reductions in the oxidation of glutamine and palmitate, but not glucose in Rn cells. Mp cells interestingly had a defect in OCR without any obvious reduction in the oxidation of exogenous fuel substrates, and similarly in Rn cells, the magnitude of decrease in basal OCR much more substantial than any change seen in the oxidation of glutamine or palmitate to CO_2 (Figure 3.2.2 B). The reason for these discrepancies is unclear. It is possible that other fuels such as different amino acids, might be important fuel sources in these cells, or alternatively endogenous (stored) fuels might be the major source for cellular respiration, and thus assessment of the oxidation of these nutrients (e.g. by pulse-chase experiments) might would be show more comparable defects to those seen in the OCR measurements. Other possible explanations for the lack of continuity between OCR and fuel oxidation could relate to the fact that OCR was measured in suspension and fuel oxidation in a monolayer of cells, or that there may be variable amounts of non-mitochondrial (cell surface) oxygen consumption across the different cell types, as has been reported in other cells with compromised mitochondrial function (Herst & Berridge, 2007). Despite the disparate findings, it was important to note that ATP levels in the cells were maintained in normal media, and were not markedly affected in galactose conditions. Thus from a bioenergetic perspective, the enhanced glycolytic flux appeared to rescue any major defect in ATP production and the

increased channelling of glucose carbons into other macromolecular pools (e.g. nucleic acids, lipid) in Rn cells likely contributed to the maintained proliferation and viability. Despite obvious differences to the current study, it is of interest to note that a recent publication proposed that over and above an adequate supply of energy and building blocks, mitochondrial membrane potential has a critical influence on cellular proliferation (Martinez-Reyes et al., 2016), yet the Mp and Rn cells maintained proliferation despite marked reductions in membrane potential. Collectively, the findings in the cybrids highlight that in the face of chronic mitochondrial stress these cells have found a way to adapt metabolic pathways to allow them to behave essentially as normal cells do. To more fully characterise the precise changes in metabolic pathways would require detailed nutrient tracing techniques (e.g. fluxomics).

The observation that there were no changes in uniformly labelled glucose oxidation with marked ETC defects (Figure 3.2.2 A) was initially perplexing but led me to hypothesise that there was more glucose being channelled through the PPP than TCA cycle. Subsequent C1 and C6 glucose tracers supported this idea but it was unfortunately unfeasible to repeat the experiment (Figure 3.2.). More glucose was converted into nucleic acids though in Rn compared with Mm cells (Figure 3.2.6 A) which is consistent with the idea of more glucose going through the PPP. This may serve as a cautionary tale for use of uniformly labelled glucose oxidation as an assay for mitochondrial glucose utilisation and I suggest that pyruvate oxidation may be a more valuable assay in future studies. Although it did not serve the purpose of answering of illustrating mitochondrial glucose utilisation with ETC defects, it shed light on the extent to which glucose is channelled into the PPP in immortalized cell lines in culture. Further evidence for this came from the finding that inhibition of G6PD reduced OCR by 40% (Figure 3.2.6 E) suggesting that flux through the PPP is responsible for almost half of glucose oxidation in these cell lines. This finding in conjunction with the rate of glutamine oxidation being double that of glucose oxidation (Figure 3.2.2), indicates that the cells heavily rely on glutamine for OXPHOS and much of the glucose is channelled through the PPP. This is a recognised metabolic feature of cancer cells (Cairns, Harris, & Mak, 2011; Pavlova & Thompson, 2016) and these data suggest it may be an underappreciated feature of any rapidly proliferating, immortalized cell lines in culture. This finding also led me to an unexpected but interesting hypothesis that a defect in

catabolic metabolism causes a shift towards anabolic metabolism. The fact that more glucose is probably going through the PPP in Rn cells than Mm cells was interesting as it is consistent with cancer cell metabolism (Cairns et al., 2011). It appears that cells experiencing ETC stress may acquire some of the metabolic features displayed in cancer cells.

Mitochondrial Stress Responses –

The overarching aim was to explore mitochondrial stress signaling and so while glycolysis was clearly an important adaptation for cellular proliferation and viability, I aimed to explore whether there were accompanying signaling pathways above and beyond glycolysis rescuing the ETC-compromised cells. I observed no coordinated changes in mtUPR or levels of the critical mitochondrial antioxidant enzyme Sod2. An early study that showed induction of mtUPR in mammalian cells used a model overexpressing mutant (and not properly folded) ornithine transcarbamylase (OTC) into COS-7 cells (Horibe & Hoogenraad, 2007). This resulted in a large induction of mitochondrial protein folding chaperones at the protein level (measured by immunoblotting). Interestingly, overexpression of the wild type control also resulted in mtUPR activation, albeit to a lesser degree than the mutant (Kageyama et al., 2014). This suggests that mtUPR activation in mammalian cells is proportional to mitochondrial unfolded protein load. In another mammalian cell model, mouse hepatocytes treated with the mTOR inhibitor, rapamycin exhibited induction of an mtUPR (Houtkooper et al., 2013). Collectively, the findings from the current study and the literature suggest that in mammalian cells, the mtUPR is activated more in response to perturbed proteostasis, rather than by an ETC stress. Since mitochondrial protein import requires an intact mitochondrial membrane potential and is dependent on mitochondrial ATP, it is possible that there was no overwhelming change in the mtUPR with the ETC defects in the cyrbid cells, as their compromised bioenergetic state may slow down protein import and reduce the subsequent protein load, although this would need to be tested experimentally. In contrast to this notion, it was recently reported that primary cultures of mouse fibroblasts with a Complex IV defect do exhibit a mtUPR (Pharaoh, Pulliam, Hill, Sataranatarajan, & Van Remmen, 2016). It is therefore possible that in mammalian cells the mtUPR might relate more closely to alterations in Complex

IV, and of note although there was no coordinated change in mtUPR markers, there was a mild upregulation of ClpP in Mp cells, which have been reported to selectively manifest a reduction in Complex IV activity (McKenzie et al., 2003). A final point to note is that our understanding of the mtUPR in mammalian cells is continuing to evolve and it is possible that it may be an adaptive response to mitochondrial stress to promote cell survival without a major induction of chaperones, as described in lower organisms (Fiorese et al., 2016). Hence it is possible that mtUPR may be an adaptive response to mitochondrial stress to promote cell survival through non chaperone mechanisms. Another alternate explanation is that since antioxidant and mtUPR responses are important and may be constitutively expressed at a high level in cultured cells and it may be difficult to detect a strong induction above baseline.

Kinase Signaling –

Since metabolic reprogramming was a crucial adaptation and mtUPR was largely unchanged, I aimed to explore potential signaling adaptations that were linked with perturbations in molecular metabolism. It was found that pro-survival kinases Akt and AMPK were both activated in Rn cells. Despite a decrease in oxygen consumption, Mp cells showed a mild increase in AMPK phosphorylation, without any change in Akt. While AMPK is well known to be activated in mitochondrial stress (Shirwany & Zou, 2014) and has shown to be an important adaptation, (Distelmaier et al., 2015; S. B. Wu, Wu, Wu, & Wei, 2014) there is less literature on Akt activation. Akt is transiently activated by a Complex I inhibitor (Guha, Fang, Monks, Birnbaum, & Avadhani, 2010; T. Zheng et al., 2015) and OXPHOS uncouplers (Guha, Fang, et al., 2010). These studies collectively support the idea that Akt can be engaged by transient mitochondrial stress but the results presented in this chapter are the first to my knowledge that have showed Akt constitutive overactivation in a chronic model of ETC stress. The Akt signaling pathway is commonly overactivated in cancer cells (Bellacosa, Kumar, Di Cristofano, & Testa, 2005) which is of interest because as discussed above, the Rn cells displayed some metabolic features of cancer cells. Akt signaling is known to promote glycolysis (Robey & Hay, 2009) and this chapter highlights the potential for metabolic reprogramming to drive signaling, in addition to signaling driving the metabolic

program. Such findings are consistent with those reported by (Trefely et al., 2015) who showed that glycolytic metabolism could impact the insulin signaling pathway.

ATM Kinase as a Mitochondrial Stress Response -

Pharmacological inhibition of ATM kinase resulted in an attenuation of adaptations to ETC stress, including pro-survival signaling and glucose uptake exclusively in Rn and not in Mm cells (Figure 3.2.13). This result reveals a role for ATM kinase as an important player in the mitochondrial stress response. ATM kinase signaling is activated during a DNA damage response and cell cycle regulation (Awasthi et al., 2015). In addition to its role in genomic stability, ATM was also of interest as it has been reported to also have functions in metabolism. ATM activity is required for full activation of Akt phosphorylation in response to insulin (Halaby et al., 2008; Viniegra et al., 2005). ATM activity is also required for AMPK phosphorylation (and subsequent phosphorylation of ACC) in response to AMP analogue AICAR (Takagi et al., 2015). (Y. Sun et al., 2007). An increase in the AMP/ATP ratio is considered to be the mechanism by which mitochondrial dysfunction activates AMPK signaling, but the current study and that by (Y. Sun et al., 2007) suggests that following bioenergetic stress ATM kinase is also required. Assessment of ATM-deficient cells exposed to mitochondrial stress would be one way to determine the relative importance of adenine nucleotide changes vs. ATM kinase in the activation of AMPK.

ATM kinase has also been demonstrated in increase flux through the PPP through phosphorylation of hsp27 which then interacts with and activates glucose 6 phosphate dehydrogenase (G6PD) (Cosentino et al., 2011) which is the rate limiting enzyme of PPP. Preliminary results examining the oxidation of 1-^{14}C-glucose (can only be oxidised in PPP) with 6-^{14}C glucose (can be oxidised in the PPP and mitochondria) suggested increased flux through the PPP in Rn cells, but more detailed studies with 13C-glucose are required to definitively explore this.

Glycolytic flux may also be increased by ATM activation as it has been demonstrated to initiate phosphorylation and subsequent translocation of GLUT1 (Andrisse et al., 2013) as well as phosphorylation and stabilisation of HIF1α (Cam, Easton, High, & Houghton, 2010). Intriguingly, 2-deoxy glucose, a glycolysis inhibitor, attenuates ATM

activation (T. Tanaka et al., 2006) suggesting that ATM activity may be in some way activated by glycolysis and promotes glycolysis as a positive feedback loop. I found that Akt signaling was reversed (Figure 3.2.12) along with glucose uptake (Figure 6.2.13) upon ATM inhibition in Rn cells. As glucose uptake is also known to be affected by Akt signaling (Robey & Hay, 2009) it is impossible to conclude in our model, whether the enhanced glucose uptake phenotype of Rn cells was because of a direct effect of ATM activation or an indirect effect of Akt activation.

ATM is also activated by reactive oxygen species through reduction of residue cysteine 2991 (Z. Guo et al., 2010) and is activated by nitrosative stress (Tripathi et al., 2013). These findings collectively demonstrate ATMs sensitivity to cellular stress caused by reactive species. The aforementioned studies looked at oxidative stress in an acute, supraphysiological setting through incubation with hydrogen peroxide. Another study that has found that physiological levels of ROS results in constitutive overactivation of ATM in cancer associated fibroblasts compared with normal fibroblasts (S. Tang et al., 2015). Because ATM is well known for its nuclear role in a DNA damage response, what needs to be considered is if this is due to a DNA damage response. This has been further confirmed by a study that found mitochondria are dependent for activation of ATM kinase by extranuclear ROS in a non DNA double strand break dependent manner (Morita, Tanimoto, Murakami, Morinaga, & Hosoi, 2014). Interestingly, my results show that there is a mild oxidative stress phenotype with Mp and even Md cells (Figure 3.2.3 A). Intriguingly treatment with antioxidants did not attenuate signaling (Figure3.2.3 B) suggesting that it is not via a ROS dependent mechanism. Based off results of the present study and other literature (T. Tanaka et al., 2006), I speculate that glycolytic flux (potentially by intracellular lactate) activates ATM kinase.

My results show that metabolic signaling can initiate activation of ATM which can affect nuclear targets. Other literature to suggest that genotoxic stress may signal ATM to promote metabolic adaptations. For example, topisomerase inhibitors enhance glycolysis in an ATM dependent manner (Demel et al., 2015). Replication stress activates ATM to promote accompanying metabolic adaptations (Aird et al., 2015). Based on my data and others, ATM feeds both backwards and forwards between

metabolism and the nucleus and hence I propose that ATM kinase truly is a nexus of metabolism and cell cycle regulation.

Conclusions –

Results from this chapter reveal that activation of ATM kinase is a novel mechanism by which mammalian cells adapt to mitochondrial stress through metabolic reprogramming and altered cell signaling. While the aim of the chapter was initially intended at exploring adaptations to mitochondrial stress, the implications have also been more general by expanding on our knowledge of how metabolism affects cell cycle regulation which may provide insight into how cancer metabolism enables cells to enhance proliferation. Although there is a growing appreciation that there is an intimate connection between cellular metabolism and cell cycle regulation, the dominant view in the literature is that cell cycle progression affects metabolism (Fajas, 2013). Surprisingly the mechanisms linking metabolic control over the cell cycle have not been elucidated (I. H. Lee & Finkel, 2013). My work in this chapter provides a novel mechanism by which metabolism can influence the cell cycle.

CHAPTER 4: INVESTIGATING CELL-TO-CELL COMMUNICATION OF MITOCHONDRIAL STRESS IN HEK293 CELLS

4.1 Introduction

Following identification of a novel intracellular signaling pathway in response to mitochondrial stress, the next aim of this thesis was to explore cell non-autonomous or cell-to-cell communication of mitochondrial stress. Interest in this was first triggered by a seminal finding in *C.elegans* whereby mitochondrial stress in neurons resulted in a mitochondrial stress response in a distal tissue, indicating that a secreted factor may be involved in mediating cell non-autonomous communication of cellular energetic status (Durieux et al., 2011). Since then, more studies providing evidence for cell non-autonomous communication of mitochondrial stress have been reported including a mouse model of muscle specific mitochondrial dysfunction, where FGF21 was secreted, eliciting changes in other tissues (K. H. Kim et al., 2013). Growth and differentiation factor 15 (GDF15) is similarly secreted from muscle in response to mitochondrial stress and communicates changes to other tissues (Chung et al., 2017). In these cases, secreted proteins act as the cell non-autonomous communicators of mitochondrial stress. Studies have also shown that peptides encoded by small open reading frames of the mitochondrial genome can participate in cell non-autonomous communication (C. Lee et al., 2013; C. Lee et al., 2015). Further, mtDNA has been amplified from microvesicles (Guescini, Genedani, et al., 2010; Guescini, Guidolin, et al., 2010) indicating a potential for mitochondrial nucleic acid components to be involved in cell non-autonomous mitochondrial signaling.

As discussed in the literature review in chapter 1, mitochondrial stress is undoubtedly associated with complex diseases and ageing e.g. neurodegeneration and diabetes, but whether it is cause or consequence is contentious (section 1.4.2-1.4.3). Regardless, there is plenty of evidence that mitochondrial dysfunction at least exacerbates or promotes progression of these conditions (section 1.4.2-1.4.3). Since the complex diseases and ageing are by nature generally multi-systemic and progressive conditions, cell-to-cell communication unsurprisingly plays a role in the progression of disease processes. For example, pathogenic proteins in neurodegenerative diseases are reported to be

transmitted in a cell non-autonomous fashion promoting progression of the disease (J. L. Guo & Lee, 2014) and cross-talk between neurons and microglia/ astrocytes is dysregulated in neurodegeneration (L. Tian, Ma, Kaarela, & Li, 2012). Similarly, cardiomyocyte secreted proteins have been proposed to be important in heart disease pathology (Jahng, Song, & Sweeney, 2016) In metabolic diseases there is substantial remodelling of the secreted proteins derived from white adipose tissue, skeletal muscle and liver to mediate whole body coordination of energy metabolism (Oh et al., 2016) and secreted proteins from adipocytes and hepatocytes will be explored in this context in the next 2 chapters.

More generally, cellular stress conditions are known to cause changes to secreted proteins including ER stress (Genereux & Wiseman, 2015), hypoxia (Riis et al., 2016; S. W. Song et al., 2016), ageing (W. H. Yang et al., 2015), oxidative stress and cellular senescence (J. L. Guo & Lee, 2014) and as noted earlier, FGF21 and GDF15 are secreted with mitochondrial stress (Chung et al., 2017). Despite this, there are currently no published studies that have mapped the complete secreted proteome (secretome) in response to mitochondrial stress. The aim of this study is to characterise the secretome of cells exposed to ETC stress, with a goal of providing insight into potential protein mediators of cell non-autonomous mitochondrial stress signaling.

4.2 Methods Summary

Detailed methods are provided in sections 2 with a brief summary of the workflow provided below.

Oxygen consumption rate dose response curves to ETC toxins were characterised using the Seahorse XF-96 Bioanalyser in HEK293 cells. Following selection of doses, cell viability and cell death were determined using AlamarBlue stains. Cells were stringently washed then incubated with ETC toxins at the respective doses in serum free medium then 24 hours later conditioned medium was collected by spinning and filtering the pellet to clear cell debris. Following an acetone precipitation trypsin digestion, peptides were separated and mass analysed by LC-MS/MS and raw files were subjected to MaxQuant analysis and data processing in the R environment using R studio. Many previous studies characterising the secretome have enriched for classically secreted protein, but it is now appreciated that most proteins are secreted by non-conventional protein secretion (Rabouille, 2016). It was for this reason, I used an acetone precipitation of conditioned medium to analyse the complete proteome being secreted by cells.

4.3 Results

4.3.1 Model of Mitochondrial Stress

In order to establish a model of low and high grade mitochondrial stress in HEK293 cells, oxygen consumption rate (OCR) was measured in a dose response fashion with acute treatment of rotenone, antimycin A and dinitrophenol using the Seahorse Bioanalyser XF-96 (Figure 4.3.1). The effect of all compounds was sigmoidal, with mild respiratory inhibition observed at ~10 nM with both rotenone and antimycin A, while micromolar doses of DNP were required to stimulate oxygen consumption substantially.

Concentrations that approximated IC_{10} and IC_{50} doses were applied to HEK293 cells overnight to determine if they were cytotoxic (Figure 4.3.2). This was critical as cell lysis and subsequent release of intracellular proteins can contaminate conditioned medium. As can be seen in Figure 4.3.2, the chosen doses of compounds did not significantly alter cellular viability. For antimycin A only the high dose is shown, as there were technical difficulties with the secretome analysis of the low dose samples.

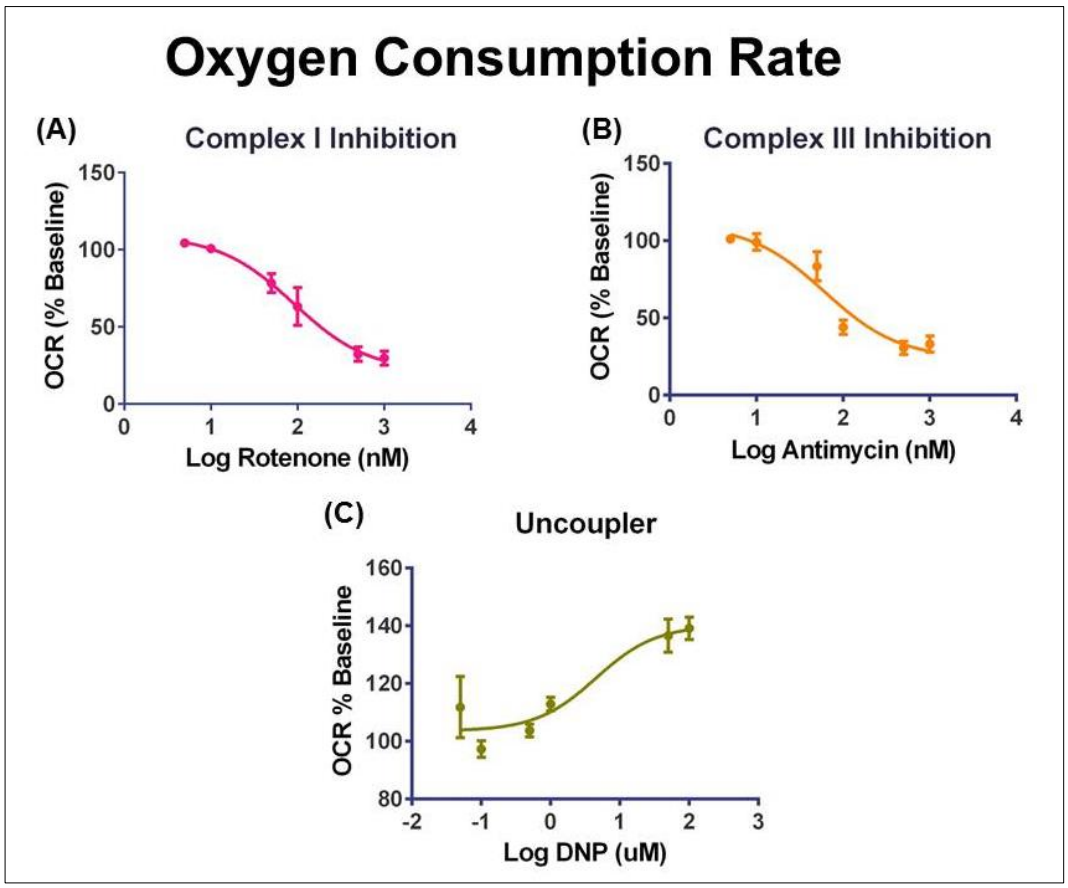

Figure 4.3.1 Dose Response of ETC Inhibitors in HEK293 Cells

Baseline oxygen consumption rate (OCR) was established by taking the average of 5 basal readings then the drugs – rotenone (A), antimycin A (B), dinitrophenol (C) were injected and 6 basal readings were taken afterwards. Results are expressed as a percentage of the baseline OCR after drug injection. Points on curves represent the mean for a given drug dose with error bars representing standard error of the mean. The experiment was performed 3 independent times.

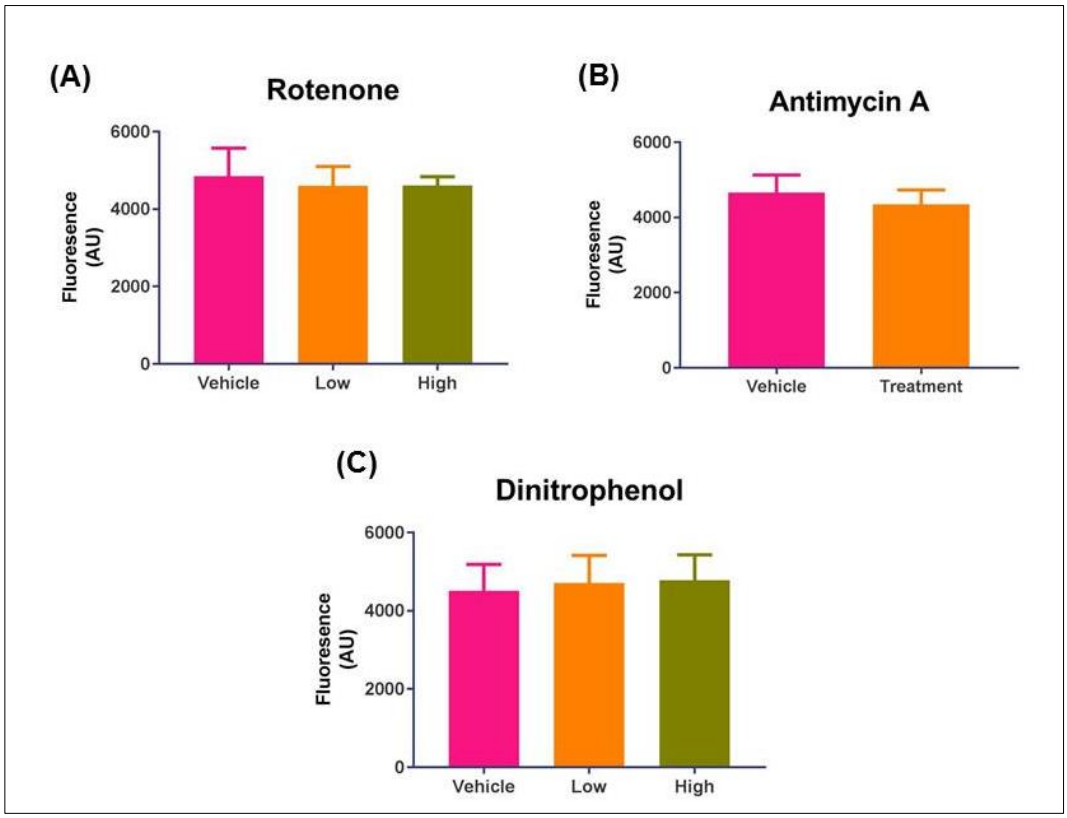

Figure 4.3.2 Cell Viability of HEK293 cells Treated with Defined Doses of Inhibitors

HEK293 treated for 24 hours with DMSO vehicle, 25 nM, 250 nM rotenone (A), Ethanol vehicle or 100 nM antimycin A (B) and H_2O vehicle, 50 µM and 100 µM dinitrophenol (C) labelled "vehicle", "Low" for low dose and "High" for high dose respectively. Alamar blue fluorescence was measured (A), (B) & (C) presented in fluorescence arbitrary units.

4.3.2 Proteins Detected by Mass Spectrometry

Peptides from conditioned medium from HEK293 cells treated with mitochondrial toxins were subjected to LC-MS/MS analysis (see section 2.3). Identified proteins were initially filtered to exclude proteins that are common contaminants in database, peptides identified by reverse sequence and proteins only identified by a peptide modification site. These filtering steps are necessary for data quality. To increase confidence in protein detection, proteins were filtered such that they were identified by at least 2 unique peptides. Next, proteins were filtered such that they were present in at least 2 out of 3 replicates or 3 out of 4 replicates.

After filtering, I performed *in silico* analysis of all detected proteins in each data set. Analysis was performed on every detected protein in each dataset. This included all proteins in vehicle and treatment groups pooled and included all proteins whether or not they were significantly changed. The SecretomeP tool (accessed http://www.cbs.dtu.dk/services/SecretomeP/) was also used to calculate the percentage of proteins that were predicted to have a signal peptide for classical protein secretion (Figure 4.3.3). For the rotenone, antimycin A and dinitrophenol datasets, there were a total of 401, 643 and 368 proteins identified respectively after filtering. Of the identified proteins, 30%, 20% and 40% of total proteins had a secretion signal peptide for classical protein secretion for rotenone, antimycin A and DNP respectively (Figure 4.3.3). Cellular component analysis by gene ontology was also performed to test whether proteins detected could be annotated as having a role in cellular protein secretion or an extracellular function (Figure 4.3.3). For rotenone, antimycin A and DNP respectively, 78%, 68% and 78% of proteins were consistent with an extracellular annotation by gene ontology (Figure 4.3.4). This suggests that largely extracellular proteins were detected in our LC-MS/MS analysis, which increases confidence in the data, with roughly one third of proteins are likely to be secreted through the classical protein secretion pathway.

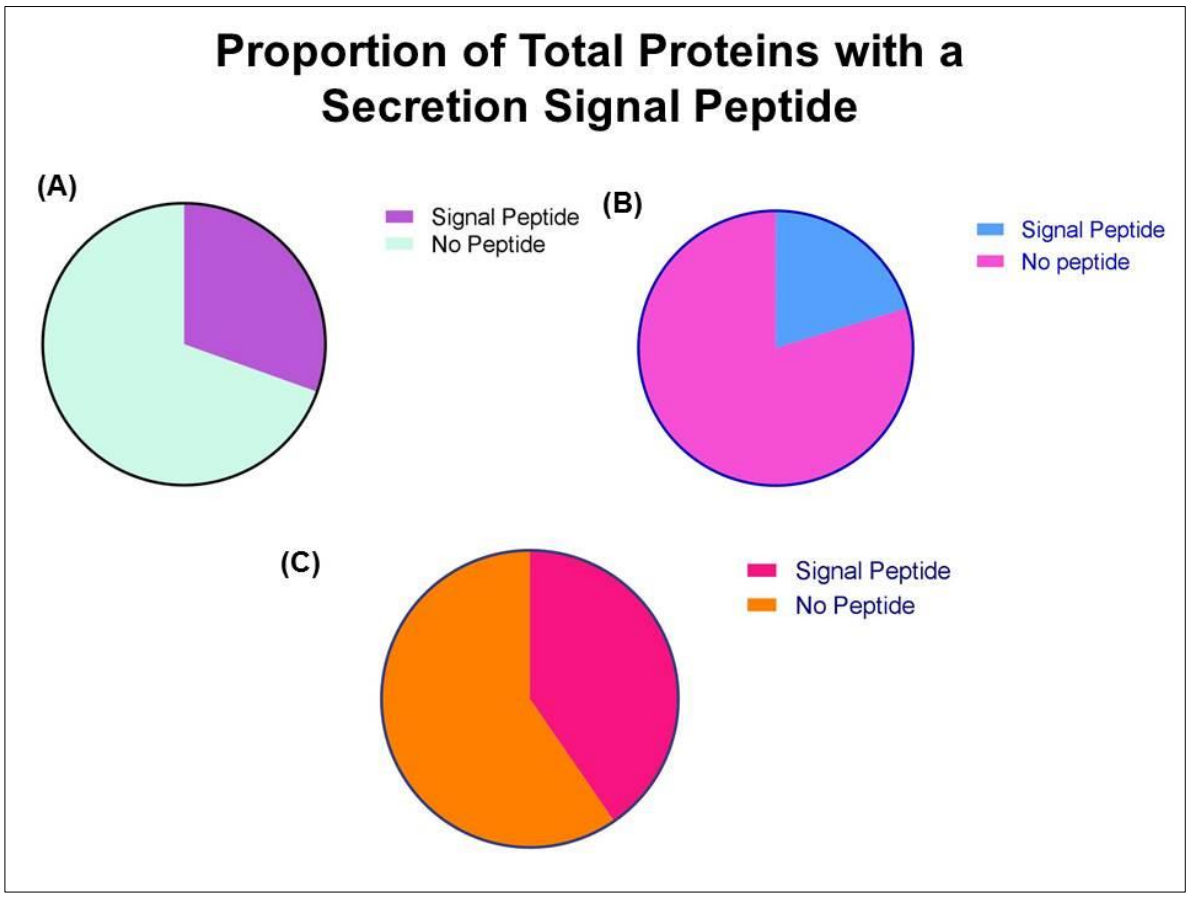

Figure 4.3.3 Proportion of all Detected Proteins with a Predicted Secretion Signal Peptide by Sequence Analysis in HEK293 Cells

All proteins detected by LC-MS/MS in each experimental group were pooled after data filtering for the Rotenone dataset (A), the Antimycin A dataset (B) and the Dinitrophenol dataset (C). Amino acid sequences were exported to the SecretomeP tool that predicts whether or not a protein has a secretion signal peptide based on sequence.

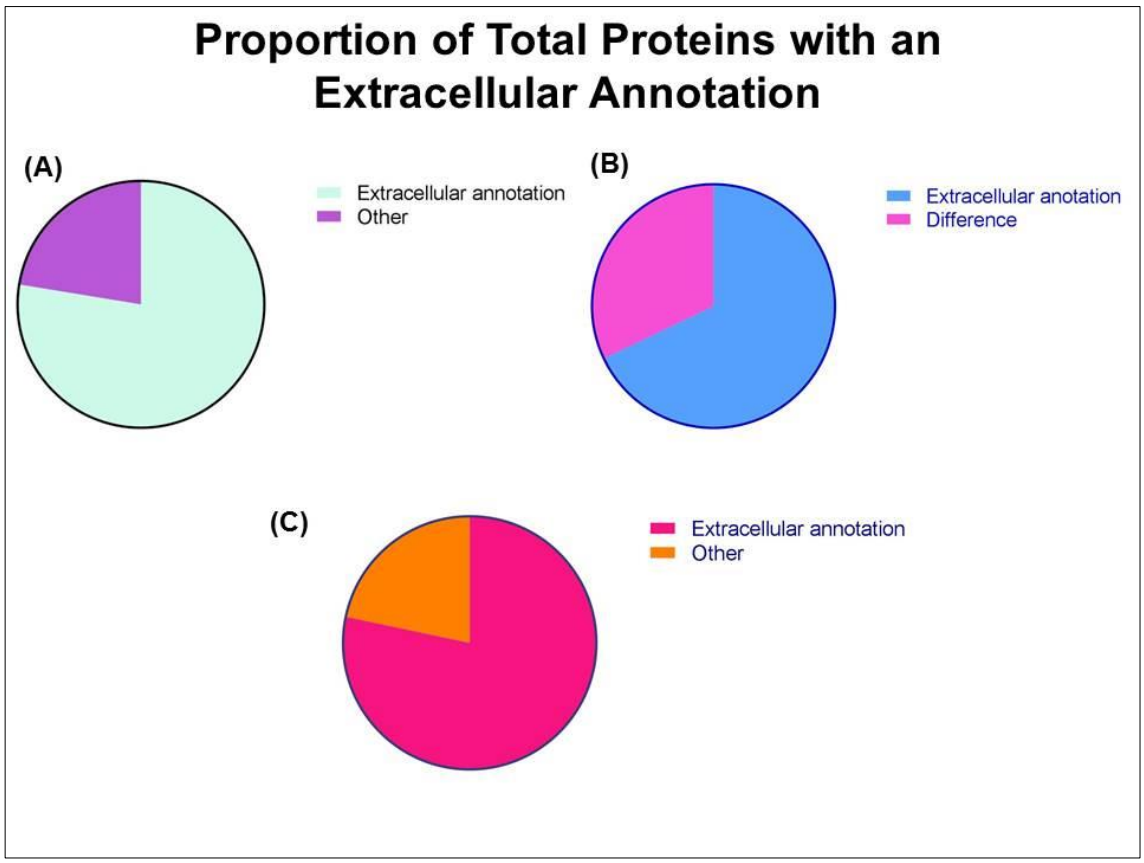

Figure 4.3.4 Proportion of all Detected Proteins with an Extracellular Annotation by Gene Ontology in HEK293 Cells

All proteins detected by LC-MS/MS in each experimental group were pooled after data filtering for the Rotenone dataset (A), the Antimycin A dataset (B) and the Dinitrophenol dataset (C). Cellular Component Analysis by Gene ontology was performed and the number of proteins that had an extracellular annotation (removing duplicates when a protein was annotated under multiple extracellular annotations) are graphed as a percentage of total proteins where "Extracellular Annotation" refers to proteins with an extracellular annotation and "other" refers to the remainder of proteins. For adipocytes, there were 6 extracellular annotations included in the analysis: "Extracellular Exosome", "Extracellular Vesicle", "Extracellular Region Part" , "Extracellular Region", "Extracellular Space", "Extracellular Matrix", "Proteinaceous Extracellular Matrix" and "Extracellular Matrix Component".

4.3.2 Data Quality Check

With large, shotgun proteomics experiments it is important to ensure data quality before proteomics analysis. After data filtering was performed as described above, data correlation and replicate reproducibility was assessed to ensure the data was of good quality. Multiscatter analysis of (Figure 4.3.5-4.3.7) and frequency histograms (Figure 3.3.9) of log_2 transformed LFQ Intensity values were performed for each replicate to analyse correlation between replicates. The 'LFQ Intensity' value which is computed in MaxQuant software (for more information on the algorithm refer to section 2.3) is used marker of 'abundance' for label free quantification.

The multiscatter plots compares the LFQ Intensity of each protein each individual replicate with all other replicates. The current dataset showed good correlation of log_2 transformed LFQ intensity values across the different groups (Figure 4.3.5-4.3.7). For the dinitrophenol dataset all Pearson's Correlation Coefficient values were greater than 0.9 suggesting tight correlation between replicates within this group. For the rotenone and antimycin A datasets, most samples were above 0.85 with some being lower.

Figure 4.3.9 illustrated that for all experimental groups except for the high dose of rotenone, the merged frequency histograms of individual replicates were very well superimposed (i.e. most of the colour in the individual columns overlaps). This indicates that the distribution of frequencies of log_2 LFQ intensity values were quite reproducible between replicates.

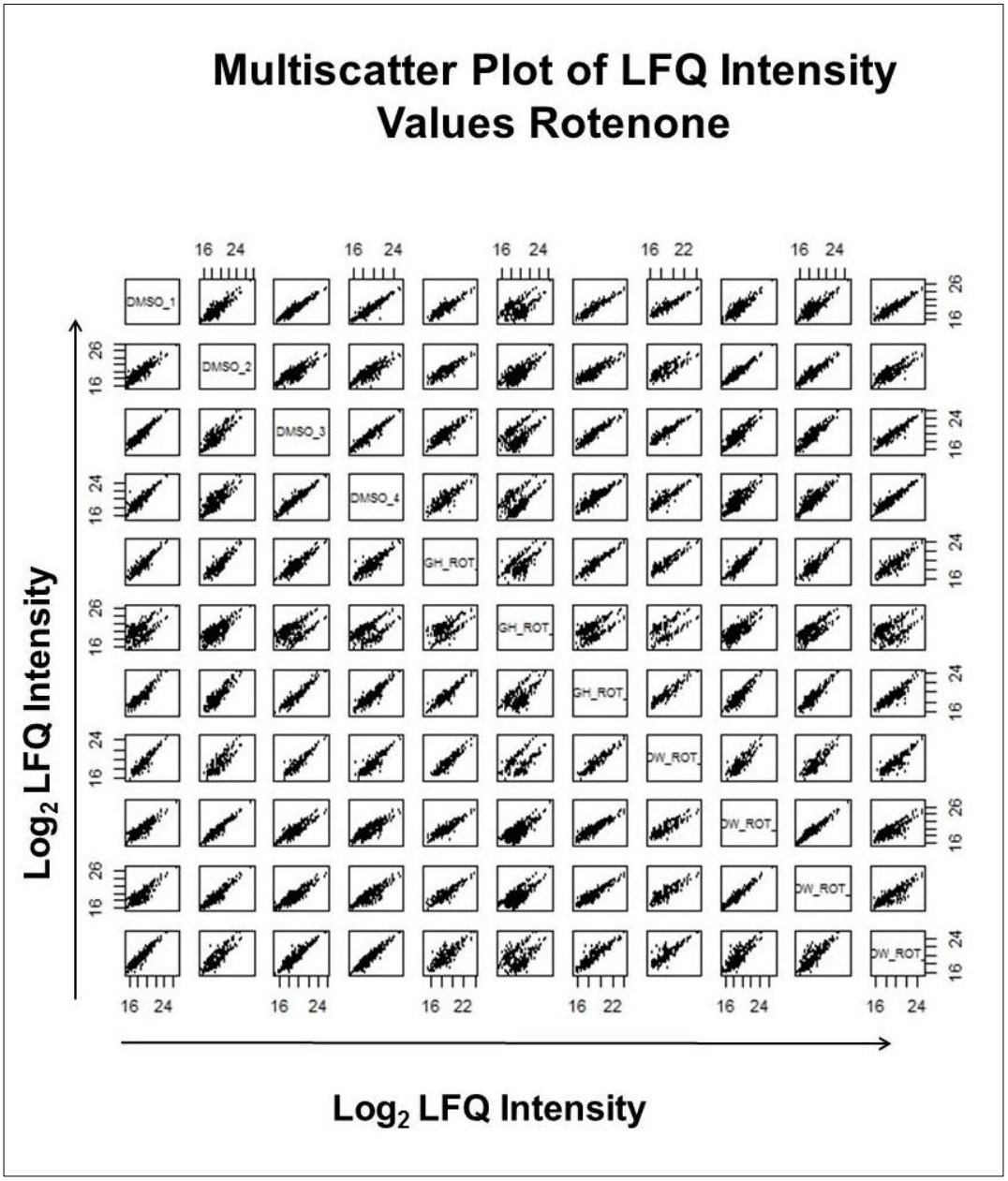

Figure 4.3.5 Multiscatter Plot of every LFQ Intensity values from Individual Samples for Rotenone Dataset in HEK293 cells

Log_2 transformed LFQ Intensity values for each single protein after filtering were plotted (one dot represents the Log_2 transformed LFQ Intensity value of one detected protein) for each sample of the rotenone dataset. From left to right – the first 4 samples are the 4 replicates of the Vehicle group; the following 3 samples are the 3 replicates of the high dose rotenone group; and the following 4 samples are the 4 replicates of the low dose rotenone group.

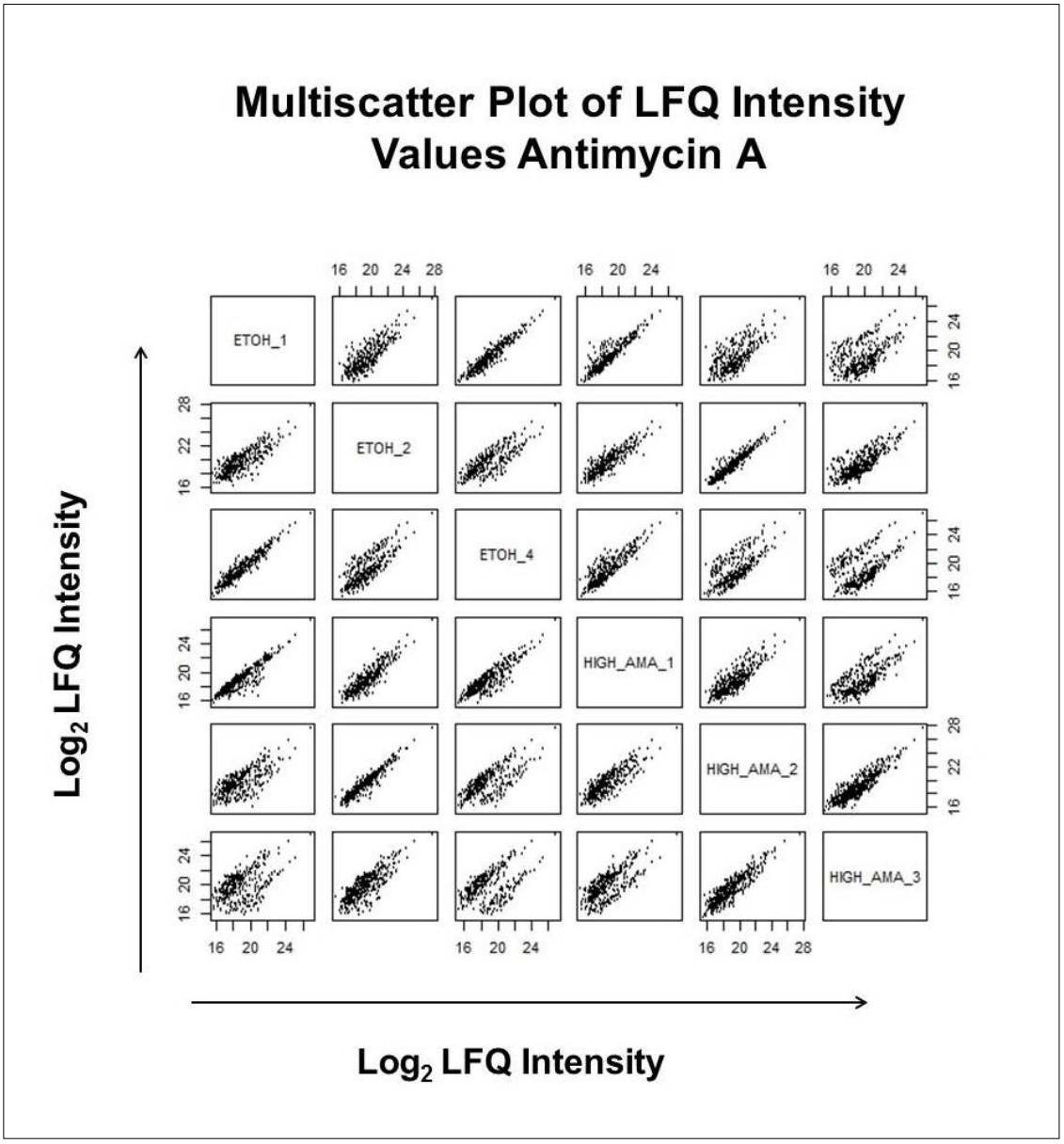

Figure 4.3.6 Multiscatter Plot of every LFQ Intensity values from Individual Samples for Antimycin A Dataset in HEK293 cells

Log_2 transformed LFQ Intensity values for each single protein after filtering were plotted (one dot represents the Log_2 transformed LFQ Intensity value of one detected protein) for each sample of the rotenone dataset. From left to right – the first 3 samples are the 3 replicates of the Vehicle group; the following 3 samples are the 3 replicates of the antimycin A group.

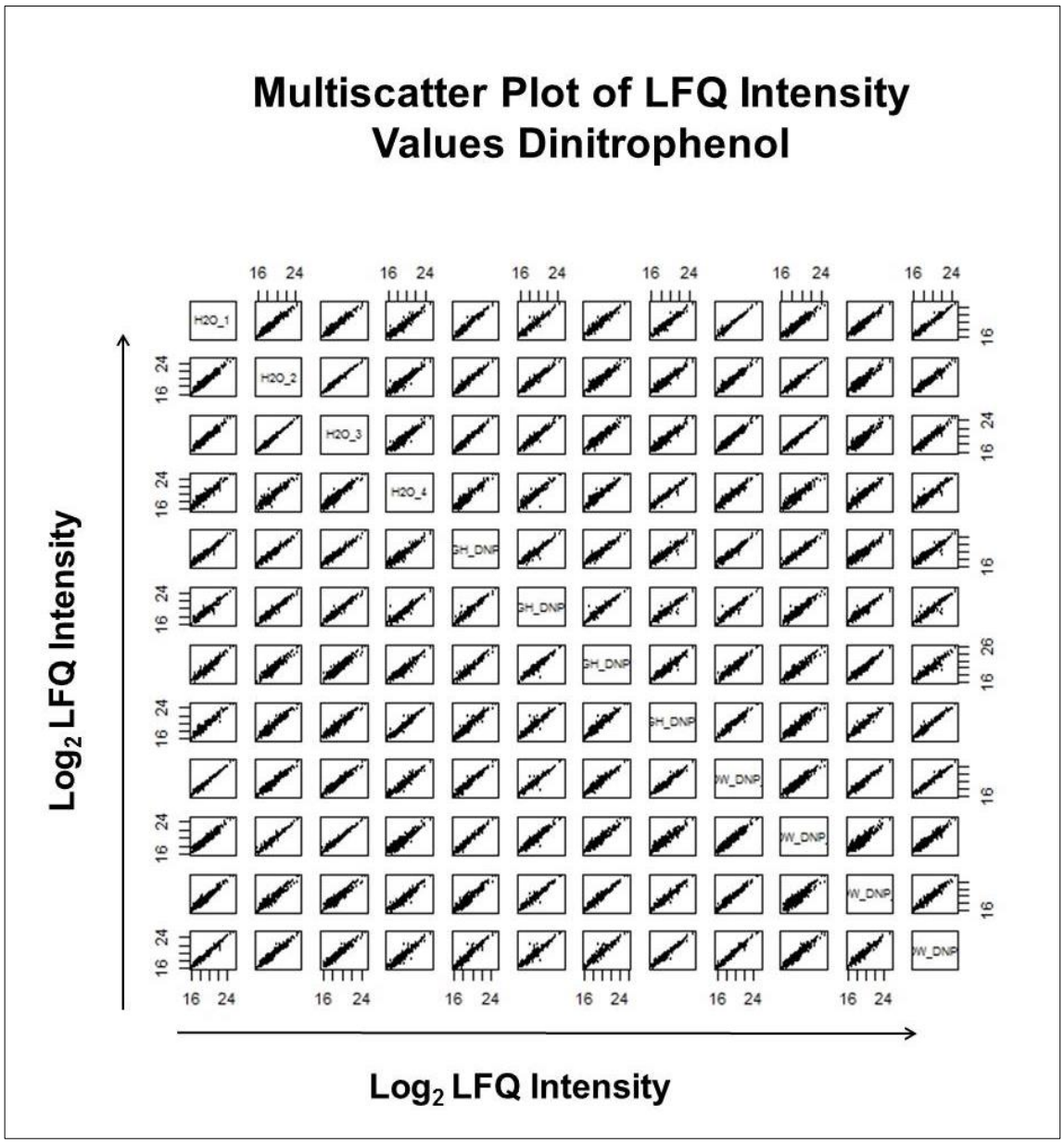

Figure 4.3.7 Multiscatter Plot of every LFQ Intensity values from Individual Samples for Dinitrophenol Dataset in HEK293 cells

Log_2 transformed LFQ Intensity values for each single protein after filtering were plotted (one dot represents the Log_2 transformed LFQ Intensity value of one detected protein) for each sample of the rotenone dataset. From left to right – the first 4 samples are the 4 replicates of the Vehicle group; the following 4 samples are the 4 replicates of the high dose dinitrophenol group; and the following 4 samples are the 4 replicates of the low dose dinitrophenol group.

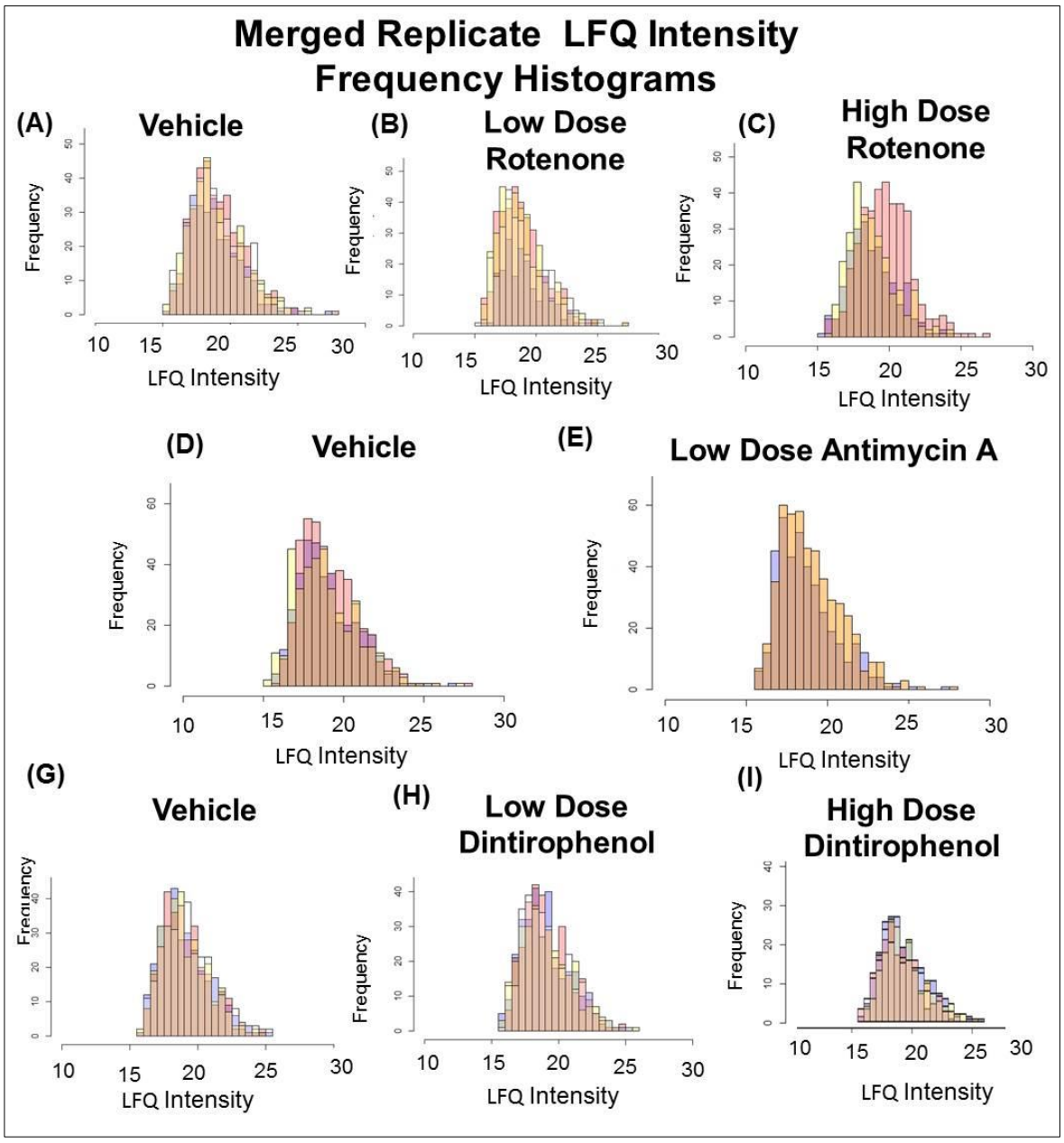

Figure 4.3.8 Merged Replicate Frequency Histograms of Log2 LFQ Intensity Values

Log_2 transformed LFQ Intensity Values were plotted as frequency histograms for each replicate and merged within each experimental group – (A) Vehicle for rotenone dataset, (B) low dose rotenone treatment, (C) High Dose rotenone, (D) Vehicle for antimycin A dataset, (E) antimycin A treatment, (G) Vehicle for dinitrophenol dataset, (H) low dose dinitrophenol treatment, (I) high dose dinitrophenol treatment. Different colours represent individual replicates.

I also performed replicate Venn diagrams on protein IDs (Figures 4.3.10 – 4.3.12) to measure the overlap of proteins identified by MS within an experimental group. Overlap analysis of detected proteins revealed that for the rotenone dataset, 62%, with 79% of proteins being detected in 3 out of 4 replicates were present in the vehicle and 42% with 71% of proteins being detected in 3 out of 4 replicates in the low dose rotenone group (Figure 3.3.8). For the high dose rotenone samples, there is good overlap of 2 of 3 replicates but one replicate has 206 individual proteins that are distinct from the other 2 replicates. This is 41% of the total proteins detected in the sample indicating that that sample (Figure 3.3.8 C). This is also reflected in the merged histograms (Figure 3.) where one replicate has a higher frequency of higher LFQ intensities that does not overlap with other replicates. For the antimycin A dataset, the vehicle group had 68% of proteins were detected in 3 out of 3 replicates and 76% of proteins were detected in at least 2 out of 3 replicates. The antimycin A drug treated group had 62% overlap in 3 out of 3 replicates and 85% overlap in at least 2 out of 3 replicates. 84, 76, 74 % overlap in 4 out of 4 replicates for the vehicle, low dose and high dose experimental groups respectively of the dinitrophenol dataset. This is considered good overlap in large label free shotgun MS/MS experiments.

Collectively, this data quality check indicates that the dintriophenol dataset is of very high quality for label free MS. The rotenone and antimycin A datasets were also of quite good quality, although a bit more variable.

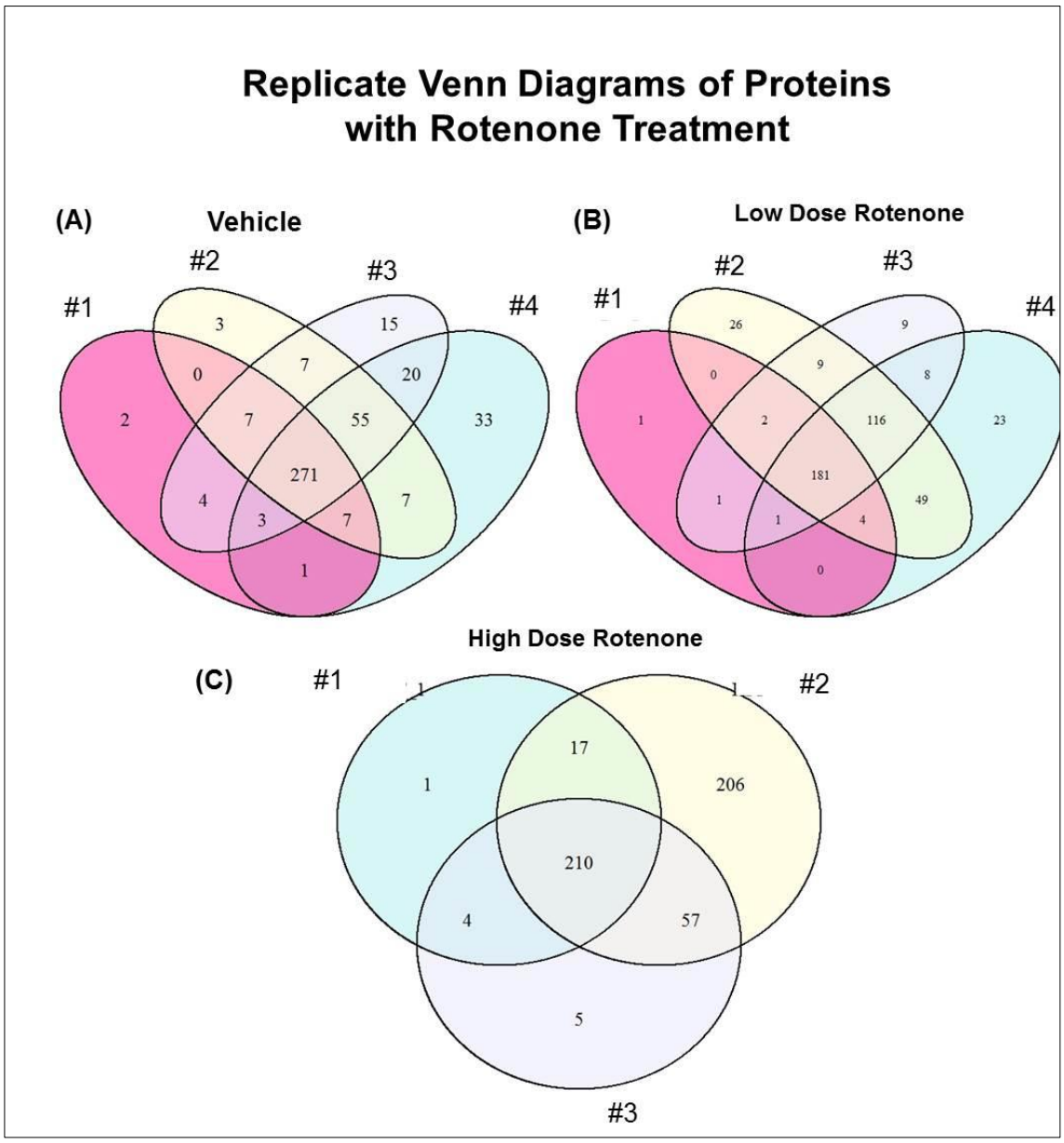

Figure 4.3.9 Overlap Analysis of Protein IDs detected in Individual Replicates for Rotenone Dataset

Venn Diagrams illustrating overlap of Protein IDs in each replicate Vehicle (A), low dose rotenone treatment (B) and high dose rotenone treatment (C). Different colours represent individual replicates.

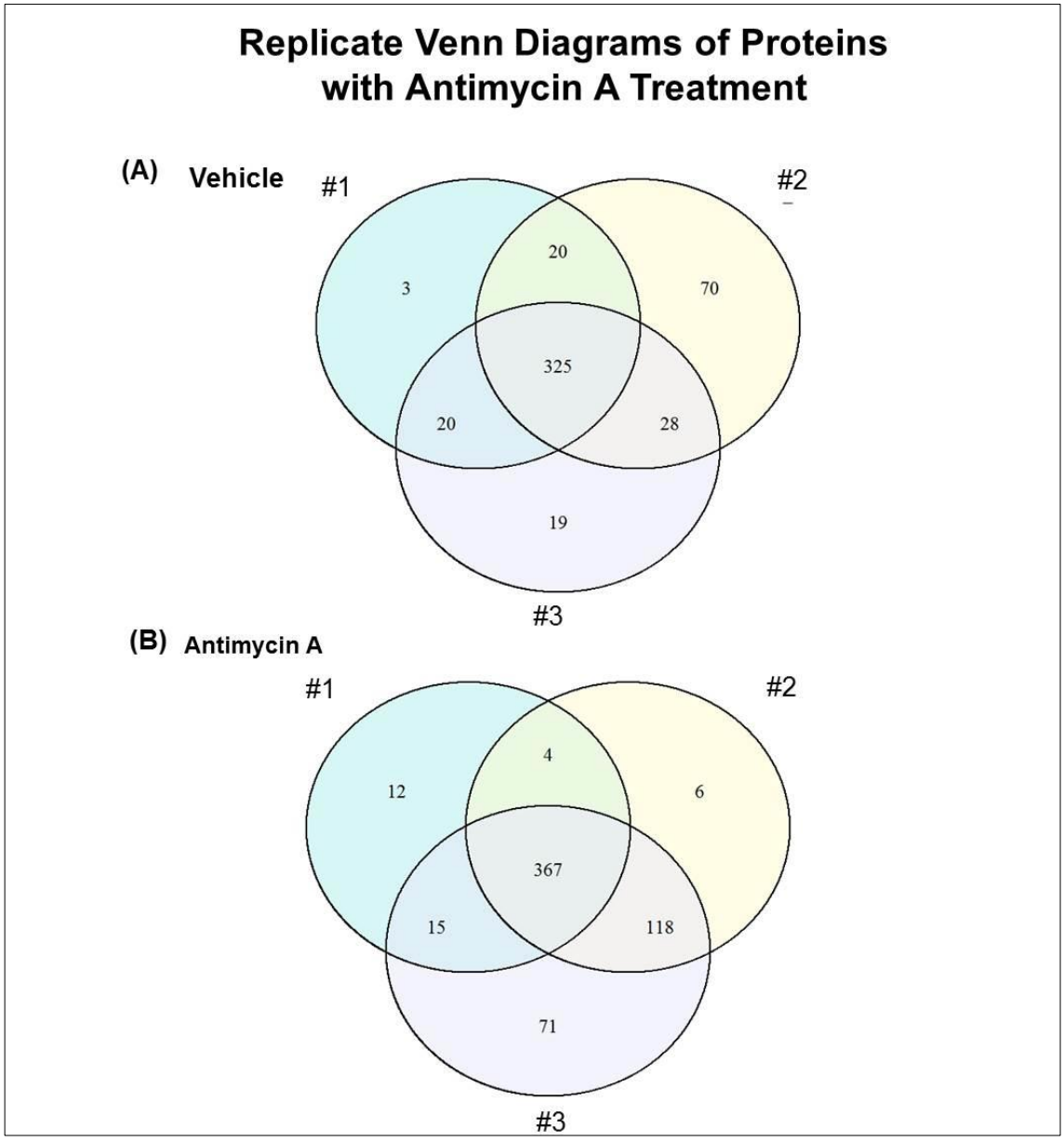

Figure 4.3.10 Overlap Analysis of Protein IDs detected in Individual Replicates for Antimycin A Dataset

Venn Diagrams illustrating overlap of Protein IDs in each replicate Vehicle (A) and high dose antimycin A treatment (B). Different colours represent individual replicates.

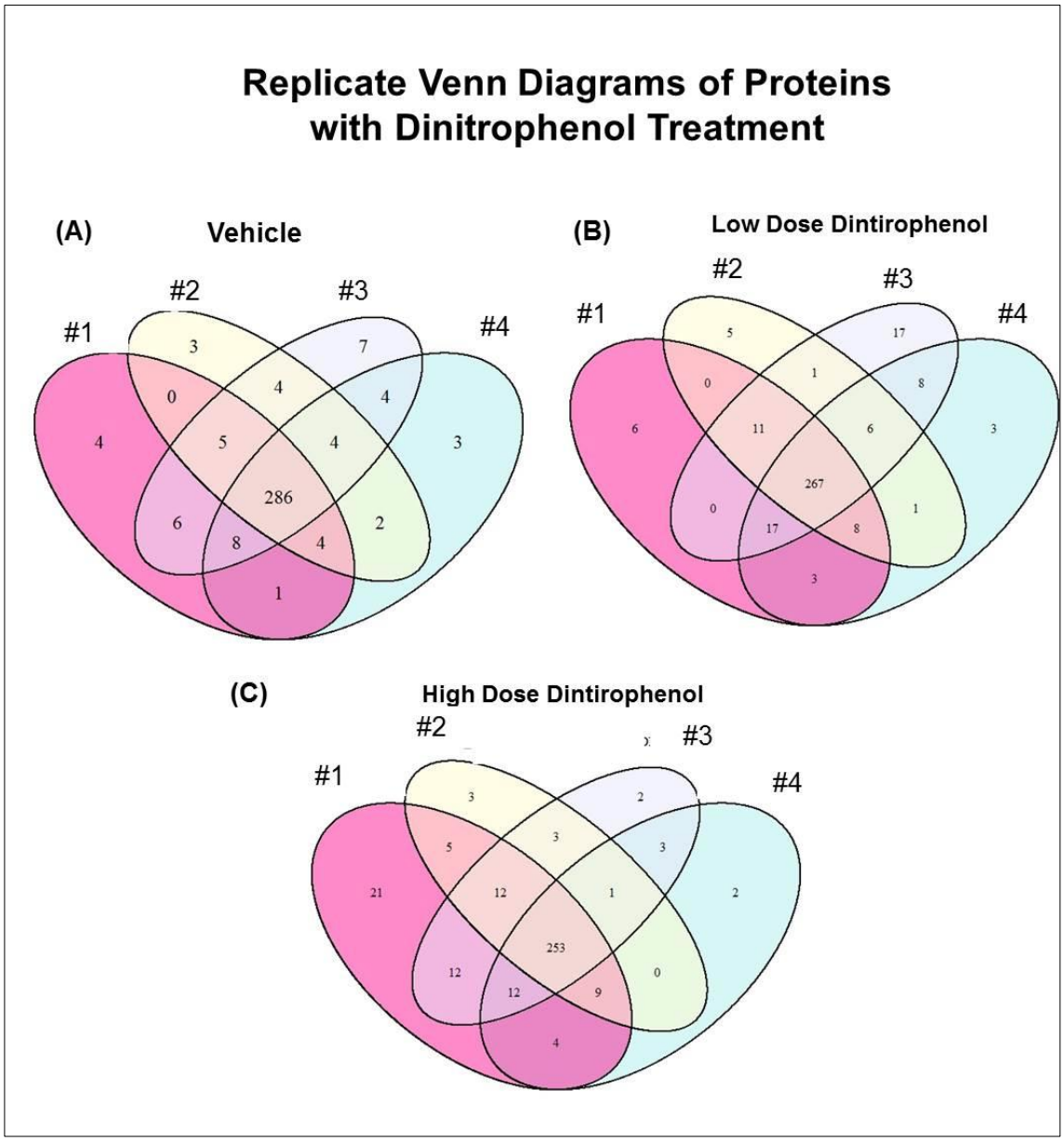

Figure 4.3.11 Overlap Analysis of Protein IDs detected in Individual Replicates for dinitrophenol Dataset

Venn Diagrams illustrating overlap of Protein IDs in each replicate Vehicle (A), low dose dinitrophenol treatment (B) and high dose dinitrophenol treatment (C). Different colours represent individual replicates.

4.3.3 Proteomics Analysis

The preceding graphs indicated that the protein data generated by the LC-MS/MS was of good quality and proteomics analysis was subsequently performed to examine changes in protein secretion in across the groups. Principle component analysis was first performed for visualisation of global trends (Figure 4.3.12) and then statistical analysis was performed on individual proteins.

Overall, the principle component analysis (PCA) shows that the different groups do not strongly cluster, indicating that there is no overwhelming trend for a global remodelling of the secretome in response to ETC toxins (Figure 4.3.1) The dinitrophenol dataset showed particularly random placement on PCA planes, indicating that dinitrophenol treatment had no coordinated effect on secreted proteins in HEK293 cells. With antimycin A treatment, there appeared to be a trend for vehicle and drug treated samples to be clustered apart, with one vehicle outlier. Lack of large global trends does not preclude there being specific groups of proteins that are significantly changed in abundance. After visualising the data, I performed statistical analysis of each protein. ANOVA or a two-sided t-test for antimycin A dataset were performed followed by a Benjamini-Hochberg correction to obtain false discovery rate values (FDR) which is statistically required due to the high chance of type I errors with multiple testing.

Statistical analysis revealed no significant changes for individual proteins for dinitrophenol which was consistent with the PCA analysis (Figure 3.3.11 C) where no clustering of different groups were displayed. Based on sample variability, FDRs of 10% and 15% were used for the rotenone and Antimycin A datasets respectively. In the literature, up to 20% FDR is used (Ting et al., 2009). Median abundances of proteins were calculated and then combined with ‘significant proteins’ to generate heat maps of significant proteins displayed in Figure 3.3.12.

The heat map illustrating the effect of Antimycin A treatment on the HEK293 secretome reveals that roughly one third of the significantly changed proteins were decreased in abundance and two thirds were increased (Figure 4.3.4). Heat maps are a useful way of visualising global trends in data. Data for individual proteins are presented in tables 4.3.2 and 4.3.3. With rotenone treatment, only one protein was

increased by at least 2 fold. This was Calsyntenin-1 and was increased 7.6 and 3.6 fold with low dose and high dose of rotenone respectively (FDR 0.06).

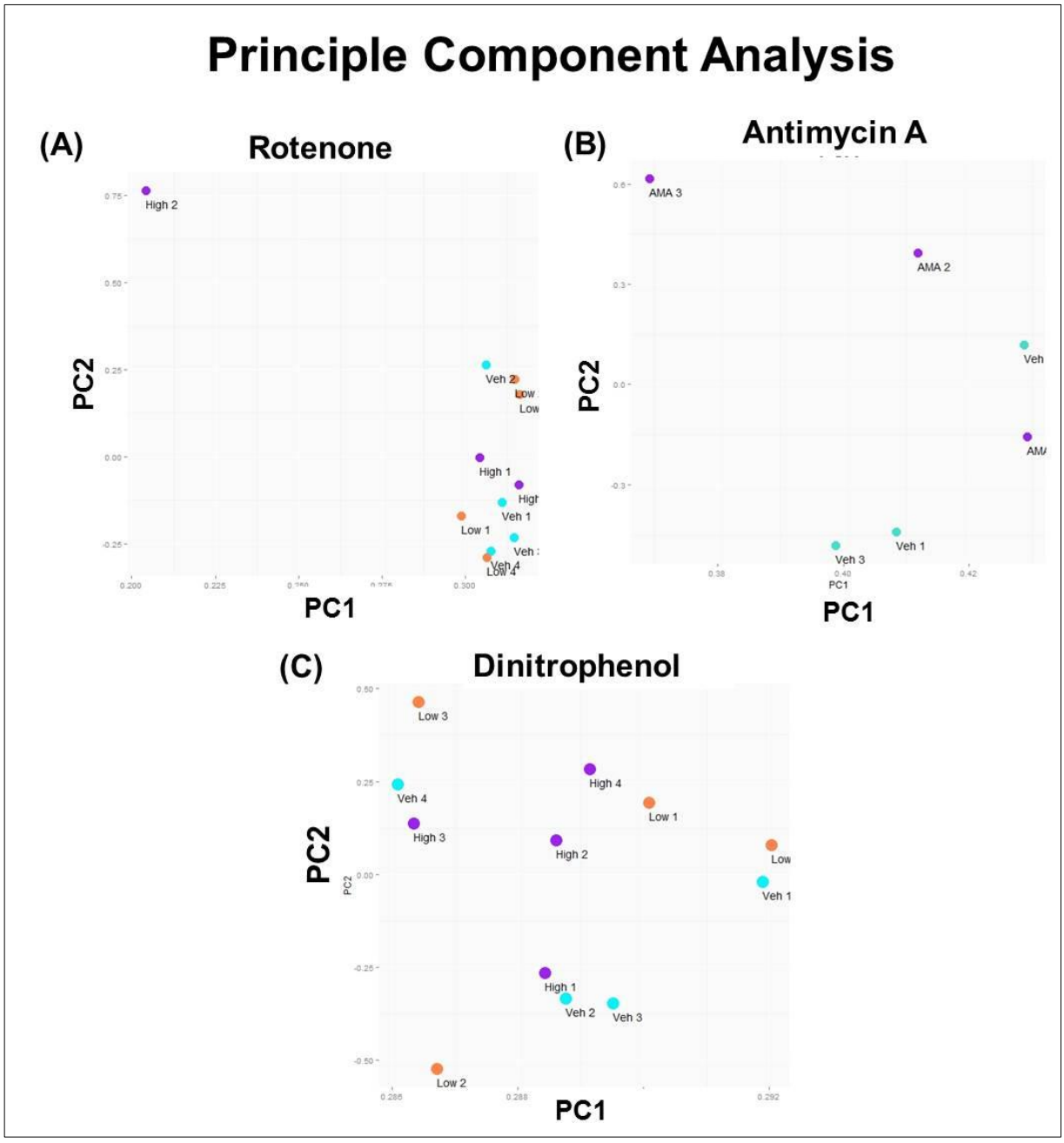

Figure 4.3.12 Principle Component Analysis (PCA) of Secreted Proteins from HEK293

PCA analysis of secreted proteins from HEK293 cells for the Rotenone dataset (A); the Antimycin A dataset (B) and the dinitrophenol dataset (C). PC1 on the x axis represents Protein IDs and PC2 on the y axis represents abundance. Replicates within one group are represented as one colour.

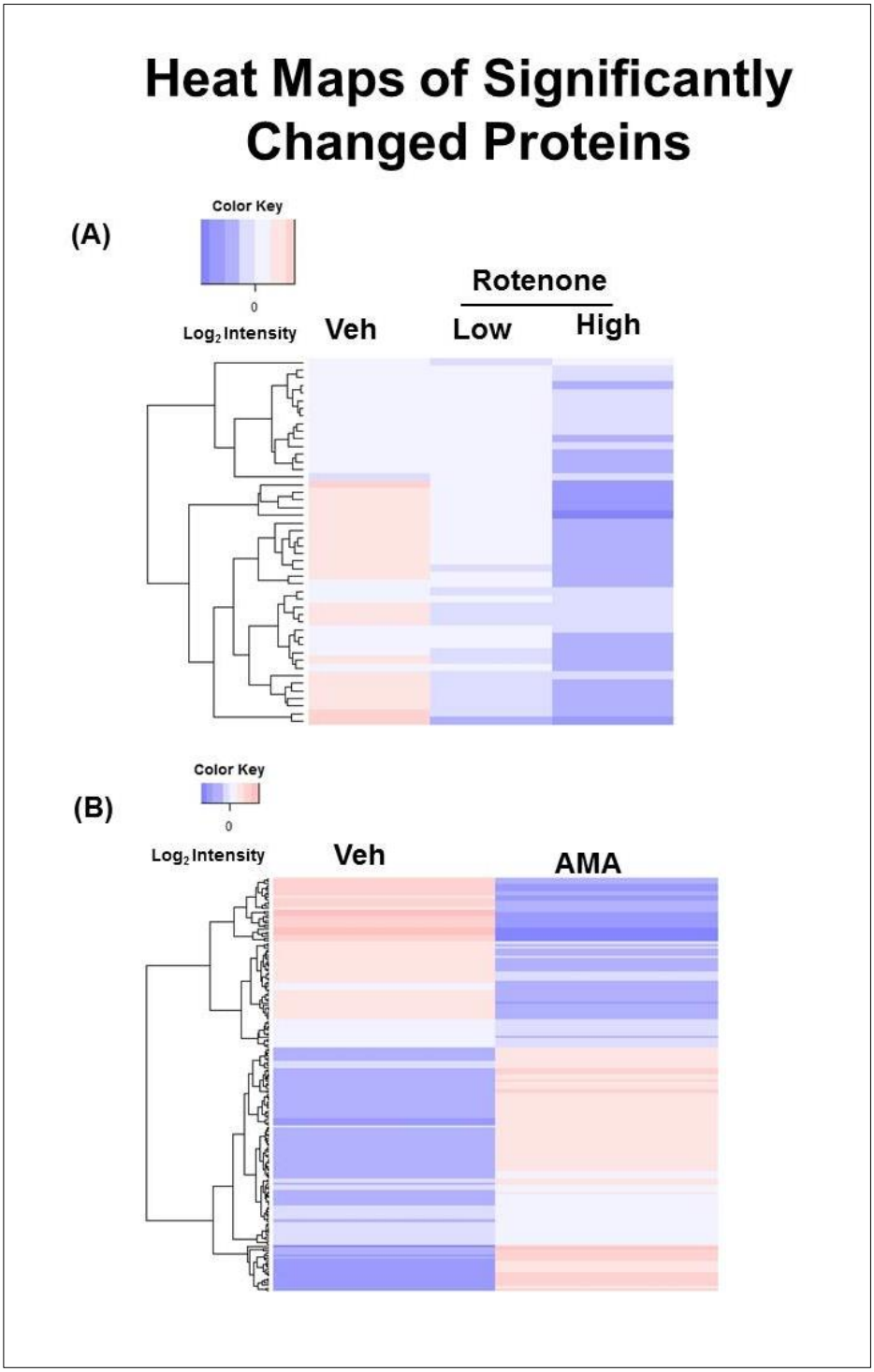

Figure 4.3.13 Abundance Heat maps of Significantly Changed Proteins in HEK293 cells

Heat map illustrating secreted proteins from HEK293 cells that were changed ($p<0.05$, with less than 10% false discovery rate) with rotenone treatment (A) and changed ($p<0.05$, with less than 15% false discovery rate) with treatment of antimycin A (B) with hierarchical clustering. Abundance was $\log_2$ transformed with the colour

representing abundance. The colour key present is coded such that white = 0, red for positive and blue for negative values. Individual proteins are represented in tables below

Table 4.3.1 Secreted Proteins Decreased in Abundance by Rotenone in HEK293 cells

Protein ID	Protein Name	Median Abundance			Fold Change		FDR
		Vehicle	Low ROT	High ROT	Low vs. Veh	High vs. Veh	
P02751	Fibronectin	4.23	0.52	0.26	0.12	0.06	0.033
Q15904	V-type proton ATPase subunit S1	1.93	0.43	1.17	0.22	0.60	0.033
O60568	Procollagen-lysine,2-oxoglutarate 5-dioxygenase 3	1.37	1.67	0.53	1.22	0.38	0.033
O75787	Renin receptor	1.32	1.70	0.47	1.28	0.35	0.033
P10909	Clusterin	2.77	0.55	0.38	0.20	0.14	0.040
Q9NS15	Latent-transforming growth factor beta-binding protein 3	3.28	0.74	0.28	0.22	0.08	0.040
P08572	Collagen alpha-2(IV) chain	1.61	1.10	0.52	0.68	0.33	0.040
Q8NBJ4	Golgi membrane protein 1	1.54	1.47	0.43	0.96	0.28	0.040
P16870	Carboxypeptidase E	5.91	0.59	0.12	0.10	0.02	0.040
Q9HBR0	Putative sodium-coupled neutral amino acid transporter 10	3.72	1.44	0.20	0.39	0.05	0.040
Q15019	Septin-2	2.41	1.18	0.38	0.49	0.16	0.040
Q86X29	Lipolysis-stimulated lipoprotein receptor	1.85	0.95	0.60	0.52	0.33	0.040
P24821	Tenascin	1.69	1.15	0.48	0.68	0.29	0.040
P16278	Beta-galactosidase	2.49	2.16	0.26	0.87	0.10	0.040
O15230	Laminin subunit alpha-5	1.78	1.72	0.29	0.97	0.16	0.040
P50897	Palmitoyl-protein thioesterase 1	1.33	1.44	0.42	1.08	0.32	0.040
P02649	Apolipoprotein E	2.26	0.98	0.61	0.43	0.27	0.045
Q14112	Nidogen-2	1.43	1.48	0.50	1.03	0.35	0.045
P11047	Laminin subunit gamma-1	2.22	1.03	0.35	0.47	0.16	0.049
Q02809	Procollagen-lysine,2-oxoglutarate 5-dioxygenase 1	2.09	0.62	0.57	0.30	0.27	0.049
O00468	Agrin	1.58	1.31	0.50	0.82	0.31	0.049
P06280	Alpha-galactosidase A	4.04	0.43	0.25	0.11	0.06	0.053
G3XAI2	Laminin subunit beta-1	3.03	0.55	0.37	0.18	0.12	0.053
P35556	Fibrillin-2	1.97	1.21	0.50	0.62	0.26	0.055

Q9HB40	Retinoid-inducible serine carboxypeptidase	1.55	1.11	0.50	0.72	0.32	0.055
Q02818	Nucleobindin-1	1.55	1.12	0.55	0.73	0.36	0.055
Q9H3G5	Probable serine carboxypeptidase CPVL	1.61	1.36	0.47	0.84	0.29	0.055
Q969P0	Immunoglobulin superfamily member 8	1.57	1.52	0.38	0.97	0.25	0.055
O00391	Sulfhydryl oxidase 1	1.22	1.42	0.48	1.17	0.40	0.055
O43405	Cochlin	1.29	1.52	0.54	1.18	0.42	0.055
Q92626	Peroxidasin homolog	2.46	0.63	0.54	0.25	0.22	0.058
P98160	Basement membrane-specific heparan sulfate proteoglycan core protein	2.42	0.87	0.51	0.36	0.21	0.058
P19022	Cadherin-2	4.49	1.64	0.11	0.37	0.03	0.058
A0A0A0MQS9	Laminin subunit alpha-4	4.04	1.50	0.57	0.37	0.14	0.058
O43854	EGF-like repeat and discoidin I-like domain-containing protein 3	2.01	0.97	0.46	0.48	0.23	0.058
Q99538	Legumain	3.74	1.93	0.12	0.52	0.03	0.058
P33908	Mannosyl-oligosaccharide 1,2-alpha-mannosidase IA	1.81	1.16	0.46	0.64	0.25	0.058
O14786	Neuropilin-1	2.68	1.01	0.45	0.38	0.17	0.065
P12109	Collagen alpha-1(VI) chain	1.66	1.44	0.38	0.87	0.23	0.066
P48723	Heat shock 70 kDa protein 13	1.04	0.46	1.63	0.44	1.57	0.066
Q13510	Acid ceramidase	2.13	1.05	0.39	0.49	0.18	0.070
P14543	Nidogen-1	1.80	0.97	0.49	0.54	0.27	0.070
H3BP20	Beta-hexosaminidase subunit alpha	2.13	0.83	0.57	0.39	0.27	0.082
C9JIZ6	Proactivator polypeptide	1.91	1.06	0.43	0.56	0.22	0.084
Q9BRK5	45 kDa calcium-binding protein	1.78	1.08	0.66	0.60	0.37	0.091
A0A087WSV8	Nucleobindin-2	1.32	1.08	0.56	0.82	0.43	0.091

Table 4.3.3 illustrates proteins secreted by HEK293 cells that displayed significantly decreased abundance with respect to vehicle upon rotenone treatment with less than 10% chance of false discovery. Rows of the table are displayed by adjusted pvalue from lowest to highest. Uniprot ID, protein name are provided along with median abundance of replicates with abundance calculated by LFQ Intensity algorithm using MaxQuant Software. “Vehicle” refers to the vehicle group, “Low ROT” refers to the low doses of rotenone group and “High ROT” refers to the high dose rotenone group. Fold changes were calculated by the median abundance treatment group / medium abundance vehicle group. FDR refers to the false discovery rate tested with a Benjamini-Hochberg

correction analysis to estimate the change of a significant pvalue in ANOVA analysis being a false discovery

Table 4.3.2 Secreted Proteins Increased in Abundance by Antimycin A treatment of HEK293 cells

Protein ID	Protein name	Median Abundance		Fold Change	FDR
		Veh	AMA		
O00469	Procollagen-lysine,2-oxoglutarate 5-dioxygenase 2	0.24	5.23	21.90	0.037
Q9H3G5	Probable serine carboxypeptidase CPVL	0.10	6.27	65.56	0.037
H3BP20	Beta-hexosaminidase subunit alpha	0.63	1.73	2.75	0.080
P07686	Beta-hexosaminidase subunit beta	0.47	1.78	3.78	0.080
O14773	Tripeptidyl-peptidase 1	0.34	2.42	7.06	0.080
C9JIZ6	Proactivator polypeptide	0.15	3.70	25.25	0.080
Q9HB71	Calcyclin-binding protein	0.13	4.04	31.17	0.080
Q8NHP8	Putative phospholipase B-like 2	0.30	3.23	10.74	0.089
Q99538	Legumain	0.20	4.01	19.82	0.093
O75083	WD repeat-containing protein 1	0.42	1.96	4.66	0.094
Q12905	Interleukin enhancer-binding factor 2	0.31	4.66	14.96	0.114
Q15691	Microtubule-associated protein RP/EB family member 1	0.39	1.95	5.00	0.125
P16278	Beta-galactosidase	0.24	3.92	16.46	0.131
O00154	Cytosolic acyl coenzyme A thioester hydrolase	0.68	1.66	2.44	0.133
Q16658	Fascin	0.69	1.75	2.54	0.133
P55072	Transitional endoplasmic reticulum ATPase	0.62	1.67	2.68	0.133
P07339	Cathepsin D	0.69	1.86	2.70	0.133
P01033	Metalloproteinase inhibitor 1	0.62	1.75	2.81	0.133
Q9BQT9	Calsyntenin-3	0.52	1.52	2.94	0.133
P09211	Glutathione S-transferase P	0.54	1.65	3.02	0.133
P01137	Transforming growth factor beta-1	0.56	1.74	3.09	0.133
Q02487	Desmocollin-2	0.56	1.81	3.24	0.133
A0A087WV23	SH3 domain-binding glutamic acid-rich-like protein 3	0.53	1.76	3.30	0.133
Q9Y3F4	Serine-threonine kinase receptor-associated protein	0.56	2.01	3.60	0.133
Q99519	Sialidase-1	0.51	1.86	3.64	0.133
O14672	Disintegrin and metalloproteinase domain-containing protein 10	0.52	1.94	3.73	0.133
A2AEA2	HLA class I histocompatibility antigen, Cw-7 alpha chain	0.57	2.15	3.78	0.133
Q02818	Nucleobindin-1	0.46	1.83	3.99	0.133
K7ELL7	Glucosidase 2 subunit beta	0.45	1.83	4.04	0.133
P61204	ADP-ribosylation factor 3	0.50	2.09	4.21	0.133
P16035	Metalloproteinase inhibitor 2	0.45	1.89	4.22	0.133
X6R8A1	Lysosomal protective protein	0.45	1.90	4.27	0.133

Q13838	Spliceosome RNA helicase DDX39B	0.45	2.00	4.40	0.133
Q9Y617	Phosphoserine aminotransferase	0.45	2.02	4.51	0.133
Q9Y5S9	RNA-binding protein 8A	0.41	1.90	4.60	0.133
Q9UQ80	Proliferation-associated protein 2G4	0.56	2.63	4.66	0.133
P49419	Alpha-aminoadipic semialdehyde dehydrogenase	0.59	2.80	4.76	0.133
P00441	Superoxide dismutase [Cu-Zn]	0.49	2.36	4.82	0.133
P13796	Plastin-2	0.43	2.06	4.83	0.133
Q9UNM6	26S proteasome non-ATPase regulatory subunit 13	0.50	2.44	4.84	0.133
P23284	Peptidyl-prolyl cis-trans isomerase B	0.43	2.13	4.90	0.133
P07814	Bifunctional glutamate/proline--tRNA ligase	0.46	2.25	4.92	0.133
P09651	Heterogeneous nuclear ribonucleoprotein A1	0.45	2.25	4.99	0.133
P61289	Proteasome activator complex subunit 3	0.47	2.43	5.16	0.133
O43852	Calumenin	0.63	3.26	5.21	0.133
P78527	DNA-dependent protein kinase catalytic subunit	0.42	2.26	5.43	0.133
P27348	14-3-3 protein theta	0.40	2.22	5.53	0.133
P62266	40S ribosomal protein S23	0.41	2.29	5.56	0.133
O15230	Laminin subunit alpha-5	0.42	2.51	5.95	0.133
Q9BTY2	Plasma alpha-L-fucosidase	0.46	2.73	5.95	0.133
P50395	Rab GDP dissociation inhibitor beta	0.41	2.53	6.15	0.133
P33991	DNA replication licensing factor MCM4	0.37	2.44	6.51	0.133
Q86X29	Lipolysis-stimulated lipoprotein receptor	0.33	2.25	6.88	0.133
P02458	Collagen alpha-1(II) chain	0.36	2.52	7.06	0.133
P55060	Exportin-2	0.45	3.42	7.58	0.133
P40926	Malate dehydrogenase, mitochondrial	0.42	3.21	7.67	0.133
P07858	Cathepsin B	0.34	2.64	7.72	0.133
Q9Y266	Nuclear migration protein nudC	0.43	3.39	7.87	0.133
P19022	Cadherin-2	0.36	2.86	8.00	0.133
P31939	Bifunctional purine biosynthesis protein PURH	0.33	2.73	8.31	0.133
P12081	Histidine--tRNA ligase, cytoplasmic	0.33	2.88	8.80	0.133
P63104	14-3-3 protein zeta/delta	0.39	3.42	8.82	0.133
O43405	Cochlin	0.41	3.59	8.84	0.133
P50914	60S ribosomal protein L14	0.36	3.27	9.07	0.133
P39060	Collagen alpha-1(XVIII) chain	0.34	3.07	9.16	0.133
P14543	Nidogen-1	0.25	2.38	9.55	0.133

Q15008	26S proteasome non-ATPase regulatory subunit 6	0.28	2.72	9.65	0.133
O00231	26S proteasome non-ATPase regulatory subunit 11	0.30	2.89	9.72	0.133
P48723	Heat shock 70 kDa protein 13	0.33	3.21	9.76	0.133
P31946	14-3-3 protein beta/alpha	0.37	3.77	10.15	0.133
Q12906	Interleukin enhancer-binding factor 3	0.33	3.52	10.56	0.133
P62993	Growth factor receptor-bound protein 2	0.43	4.77	11.15	0.133
Q12841	Follistatin-related protein 1	0.34	3.88	11.29	0.133
O60568	Procollagen-lysine,2-oxoglutarate 5-dioxygenase 3	0.25	2.83	11.47	0.133
P41252	Isoleucine--tRNA ligase, cytoplasmic	0.39	4.66	11.90	0.133
Q9HBR0	Putative sodium-coupled neutral amino acid transporter 10	0.31	3.78	12.32	0.133
P35268	60S ribosomal protein L22	0.30	4.01	13.18	0.133
Q9BRK5	45 kDa calcium-binding protein	0.32	4.29	13.55	0.133
H3BLZ8	Probable ATP-dependent RNA helicase DDX17	0.28	4.00	14.45	0.133
Q14766	Latent-transforming growth factor beta-binding protein 1	0.23	3.55	15.41	0.133
P13611	Versican core protein	0.27	4.50	16.67	0.133
P13797	Plastin-3	0.23	3.83	16.84	0.133
P62258	14-3-3 protein epsilon	0.21	3.88	18.16	0.133
P26639	Threonine--tRNA ligase, cytoplasmic	0.25	5.78	22.77	0.133
P18206	Vinculin	0.20	5.08	25.19	0.133
Q08380	Galectin-3-binding protein	0.26	8.45	32.31	0.133
E9PB61	THO complex subunit 4	0.15	5.50	37.06	0.133
Q92598	Heat shock protein 105 kDa	0.40	2.93	7.31	0.134
P12955	Xaa-Pro dipeptidase	0.31	3.95	12.93	0.137
P11047	Laminin subunit gamma-1	0.27	3.31	12.35	0.139
E7EUF1	Ectonucleotide pyrophosphatase/phosphodiesterase family member 2	0.48	1.53	3.20	0.140
Q9NZI8	Insulin-like growth factor 2 mRNA-binding protein 1	0.33	2.13	6.44	0.140
O00391	Sulfhydryl oxidase 1	0.19	3.36	17.67	0.140
P54136	Arginine--tRNA ligase, cytoplasmic	0.29	6.47	22.20	0.140
P33908	Mannosyl-oligosaccharide 1,2-alpha-mannosidase IA	0.18	4.57	24.82	0.140
P63244	Guanine nucleotide-binding protein subunit beta-2-like 1	0.21	5.41	25.17	0.140
P07437	Tubulin beta chain	0.41	2.03	4.93	0.142
Q9H4F8	SPARC-related modular calcium-binding protein 1	0.44	2.54	5.82	0.142
Q15631	Translin	0.23	2.40	10.39	0.142

P18669	Phosphoglycerate mutase 1	0.59	1.60	2.70	0.143
P32119	Peroxiredoxin-2	0.23	4.67	20.19	0.144
P11413	Glucose-6-phosphate 1-dehydrogenase	0.19	4.02	20.68	0.144

Table 4.3.2 illustrates proteins secreted by HEK293 cells that displayed significantly increased abundance with respect to vehicle upon antimycin A treatment with less than 15% chance of false discovery. Rows of the table are displayed by adjusted pvalue from lowest to highest. Uniprot ID, protein name are provided along with median abundance of replicates with abundance calculated by LFQ Intensity algorithm using MaxQuant Software. “Vehicle” refers to the vehicle group and “AMA” refers to the antimycin A group. Fold changes were calculated by the median abundance treatment group / medium abundance vehicle group. FDR refers to the false discovery rate tested with a Benjamini-Hochberg correction analysis to estimate the change of a significant pvalue in ANOVA analysis being a false discovery.

Table 4.33 Secreted Proteins Decreased in Abundance by Antimycin A treatment of HEK293 cells

Protein ID	Protein Name	Median Abundance		Fold Change	FDR
		Veh	AMA		
P50897	Palmitoyl-protein thioesterase 1	8.93	0.22	0.02	0.037
O00115	Deoxyribonuclease-2-alpha	9.23	0.12	0.01	0.080
A0A087X1N8	Serpin B6	7.07	0.16	0.02	0.094
O43684	Mitotic checkpoint protein BUB3	13.54	0.12	0.01	0.133
Q14112	Nidogen-2	10.67	0.12	0.01	0.133
Q8NBJ4	Golgi membrane protein 1	6.29	0.09	0.01	0.133
P06280	Alpha-galactosidase A	7.64	0.12	0.02	0.133
A0A087WZM2	Ribonuclease T2	8.01	0.17	0.02	0.133
P28066	Proteasome subunit alpha type-5	10.42	0.26	0.03	0.133
P51991	Heterogeneous nuclear ribonucleoprotein A3	6.10	0.18	0.03	0.133
B0QY89	Eukaryotic translation initiation factor 3 subunit L	4.87	0.16	0.03	0.133
J3KPS3	Fructose-bisphosphate aldolase A	6.40	0.21	0.03	0.133
P53634	Dipeptidyl peptidase 1	6.67	0.29	0.04	0.133
P08670	Vimentin	5.19	0.24	0.05	0.133
P12814	Alpha-actinin-1	4.69	0.23	0.05	0.133
P00492	Hypoxanthine-guanine phosphoribosyltransferase	4.91	0.24	0.05	0.140
P55268	Laminin subunit beta-2	7.74	0.08	0.01	0.140
P11908	Ribose-phosphate pyrophosphokinase 2	5.82	0.14	0.02	0.140

Table 4.3.3 illustrates proteins secreted by HEK293 cells that displayed significantly decreased abundance with respect to vehicle upon antimycin A treatment with less than 15% chance of false discovery. Rows of the table are displayed by adjusted pvalue from lowest to highest. Uniprot ID, protein name are provided along with median abundance of replicates with abundance calculated by LFQ Intensity algorithm using MaxQuant Software. “Vehicle” refers to the vehicle group and “AMA” refers to the antimycin A group. Fold changes were calculated by the median abundance treatment group / medium abundance vehicle group. FDR refers to the false discovery rate tested with a Benjamini-Hochberg correction analysis to estimate the change of a significant pvalue in ANOVA analysis being a false discovery

Following statistics, biological interpretation of data was analysed. Network analysis and KEGG analysis were performed on proteins that were significantly downregulated by rotenone, upregulated by antimycin A and downregulated by antimycin A. To approach this, Protein IDs were exported to string database (www.string-db.org) using "high confidence (0.7) for the minimum required interaction score and only selecting experiments and databases parameters for active interaction sources. The parameters selected above are fairly stringent. This data was subject to KEGG pathway enrichment analysis presented in Table 4.3.4.

KEGG enrichment analysis for proteins with reduced secretion by rotenone showed that "ECM-receptor interaction" was the top enriched pathway with 9 proteins which included the following genes AGRN, COL4A2, COL6A1, FN,1 HSPG2, LAMA5, LAMB, LAMC1 and TNC. The next enriched pathway was "lysosome". This included 7 proteins encoded by the following genes ASAH1, ATP6AP1, GLA, GLB1, HEXA, LGMN, PPT1, PSAP. "Focal adhesion", "small cell lung cancer", "amoebiasis" and "PI3K-Akt signaling pathway" included several genes that were also annotated under "ECM-receptor interaction". Other enriched pathways included "sphingolipid metabolism" which genes including ASAH1, GLA and GLB1. Note that 2 of these genes were also annotated under "Lysosome". After regarding genes that were annotated under multiple pathways or related pathways, the KEGG data overall shows that that lysosomal proteins and extracellular matrix proteins were the primary networks altered with mitochondrial inhibition.

There were several KEGG pathways that were significantly enriched by proteins increased in abundance with antimycin A treatment. "Lysosome" was also a top enriched pathway for proteins that were upregulated by antimycin A, along with "Other glycan degradation", Aminoacyl-tRNA biosynthesis" and "Cell cycle". Other enriched pathways that included proteins also annotated under "Lysosome" included "Other glycan degradation", "glycosphingolipid biosynthesis – ganglio series" and "Glycosaminoglycan degradation" the pathways "other glycan degradation", "glycosaminoglycan degradation", "Fatty acid elongation" and "galactose metabolism" (Table 4.3.4). This is consistent with the rotenone dataset. Similarly to the rotenone dataset, "ECM-receptor interaction" and some other pathways included proteins

annotated under that pathway ID. The only enriched KEGG pathway for proteins decreased in abundance with antimycin A (FDR<1%) was also “Lysosome” with 4 proteins contributing to the annotation encoded by CTSC, DNASE2, GLA and PPT1.

Table 4.3.4 KEGG Enrichment Analysis on Secreted Proteins Decreased in Abundance by Rotenone

Pathway ID	Pathway Description	Observed Gene Count	FDR
4512	ECM-receptor interaction	9	4.32E-11
4142	Lysosome	8	2.36E-08
4510	Focal adhesion	7	2.22E-05
5222	Small cell lung cancer	5	7.11E-05
5146	Amoebiasis	5	0.000164
4151	PI3K-Akt signaling pathway	7	0.000329
600	Sphingolipid metabolism	3	0.00578

Table 4.3.4 displays significantly enriched (FDR<1%) KEGG pathways by gene ontology on Secreted Proteins that were Decreased in response to Complex I inhibition in HEK293 cells. The table provides the KEGG “Pathway ID” and “Pathway Description”. The number of proteins that were annotated under a particular pathway was represented as “Observed Gene Count” and the FDR is provided.

Table 4.3.5 KEGG Enrichment Analysis on Secreted Proteins Increased and decreased in Abundance by Antimycin A

Pathway ID	Pathway Description	Observed Gene Count	FDR
Increased with Antimycin A			
511	Other glycan degradation	4	0.000117
970	Aminoacyl-tRNA biosynthesis	5	0.000117
4110	Cell cycle	7	0.000117
4142	Lysosome	7	0.000117
5169	Epstein-Barr virus infection	8	0.000161
604	Glycosphingolipid biosynthesis - ganglio series	3	0.00192
3050	Proteasome	4	0.00192
531	Glycosaminoglycan degradation	3	0.0032
5146	Amoebiasis	5	0.00396
4151	PI3K-Akt signaling pathway	8	0.00492
5203	Viral carcinogenesis	6	0.00522
4612	Antigen processing and presentation	4	0.00603
Decreased with Antimycin A			
4142	Lysosome	4	0.000557

Table 4.3.5 displays significantly enriched (FDR<1%) KEGG pathways by gene ontology in response to Complex III inhibition in HEK293 cells. Secreted proteins that were significantly increased in abundance by antimycin A compared with vehicle (titled – "Increased with Antimycin A") and decreased by antimycin A (titled – "Decreased with Antimycin A") were separately subject to KEGG pathway enrichment analysis by gene ontology. The table provides the KEGG "Pathway ID" and "Pathway Description". The number of proteins that were annotated under a particular pathway was represented as "Observed Gene Count" and the FDR is provided.

4.3 Discussion

This chapter characterised the complement of proteins secreted from HEK293 cells in response to ETC stress. Principle component analysis and high FDR values obtained when proteins were analysed statistically revealed that overall there were no major trends for remodelling of secreted proteins from HEK293 cells in response to dinitrophenol. Rotenone treatment reduced the secretion of a number of proteins, but there were more differences with antimycin A despite variability. Antimycin A treatment caused many proteins to have altered secretion both increased and decreased. The fact that many proteins showed reduced secretion in response to rotenone and antimycin A, argues against a "leak" of intracellular proteins into the media from dead cells. Indeed the fact that cell viability was relatively unaffected with the chosen doses of compounds, provides support for these being bona fide secretion changes. Interestingly, although there were some similarities in terms of which proteins had decreased secretion with rotenone and antimycin A, there were many proteins which were not concordant, suggesting that there are site-specific effects with mitochondrial inhibition. The reason for such differences between Complex I and III remains to be determined.

Pathway analysis revealed that strikingly, lysosomal proteins responded dynamically to ETC stress. This was evidenced by 'lysosomes' being amongst the top enriched pathways with both antimycin A and rotenone treatment. Also many of the other pathways hits included proteins that were also annotated under lysosomes. Lysosomes are acidic organelles that are rich in hydrolytic and proteolytic enzymes that degrade proteins and other biomolecules. More recently, it has been appreciated that lysosomes play a role in autophagy, cellular signaling and can also be trafficked to the plasma membrane where they undergo exocytosis (Abrahamsen & Stenmark, 2010). In fact, lysosomal exocytosis is considered to be a pathway of non-conventional protein secretion (Johansson, Nandakumar, Persson, Olsson, & Hansson, 2009; Luo et al., 2011; Nickel, 2003). Extending on this idea, contents of autophagosomes can be trafficked to the plasma membrane and secreted in vesicles in a process recently termed 'secretory autophagy' or 'exophagy' which is also considered a process of non-classical protein secretion (Abrahamsen & Stenmark, 2010; Manjithaya & Subramani, 2011; Ponpuak et al., 2015). The process of lysosomal exocytosis was mostly thought to occur

in myeloid cells in response to pathogens (Griffiths, 2016) whereas secretory autophagy is not cell type specific (Abrahamsen & Stenmark, 2010). Therefore, it is most likely that the enrichment of lysosomal proteins being secreted from the HEK293 cells in the current study is from secretory autophagy.

Lysosomal function can be heavily influenced by changes in nutrient turnover and signaling through metabolic pathways (Mony, Benjamin, & O'Rourke, 2016; Settembre, Fraldi, Medina, & Ballabio, 2013) and thus it is not surprising that lysosomal function is sensitive to mitochondrial inhibition (C. Y. Lim & Zoncu, 2016). Given that lysosomes are metabolically sensitive and mitochondria are the primary site of energy production within in the cell, it is conceivable that mitochondrial function is communicated to lysosomes. Indeed a recent literature trend highlights mitochondrial-lysosomal cross-talk as being important for cellular fitness (Raimundo, Fernandez-Mosquera, Yambire, & Diogo, 2016). It has been demonstrated in several models over the last few years that lysosomal dysfunction results in an accumulation of dysfunctional mitochondria through defective mitophagy but more recently it was shown that the converse is true whereby mitochondrial respiration affects lysosomal function (Baixauli et al., 2015). This provides evidence that perturbations of mitochondrial function are communicated to lysosomes. While autophagy is generally considered to be a response to cellular stress, one of the strongest stimuli is starvation (R. Singh & Cuervo, 2011). Further, limited availability of nutrients including amino acids, lipids and glucose also trigger autophagy (R. Singh & Cuervo, 2011). It is of interest to note that a starvation-like response is observed in muscle from a mouse model of late-onset mitochondrial myopathy (Tyynismaa et al., 2010). The transcription factor TFEB is well characterised in controlling lysosome and autophagic function in response to cellular stressors such as ER stress. A related transcription factor, TFE3 is now known to control lysosomal physiology and autophagy but in response to nutritional and metabolic stimuli (Martina et al., 2014). This reveals a mechanistic link between metabolic/ nutritional status and autophagy.

Since the proteomics data presented in this chapter is concerned with secreted proteins it is important to consider whether mitochondrial stress signals changes in lysosomal function that could result in exit of lysosomes or autophagosomes. An obvious

mechanism by which this may occur is other reason this mitochondria-lysosomal communication being coupled with non-conventional protein secretion is interesting, is because mitochondrial dysfunction can result in mitophagy (section 1.3). Since 'secreted autophagy' or 'exophagy' is a mechanism of non-conventional protein secretion, perhaps mitophagy is similarly coupled with protein secretion in a process that could be termed 'exomitophagy'. This could explain older observations that mtDNA can be amplified in microvesicles (Guescini, Genedani, et al., 2010; Guescini, Guidolin, et al., 2010). However, the secretion dataset from the HEK293 cells did not show a strong enrichment for mitochondrial proteins like it did for lysosomes. Extracellular acidification of breast cancer cells causes trafficking of lysosomes from perinuclear regions to the plasma membrane for exocytosis (Glunde et al., 2003) which is interesting as Complex I or III defects could acidify media by lactate. Further, lysosomal exocytosis is also triggered by the nutrient sensitive transcription factor TFE3 mentioned above (Martina et al., 2014) which makes it plausible that metabolic status could control lysosomal exocytosis. There is also an idea in the literature that autophagy can be coupled with exosome shedding (Baixauli, Lopez-Otin, & Mittelbrunn, 2014) which is another potential pathway by which lysosomal contents may be secreted from the cell.

While it is plausible that mitochondrial stress or cellular metabolic perturbations could affect lysosomal function and potentially lead to secretion of lysosomal components, a challenge with the interpretation of this data is that although secretion of lysosomal proteins were increased with antimycin A treatment and also downregulated by antimycin A and rotenone. This may suggest that lysosomal exocytosis and/ or secretory autophagy are altered with contents varying in a selective, highly regulated fashion. While degradative autophagy is a regulated, selective process (Johansen & Lamark, 2011), there is currently no evidence for cargo selection in secretory autophagy (Ponpuak et al., 2015). Further, published studies that have characterised the proteome of lysosomes have not addressed secretory lysosomes. This makes it difficult to speculate why some lysosomal proteins were upregulated and some lysosomal proteins were downregulated. Further, different lysosomal proteins did not change in the same ratio. With antimycin A treatement Cathepsin B was upregulated ~8 fold while Cathepsin D just ~3 fold. This suggests that it is not simply a process whereby

lysosomal proteins are all stochiometrically exported but rather the cargo being exported is selectively regulated. Further, the abundance of lysosomal proteins that were downregulated had higher levels in the vehicle group than lysosomal proteins that were upregulated which suggests that there is some activity in a basal state that is an inherently different process to what occurs in response to mitochondrial stress. It is also important to consider that these experiments were performed in serum-free culture conditions and serum-free conditions are a stimulus for autophagy (R. Singh & Cuervo, 2011). Hence the vehicle may have had a supraphysiological 'baseline' activity.

Although there is not enough literature on the topic to speculate why secretion of some lysosomal proteins are increased and others are decreased (Ponpuak et al., 2015), I noticed that the proteins Ceroid-lipofuscinosis neuronal protein 5 and Tripeptidyl-peptidase 1 that were upregulated with antimycin A are associated with lipofuscin-loaded lysosomes. Density of lipofuscin-loaded lysosomes are known to increase with ageing and senescence (Terman, Kurz, Navratil, Arriaga, & Brunk, 2010). Interestingly, although lipofuscin can form from any type of cellular material, mitochondria are an important source (Terman, Gustafsson, & Brunk, 2006). Hence it is possible that large loads of mitochondrial stress impose cause lysosomes to accumulate lipofuscin but it is not known whether lipofuscin-loaded lysosomes are coupled with secretion.

Other strongly enriched pathways from proteins downregulated with rotenone included 'ECM-receptor interaction' and 'focal adhesion'. Many of these genes are extracellular matrix proteins are highly secreted proteins involved in basement membrane deposition. These proteins are highly secreted from mammalian cells and are required to maintain integrity and support of physiological tissues and they also generally decline with the ageing process (Kurtz & Oh, 2012). The secretion of these proteins may be a bioenergetically demanding process, explaining the reduction in secretion of these proteins with mitochondrial stressors.

Although proteins networked together well in these datasets, there were some orphan proteins that were of interest due to potential roles in progression of complex disease including amyloid proteins, insulin-like growth factor binding proteins and transforming growth factor related proteins. Secretion of Amyloid beta A4 protein (APP) and

Amyloid beta precursor-like protein 2 (APLP2) were both increased with antimycin A treatment (Table 4.2.2). They are ubiquitously expressed proteins that are important for growth and development and known to be secreted and present in conditioned medium (Dyrks, Monning, Beyreuther, & Turner, 1994; R. Wang, Meschia, Cotter, & Sisodia, 1991; Webster et al., 1995). Enhanced expression is associated with cancer progression (Pandey et al., 2016) and dysfunction is associated with Alzheimer's disease. Mitochondrial stress has been shown to promote amyloid beta formation and cellular stress but this is the first report to my knowledge of mitochondrial stress causing secretion of these proteins. Interestingly, autophagy mediates the secretion of amyloid beta (Nilsson & Saido, 2014) which is consistent with the observation of many lysosomal proteins being secreted with antimycin A treatment discussed earlier.

Secretion of insulin-like growth factor binding protein 2 (IGFBP2) was increased by antimycin A treatment. This is interesting because a *Drosophila* IGFBP homologue has been shown to link mitochondrial stress with lifespan extension through dampened IGF signaling (Owusu-Ansah et al., 2013) Secretion of latent-transforming growth factor beta-binding protein 3 (LTBP3) and transforming growth factor beta-1 (TGFβ1) were both decreased with antimycin A treatment. LTBP3 secretion was also reduced by rotenone. TGFβ is a cytokine that has been shown to inhibit mitochondrial function promoting glycolysis (Jiang et al., 2015; S. Y. Lee et al., 2015).

As outlined in the introduction of this chapter, a major motive for exploring cell non-autonomous communication in mammalian cells was inspired by work that found cell non-autonomous induction of mitochondrial stress in *C.elegans* (Durieux et al., 2011). The authors have readdressed this finding and found that the effect is mediated by neuropeptide alterations (Berendzen et al., 2016) which was also supported by another study (Shao, Niu, & Liu, 2016). Hence it is most likely a neuron specific effect that is not even necessarily evolutionarily conserved. By using a broader approach, where I characterised proteins being secreted from a well characterised, standard cellular model HEK293, I found that secretion of lysosomal proteins were dynamically regulated by ETC stress and I speculate that mitochondria-lysosome communication coupled with secreted autophagy or lysosomal exocytosis may be a pathway in which mitochondrial stress is linked with non-conventional protein secretion. Although, since the PCA

showed that there was no convincing remodelling of the secretome in response to ETC stress in HEK293 cells, I next wanted to explore the question in cell types that are considered more professional secretory cells and play large roles in whole body physiology in the subsequent chapters.

CHAPTER 5: CHARACTERISING THE SECRETOME OF PRIMARY MURINE HEPATOCYTES UNDER MITOCHONDRIAL STRESS

5.1 Introduction

In the previous chapter, there were changes in the secretion of certain proteins in response to Complex I and Complex III inhibition, but no evidence for an overwhelming remodelling of the secretome in HEK293 cells in response to mitochondrial stress. I next wanted to explore the same question in cells that are involved in regulation of whole body energy metabolism and are known to secrete a large number of proteins (more recognised secretory cells) as I hypothesised that these cells may be more likely to undergo more extensive remodelling of the secretome in response to mitochondrial perturbations. Some of the major organs secreting bioactive factors involved in whole body energy metabolism include muscle, liver and adipose tissue (Oh et al., 2016). Secreted proteins in response to mitochondrial stress in muscle include Fibroblast growth factor 21 (FGF21) (Davis et al., 2013; K. H. Kim et al., 2013) and Growth and differentiation factor 15 (GDF15) (Chung et al., 2017; Ji et al., 2016). Secretions in response to mitochondrial stress from liver and adipose tissue are currently largely unexplored. I therefore aimed to characterise the secretome in hepatocytes (present chapter) and adipocytes (next chapter).

Liver is a visceral organ primarily composed of hepatocytes and long known to have important roles in production of plasma proteins (Miller, Bly, Watson, & Bale, 1951), packageing and secretion of lipoproteins and cholesterol (Janero, Siuta-Mangano, Miller, & Lane, 1984; Vance & Vance, 1986), xenobiotic detoxification (Grant, 1991), bile production (Coleman, 1987) and secretion of inflammatory proteins (Robinson, Harmon, & O'Farrelly, 2016). More recently, the liver and hepatocytes have been shown to secrete proteins with important roles regulating whole body energy homeostasis (Iroz, Couty, & Postic, 2015; Stefan & Haring, 2013). For example, Fetuin-A is a hepatokine (Lebensztejn, Flisiak-Jackiewicz, Bialokoz-Kalinowska, Bobrus-Chociej, & Kowalska, 2016) that promotes lipid induced insulin resistance (Pal et al., 2012) and development of T2DM (Stefan et al., 2014). Fetuin-B is also a hepatokine

(Dietzel et al., 2013) that has recently been demonstrated to cause glucose intolerance in muscle (Meex et al., 2015).

Mitochondrial dysfunction is associated with metabolic conditions including insulin resistance (Koliaki & Roden, 2016) and non-alcoholic hepatic steatosis (Sunny, Bril, & Cusi, 2016). Less liver-specific mouse models of mitochondrial dysfunction have been reported than other tissues. One study using a conditional liver knockout of the COX10 gene, a subunit of cytochrome c oxidase or Complex IV, found that the hepatocytes could meet bioenergetic needs by glycolysis and gluconeogenesis *in vivo* for long periods but did not look at distal tissues (Diaz et al., 2008) so cell non-autonomous signaling of liver specific mitochondrial stress cannot be speculated. Similarly, mice with a liver-specific PGC-1β deficiency have decreased hepatic mitochondrial fatty acid oxidation but similarly effects in distal tissues were not characterised (Chambers et al., 2012) and a liver-specific mouse model of mtDNA depletion showed enhanced diet induced liver dysfunction (Bottani et al., 2014), but in neither of these models were the metabolic vulnerabilities or adaptions in other tissues like adipose or muscle explored. Overall, cell non-autonomous effects of hepatic mitochondrial dysfunction have not been studied to date.

Studies characterising the secretome of hepatocytes using a shotgun based proteomics approach include a comparison of different hepatocyte cell lines (Slany et al., 2010), of human hepatocytes in response to inflammatory stimuli including IL-6 stimulation (Nakata et al., 2014) and dengue fever viral infection (Higa et al., 2008), and in hepatocyte models of perturbed lipid homeostasis (Meex et al., 2015). T2DM patients treated with pioglitazone, a PPAR-γ agonist which stimulates mitochondrial biogenesis, but not metformin which is known to inhibit mitochondrial function, displayed reduced Fetuin-A levels (Mori et al., 2008) suggesting that alterations in mitochondrial function may affect the levels of protein secreted from the liver. Thyroid hormone treatment, which is known to stimulate mitochondrial biogenesis of hepatocytes, increases secretion of major liver-produced, plasma proteins (Hertzberg, Pindyck, Mosesson, & Grieninger, 1981). Senescence, which is typically associated with mitochondrial decline, also causes an altered secretome in hepatocytes (Irvine et al., 2014). These studies collectively imply a connection between mitochondria and secretion of proteins

from liver, however, there are no published studies that have analysed the secretome of hepatocytes in direct response to ETC stressors.

Thus the aim of this chapter was to characterise the ETC sensitive secretome of primary murine hepatocytes (hepatocytes) by performing LC-MS/MS based shotgun proteomics on the conditioned medium collected from hepatocytes treated with an ETC Complex I inhibitor, rotenone, ETC Complex III inhibitor, antimycin A and an OXPHOS uncoupler, dinitrophenol.

5.2 Methods Summary

Hepatocyte isolation and culture was performed as described in section 2.1 In brief, livers of anaesthetised mice were perfused with collagenase to digest liver. The liver was then excised and membrane gently torn to release hepatocytes which were strained and washed, then counted and plated in a medium containing insulin, dexamethasone, FBS and BSA. Four hours later, the medium was changed to a serum and albumin free media with only dexamethasone.

Oxygen consumption rate dose response curves to ETC toxins were characterised using the Seahorse XF-96 Bioanalyser in HEK293 cells. Following selection of doses, cell viability and cell death were determined using propidium iodide, and AlamarBlue stains. Cells were stringently washed then incubated with ETC toxins at the respective doses in serum free medium then 24 hours later conditioned medium was collected by spinning and filtering to pellet and clear cell debris to prevent contamination the samples with intracellular proteins. An acetone precipitation was performed and trypsin digest was performed according to methods.

Peptides were separated and mass analysed by LC-MS/MS on ThermoXCalibur raw files were subjected to MaxQuant Analysis to map peptide sequences with protein IDs. MaxQuant calculates an LFQ intensity algorithm as a surrogate for protein abundance. Data analysis was performed in the R language using R studio.

5.3 Results

5.3.1 Model of ETC Stress in Primary Hepatocytes

As with the previous chapter, oxygen consumption rate (OCR) was measured in dose response in primary hepatocytes for rotenone, to model Complex I inhibition, antimycin A, to model Complex III inhibition and 2,4-dinitrophenol (DNP) to model an OXPHOS uncoupler using (Figure 5.2.1). The OCR for rotenone-treated hepatocytes showed a similar sigmoidal curve to that observed in HEK293 cells in the last chapter, albeit with slightly less sensitivity (Fig 5.2.1A). The OCR response for Antimycin A (Figure 5.2.1B) was unusual, having little effect on hepatocytes and then causing a steep drop. Because of the strange shape of this curve, I repeated this experiment with antimycin A sourced from a different laboratory and saw the same shaped curve, indicating that it is a real effect in primary hepatocytes. DNP cause a steep incline in OCR in the range of 50-100μM (Fig 5.2.1C). Due to the disparity in these dose response relationships, a low (IC_{10}) and high (IC_{50}) was selected for rotenone, while a single dose of compound was examined for antimycin A and DNP.

Despite the variable effects of the different compounds, two independent tests (alamar blue and propidium iodide staining) showed that cell viability was not affected with overnight treatment with the selected doses (Fig 5.2.2).

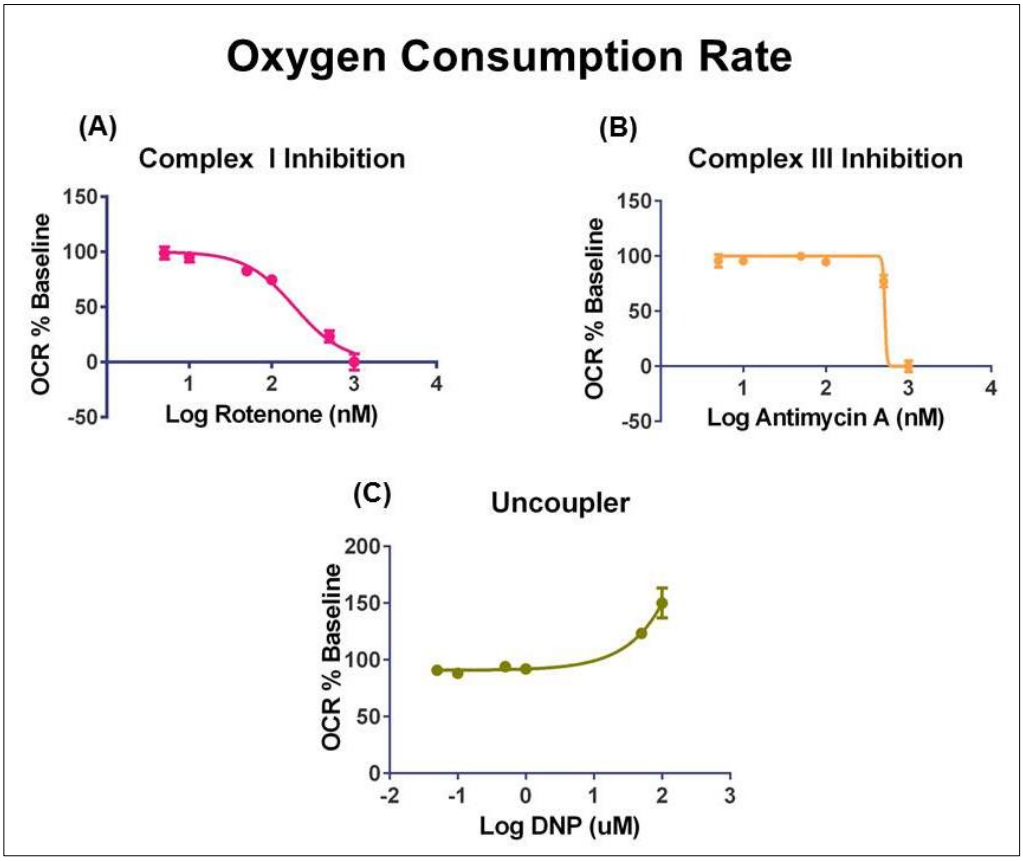

Figure 5.2.1 Dose Response Curves of ETC Inhibitors in Primary Murine Hepatocytes

Oxygen consumption rate (OCR) was measured by Seahorse-XF96 Bioanalyser before and after drug injections in dose response. Results are expressed as a percentage of the baseline OCR reading after corresponding drug dose. (A) Complex I inhibitor Rotenone, (B) Complex III inhibitor Antimycin A (C) OXPHOS/ETC Uncoupler 2,4-dinitrophenol.

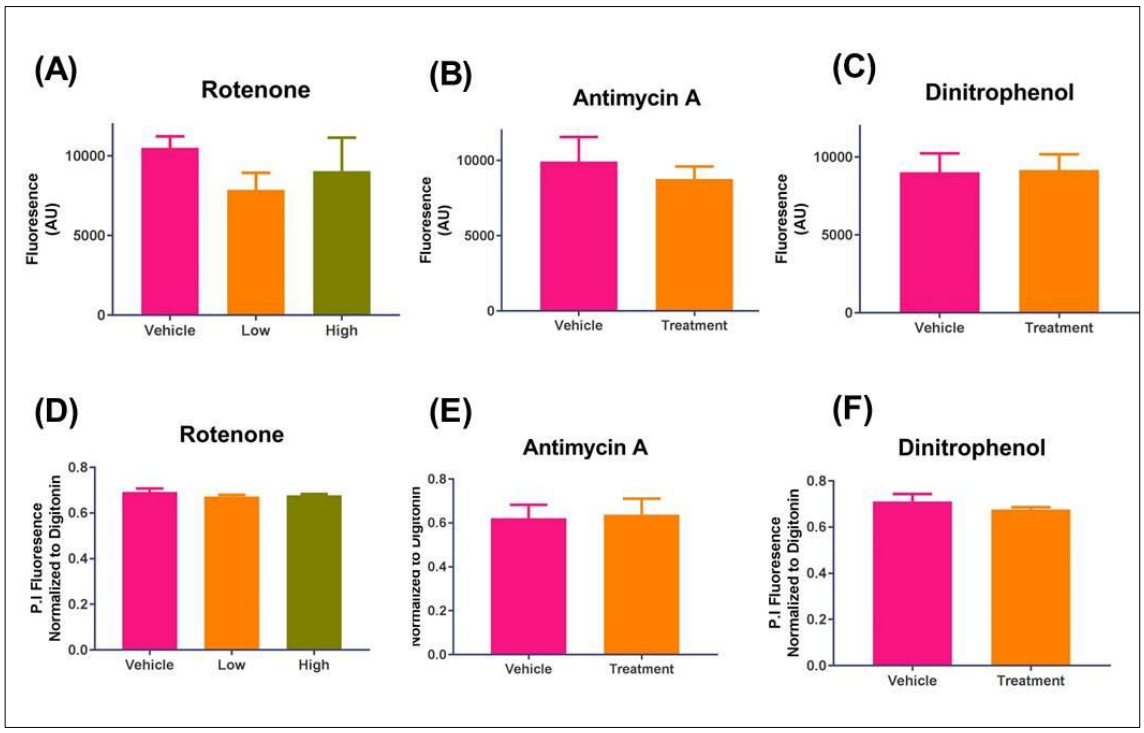

Figure 5.3.2 Cell Viability of Hepatocytes Treated with Defined Doses of Inhibitors

Hepatocytes treated for 48 hours with DMSO vehicle, 50 nM and 500 nM rotenone (A) & (E); Ethanol vehicle and 100 nM antimycin A (B) & (F); and H_2O vehicle and 100 µM dinitrophenol (C) & (G) labelled "vehicle", "Low" for low dose and "High" for high dose respectively. Alamar blue fluorescence was measured (A), (B) & (C) presented in fluorescence arbitrary units. Propidium iodide (P.I) fluorescence was measured, then measured again after a 30 minute incubation with 600 µM digitonin as a positive control of permeable cells. Fluroescence data was normalised to digitonin.

5.2.3 Validation of Extracellular Location of Detected Proteins

In total there were 656, 610 and 682 independent proteins identified in the media from the rotenone, antimycin A or DNP datasets respectively after data filtering. Whether or not proteins detected by MS were likely to be secreted was assessed by examining the presence of a secretion signal peptide (Figure 5.3.3) or whether the proteins were annotated as being localised to the extracellular compartments were determined using gene ontology (Figure 5.3.4). Of total proteins detected to be secreted from hepatocytes, 31%, 32% and 31% had a secretion signal peptide for classical protein secretion in the rotenone, antimycin A and dinitrophenol datasets, respectively (Figure 5.3.3). Annotation analysis by gene ontology showed that 67%, 68% and 68% of proteins were consistent with being extracellular (Figure 5.3.4). These numbers are similar to those observed in HEK293 cells in the previous chapter.

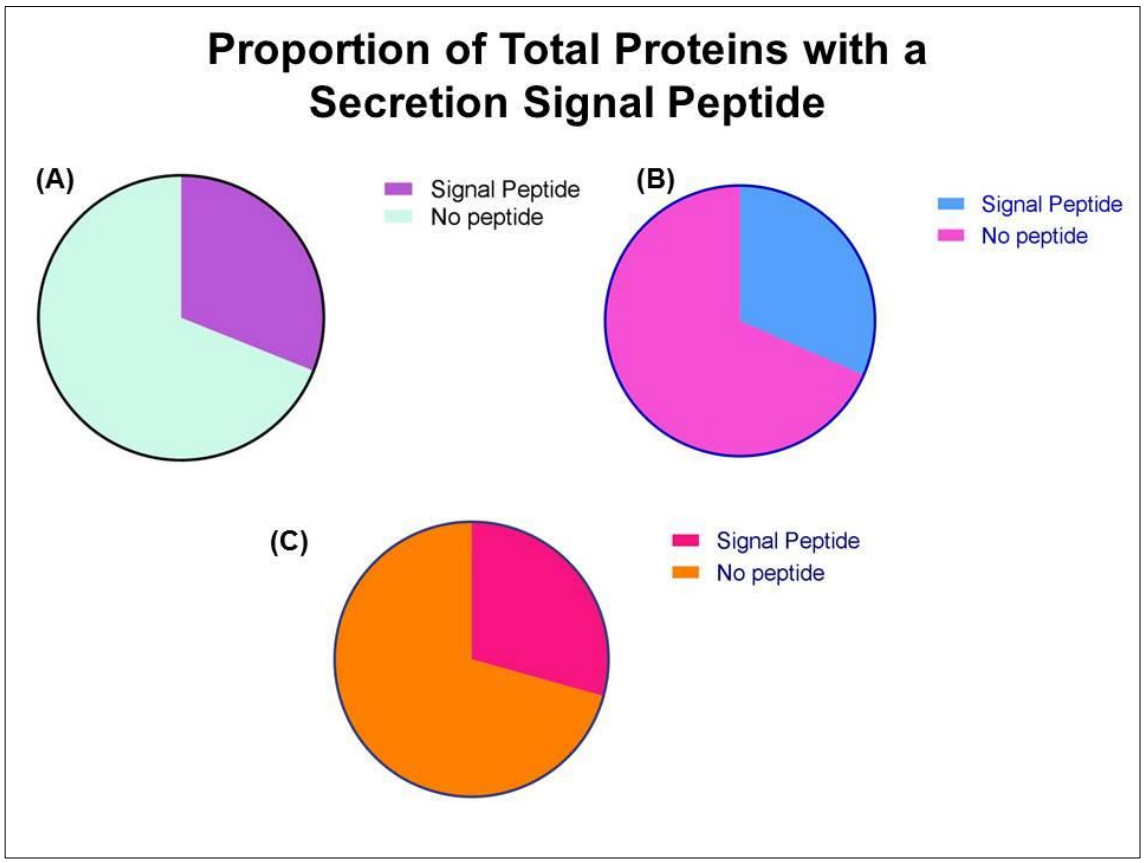

Figure 5.3.3 Proportion of all Detected Proteins with a Predicted Secretion Signal Peptide by Sequence Analysis in Hepatocytes

All proteins detected by LC-MS/MS in each experimental group were pooled after data filtering for the Rotenone dataset (A) the Antimycin A dataset (B) and the Dinitrophenol dataset (C). Amino acid sequences were exported to the SecretomeP tool that predicts whether or not a protein has a secretion signal peptide based on sequence.

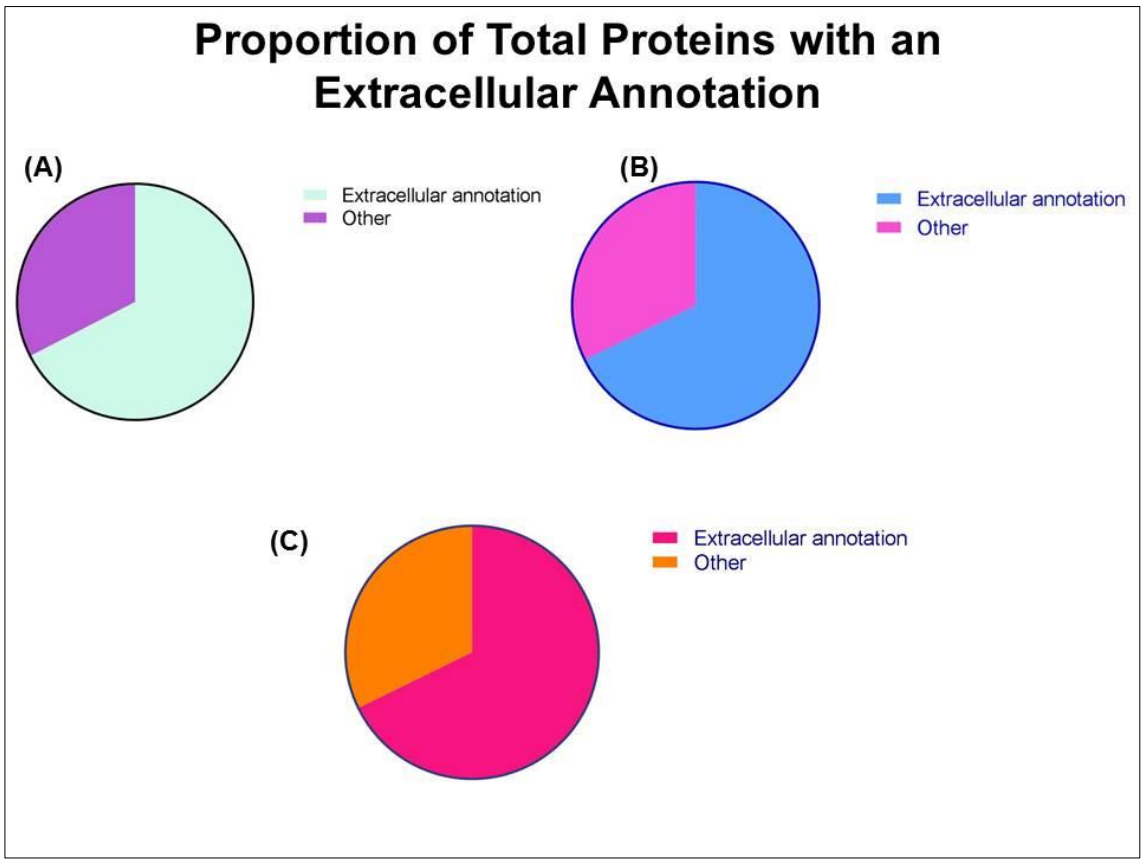

Figure 5.3.4 Proportion of all Detected Proteins with an Extracellular Annotation by Gene Ontology in Hepatocytes

All proteins detected by LC-MS/MS in each experimental group were pooled after data filtering for the Rotenone dataset (A), the Antimycin A dataset (B) and the Dinitrophenol dataset (C). Cellular Component Analysis by Gene ontology was performed and the number of proteins that had an extracellular annotation (removing duplicates when a protein was annotated under multiple extracellular annotations) are graphed as a percentage of total proteins where "Extracellular Annotation" refers to proteins with an extracellular annotation and "other" refers to the remainder of proteins. For hepatocytes, there were 6 extracellular annotations included in the analysis: "Extracellular Exosome", "Extracellular Vesicle", "Extracellular Region Part" , "Extracellular Region", "Extracellular Space", "Extracellular Matrix", "Proteinaceous Extracellular Matrix" and "Extracellular Matrix Component".

5.2.2 Assessment of Data Quality and Correlation

To confirm for data quality, data correlation and replicate reproducibility was assessed by performing multiscatter analysis of (Figures 5.3.6 – 5.3.8) and frequency histograms (Figure 5.3.9) of log_2 transformed LFQ Intensity values. were performed for each replicate to analyse correlation between replicates. Overlap of Protein IDs amongst replicates for each group is presented as venn diagrams (Figures 5.3.10 – 5.3.12) to measure the overlap of proteins identified by MS within an experimental group.

Multiscatter plots illustrated that samples were very tightly correlated amongst groups with Pearson's Correlation Coefficient values all greater than 0.9 (except Vehicle replicate 2 vs. DNP replicate 4 which had a R^2 value of 0.89). Indeed most were greater than 0.95 suggesting extremely good correlation between the different replicates.

Figure 5.3.9 illustrated that for all experimental groups the merged frequency histograms of individual replicates were very well superimposed, which indicates that the distribution of frequencies of log_2 LFQ intensity values were reproducible between replicates.

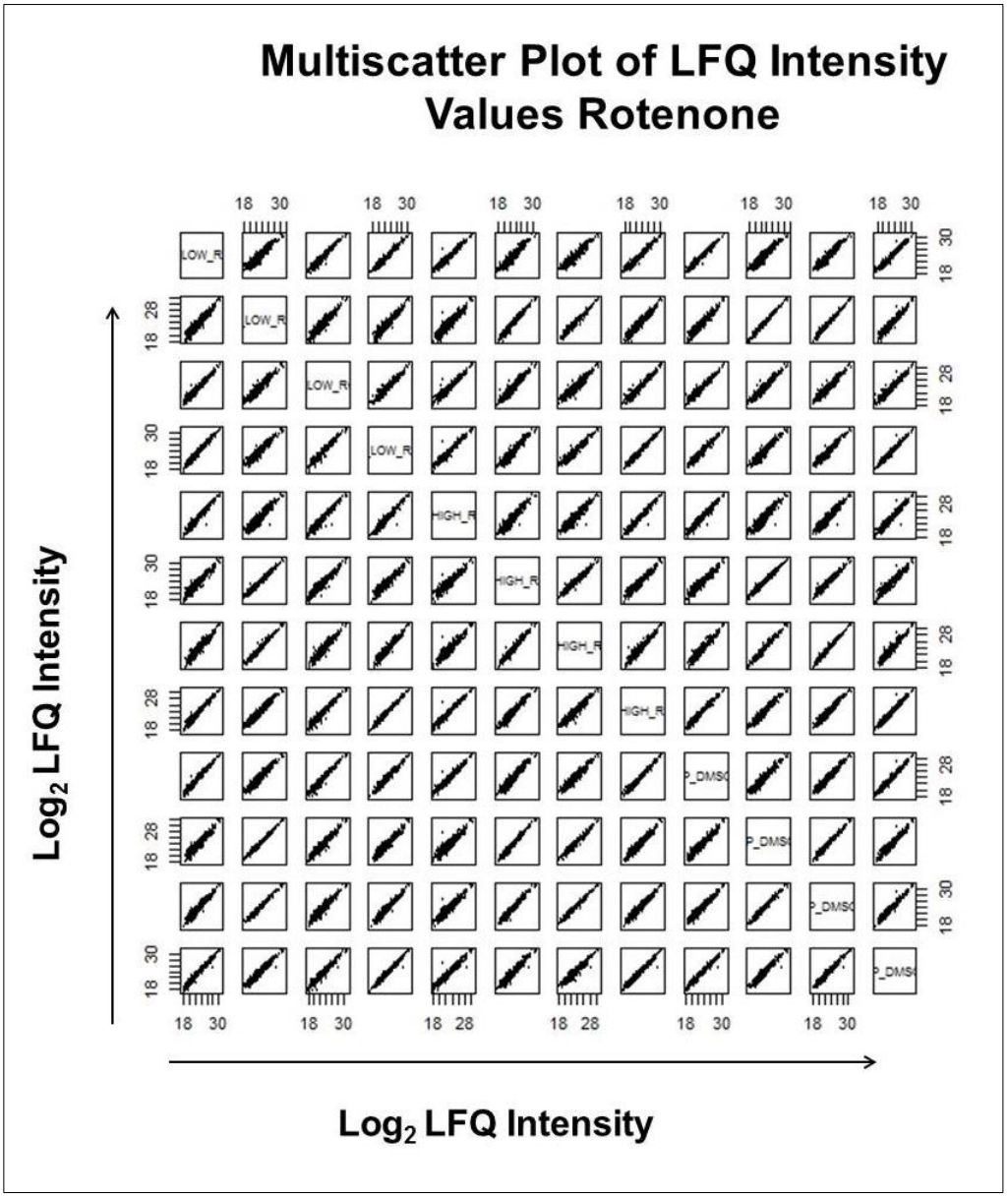

Figure 5.3.5 Multiscatter Plot of every LFQ Intensity values from Individual Samples for Rotenone Dataset in Hepatocytes

Log_2 transformed LFQ Intensity values for each single protein after filtering were plotted (one dot represents the Log_2 transformed LFQ Intensity value of one detected protein) for each sample of the rotenone dataset. From left to right – the first 4 samples are the low dose rotenone group; the following 4 samples are the 4 replicates of the high dose rotenone group; and the following 4 samples are the 4 replicates of the vehicle group.

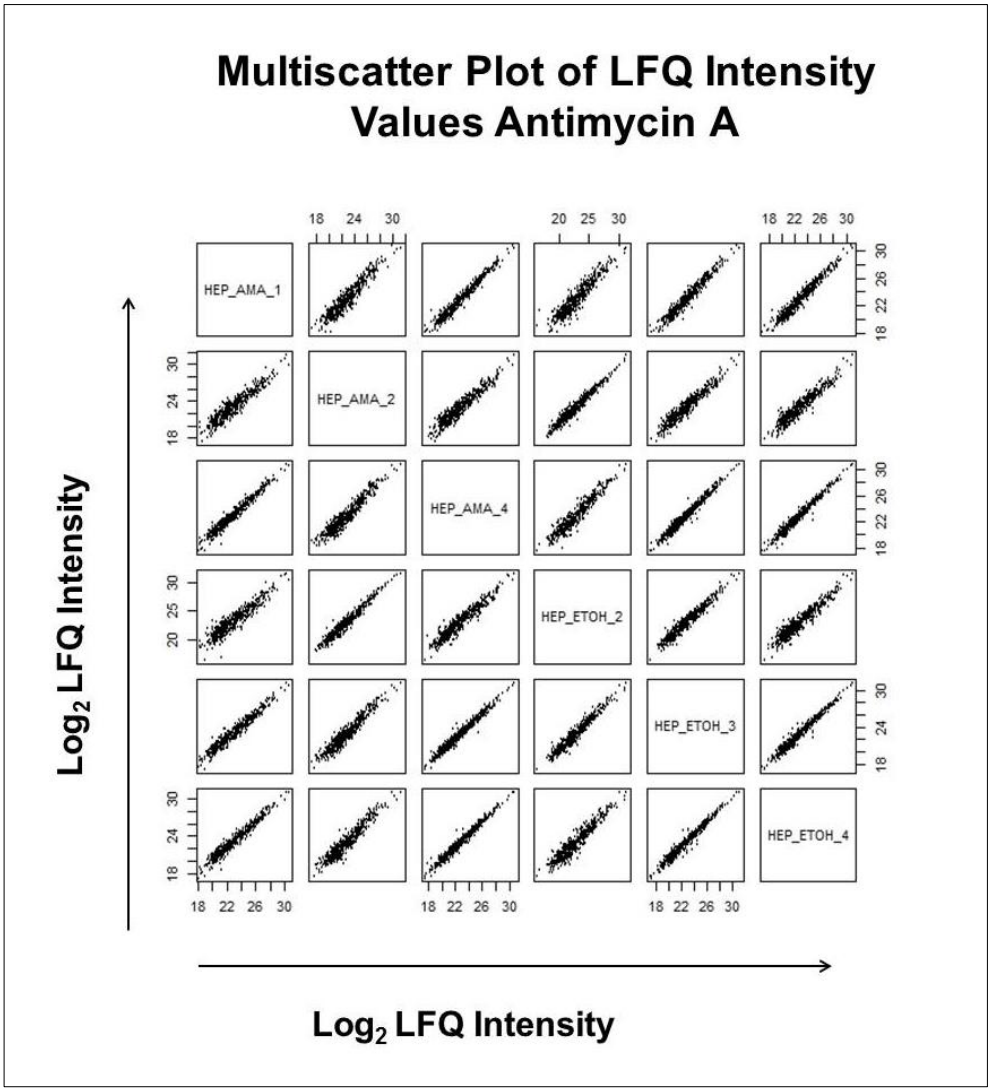

Figure 4.3.6 Multiscatter Plot of every LFQ Intensity values from Individual Samples for Antimycin A Dataset in Hepatocytes

Log_2 transformed LFQ Intensity values for each single protein after filtering were plotted (one dot represents the Log_2 transformed LFQ Intensity value of one detected protein) for each sample of the rotenone dataset. From left to right – the first 3 samples are the 3 replicates of the antimycin A treated group and the following 3 replicates are the 3 replicates of the vehicle group.

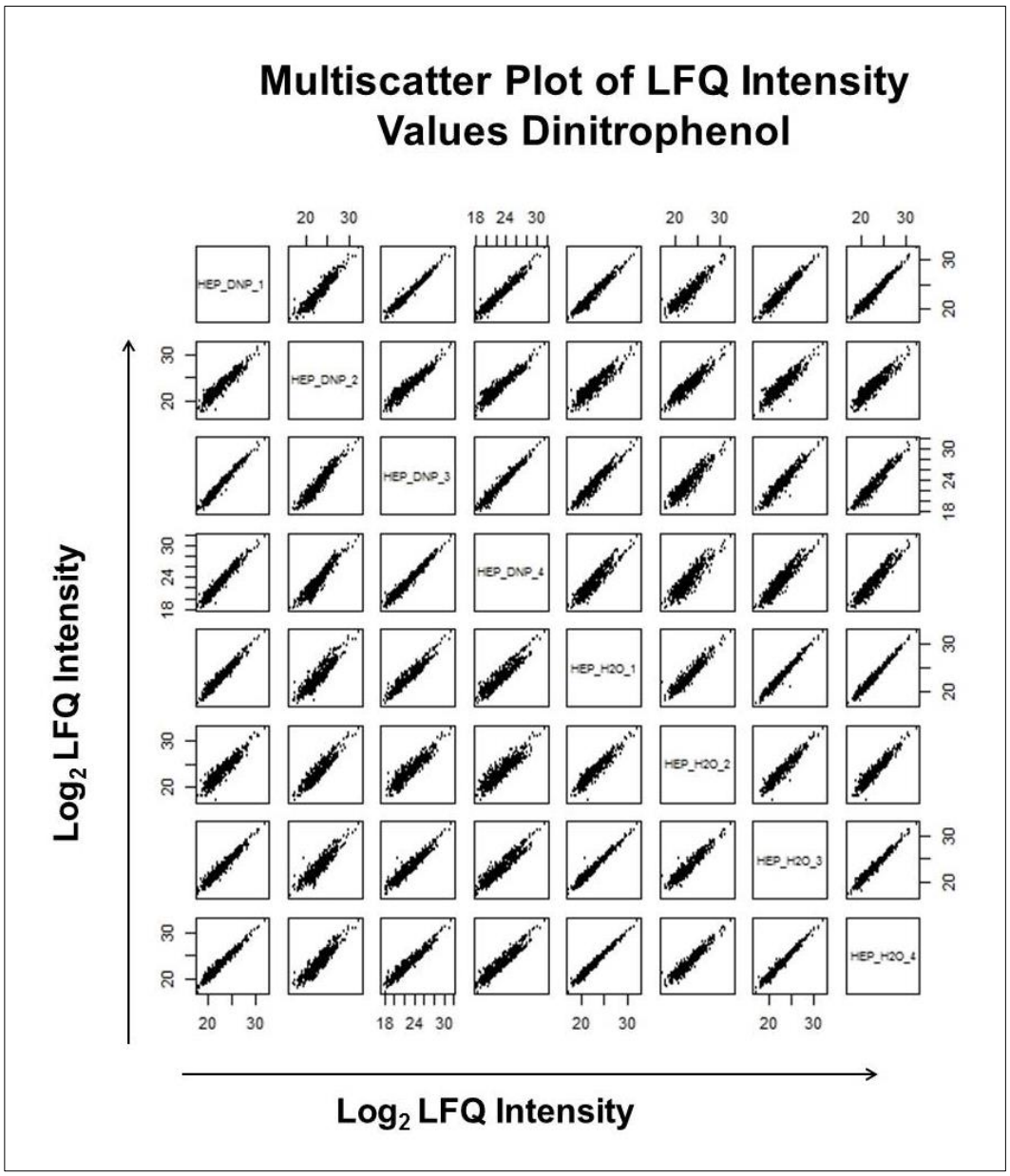

Figure 5.3.7 Multiscatter Plot of every LFQ Intensity values from Individual Samples for Dinitrophenol Dataset in Hepatocytes

Log_2 transformed LFQ Intensity values for each single protein after filtering were plotted (one dot represents the Log_2 transformed LFQ Intensity value of one detected protein) for each sample of the rotenone dataset. From left to right – the first 4 samples are the 4 replicates of the high dose dinitrophenol group; the following 4 samples are the 4 replicates of the; low dose dinitrophenol group and the following 4 samples are the 4 replicates of the vehicle group.

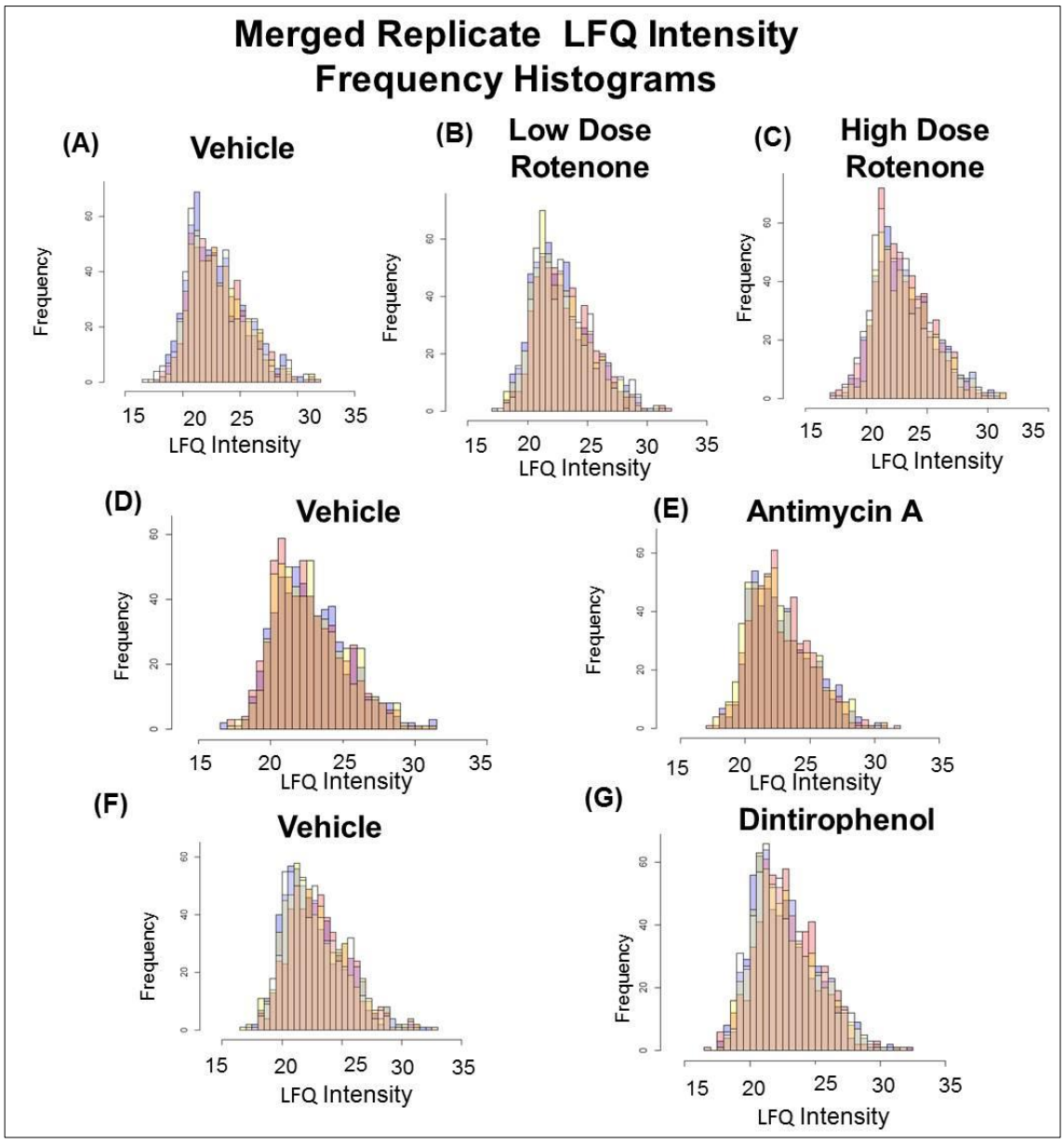

Figure 5.3.8 Merged Replicate Frequency Histograms of Log2 LFQ Intensity Values

Log_2 transformed LFQ Intensity Values were plotted as frequency histograms for each replicate and merged within each experimental group – (A) Vehicle for rotenone dataset, (B) low dose rotenone treatment, (C) High Dose rotenone, (D) Vehicle for antimycin A dataset, (E) antimycin A treatment, (F) Vehicle for dinitrophenol dataset, (G) dinitrophenol treatment, Different colours represent individual replicates.

Venn diagrams on protein IDs (Figures 5.3.9 – 5.3.11) were constructed to measure the overlap of proteins identified by MS within an experimental group. For the rotenone dataset, protein ID overlap between 4 out of 4 replicates was 79%, 79% and 73% for vehicle, low dose and high dose experimental groups respectively. For vehicle and Antimycin A 82% and 80% overlap of protein IDs was observed for the vehicle and antimycin A groups respectively in 3 out of 3 replicates. Similarly, 81% overlap of protein IDs was displayed in both the vehicle and the dinitrophenol treated groups in 4 out of 4 replicates.

Analysis of data correlation and replicate reproducibility illustrated that the data is of good quality for label free MS. Overall, the data correlation and replicate reproducibility was of high quality and of greater quality than that obtained for HEK293 cells in chapter 4.

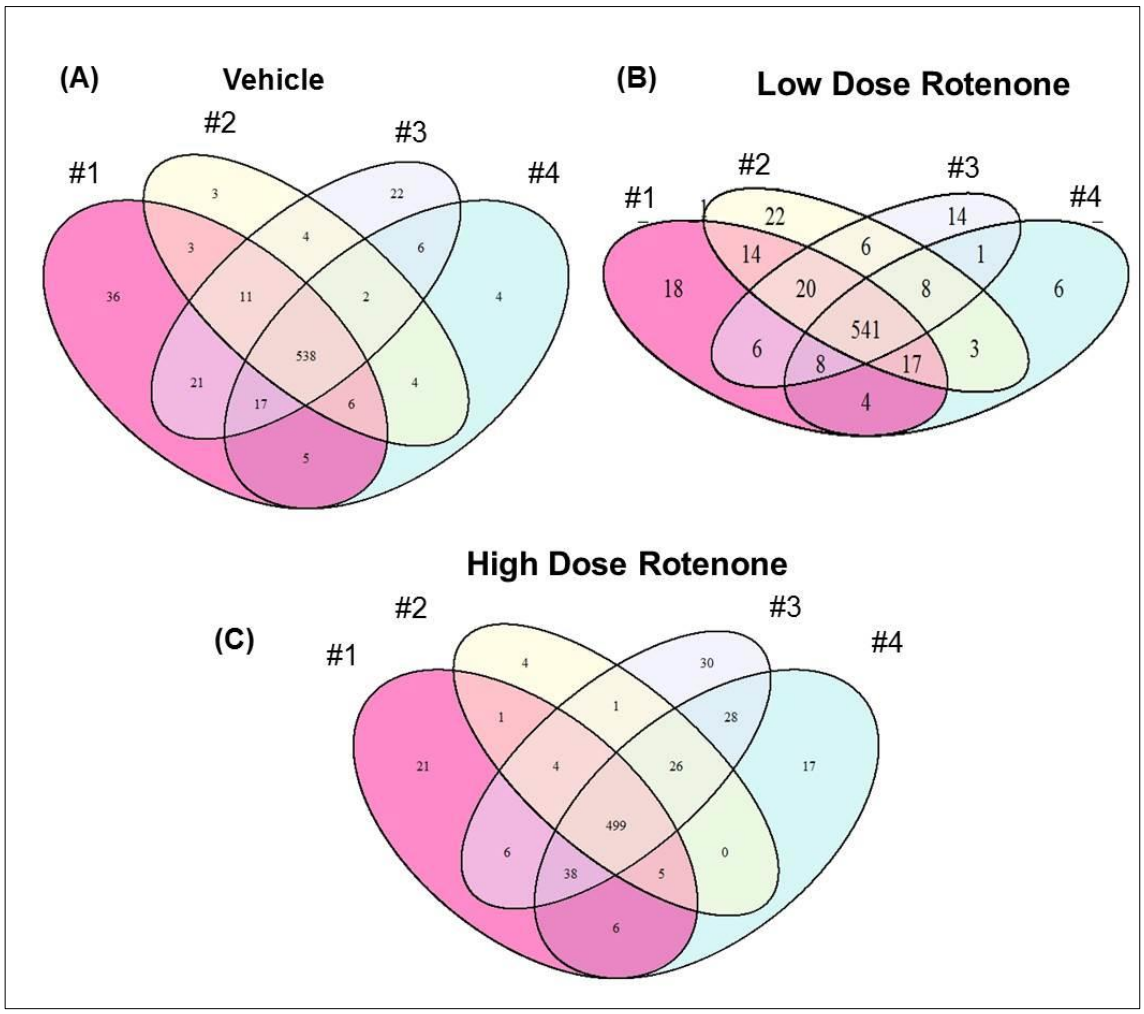

Figure 5.3.9 Overlap Analysis of Protein IDs detected in Individual Replicates for Rotenone Dataset in Hepatocytes

Venn Diagrams illustrating overlap of Protein IDs in each replicate Vehicle (A), low dose rotenone treatment (B) and high dose rotenone treatment (C). Different colours represent individual replicates.

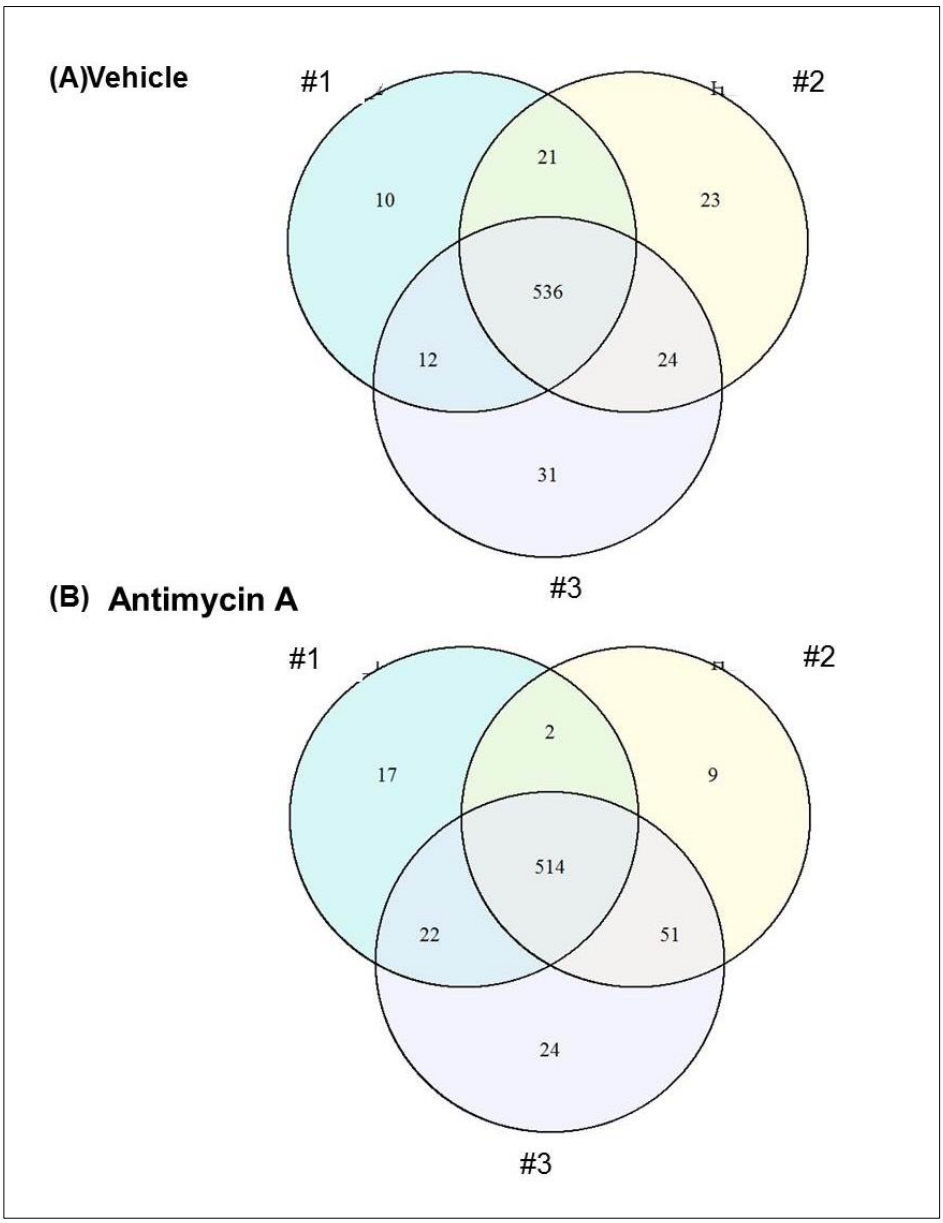

Figure 5.3.10 Overlap Analysis of Protein IDs detected in Individual Replicates for Antimycin A Dataset in hepatocytes

Venn Diagrams illustrating overlap of Protein IDs in each replicate Vehicle (A) and antimycin A treatment (C). Different colours represent individual replicates.

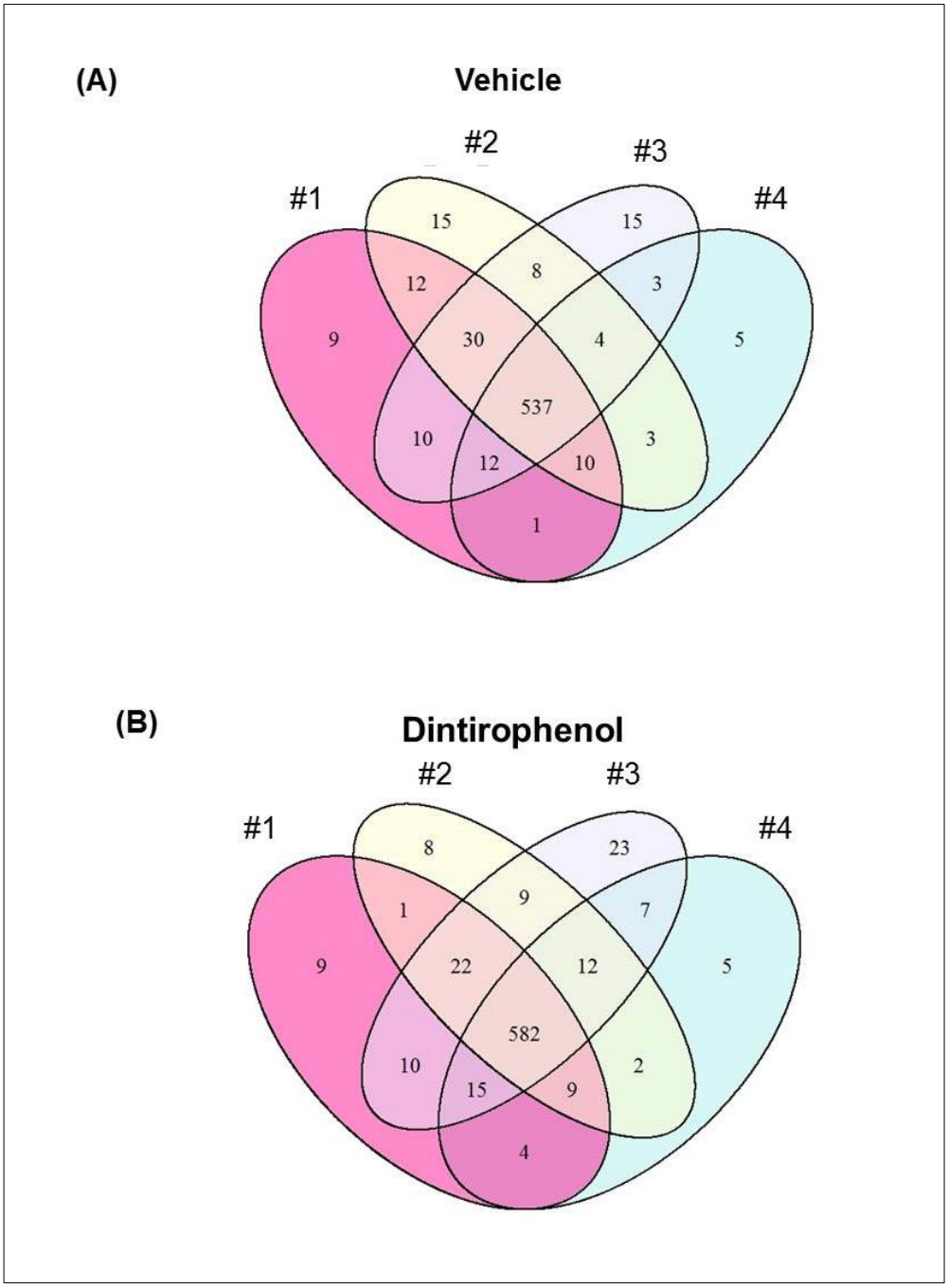

Figure 5.3.11 Overlap Analysis of Protein IDs detected in Individual Replicates for dinitrophenol Dataset

Venn Diagrams illustrating overlap of Protein IDs in each replicate Vehicle (A), low dose dinitrophenol treatment (B) and dinitrophenol treatment (C). Different colours represent individual replicates.

5.2.3 Proteomics Analysis

After ensuring data quality, proteomics analysis was performed. First, data was visualised using principle component analysis (PCA) to reveal global trends. PCA of the rotenone dataset showed a tendency for vehicle samples to cluster away from samples that were drug treated, but the data appeared variable with no tight clustering of experimental groups (Figure 5.3.12A). For the antimycin A dataset, PCA revealed that vehicle and drug treatment did not separate well indicating that there were no overwhelming changes in the secretome in response to Complex III inhibition (Figure 5.3.12B). PCA revealed that for hepatocytes, dinitrophenol treatment caused clustering of vehicle samples and clustering of drug treated samples separate from the vehicle (Figure 5.3.12C). This suggests that there are overall trends towards a global remodelling of the secretome in hepatocytes in response to OXPHOS uncoupling.

After data PCA visualisation, I performed subsequent statistical analysis. As in chapter 4, ANOVA or two sided, unpaired t-test were performed followed by a Benjamini-Hochberg correction analyses to estimate the false discovery rate. Statistical analysis revealed many significantly changed proteins with dinitrophenol treatment, some changes with rotenone and relatively few changes with antimycin A. This is in concordance with the PCA results.

Changed proteins were combined with abundance for visualisation by heat map analysis (Figure 5.3.13). A FDR of 5-10% was applied to the data. Median abundances of proteins were calculated and then combined with 'significant proteins' to generate heat maps displayed in Figure 5.3.13, while data for individual proteins are displayed in below tables 5.3.1-5.3.4.

The heat map illustrating the effect of rotenone, Antimycin A and DNP treatment on the primary hepatocyte secretome reveals that roughly one third of the significantly changed proteins were increased in abundance and two thirds were decreased with the respective treatments (Figure 5.3.13). Data for individual proteins are presented in tables 5.3.1-5.3.3. For rotenone the protein with the greatest increase in secretion was Filamin-B, which was elevated by ~100-fold (Table 5.3.1). Conversely 40S ribosomal protein S10 was reduced by ~25-fold Table 5.3.1). For Antimycin A the 4 proteins that

increased in abundance with mitochondrial stress were elevated between 4-37-fold, while most proteins were downregulated 2-3-fold, except Carboxylesterase 1C which was reduced in abundance by 2 orders of magnitude (Table 5.3.2). Remodelling of the secretome was far more extensive with DNP, with the most upregulated (annotated) protein being Phytanoyl-CoA dioxygenase domain-containing protein 1 (~35-fold) (Table 5.3.3), and the greatest reduction in abundance observed for Heparin cofactor 2, which was reduced by nearly 500-fold (Table 5.3.4).

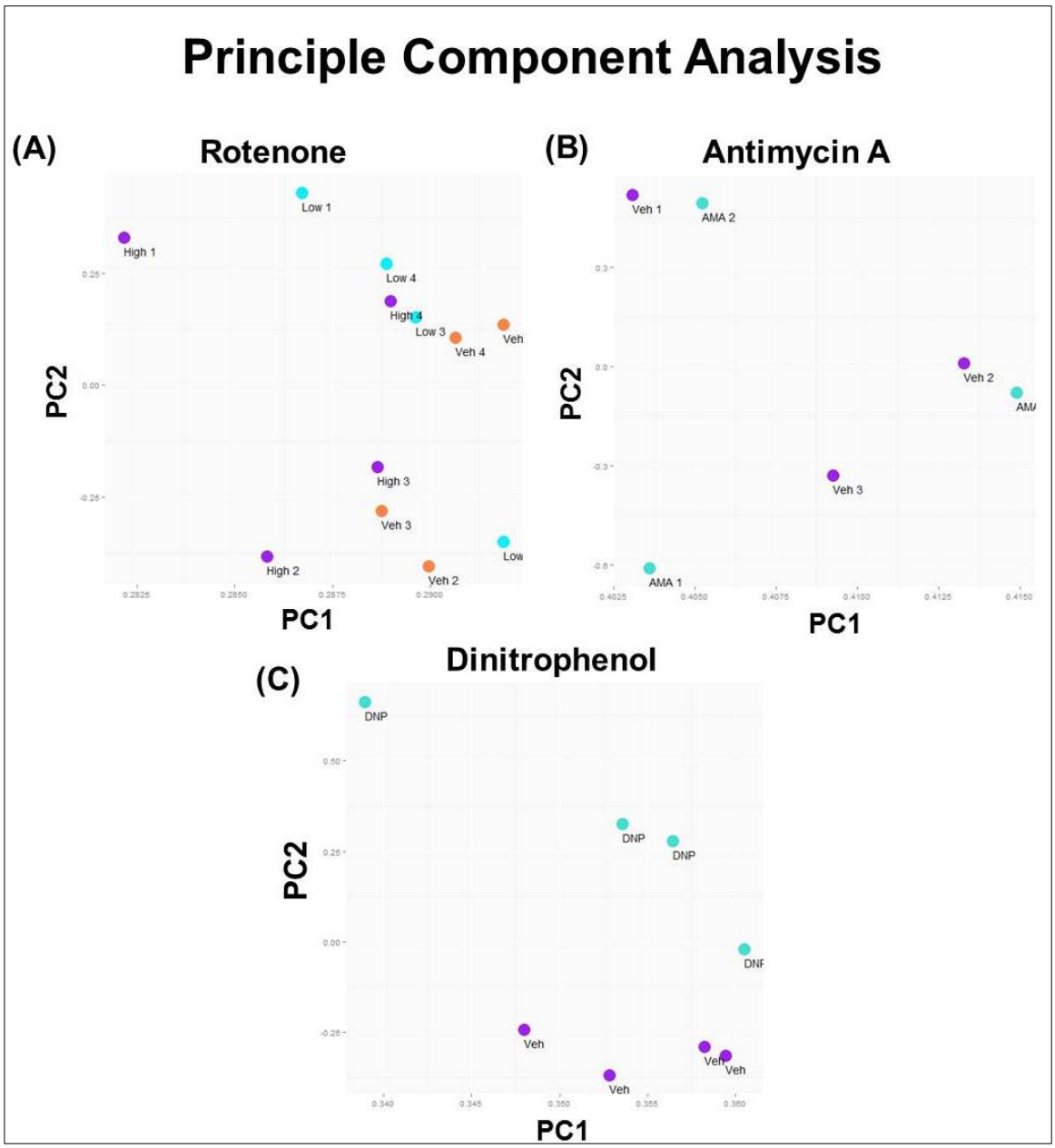

Figure 5.3.12 Principle Component Analysis (PCA) of Secreted Proteins from Hepatocytes

PCA analysis of secreted proteins from hepatocytes for the Rotenone dataset (A); the Antimycin A dataset (B) and the dinitrophenol dataset (C). PC1 on the x axis represents Protein IDs and PC2 on the y axis represents abundance. Replicates within one group are represented as one colour.

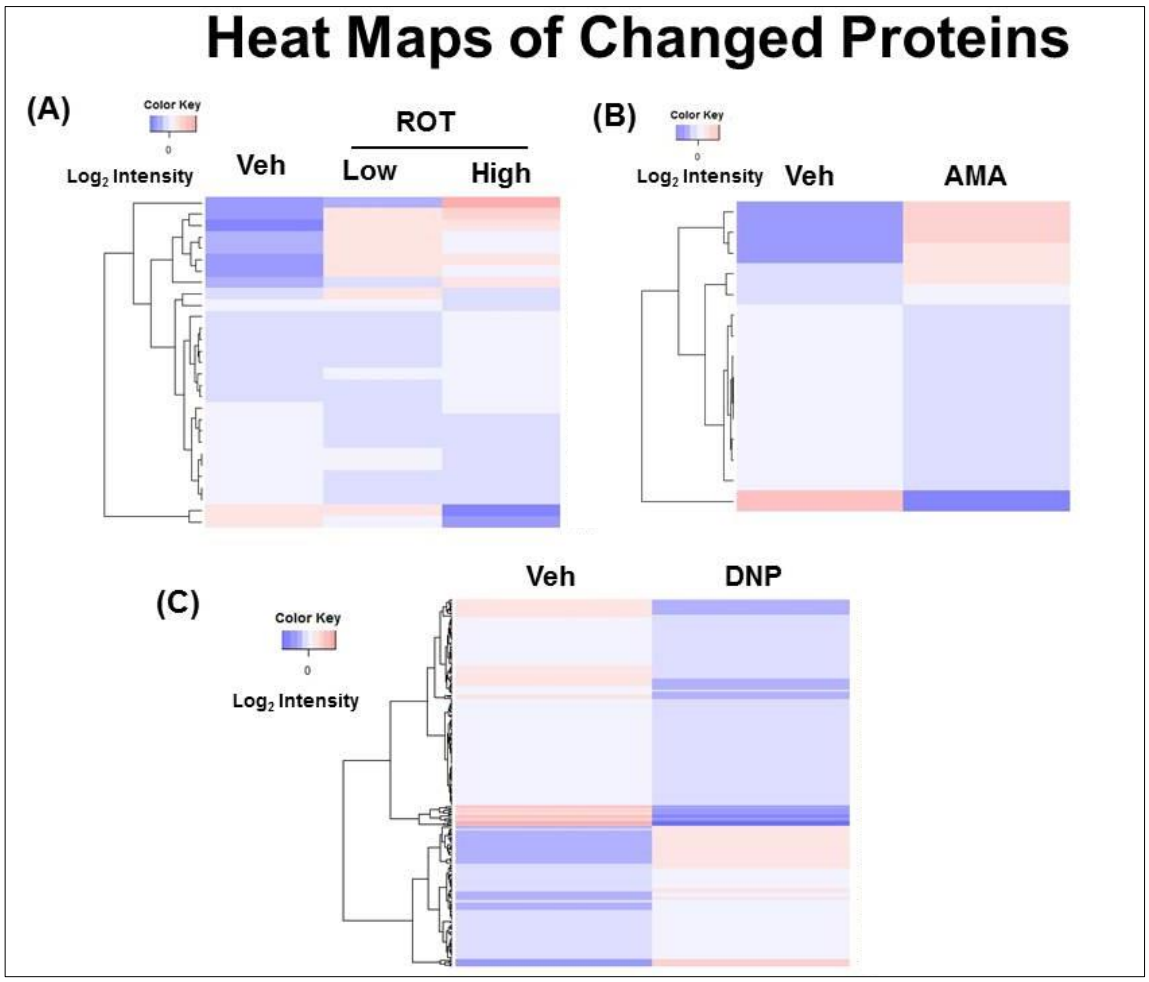

Figure 5.3.13 Abundance Heat maps of Significantly Changed Proteins in hepatocytes

Heat maps illustrating abundance of secreted proteins from hepatocytes that were significantly changed ($p<0.05$, with FDR <0.1% for rotenone and antimycin A and FDR<0.05 for dinitrophenol) with hierarchical clustering following treatment of rotenone (B); antimycin A (B) and dinitrophenol (D). Abundance was log_2 transformed with the colour representing abundance. The colour key present is coded such that white = 0, red for positive and blue for negative values. Data for individual proteins are presented in tables below.

Table 5.2.1 Secreted Proteins from Hepatocytes Changed in Abundance by Rotenone treatment

Increased with Rotenone							
Protein ID	**Protein Name**	**Median Abundance**			**Fold Change**		**FDR**
		DMSO	**Low ROT**	**High ROT**	**Low vs. Veh**	**High vs. Veh**	
A0A0J9YUI8	Glucokinase regulatory protein	0.42	0.98	2.93	2.36	7.06	0.009
P34884	Macrophage migration inhibitory factor	0.80	0.87	1.56	1.10	1.96	0.071
P01898	H-2 class I histocompatibility antigen, Q10 alpha chain	0.10	3.21	2.33	33.10	24.08	0.071
P28665	Murinoglobulin-1	0.65	1.06	1.39	1.62	2.13	0.082
P49722	Proteasome subunit alpha type-2	0.30	2.32	1.72	7.65	5.66	0.082
P62281	40S ribosomal protein S11	0.19	2.73	1.65	14.00	8.45	0.082
B9EK13	2-oxo-4-hydroxy-4-carboxy-5-ureidoimidazoline decarboxylase	0.16	2.42	2.31	15.06	14.39	0.082
B2RXW1	Histidine ammonia-lyase	0.16	3.83	4.34	24.13	27.35	0.082
Q80X90	Filamin-B	0.24	0.36	23.70	1.53	100.12	0.082
Q00897	Alpha-1-antitrypsin 1-4	0.51	2.45	0.90	4.81	1.76	0.094
P60867	40S ribosomal protein S20	0.26	2.39	1.59	9.19	6.11	0.094
Decreased with Rotenone							
Protein ID	**Protein Name**	**Median Abundance**			**Fold Change**		**FDR**
		DMSO	**Low ROT**	**High ROT**	**Low vs. Veh**	**High vs. Veh**	
P63325	40S ribosomal protein S10	2.75	3.73	0.12	1.36	0.04	0.035
A2ARD6	Kynureninase	2.18	1.80	0.17	0.83	0.08	0.071
A2RTI3	Legumain	1.35	1.47	0.51	1.09	0.38	0.009

Table 5.2.1 illustrates proteins secreted by hepatocytes that displayed significantly increased abundance with respect to vehicle upon rotenone treatment with FDR<10% (titled – “Increased with Rotenone”) and displayed significantly decreased abundance with respect to vehicle upon rotenone treatment with FDR<10% (titled – “Decreased

with Rotenone"). Rows of the table are displayed by adjusted pvalue from lowest to highest. Uniprot ID, protein name are provided along with median abundance of replicates with abundance calculated by LFQ Intensity algorithm using MaxQuant Software. "Low ROT" and "High ROT" refers to low and high dose treatments of rotenone respectively with "Low vs. Veh" and "High vs. Veh" representing fold changes respect to vehicle control of low and high doses of antimycin A treatment respectively. FDR value refers to the false discovery rate calculated by a Benjamini-Hochberg correction analysis to estimate the change of a significant pvalue in ANOVA analysis being a false discovery

Table 5.3.2 Secreted Proteins from Hepatocytes Changed in Abundance by Antimycin A treatment

Increased with Antimycin A					
Protein ID	**Protein Name**	**Median Abundance**		**Fold Change**	**FDR**
		Vehicle	AMA		
P01027	Complement C3	0.54	2.04	3.74	0.028
Q9DCW4	Electron transfer flavoprotein subunit beta	0.23	5.13	22.77	0.036
Q61838	Alpha-2-macroglobulin	0.18	6.77	37.21	0.036
P49182	Heparin cofactor 2	0.23	3.85	17.10	0.071
Decreased with Antimycin A					
Protein ID	**Protein Name**	**Median Abundance**		**Fold Change**	**FDR**
		Vehicle	AMA		
Q91VD9	NADH-ubiquinone oxidoreductase 75 kDa subunit, mitochondrial	1.44	0.65	0.45	0.028
P23953	Carboxylesterase 1C	8.78	0.11	0.01	0.098
P07309	Transthyretin	1.76	0.54	0.31	0.098
B8JJN0	Complement factor B	1.58	0.64	0.41	0.036
Q8K182	Complement component C8 alpha chain	1.41	0.70	0.49	0.098

Table 5.2.2 illustrates proteins secreted by hepatocytes that displayed significantly increased abundance with respect to vehicle upon antimycin A treatment with FDR<10% (titled – "Increased with Antimycin A") and displayed significantly decreased abundance with respect to vehicle upon rotenone treatment with FDR<10% (titled – "Increased with Antimycin A"). Rows of the table are displayed by adjusted pvalue from lowest to highest. Uniprot ID, protein name are provided along with median abundance of replicates with abundance calculated by LFQ Intensity algorithm using MaxQuant Software. "AMA" refers to antimycin A treatment and fold change refers to the fold change of treatment with respect to vehicle control of low and high doses of antimycin A treatment respectively. FDR value refers to the false discovery

rate calculated by a Benjamini-Hochberg correction analysis to estimate the change of a significant pvalue in ANOVA analysis being a false discovery

Table 5.3.3 Increased Abundance of Secreted Proteins by Dinitrophenol Treatment of Hepatocytes

Protein ID	Protein Name	Median Abundance		Fold Change	FDR
		Vehicle	DNP		
P80317	T-complex protein 1 subunit zeta	0.62	1.77	2.84	0.008
Q00897	Alpha-1-antitrypsin 1-4	0.59	1.82	3.10	0.008
P16015	Carbonic anhydrase 3	0.52	1.94	3.73	0.008
Q61805	Lipopolysaccharide-binding protein	0.53	1.99	3.74	0.008
Q8R121	Protein Z-dependent protease inhibitor	0.51	1.95	3.85	0.008
P01899	H-2 class I histocompatibility antigen, D-B alpha chain	0.48	2.11	4.37	0.008
P97823	Acyl-protein thioesterase 1	0.50	2.27	4.53	0.008
Q8VCG4	Complement component C8 gamma chain	0.31	3.09	10.11	0.008
Q9D9V3	Ethylmalonyl-CoA decarboxylase	0.16	4.84	31.05	0.008
Q91X72	Hemopexin	0.70	1.45	2.08	0.011
Q9DBA8	Probable imidazolonepropionase	0.64	1.46	2.27	0.011
Q540D7	Alcohol dehydrogenase [NADP(+)]	0.57	1.46	2.55	0.011
O88783	Coagulation factor V	0.57	1.85	3.25	0.011
Q64726	Zinc-alpha-2-glycoprotein	0.56	1.96	3.47	0.011
P34884	Macrophage migration inhibitory factor	0.51	1.80	3.54	0.011
Q61704	Inter-alpha-trypsin inhibitor heavy chain H3	0.52	1.88	3.59	0.011
Q3UKW2	Calmodulin	0.49	1.89	3.82	0.011
Q3UEF5	Angiopoietin-related protein 3	0.50	1.91	3.84	0.011
P58252	Elongation factor 2	0.43	2.11	4.86	0.011
Q8VC30	Bifunctional ATP-dependent dihydroxyacetone kinase/FAD-AMP lyase (cyclizing)	0.47	2.30	4.87	0.011
P16331	Phenylalanine-4-hydroxylase	0.46	2.41	5.23	0.011
Q07797	Galectin-3-binding protein	0.42	2.32	5.58	0.011
Q8R0Y6	Cytosolic 10-formyltetrahydrofolate dehydrogenase	0.56	1.79	3.19	0.013
P00493	Hypoxanthine-guanine phosphoribosyltransferase	0.34	2.52	7.42	0.013
Q01279	Epidermal growth factor receptor	0.62	1.78	2.89	0.013
E9Q509	Pyruvate kinase	0.51	1.82	3.59	0.013
O89023	Tripeptidyl-peptidase 1	0.54	2.02	3.72	0.014
B2RXW1	Histidine ammonia-lyase	0.37	2.86	7.84	0.014
G3X8T9	Serine protease inhibitor A3N	0.50	2.09	4.17	0.014
A0A0A0MQF6	Glyceraldehyde-3-phosphate dehydrogenase	0.57	1.72	3.02	0.015
Q9D1A2	Cytosolic non-specific dipeptidase	0.49	1.91	3.93	0.015

Q9JHH6	Carboxypeptidase B2	0.52	1.79	3.47	0.015
Q08EE6	Tsukushin	0.53	1.84	3.50	0.015
B2RTL5	Aldehyde dehydrogenase, cytosolic 1	0.66	1.59	2.40	0.016
P01898	H-2 class I histocompatibility antigen, Q10 alpha chain	0.64	1.60	2.50	0.016
Q91XL1		0.64	1.72	2.70	0.016
Q9CR16	Peptidyl-prolyl cis-trans isomerase D	0.49	1.82	3.71	0.016
P09411	Phosphoglycerate kinase 1	0.55	1.77	3.23	0.016
Q922B2	Aspartate--tRNA ligase, cytoplasmic	0.42	2.24	5.38	0.016
A2RTT4	Ubiquitin-conjugating enzyme E2 N	0.59	1.58	2.68	0.016
P21614	Vitamin D-binding protein	0.51	2.12	4.14	0.016
O70435	Proteasome subunit alpha type-3	0.46	1.93	4.16	0.016
Q3V117	ATP-citrate synthase	0.21	4.04	19.23	0.017
P68040	Guanine nucleotide-binding protein subunit beta-2-like 1	0.59	1.99	3.41	0.018
P11276	Fibronectin	0.44	2.33	5.24	0.018
Q499J3	Alpha-tocopherol transfer protein	0.57	2.04	3.60	0.019
Q922D8	C-1-tetrahydrofolate synthase, cytoplasmic	0.62	1.51	2.44	0.019
P16301	Phosphatidylcholine-sterol acyltransferase	0.58	1.93	3.31	0.019
P17182	Alpha-enolase	0.57	1.65	2.91	0.020
Q566C3	Alanine aminotransferase 1	0.43	2.25	5.21	0.020
B8JJN0	Complement factor B	0.41	2.44	6.00	0.020
A0A0R4J137	Phytanoyl-CoA dioxygenase domain-containing protein 1	0.15	5.33	34.68	0.021
Q3U2G2	Heat shock 70 kDa protein 4	0.64	1.66	2.61	0.024
Q80X90	Filamin-B	0.49	1.94	3.91	0.024
P23116	Eukaryotic translation initiation factor 3 subunit A	0.45	3.90	8.67	0.024
Q91YI0	Argininosuccinate lyase	0.60	1.59	2.63	0.025
Q8K182	Complement component C8 alpha chain	0.52	1.79	3.45	0.025
P19157	Glutathione S-transferase P 1	0.71	1.49	2.11	0.025
P07724	Serum albumin	0.62	1.89	3.03	0.025
P35505	Fumarylacetoacetase	0.48	1.98	4.10	0.025
A2AJL3	FGGY carbohydrate kinase domain-containing protein	0.45	2.00	4.42	0.025
Q3UZZ6	*	0.14	7.73	54.83	0.025
P80314	T-complex protein 1 subunit beta	0.25	3.01	12.02	0.025
E9Q414	*	0.54	1.44	2.69	0.025
P20918	Plasminogen	0.40	3.06	7.57	0.027
Q06890	Clusterin	0.54	1.77	3.29	0.027
Q3U9N4	Granulins	0.50	2.39	4.82	0.027

P29268	Connective tissue growth factor	0.39	2.55	6.52	0.027
P07361	Alpha-1-acid glycoprotein 2	0.33	3.17	9.48	0.027
A0A0R4J0I1		0.66	1.53	2.31	0.027
P24456	Cytochrome P450 2D10	0.57	2.11	3.72	0.027
P80313	T-complex protein 1 subunit eta	0.57	1.65	2.88	0.030
P62852	40S ribosomal protein S25	0.39	2.54	6.57	0.030
Q07456	Protein AMBP	0.54	1.91	3.50	0.030
P11352	Glutathione peroxidase 1	0.58	1.77	3.04	0.030
Q60590	Alpha-1-acid glycoprotein 1	0.56	1.80	3.22	0.031
Q91V76	Ester hydrolase C11orf54 homolog	0.63	1.61	2.55	0.031
Q91X52	L-xylulose reductase	0.40	2.28	5.67	0.031
P14206	40S ribosomal protein SA	0.46	2.01	4.36	0.031
Q8BVI4	Dihydropteridine reductase	0.50	1.80	3.59	0.032
Q8BGL3	*	0.57	1.64	2.90	0.033
P97290	Plasma protease C1 inhibitor	0.40	2.48	6.26	0.033
P17751	Triosephosphate isomerase	0.68	1.50	2.19	0.033
Q3TVK3	Aspartyl aminopeptidase	0.36	2.74	7.70	0.034
B2RXY7	Carbonyl reductase [NADPH] 1	0.47	2.03	4.36	0.035
P50247	Adenosylhomocysteinase	0.23	4.50	19.59	0.035
A0A0R4J0S2	Insulin-like growth factor-binding protein complex acid labile subunit	0.56	1.75	3.14	0.037
A0A0R4IZW5	Cadherin-1	0.34	2.63	7.81	0.038
Q3UEL9	Thyroxine-binding globulin	0.33	3.33	10.01	0.043
A8IP69	14-3-3 protein gamma	0.49	2.52	5.20	0.044
Q3UGC8	Propionyl-CoA carboxylase alpha chain, mitochondrial	0.60	1.75	2.91	0.045
P97461	40S ribosomal protein S5	0.31	3.17	10.23	0.046
Q9WVL0	Maleylacetoacetate isomerase	0.62	1.79	2.89	0.049

Table 5.3.4 illustrates proteins secreted by hepatocytes that displayed significantly increased abundance with respect to vehicle upon dinitrophenol treatment with less than 5% chance of false discovery. Rows of the table are displayed by adjusted pvalue from lowest to highest. Uniprot ID, protein name are provided along with median abundance of replicates with abundance calculated by LFQ Intensity algorithm using MaxQuant Software. “Vehicle” refers to the vehicle group and “DNP” refers to the dinitrophenol group. Fold changes were calculated by the median abundance treatment group / medium abundance vehicle group. FDR refers to the false discovery rate tested with a Benjamini-Hochberg correction analysis to estimate the change of a significant pvalue in ANOVA analysis being a false discovery.
* denotes unnamed protein

Table 5.2.4 Decreased Abundance of Secreted Proteins by Dinitrophenol Treatment of Hepatocytes

Protein ID	Protein Name	Median Abundance		Fold Change	FDR
		Vehicle	DNP		
A2AS37	*	1.74	0.56	0.32	0.008
Q6ZWX6	Eukaryotic translation initiation factor 2 subunit 1	5.40	0.25	0.05	0.011
P19096	Fatty acid synthase	1.97	0.58	0.29	0.011
G3X977	Inter-alpha-trypsin inhibitor heavy chain H2	1.56	0.62	0.40	0.011
P40936	Indolethylamine N-methyltransferase	1.55	0.58	0.37	0.011
A0A0R4J0E1	Fibrinogen-like protein 1	3.43	0.60	0.17	0.011
P50431	Serine hydroxymethyltransferase, cytosolic	2.03	0.49	0.24	0.011
E9QPX1	Collagen alpha-1(XVIII) chain	2.26	0.58	0.26	0.011
Q8VCU2	Phosphatidylinositol-glycan-specific phospholipase D	2.05	0.54	0.26	0.011
P01027	Complement C3	1.97	0.57	0.29	0.011
P97449	Aminopeptidase N	1.76	0.57	0.32	0.011
O70475	UDP-glucose 6-dehydrogenase	1.91	0.64	0.33	0.011
P01029	Complement C4-B	1.66	0.58	0.35	0.011
Q9D0F9	Phosphoglucomutase-1	1.58	0.60	0.38	0.011
Q8CGC7	Bifunctional glutamate/proline--tRNA ligase	1.51	0.64	0.43	0.011
Q9JM62	Receptor expression-enhancing protein 6	1.52	0.65	0.43	0.011
P41317	Mannose-binding protein C	1.47	0.66	0.45	0.011
Q9CWS0	N(G),N(G)-dimethylarginine dimethylaminohydrolase 1	1.51	0.68	0.45	0.011
Q91WT7	*	1.46	0.68	0.46	0.011
Q8R1G2	Carboxymethylenebutenolidase homolog	1.77	0.60	0.34	0.012
Q00898	Alpha-1-antitrypsin 1-5	2.07	0.49	0.24	0.012
P47199	Quinone oxidoreductase	1.80	0.56	0.31	0.013
Q5ND36	Alpha-2-antiplasmin	1.48	0.66	0.45	0.013
Q61702	Inter-alpha-trypsin inhibitor heavy chain H1	1.60	0.62	0.39	0.014
P10605	Cathepsin B	12.42	0.08	0.01	0.014
P23953	Carboxylesterase 1C	1.85	0.58	0.32	0.016
P24549	Retinal dehydrogenase 1	1.66	0.68	0.41	0.016
Q5BKQ9	26S proteasome non-ATPase regulatory subunit 11	1.98	0.47	0.24	0.016
E9PZF0	Nucleoside diphosphate kinase	2.02	0.58	0.28	0.016
P70694	Estradiol 17 beta-dehydrogenase 5	1.69	0.59	0.35	0.016
Q3UER8	Fibrinogen gamma chain	1.42	0.60	0.43	0.016

Q8R2P8	Lysyl-tRNA synthetase	1.85	0.49	0.26	0.017
Q80YC5	Coagulation factor XII	1.74	0.60	0.34	0.018
Q9QXC1	Fetuin-B	1.67	0.65	0.39	0.018
Q99J08	SEC14-like protein 2	3.90	0.16	0.04	0.018
P35700	Peroxiredoxin-1	1.54	0.63	0.41	0.018
P47877	Insulin-like growth factor-binding protein 2	1.52	0.66	0.44	0.018
A3KMP2	Tetratricopeptide repeat protein 38	1.52	0.68	0.45	0.018
P40142	Transketolase	9.98	0.14	0.01	0.019
P63101	14-3-3 protein zeta/delta	1.87	0.53	0.28	0.019
Q8R5L1	Complement component 1 Q subcomponent-binding protein, mitochondrial	1.83	0.55	0.30	0.019
P00329	Alcohol dehydrogenase 1	2.79	0.51	0.18	0.019
Q3U7Z6	Phosphoglycerate mutase	18.45	0.05	0.00	0.019
E0CZ58	Proteoglycan 4	6.43	0.12	0.02	0.019
O09173	Homogentisate 1,2-dioxygenase	1.74	0.56	0.32	0.019
Q9ET01	Glycogen phosphorylase, liver form	1.68	0.58	0.34	0.019
P30115	Glutathione S-transferase A3	1.58	0.63	0.40	0.019
A0A0R4J0M4	Apolipoprotein F	1.46	0.69	0.47	0.019
O70570	Polymeric immunoglobulin receptor	8.01	0.25	0.03	0.020
G5E8T9	Hydroxyacylglutathione hydrolase, mitochondrial	2.13	0.46	0.22	0.020
P01901	H-2 class I histocompatibility antigen, K-B alpha chain	1.48	0.71	0.48	0.020
P10126	Elongation factor 1-alpha 1	1.67	0.62	0.37	0.021
Q3UBS3	Haptoglobin	1.79	0.64	0.36	0.021
P57780	Alpha-actinin-4	2.62	0.39	0.15	0.021
P10493	Nidogen-1	2.52	0.47	0.19	0.021
A0A0A6YW77	Neutrophil gelatinase-associated lipocalin	2.18	0.47	0.22	0.021
P10810	Monocyte differentiation antigen CD14	2.17	0.52	0.24	0.021
Q61133	Glutathione S-transferase theta-2	1.83	0.55	0.30	0.021
Q9QXD6	Fructose-1,6-bisphosphatase 1	1.81	0.60	0.33	0.021
P14869	60S acidic ribosomal protein P0	1.71	0.63	0.37	0.021
P22599	Alpha-1-antitrypsin 1-2	1.60	0.62	0.38	0.021
H7BWY6	Retinol-binding protein 4	10.94	0.09	0.01	0.021
O89020	Afamin	6.38	0.19	0.03	0.022
P99027	60S acidic ribosomal protein P2	2.84	0.37	0.13	0.022
Q91XF0	Pyridoxine-5-phosphate oxidase	1.44	0.70	0.49	0.022
A0A0N4SVV4	Retinoic acid receptor responder protein 2	1.79	0.55	0.31	0.023
Q3U6G1	Flavin reductase (NADPH)	1.51	0.66	0.44	0.024
Q9DBE0	Cysteine sulfinic acid decarboxylase	1.90	0.51	0.27	0.024

P28474	Alcohol dehydrogenase class-3	7.40	0.13	0.02	0.024
E9Q035	Serotransferrin	2.48	0.37	0.15	0.024
P15626	Glutathione S-transferase Mu 2	1.86	0.56	0.30	0.024
Q9CPY7	Cytosol aminopeptidase	1.68	0.62	0.37	0.024
Q3UER1	Fructose-bisphosphate aldolase	2.53	0.45	0.18	0.024
E9QN99	Abhydrolase domain-containing protein 14B	4.66	0.14	0.03	0.024
G3X982	*	2.40	0.43	0.18	0.024
Q6S9I3	*	1.56	0.61	0.39	0.024
E9Q6D8	*	1.44	0.70	0.49	0.025
Q01853	Transitional endoplasmic reticulum ATPase	1.70	0.69	0.41	0.026
P52430	Serum paraoxonase/arylesterase 1	1.92	0.55	0.29	0.027
Q9QXF8	Glycine N-methyltransferase	1.85	0.56	0.30	0.027
Q9Z1N5	Spliceosome RNA helicase Ddx39b	1.59	0.61	0.38	0.027
K3W4L7	Phenazine biosynthesis-like domain-containing protein 1	1.64	0.53	0.32	0.027
P62075	Mitochondrial import inner membrane translocase subunit Tim13	1.56	0.66	0.42	0.027
P17427	AP-2 complex subunit alpha-2	1.66	0.53	0.32	0.027
P54869	Hydroxymethylglutaryl-CoA synthase, mitochondrial	3.41	0.34	0.10	0.027
Q9DBD0	Inhibitor of carbonic anhydrase	1.57	0.61	0.39	0.028
P62897	Cytochrome c, somatic	2.19	0.40	0.18	0.028
Q91ZJ5	UTP--glucose-1-phosphate uridylyltransferase	1.55	0.59	0.38	0.028
Q8BH35	Complement component C8 beta chain	1.73	0.63	0.36	0.028
Q9JJN5	Carboxypeptidase N catalytic chain	1.50	0.62	0.41	0.029
Q9DBB9	Carboxypeptidase N subunit 2	1.71	0.61	0.36	0.029
Q64442	Sorbitol dehydrogenase	1.35	0.68	0.50	0.030
P06728	Apolipoprotein A-IV	1.86	0.55	0.29	0.030
Q6GT24	Peroxiredoxin-6	2.25	0.47	0.21	0.030
Q91XE4	Aspartoacylase-2	1.55	0.67	0.43	0.031
O35490	Betaine--homocysteine S-methyltransferase 1	1.69	0.64	0.38	0.032
G3X8T3	Lysosomal protective protein	1.95	0.47	0.24	0.032
O09131	Glutathione S-transferase omega-1	1.56	0.66	0.42	0.033
Q61838	Alpha-2-macroglobulin	1.93	0.55	0.28	0.033
P70296	Phosphatidylethanolamine-binding protein 1	1.48	0.65	0.44	0.033
E9Q6C2	Complement C1s-A subcomponent	1.94	0.57	0.29	0.033
P06684	Complement C5	5.69	0.16	0.03	0.033
P97371	Proteasome activator complex subunit 1	1.56	0.63	0.40	0.033
Q9CQV8	14-3-3 protein beta/alpha	1.53	0.62	0.41	0.033

P62320	Small nuclear ribonucleoprotein Sm D3	1.91	0.58	0.30	0.033
A0A0A0MQC3	5-hydroxyisourate hydrolase	2.07	0.52	0.25	0.034
P98064	Mannan-binding lectin serine protease 1	2.72	0.49	0.18	0.034
Q9QUM9	Proteasome subunit alpha type-6	14.94	0.06	0.00	0.035
P62827	GTP-binding nuclear protein Ran	1.38	0.68	0.49	0.035
P49182	Heparin cofactor 2	23.76	0.05	0.00	0.035
Q91X91	Nicotinate-nucleotide pyrophosphorylase [carboxylating]	1.90	0.48	0.25	0.035
O70251	Elongation factor 1-beta	1.42	0.71	0.50	0.035
P55264	Adenosine kinase	1.54	0.65	0.43	0.036
Q9DCU9	Probable 4-hydroxy-2-oxoglutarate aldolase, mitochondrial	2.48	0.28	0.11	0.036
P06797	Cathepsin L1	1.56	0.70	0.45	0.037
Q99PT1	Rho GDP-dissociation inhibitor 1	1.49	0.65	0.43	0.037
O88968	Transcobalamin-2	1.92	0.61	0.32	0.038
Q3UTR7	Angiotensinogen	1.69	0.66	0.39	0.038
P47738	Aldehyde dehydrogenase, mitochondrial	1.50	0.70	0.47	0.038
Q3T9Z2	Glyoxylate reductase/hydroxypyruvate reductase	2.00	0.57	0.28	0.038
P62264	40S ribosomal protein S14	1.42	0.66	0.46	0.039
Q8VCX1	3-oxo-5-beta-steroid 4-dehydrogenase	2.14	0.54	0.25	0.040
A2AKN8		1.58	0.66	0.42	0.041
P29391	Ferritin light chain 1	1.98	0.54	0.27	0.041
P61458	Pterin-4-alpha-carbinolamine dehydratase	1.67	0.64	0.38	0.041
Q00519	Xanthine dehydrogenase/oxidase	1.47	0.67	0.46	0.041
P62751	60S ribosomal protein L23a	2.28	0.51	0.22	0.041
Q9JHW2	Omega-amidase NIT2	1.48	0.63	0.43	0.041
P55050	Fatty acid-binding protein, intestinal	2.70	0.46	0.17	0.042
Q91X83	S-adenosylmethionine synthase isoform type-1	1.60	0.54	0.34	0.042
Q71RI9	Kynurenine--oxoglutarate transaminase 3	2.10	0.53	0.25	0.042
F6ZIS7	*	3.88	0.27	0.07	0.042
Q8VCB3	Glycogen [starch] synthase, liver	2.21	0.51	0.23	0.042
O88569	Heterogeneous nuclear ribonucleoproteins A2/B1	1.76	0.49	0.28	0.044
P34914	Epoxide hydrolase 2	1.60	0.62	0.39	0.045
P10639	Thioredoxin	1.71	0.56	0.33	0.047
A5GZX3	Lactoylglutathione lyase	1.41	0.68	0.48	0.048
Q8CG76	Aflatoxin B1 aldehyde reductase member 2	1.91	0.58	0.30	0.049

Q4FZK2	Elongation factor 1-gamma	1.41	0.69	0.49	0.049
Q3TWN7	V-type proton ATPase subunit S1	2.90	0.39	0.14	0.050
Q3KQQ2	Major urinary protein 3	1.56	0.59	0.38	0.050
A2AE89	Glutathione S-transferase Mu 1	1.62	0.64	0.39	0.050

Table 5.3.5 illustrates proteins secreted by hepatocytes that displayed significantly decreased abundance with respect to vehicle upon dinitrophenol treatment with less than 5% chance of false discovery. Rows of the table are displayed by adjusted pvalue from lowest to highest. Uniprot ID, protein name are provided along with median abundance of replicates with abundance calculated by LFQ Intensity algorithm using MaxQuant Software. “Vehicle” refers to the vehicle group and “DNP” refers to the dinitrophenol group. Fold changes were calculated by the median abundance treatment group / medium abundance vehicle group. FDR refers to the false discovery rate tested with a Benjamini-Hochberg correction analysis to estimate the change of a significant pvalue in ANOVA analysis being a false discovery.
* denotes unnamed protein

As in chapter 4, significantly changed proteins were subjected to analysis in string database for interactions and KEGG pathway enrichment analysis was performed for biological interpretation. Due to the small number of changed proteins for the rotenone and antimycin A datasets, the only biological interpretation that can be reported is an enrichment of “complement and coagulation cascade” pathways for proteins that were significantly increased by rotenone (FDR of 0.0188). However, because of the more extensive changes, several KEGG pathways were enriched with dinitrophenol treatment (Table 5.3.5).

“Metabolic pathways” was the top-enriched pathway for both the upregulated and downregulated proteins. This is a very broad cluster of metabolic pathways, many of which are specifically noted at (with lower protein frequency counts) in Table 5.3.5 (e.g. carbon metabolism, glycolysis/gluconeogenesis). The next most significantly up-regulated and down-regulated pathway was “Complement and coagulation cascades” with 8 and 14 proteins changed in each direction respectively. “Microbial metabolism in diverse environments” respresented the third most significantly changed pathway in both direction, with many of the proteins in this group overlapping with those in “Metabolic pathways”. The remaining pathways largely represented a mix of pathways involved in metabolism and drug detoxification.

Table 5.3.5 KEGG Pathway Enrichment Analysis for Hepatocytes Treated with dinitrophenol

Pathway ID	Pathway Description	Observed gene count	FDR
Increased in Abundance with Dinitrophenol			
1100	Metabolic pathways	23	4.16E-08
4610	Complement and coagulation cascades	8	8.05E-08
1120	Microbial metabolism in diverse environments	10	1.05E-07
1230	Biosynthesis of amino acids	7	1.08E-06
1200	Carbon metabolism	7	1.13E-05
10	Glycolysis / Gluconeogenesis	5	0.000202
340	Histidine metabolism	3	0.00779
Decreased in Abundance with Dinitrophenol			
1100	Metabolic pathways	39	5.21E-16
4610	Complement and coagulation cascades	14	2.81E-15
1120	Microbial metabolism in diverse environments	16	5.06E-13
980	Metabolism of xenobiotics by cytochrome P450	8	2.84E-07
982	Drug metabolism - cytochrome P450	8	2.93E-07
5150	Staphylococcus aureus infection	7	9.13E-07
480	Glutathione metabolism	7	1.36E-06
5204	Chemical carcinogenesis	8	2.27E-06
5322	Systemic lupus erythematosus	8	2.41E-06
10	Glycolysis / Gluconeogenesis	7	2.54E-06
500	Starch and sucrose metabolism	5	0.000318
5134	Legionellosis	5	0.000557
30	Pentose phosphate pathway	4	0.000657
1200	Carbon metabolism	6	0.000932
40	Pentose and glucuronate interconversions	4	0.00106
5133	Pertussis	5	0.00121
260	Glycine, serine and threonine metabolism	4	0.00137
1230	Biosynthesis of amino acids	5	0.00137
350	Tyrosine metabolism	4	0.00158
620	Pyruvate metabolism	4	0.00165
380	Tryptophan metabolism	4	0.00189
4614	Renin-angiotensin system	3	0.00246
630	Glyoxylate and dicarboxylate metabolism	3	0.00522
4145	Phagosome	6	0.00522

Table 5.3.6 Displays significantly enriched (FDR<1%) KEGG pathways by gene ontology in response to OXPHOS uncoupling in hepatocytes. Secreted proteins that were significantly increased in abundance by dinitrophenol compared with vehicle (“Increased with Dinitrophenol”) and decreased by antimycin A (“Decreased with Dinitrophenol”) were separately subject to KEGG pathway enrichment analysis by gene

ontology. The table provides the KEGG “Pathway ID” and “Pathway Description”. The number of proteins that were annotated under a particular pathway was represented as “Observed Gene Count” and the FDR is provided.

5.4 Discussion

The liver is a key metabolic organ that secretes many proteins, including plasma proteins. In this chapter, I characterised the ETC sensitive secretome of primary murine hepatocytes and found that the hepatocyte secretome is very sensitive to an OXPHOS uncoupler but is relatively insensitive to either a ETC complex I or III inhibitor. These findings were highly surprising, given that other studies have reported secretome changes with other diverse stimuli (Higa et al., 2008; Meex et al., 2015; Nakata et al., 2014; Slany et al., 2010). One possible reason that the ETC inhibitors had limited impact is that hepatocytes have a strong capacity for xenobiotic detoxification (Grant, 1991) and they may be more effective at detoxifying rotenone or antimycin A than dinitrophenol. Indeed the shape of the antimycin A curve was peculiar compared to the seen in HEK293 cells and may relate to this aspect of hepatocyte function. Detoxification of the ETC inhibitors may be particularly relevant when considering the timeframe of the seahorse experiment that defined the relevant doses (acute) vs. the more chronic (24hr) exposure for the secretome analysis. It is possible that the hepatocytes rapidly degraded rotenone and antimycin A and thus the effective concentration of these compounds over the majority of the course of the secretome experiment was lower than what was originally applied to the cells. It is also unclear how the different compounds impacted intracellular ATP levels in the experiments. As secretion of proteins (classical and non-classical) is energy-requiring, it is perhaps not surprising that the relative concentration of more secreted proteins was decreased than increased. As noted in the previous chapter this also confirms that the proteins that were increased were unlikely arising from cells that had died and released intracellular contents (also confirmed by viability experiments).

The top KEGG pathway to be enriched by proteins both increased and decreased in abundance with dinitrophenol was “metabolic pathways” (Table 5.3.6). This is interesting as hepatocyte microvesicles can be metabolically active (Royo et al., 2017). KEGG pathway analysis also revealed changes in “Complement and Coagulation Cascades” in response to OXPHOS uncoupling (Table 5.3.6). The complement system is an innate immune response that “complements” the ability of antibodies to clear pathogens and is elicited by a group of complement proteins in the blood (Ghebrehiwet, 2016). There are three distinct complement pathways, the classical, alternative and

lectin pathways and all converge at complement protein C3 (C3) (Sarma & Ward, 2011). The liver is responsible for synthesising and secreting 80-90% of plasma complement proteins including components for all three pathways (Phieler, Garcia-Martin, Lambris, & Chavakis, 2013; Qin & Gao, 2006). Hepatocytes secreted complement proteins (Phieler et al., 2013) suggesting that hepatocytes rather than another cell type of liver have an important role in complement protein secretion. Complement proteins that had increased secretion with OXPHOS uncoupling were complement 8 alpha chain and complement 8 gamma chain were both increased with dinitrophenol ~3.5 and 10 fold respectively. Secreted complement proteins that were decreased in abundance were complement 1s which was down by about ~97% and complement 3, complement 4 beta, complex 5 and complement 8 beta which were also decreased in abundance ~70%.

As complement proteins are involved in the innate immune system, alterations in the balance of complement proteins may affect systemic inflammation. Overall, the trend is for a decrease in complement proteins with the exception of C8 beta and gamma. Strikingly, the opposite trend is observed in hepatocytes treated with antimycin A (Table 5.3.5). As uncoupling increases mitochondrial energy expenditure and fatty acid oxidation and antimycin A decreases those parameters, I speculated that perhaps metabolic perturbations are linked with complement protein secretion in liver. A recent study found that C3 was secreted from liver and primary hepatocytes in response to fasting and metabolic challenges (Magliarelli et al., 2016). This suggests that C3 secretion from liver and hepatocytes may occur in a nutrient sensitive manner (Magliarelli et al., 2016). Complement proteins can cause pancreatic beta cells to secrete insulin (King & Blom, 2016). Hence hepatic complement protein secretion could be a mechanism by which liver nutrient availability or metabolic status is communicated to the pancreas to regulate insulin secretion. Another study comparing the secretome of primary hepatocytes isolated from high fat and chow fed mice found that complement factor B and complement factor H were both increased with high fat feeding and the alternative complement pathway was enriched by pathway analysis (Meex et al., 2015). However, in that study C3 was detected in the dataset but not changed with high fat feeding (Meex et al., 2015). As mitochondrial function was not measured in the hepatocytes from the fat-fed mice in the study of Meex et al (2015) it is

unclear how much of the secretome changes related to excess supply of lipid vs. any change in mitochondrial metabolism. C3 expression has been found to be under control of the PPARα promoter in hepatocytes and treatment with a PPARα antagonist decreased C3 secretion from hepatocytes but a PPARα agonist did not increase secretion (Mogilenko et al., 2013). Metabolic perturbations have been found to increase C3 secretion in macrophages. C3 is a plasma biomarker of obesity and insulin resistance (Al Haj Ahmad & Al-Domi, 2016) and plasma C3 is decreased in obese subjects following weight loss (Hernandez-Mijares et al., 2012) but this is thought to be through adipose tissue macrophages (Al Haj Ahmad & Al-Domi, 2016) and the contribution of obese plasma C3 from liver is not well studied. Supporting this idea, in HepG2 hepatocytes phosphorylation of sterol regulatory-element binding protein (SREBP), a major regulator of lipid metabolism in the liver, resulted in secretion of C3 and alpha-1-antitrypsin (Knebel et al., 2014). However, C3 levels are associated with non-alcoholic fatty liver disease independently of other metabolic parameters (Xu et al., 2016) so perhaps its secretion is connected with hepatic lipid metabolism. In light of other literature, the differential effects of complement protein secretion with Complex III inhibition and an OXPHOS uncoupler might be related to changes in fatty acid oxidation, but this requires testing.

The mechanism by which mitochondrial oxidation (and perhaps fatty acid oxidation) leads to secretion of complement proteins is unclear. The hepatocyte nuclear factor1 alpha (HNF1α) transcription factor is expressed in liver as well as other tissues and required for expression of C8beta, C9, C3 and C5 (Pontoglio et al., 2001). It is possible that HNF1α activation in hepatocytes is decreased upon mitochondrial uncoupling. Alpha-1-antitrypsin was additionally downregulated in this dataset and it has been shown that HNF1α interacts with the alpha-1-antitrypsin promoter region to cause its transcription (Courtois, Morgan, Campbell, Fourel, & Crabtree, 1987) providing further evidence for the hypothesis that HNF1α activation may be decreased in this dataset. HNF1α interestingly controls expression of metabolic genes and is involved in metabolic processes (Pontoglio, 2000). Comparing sequences of the palindromic recognition binding site of HNF1α with genes that were 1000 bp upstream of the transcriptional start site revealed that it is unlikely to be binding to the promoter to cause active changes of transcription of these genes in response to DNP. However, it

cannot rule out enhancer binding or indirect effects on expression of those genes. To fully interrogate whether HNF1α may be activated by DNP and causing transcription of those genes, I would need to observe nuclear translocation of HNF1α in response to dinitrophenol and knockdown of HNF1α and measure mRNA levels of these genes with and without dinitrophenol.

The key findings of this chapter were that protein secretion from hepatocytes was most affected by an OXPHOS uncoupler and that treatment of hepatocytes with the OXPHOS uncoupler resulted in secretion of metabolic enzymes and an alteration in secretion of complement proteins. Given that this was not found in HEK293 cells (chapter 4) nor with rotenone or antimycin A treatment in hepatocytes, it appears to be an OXPHOS uncoupler, hepatocyte specific effect. In order to confirm this, it would be valuable to measure complement protein and fibronectin levels in culture media in response to several OXPHOS uncouplers in other hepatocyte cells lines. Based on the literature I speculate that the mechanism might be related to perturbed lipid metabolism. Enhanced secretion of complement proteins without infection can lead to systemic inflammation and the risk of cardiovascular disease.

CHAPTER 6: CHARACTERISING THE SECRETOME OF PRIMARY MURINE ADIPOCYTES UNDER MITOCHONDRIAL STRESS

6.1 Introduction

White adipose tissue (WAT) is the major energy store in the body. WAT is composed of numerous cell types including stromal vascular fraction, macrophages and adipocytes (Cinti, 2005). Adipocytes undergo *de novo* lipogenesis at high rates to convert glucose into triglyceride which is stored in lipid droplets (Gustafson & Smith, 2015). WAT contributes to whole body energy homeostasis not only by storing excess energy as triglyceride, but also through secretion of a large complement of proteins which regulate energy metabolism and inflammation in distal tissues and cells (Coelho, Oliveira, & Fernandes, 2013; Fantuzzi, 2005; Trayhurn & Beattie, 2001; Vazquez-Vela, Torres, & Tovar, 2008).

Literature has emerged in recent years showing that mitochondrial function in adipose tissue can influence the development of multi-systemic pathological changes and alter whole body energy homeostasis (Kusminski & Scherer, 2012; Vernochet et al., 2012). This renders adipocytes an interesting cell type to interrogate proteins secretion with ETC stress. For example, the adipose-specific, TFAM deletion mouse model displays enhanced metabolic syndrome phenotype in conjunction with mitochondrial dysfunction. (Vernochet et al., 2012). In cultured adipocytes, TFAM knockdown causes decreased mitochondrial respiratory function and reduced insulin stimulated glucose uptake suggesting they are less insulin sensitive (X. Shi et al., 2008). Conversely, improvement of adipose tissue specific mitochondrial function through overexpression of mitoNEET improved secretion of adiponectin and lead to healthier, albeit still obese, adipose tissue (Kusminski et al., 2012). Hence there is a reasonable amount of evidence that perturbing mitochondrial function of adipocytes can influence responsiveness to insulin and other metabolic parameters. Additionally, as discussed in section 1.4.2 mitochondrial dysfunction occurs in adipose tissue with diet-induced obesity and metabolic syndrome (Heinonen et al., 2015) and this relationship is somewhat less contentious than other tissues like muscle. As changes in secretions from adipocytes are

a major feature of adipose tissue biology under different pathologies (Coelho et al., 2013; Trayhurn & Beattie, 2001), understanding changes in the adipocyte secretome in response to mitochondrial stressors may shed light on this disease. More recently, secreted proteins from adipocytes have also been implicated in cancer progression (Booth, Magnuson, Fouts, & Foster, 2015; Guaita-Esteruelas et al., 2017; Volden et al., 2016), cellular senescence (Zhao et al., 2016) and autophagy (Liu et al., 2015).

A number of metabolic stressors have been shown to alter the adipocyte secretome. The adipocyte secretome is known to be altered with treatment of the PPARγ agonist, rosiglitazone, which stimulates mitochondrial biogenesis (X. Chen, Hunt, Cushman, & Hess, 2009; Hwang et al., 2011; Klimcakova et al., 2007). The secretome of adipocytes is also remodelled upon glucose restriction (Renes, Rosenow, Roumans, Noben, & Mariman, 2014) which represents a metabolic stress. Both hypoxia (Frazier, Gimble, Kheterpal, & Rowan, 2013) and hypoxia mimetics also change the adipocyte secretome (Rosenow, Noben, Bouwman, Mariman, & Renes, 2013) and pseudohypoxia is seen with mitochondrial dysfunction (Selak, Duran, & Gottlieb, 2006)

The aforementioned studies suggest that mitochondrial stress in adipose tissue can have whole body effects and the adipocyte secretome is sensitive to metabolic stressors. However, the effect of mitochondrial stress on the adipocyte secretome has not directly been tested. The aim of this chapter was to characterise the secretome in response to low and high doses of ETC Complex I and III inhibitors and an OXPHOS uncoupler.

6.2 Methods Summary

Adipocyte isolation and culture was performed as described in section 2.2 In brief, inguinal adipose tissue depots were collagenase digested, strained and spun to obtain the stromal vascular fraction containing preadipocytes. Preadipocytes were differentiated using an adipogenic cocktail then 48 hours later changed to maintenance medium which they were maintained on 10 days until use.

Oxygen consumption rate dose response curves to ETC toxins were characterised using the Seahorse XF-96 Bioanalyser in HEK293 cells. Following selection of doses, cell viability and cell death were determined using propidium iodide and AlamarBlue stains. Cells were stringently washed then incubated with ETC toxins at the respective doses in serum free medium then 24 hours later conditioned medium was collected by spinning and filtering to pellet and clear cell debris to prevent contamination the samples with intracellular proteins. An acetone precipitation was performed and trypsin digest was performed according to methods.

Peptides were separated and mass analysed by LC-MS/MS on ThermoXCalibur raw files were subjected to MaxQuant Analysis to map peptide sequences with protein IDs. MaxQuant calculates an LFQ intensity algorithm as a surrogate for protein abundance. Data analysis was performed in the R language using R studio.

6.3 Results

6.3.1 Development of Model

Consistent with the previous cell types, I began by characterising the adipocyte specific dose response curves of rotenone, antimycin A and dinitrophenol using oxygen consumption rate as an output (Figure 6.2.1). Rotenone and antimycin A inhibited respiration in primary adipocytes in a sigmoidal fashion, while dinitrophenol showed a very steep dose-response effect at close to 100μM (Fig 6.2.1C). Based on these findings low and high doses of 50 nM and 500 nM for rotenone, 30 nM and 100 nM for antimycin A and 50 μM and 100 μM dinitrophenol were chosen accordingly. Treatment of adipocytes with respective drug doses for 24 hours was performed and viability was assessed by both alamar blue assays and propidium iodide staining. The cells looked visibly viable and there were no significant changes in cell death (Figure 6.3.2 D, E & F). Of note, high doses of rotenone and antimycin A showed a trend to decrease Alamar blue fluorescence, but this was not reflected in the propidium iodide staining. These disparate findings are likely due to reduced mitochondrial reductase activity as adipocytes are terminally differentiated and will not proliferate.

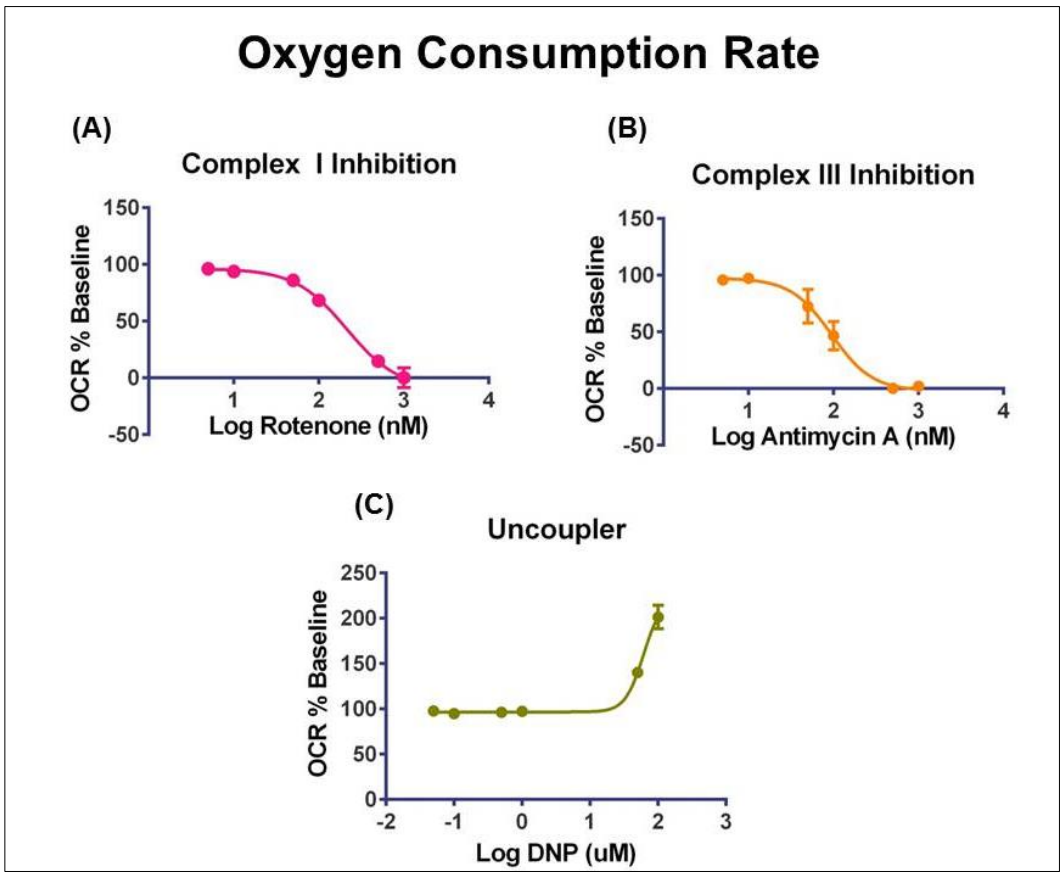

Figure 6.3.1 Dose Response Curves of ETC Inhibitors in Primary Murine Adipocytes

Oxygen consumption rate (OCR) was measured by Seahorse-XF96 Bioanalyser before and after drug injections in dose response. Results are expressed as a percentage of the baseline OCR reading after corresponding drug dose. (A) Complex I inhibitor Rotenone, (B) Complex III inhibitor Antimycin A (C) OXPHOS/ETC Uncoupler 2,4-dinitrophenol.

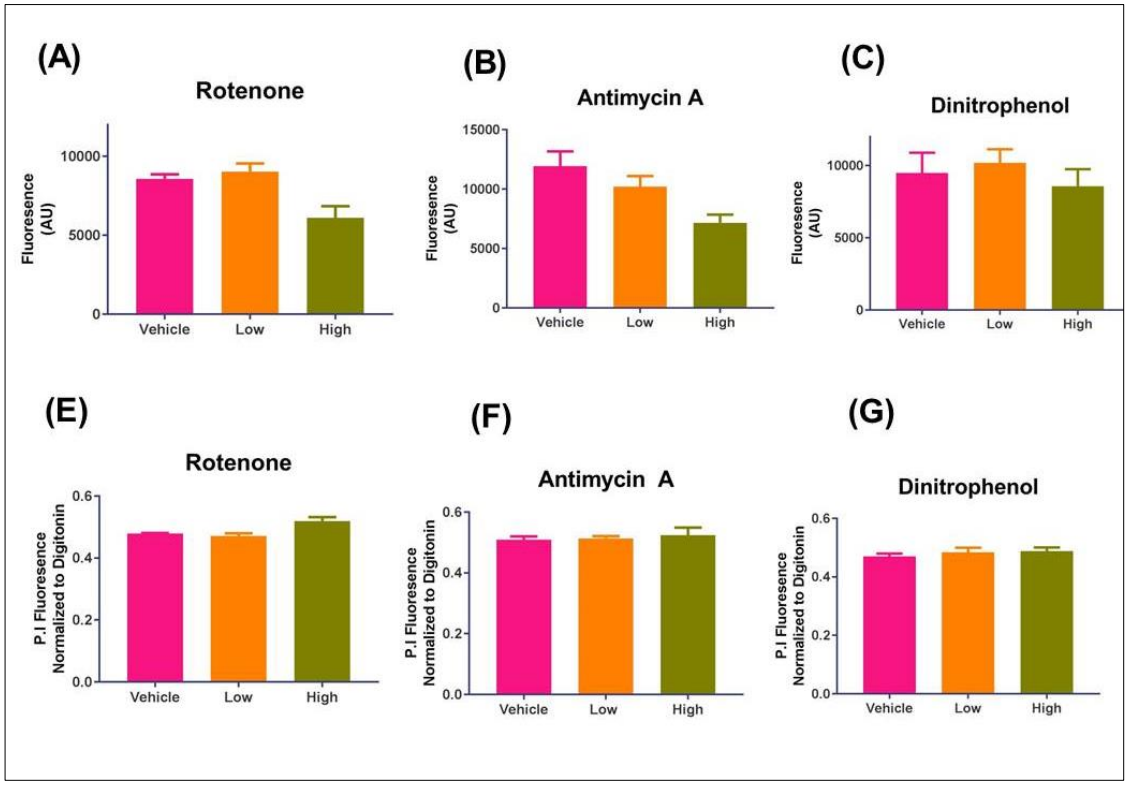

Figure 6.3.2 Cell Viability of Adipocytes Treated with Defined Doses of Inhibitors

Adipocytes treated for 24 hours with DMSO vehicle, 50 nM, 500 nM rotenone (A) & (E); Ethanol vehicle, 30 nM, 100 nM antimycin A (B) & (F); and H_2O vehicle, 50 µM and 100 µM dinitrophenol (C) & (G) labelled "vehicle", "Low" for low dose and "High" for high dose respectively. Alamar blue fluorescence was measured (A), (B) & (C) presented in fluorescence arbitrary units. Propidium iodide (P.I) fluorescence was measured,then measured again after a 30 minute incubation with 600 µM digitonin as a positive control of permeable cells. Fluroescence data was normalised to digitonin.

6.2.2 Validation of Extracellular Location of Detected Proteins

As in the other chapters, I bioinformatically assess whether proteins detected by MS were likely to be a classically secreted protein (Figure 6.3.3) or annotated as being localised to the extracellular compartments (Figure 6.3.4). A total of 205, 257 and 173 proteins were detected in the medium for the rotenone, antimycin A and dinitrophenol datasets respectively. Analysis showed that 42%, 32% and 47% of proteins had a secretion signal peptide for rotenone, antimycin A and dinitrophenol respectively for adipocytes. This was generally higher than that of HEK293 and hepatocytes in previous chapters which could be because less total proteins were detected (~170-220) in adipocytes as opposed to (~400-650) in HEK293 and hepatocytes datasets. However, the percentage of proteins with an extracellular annotation was relatively similar - 83%, 93% and 84% for rotenone, antimycin A and dinitrophenol respectively.

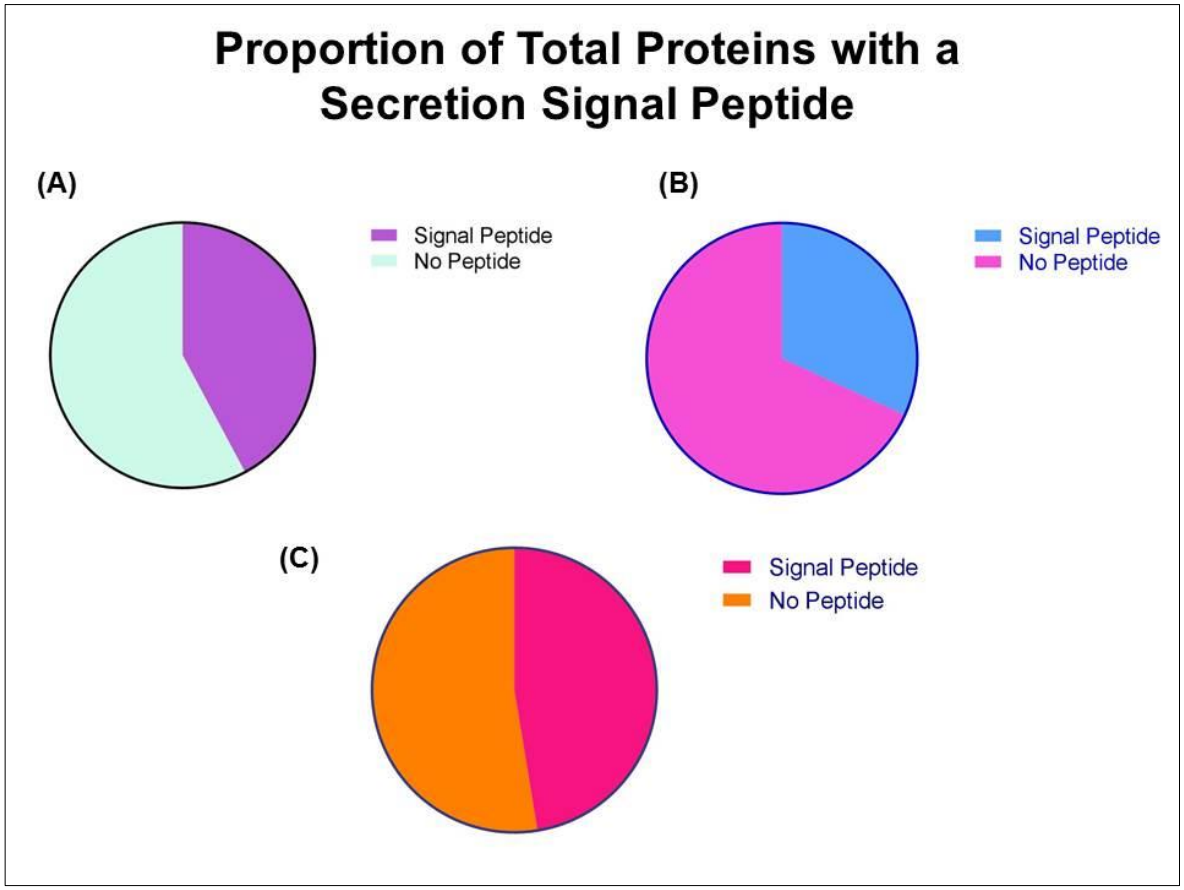

Figure 6.3.3 Proportion of all Detected Proteins with a Predicted Secretion Signal Peptide by Sequence Analysis in Adipocytes

All proteins detected by LC-MS/MS in each experimental group were pooled after data filtering for the Rotenone dataset (A) Rotenone dataset, the Antimycin A dataset (B) and the Dinitrophenol dataset (C). Amino acid sequences were exported to the SecretomeP tool that predicts whether or not a protein has a secretion signal peptide based on sequence.

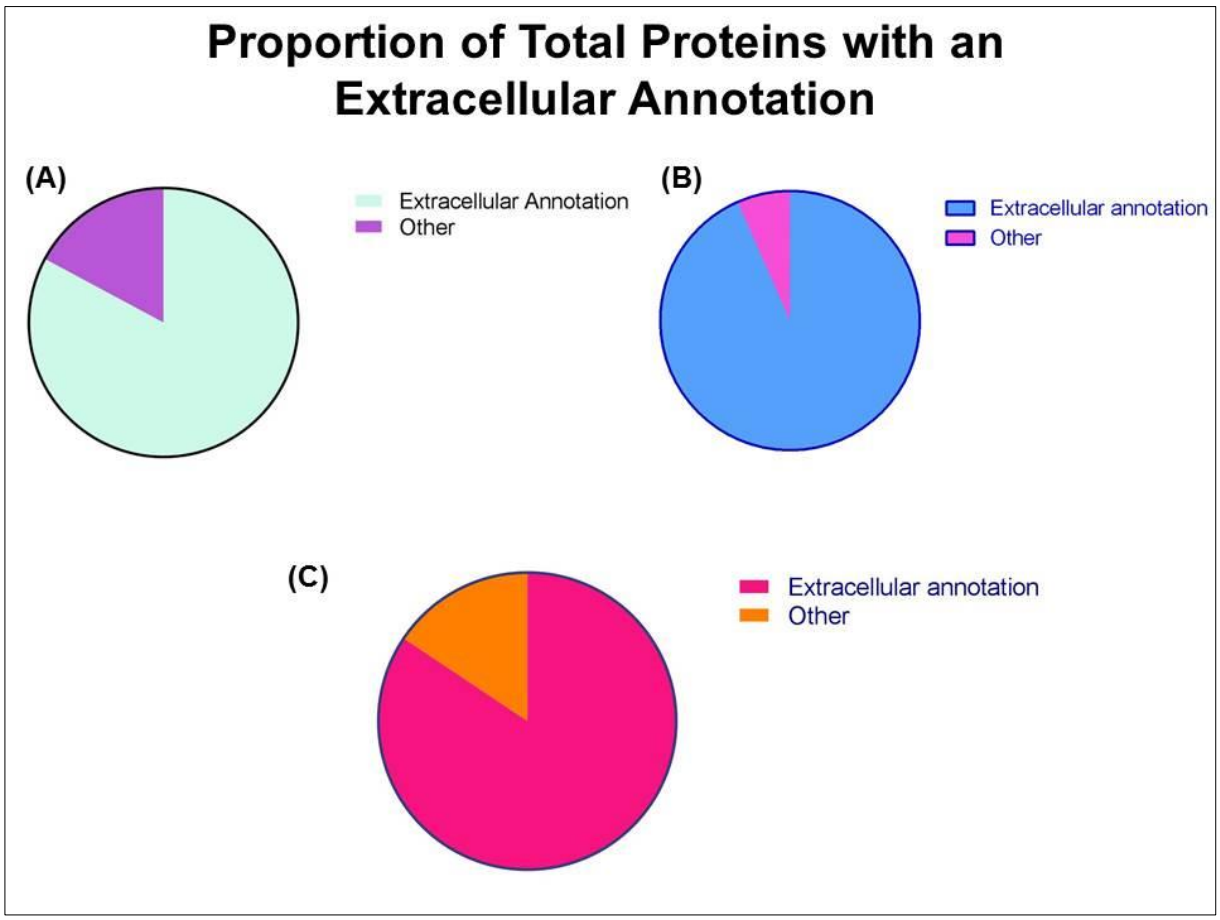

Figure 6.3.4 Proportion of all Detected Proteins with an Extracellular Annotation by Gene Ontology in Adipocytes

All proteins detected by LC-MS/MS in each experimental group were pooled after data filtering for the Rotenone dataset (A), the Antimycin A dataset (B) and the Dinitrophenol dataset (C). Cellular Component Analysis by Gene ontology was performed and the number of proteins that had an extracellular annotation (removing duplicates when a protein was annotated under multiple extracellular annotations) are graphed as a percentage of total proteins where “Extracellular Annotation” refers to proteins with an extracellular annotation and “other” refers to the remainder of proteins. For adipocytes, there were 6 extracellular annotations included in the analysis: “Extracellular Exosome”, “Extracellular Region Part”, “Extracellular Region”, “Extracellular Space”, “Extracellular Matrix”, “Proteinaceous Extracellular Matrix” and “Extracellular Matrix Component”.

6.2.3 Assessment of Data Quality and Correlation

Data correlation and replicate reproducibility were also assessed by performing multiscatter analysis of (Figures 6.3.5 – 6.3.7) and frequency histograms (Figure 6.3.8) of log_2 transformed LFQ Intensity values were performed for each replicate to analyse correlation between replicates.

Multiscatter plots show that within each experimental group most samples generally correlated well with each other, with exception of samples collected from one or two particular mice which had Pearson's Correlation Coefficient values of ~ 0.45 when compared to other replicates.

Figure 6.3.8 illustrated that for all experimental groups the merged frequency histograms of individual replicates were quite well superimposed for most groups. This indicates that the distribution of frequencies of log_2 LFQ intensity values were generally reproducible between replicates.

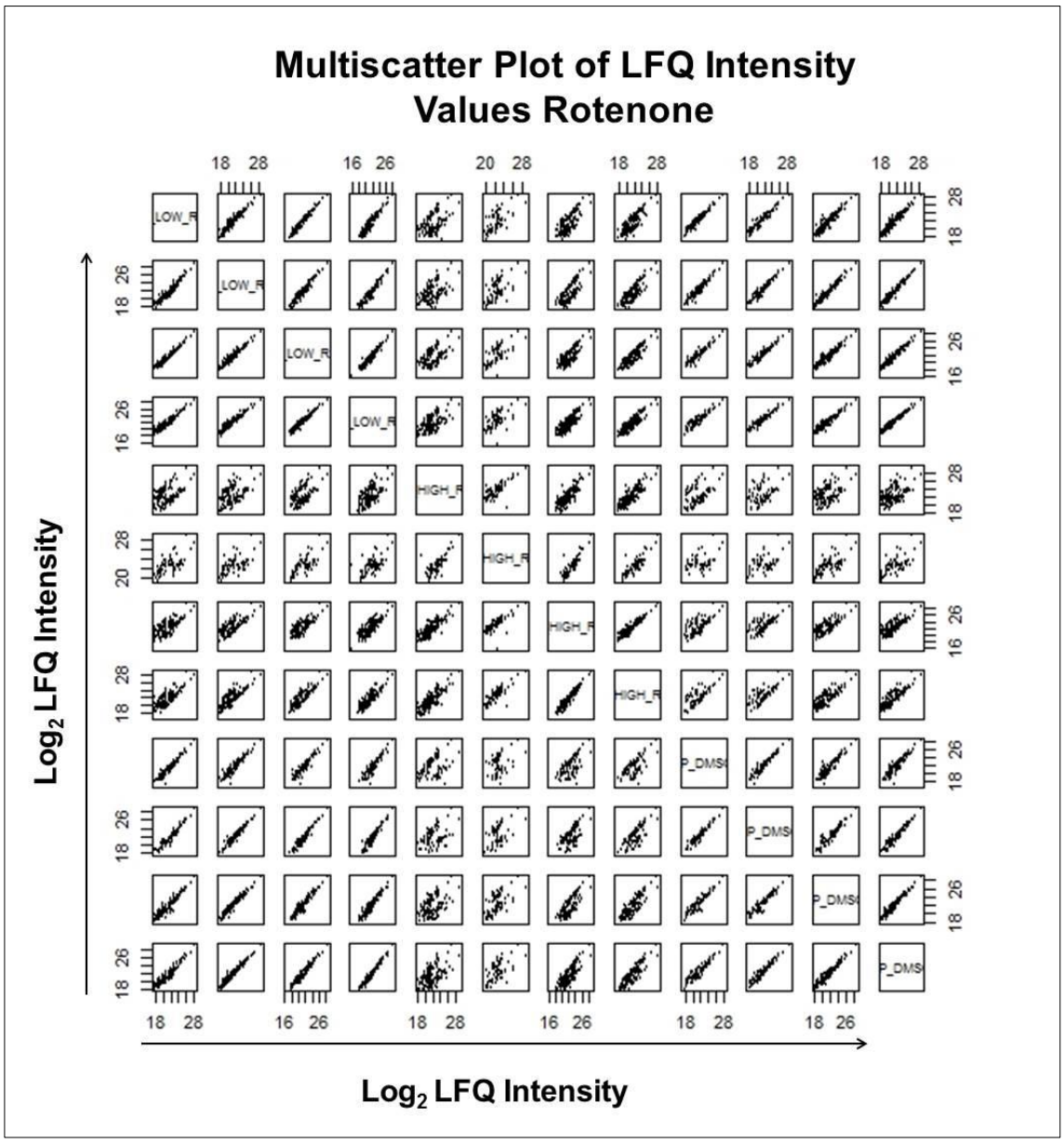

Figure 6.3.5 Multiscatter Plot of Individual Samples for Rotenone Dataset in Adipocytes

Log_2 transformed LFQ Intensity values for each single protein after filtering were plotted (one dot represents the Log_2 transformed LFQ Intensity value of one detected protein) for each sample of the rotenone dataset. From left to right – the first 4 samples are the 4 replicates the low dose rotenone group; the following 4 samples are the 4 replicates of the high dose rotenone group; and the following 4 samples are the 4 replicates of the Vehicle group.

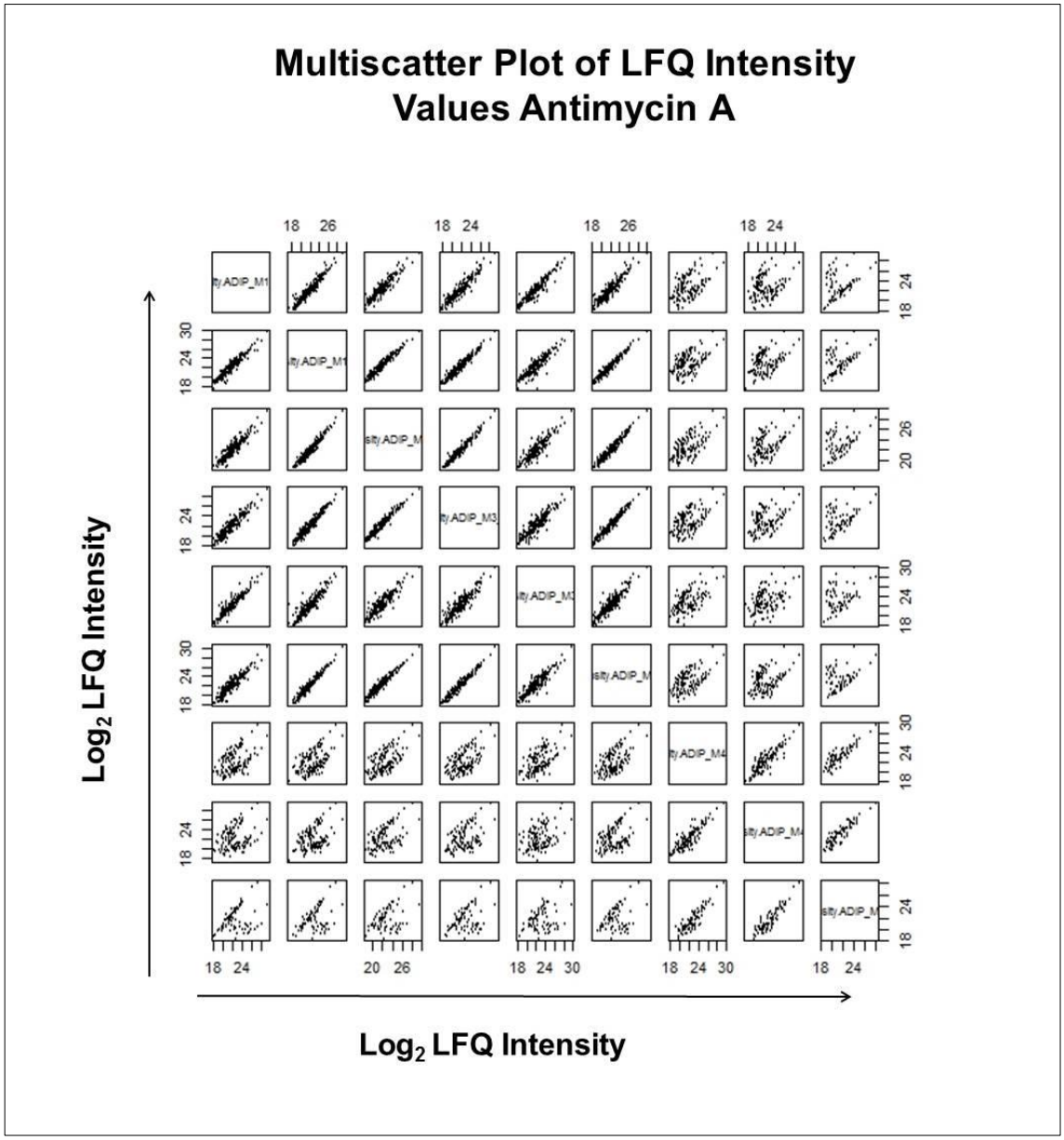

Figure 6.3.6 Multiscatter Plot of Individual Samples for Antimycin A Dataset in Adipocytes

Log_2 transformed LFQ Intensity values for each single protein after filtering were plotted (one dot represents the Log_2 transformed LFQ Intensity value of one detected protein) for each sample of the rotenone dataset. From left to right – the first 4 samples are the 4 replicates the low dose rotenone group; the following 4 samples are the 4 replicates of the high dose rotenone group; and the following 4 samples are the 4 replicates of the Vehicle group.

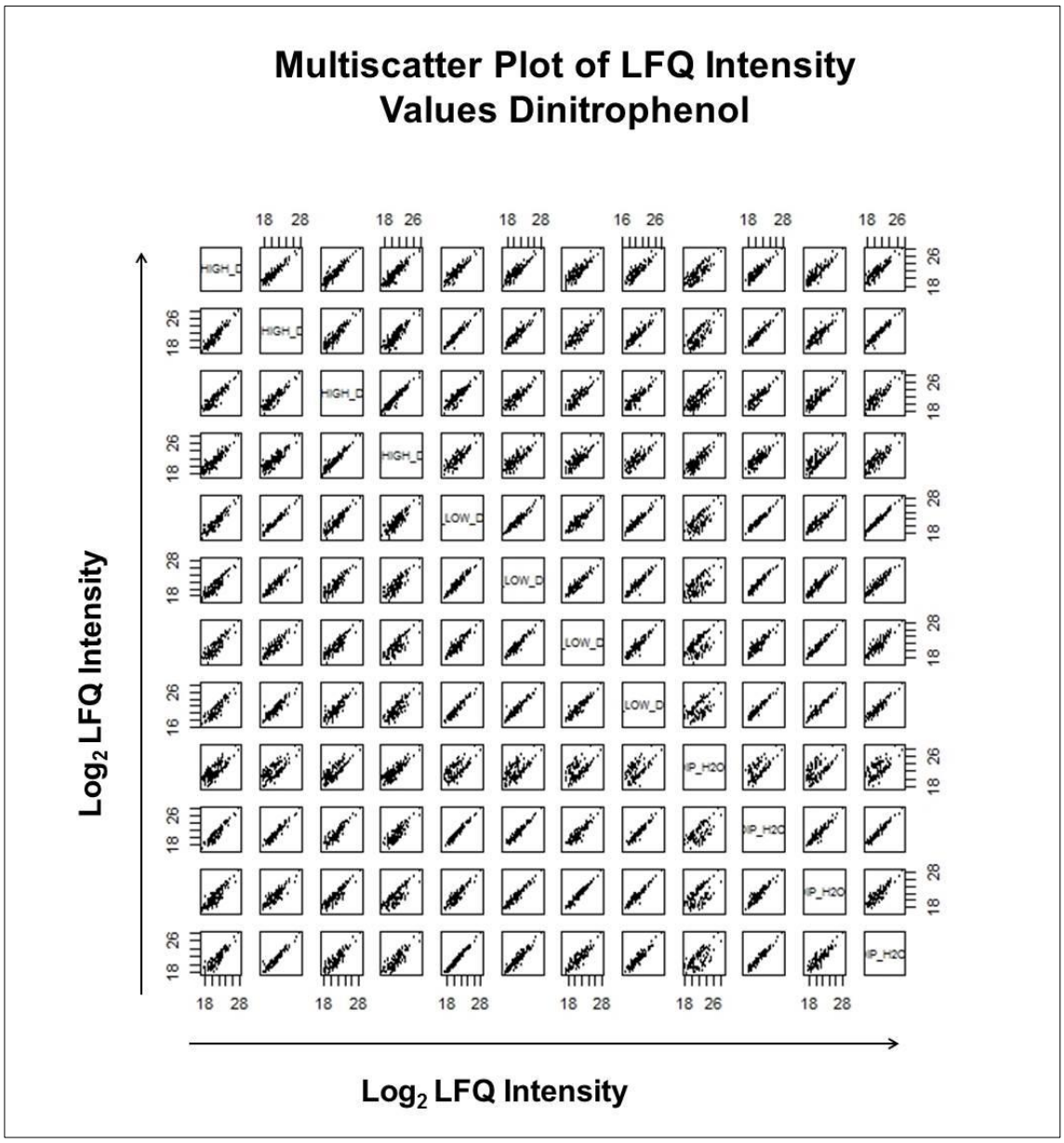

Figure 6.3.7 Multiscatter Plot of Individual Samples for Dinitrophenol Dataset in Adipocytes

Log_2 transformed LFQ Intensity values for each single protein after filtering were plotted (one dot represents the Log_2 transformed LFQ Intensity value of one detected protein) for each sample of the rotenone dataset. From left to right – the first 4 samples are the 4 replicates the low dose rotenone group; the following 4 samples are the 4 replicates of the high dose rotenone group; and the following 4 samples are the 4 replicates of the Vehicle group.

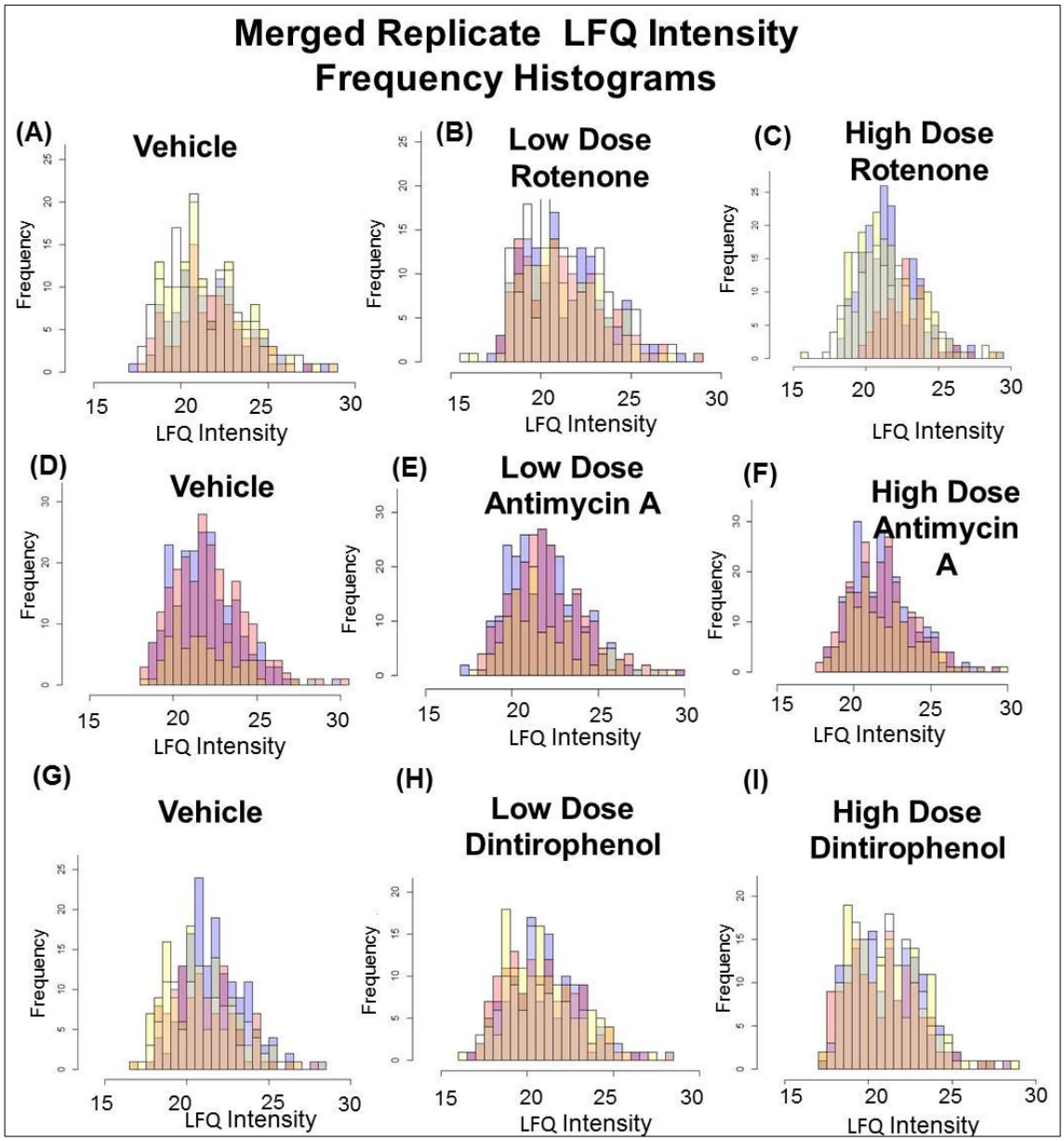

Figure 6.3.8 Merged Replicate Frequency Histograms of Log2 LFQ Intensity Values

Log_2 transformed LFQ Intensity Values were plotted as frequency histograms for each replicate and merged within each experimental group – (A) Vehicle for rotenone dataset, (B) low dose rotenone treatment, (C) High Dose rotenone, (D) Vehicle for antimycin A dataset, (E) low dose antimycin A treatment, (F) high dose antimycin A treatment (G) Vehicle for dinitrophenol dataset, (H) low dose dinitrophenol treatment, (I) high dose dinitrophenol treatment. Different colours represent individual replicates.

Overlap of Protein IDs amongst replicates for each group was also presented as venn diagrams (Figures 6.3.9 – 5.3.11) to measure the overlap of proteins identified by MS within an experimental group. For the rotenone dataset there was 62%, 75% and 76% overlap in 3 out of 4 replicates for vehicle, low dose and high dose treatments respectively. For the antimycin A dataset, there was 48%, 75% and 75% overlap in 3 out of 3 replicates for vehicle, low dose and high dose treatments respectively. For the vehicle experimental group, there was 76% overlap in 2 out of 3 replicates. 49%, 65% and 71% overlap was displayed in 4 out of 4 replicates for vehicle, low dose and high dose treatments respectively in the dinitrophenol dataset. In 3 out of 4 replicates, there was 62%, 75% and 82% overlap respectively.

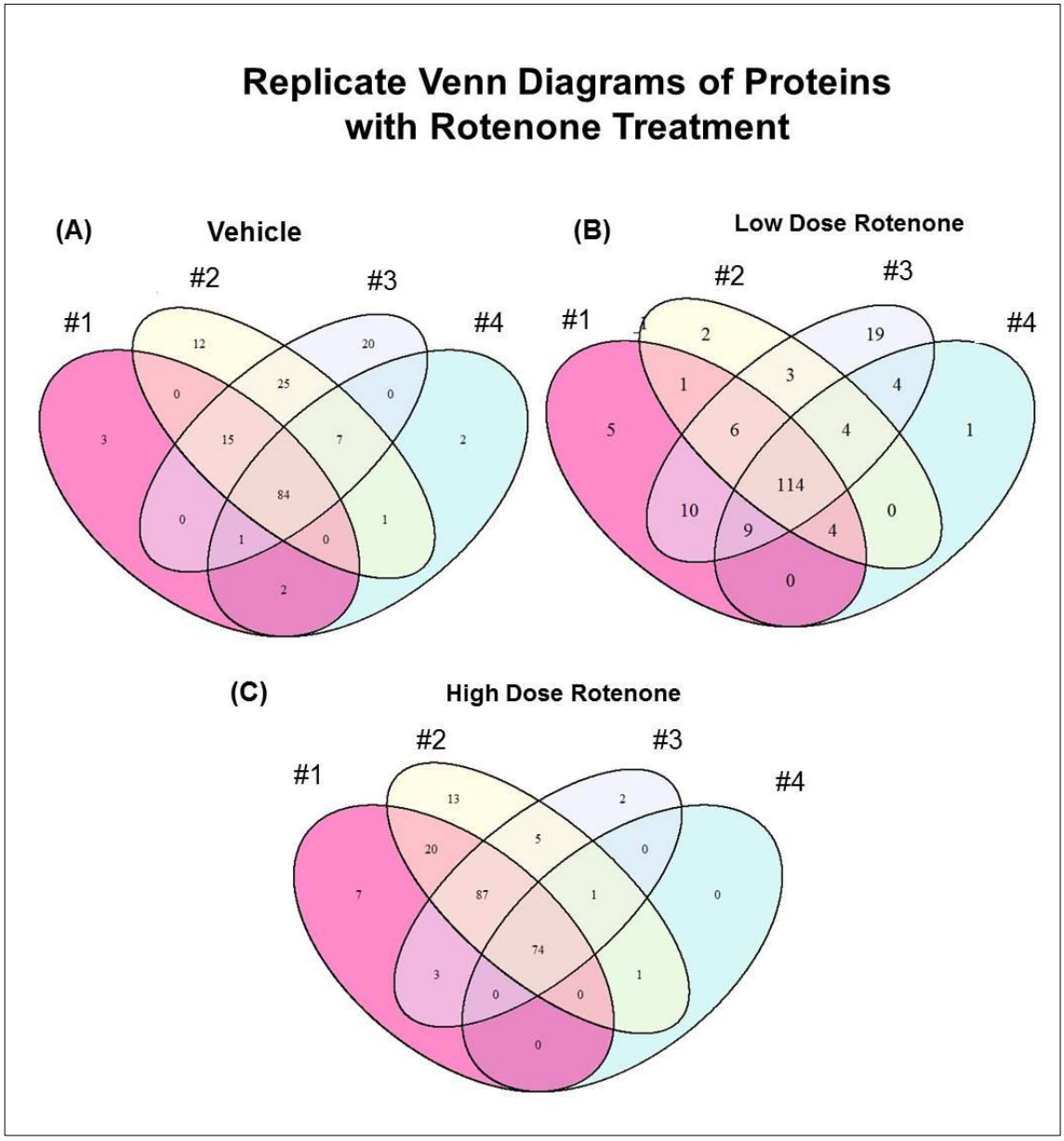

Figure 6.3.9 Overlap Analysis of Protein IDs detected in Individual Replicates for Rotenone Dataset

Venn Diagrams illustrating overlap of Protein IDs in each replicate Vehicle (A), low dose rotenone treatment (B) and high dose rotenone treatment (C). Different colours represent individual replicates.

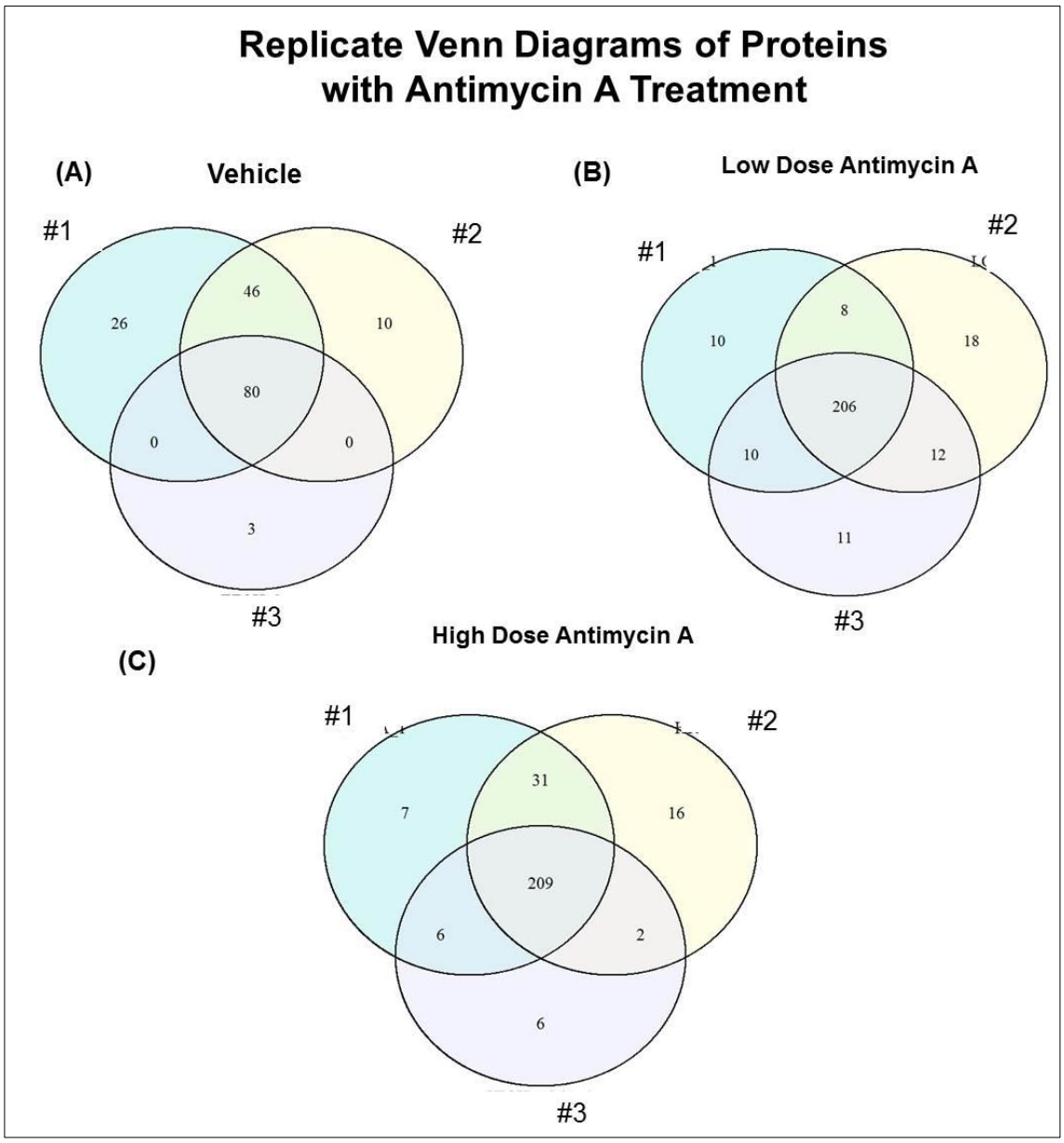

Figure 6.3.10 Overlap Analysis of Protein IDs detected in Individual Replicates for antimycin A Dataset

Venn Diagrams illustrating overlap of Protein IDs in each replicate Vehicle (A), low dose antimycin A treatment (B) and high dose antimycin A treatment (C). Different colours represent individual replicates.

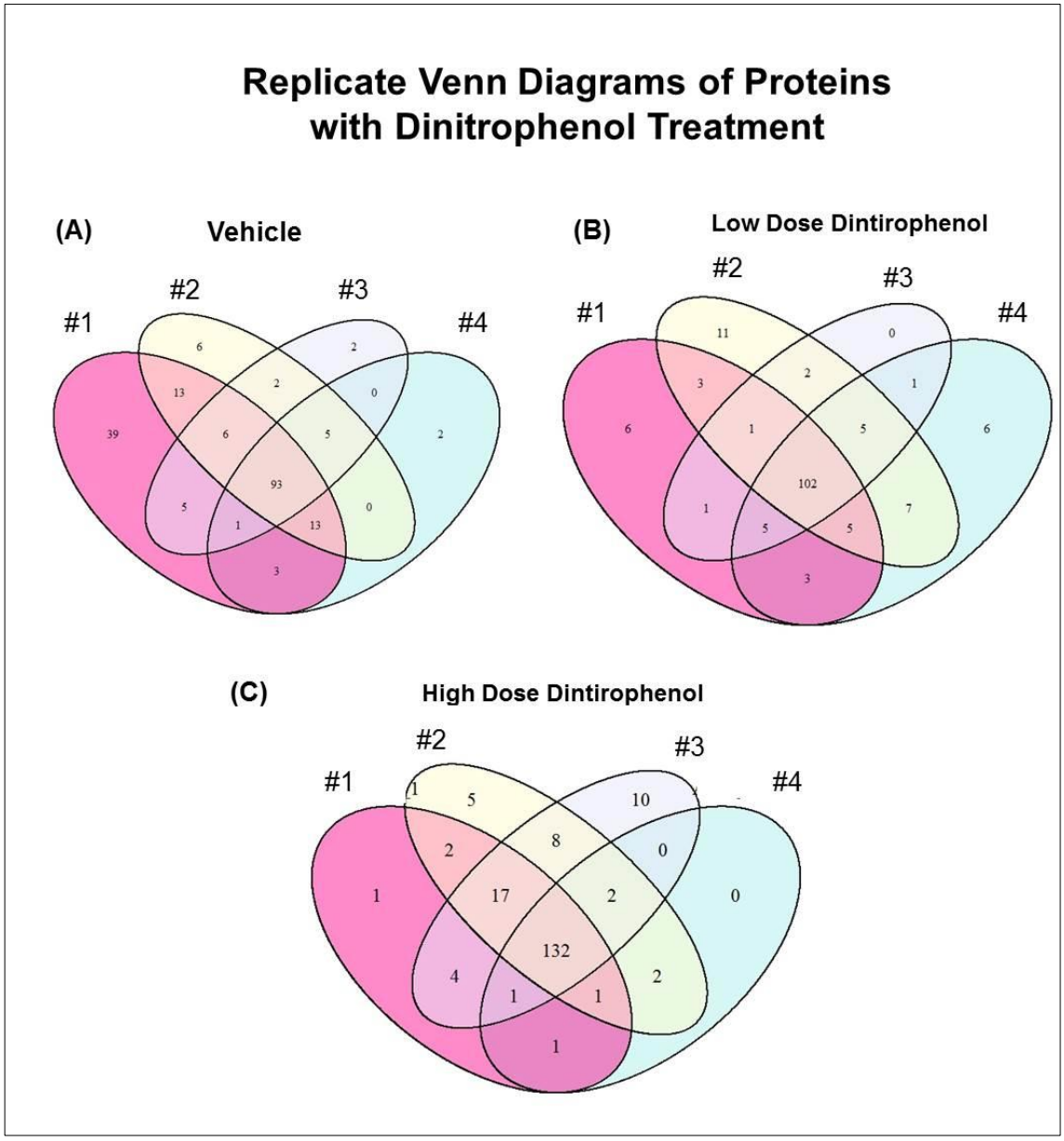

Figure 6.3.11 Overlap Analysis of Protein IDs detected in Individual Replicates for dinitrophenol Dataset

Venn Diagrams illustrating overlap of Protein IDs in each replicate Vehicle (A), low dose dinitrophenol treatment (B) and high dose dinitrophenol treatment (C). Different colours represent individual replicates.

6.2.4 Proteomics Analysis

After examining data quality, I went on to perform subsequent proteomic analysis. PCA analysis (Fig 6.3.12) was used to visualise the data and then ANOVA testing followed by a Benjamini-Hochberg correction analysis were performed for statistical analysis. PCA analysis revealed that high dose rotenone clustered away from the vehicle and low dose rotenone suggesting that a high level of Complex I inhibition causes a change to proteins secreted from adipocytes. In contrast, low dose and high dose antimycin treatment both cluster away from vehicle but not from each other suggesting that Complex III inhibition causes a remodelling of the adipocyte secretome irrespective of dose. For the dinitrophenol dataset, one of the vehicle replicates appeared as an outlier. With that aside, high dose dinitrophenol samples slightly cluster away from vehicle and low dose indicative of a pattern similar to that of rotenone.

ANOVA analysis followed by a Benjamini-Hochberg correction analysis revealed many significantly changed proteins in the antimycin A and rotenone groups which is reflected in the PCA analysis. There were no significant changes with dinitrophenol treatment. This is likely due to the outlier vehicle replicate seen in the PCA analysis.

Because many proteins were significantly changed, a more stringent FDR cutoff (0.01 or 1% FDR) was applied for subsequent proteomic analysis for antimycin A and rotenone datasets to provide an indication of the most important secretome changes. These were combined with abundance and illustrated in heat maps (Figure 6.3.13). Heat maps show that the adipocytes respond to different doses of ETC inhibitors differently between Complex I and Complex III (Figure 6.3.13). With rotenone treatment of adipocytes, there is an apparent difference with high dose treatment compared with low dose. This was also reflected above in the PCA graphs (Figure 6.3.12). While for antimycin A the changes were similar in both treatment groups. Individually changed proteins are presented in Tables 6.3.1 – 6.3.5 and in contrast to the previous cell types in chapters 4 and 5, the secretion of many more proteins were increased rather than decreased in abundance in response rotenone and antimycin A.

There were variable patterns with the changes in secretion with rotenone with many proteins generally showing concordant increases (Table 6.2.1) or decreases (Table 6.2.2), while a group of proteins (Table 6.3.3) showed significant disparate changes with the different doses (decreased in low dose, but increased in high dose). Across all the groups the protein with the highest fold increase with rotenone was Polymerase I and transcript release factor, which was increased >60-fold, while the most pronounced decrease was observed for thioredoxin (7-fold lower). For antimycin A several proteins showed relative changes in secretion that were greater than 200-fold including phosphoglycerate kinase 1, mitochondrial dihydrolipoyl dehydrogenase, Heat shock 70 kDa protein 4, 14-3-3 protein gamma, Prothymosin alpha and mitochondrial pyruvate carboxylase (Table 6.3.4). The most decreased protein in response to antimycin A treatment was mitochondrial long-chain acyl-CoA dehydrogenase, which was more than 10-fold lower.

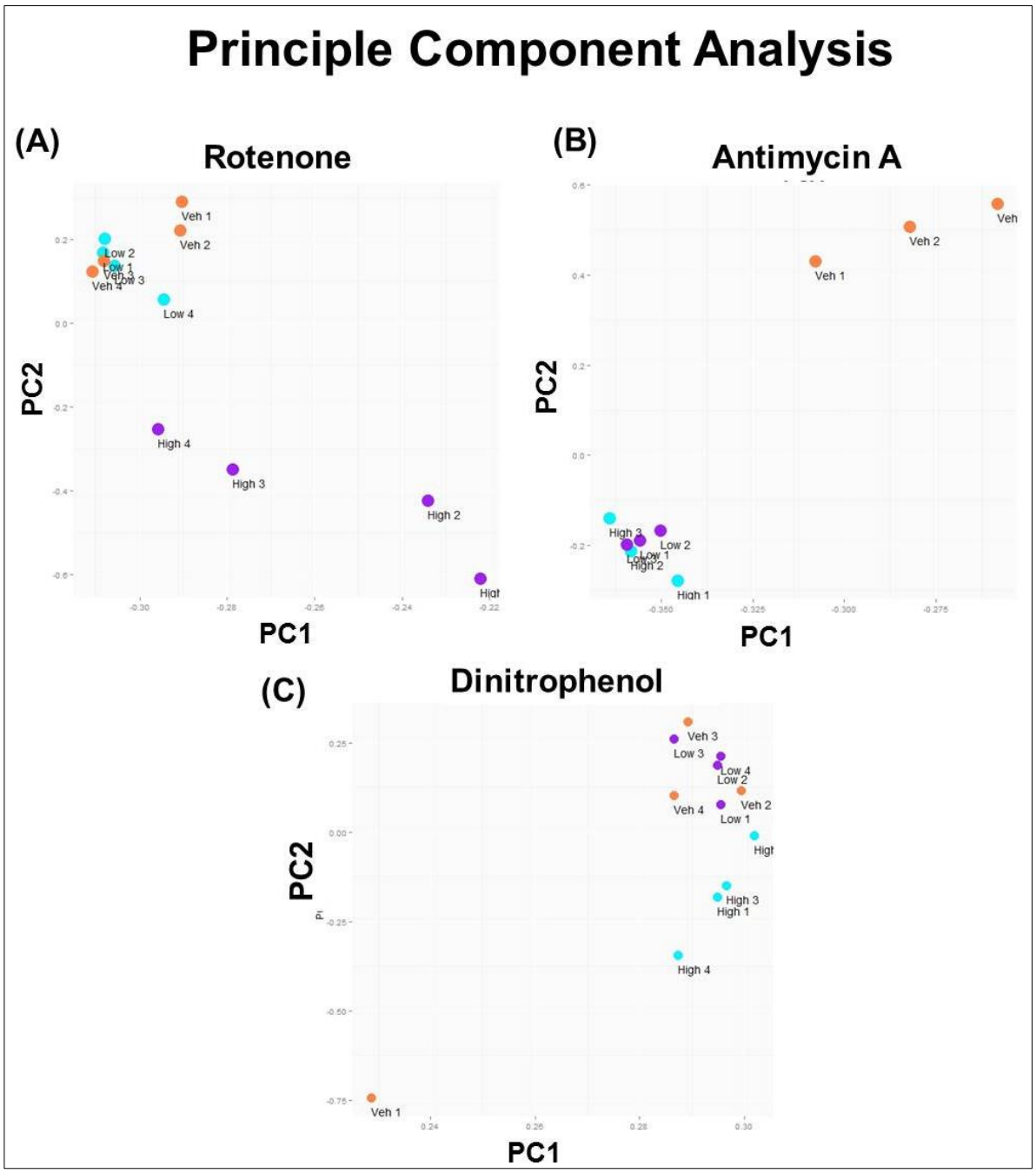

Figure 6.3.12 Principle Component Analysis (PCA) of Secreted Proteins from Adipocytes

PCA analysis of secreted proteins from hepatocytes for the Rotenone dataset (A); the Antimycin A dataset (B) and the dinitrophenol dataset (C). PC1 on the x axis represents Protein IDs and PC2 on the y axis represents abundance. Replicates within one group are represented as one colour.

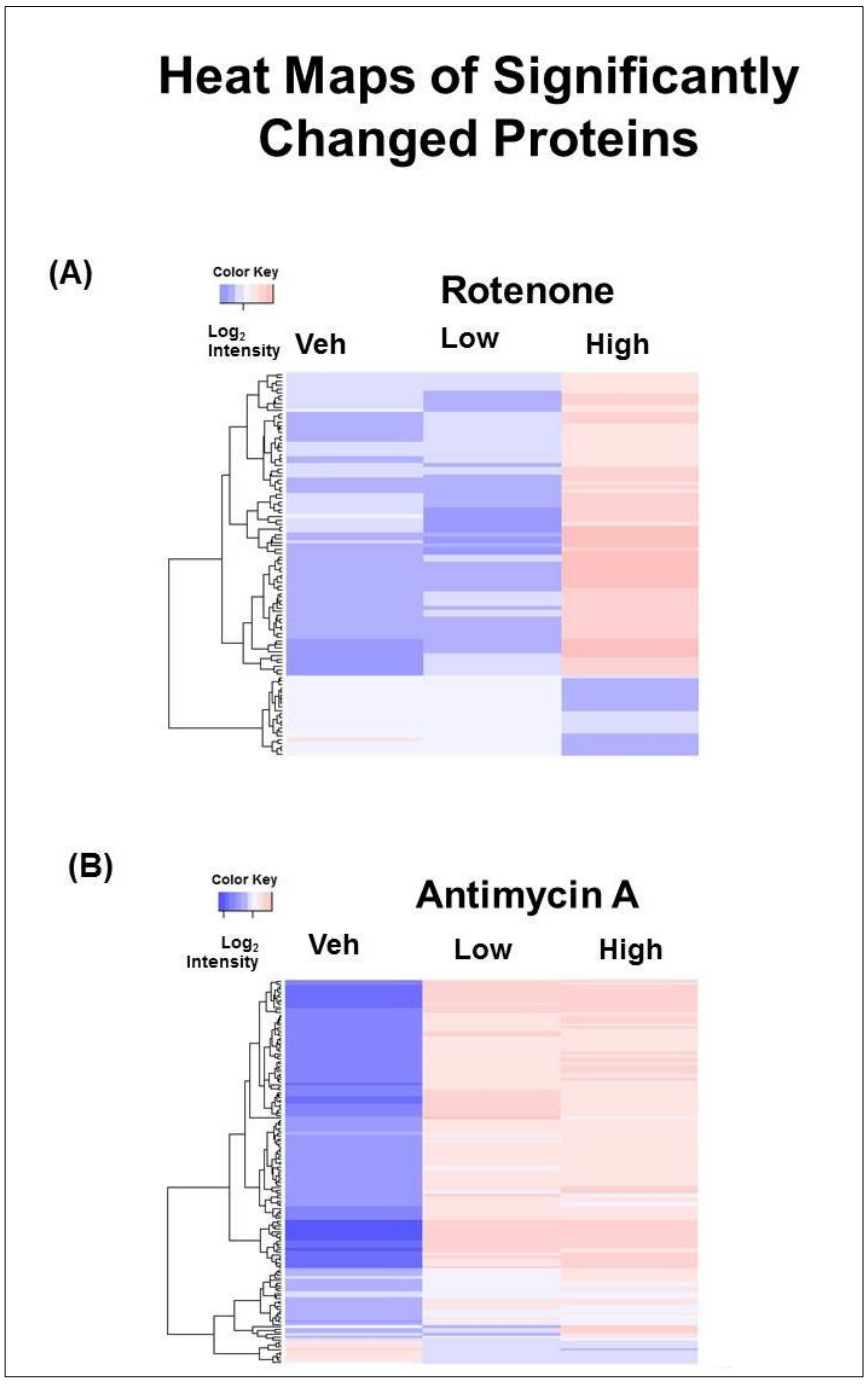

Figure 6.3.13 Abundance Heat maps of Significantly Changed Proteins in Adipocytes

Heat maps illustrating abundance of secreted proteins from adipocytes that were significantly changed ($p<0.05$, with less than 1% false discovery rate) with hierarchical clustering following treatment of rotenone (B) and antimycin A (B). Abundance was log_2 transformed with the colour representing abundance. The colour key present is coded such that white = 0, red for positive and blue for negative values. Data for individual proteins are presented in tables below.

Table 6.3.1 Secreted Proteins Increased in Abundance upon Rotenone Treatment in Adipocytes

Protein ID	Protein Name	Median Abundance			Fold Change		FDR
		DMSO	Low ROT	High ROT	Low vs. Veh	High vs. Veh	
P35505	Fumarylacetoacetase	0.51	0.54	3.83	1.06	7.52	9E-05
Q62009	Periostin	0.33	0.36	7.91	1.11	24.13	9E-05
P40142	Transketolase	0.38	0.51	6.43	1.34	16.98	9E-05
P34914	Epoxide hydrolase 2	0.37	0.56	8.04	1.52	21.89	9E-05
P19096	Fatty acid synthase	0.35	0.56	8.91	1.61	25.75	9E-05
P08249	Malate dehydrogenase, mitochondrial	0.48	0.40	3.90	0.83	8.12	1E-04
Q9DCD0	6-phosphogluconate dehydrogenase, decarboxylating	0.69	0.43	3.45	0.63	5.03	2E-04
Q3V117	ATP-citrate synthase	0.53	0.42	5.59	0.80	10.63	2E-04
A6ZI44	Fructose-bisphosphate aldolase	0.34	0.34	9.17	1.00	27.21	2E-04
G5E8N5	L-lactate dehydrogenase	0.58	0.61	3.11	1.04	5.33	2E-04
P63017	Heat shock cognate 71 kDa protein	0.34	0.39	6.12	1.13	17.79	2E-04
A8IP69	14-3-3 protein gamma	0.96	0.50	2.94	0.53	3.07	3E-04
P09411	Phosphoglycerate kinase 1	0.45	0.27	12.54	0.61	28.12	3E-04
Q99KI0	Aconitate hydratase, mitochondrial	0.74	0.52	2.77	0.71	3.76	3E-04
Q61425	Hydroxyacyl-coenzyme A dehydrogenase, mitochondrial	0.32	0.52	7.14	1.62	22.31	4E-04
P08228	Superoxide dismutase [Cu-Zn]	0.38	0.64	3.89	1.70	10.36	5E-04
Q9CQV8	14-3-3 protein beta/alpha	0.33	0.66	3.94	1.97	11.78	5E-04
E9PZF0	Nucleoside diphosphate kinase	0.39	0.69	5.21	1.76	13.36	5E-04
P06801	NADP-dependent malic enzyme	0.38	0.49	5.28	1.31	14.07	5E-04
P15105	Glutamine synthetase	0.48	0.28	8.68	0.59	18.00	6E-04
Q9D6R2	Isocitrate dehydrogenase [NAD] subunit alpha, mitochondrial	0.35	0.65	4.50	1.88	13.01	7E-04

A0A0A0MQF6	Glyceraldehyde-3-phosphate dehydrogenase	0.39	0.61	5.29	1.58	13.72	9E-04
H7BWY6	Retinol-binding protein 4	0.18	0.46	13.36	2.53	73.91	9E-04
G3X8T9	Serine protease inhibitor A3N	0.34	0.50	9.14	1.46	26.87	1E-03
Q93092	Transaldolase	0.54	0.54	3.18	1.00	5.86	1E-03
P16045	Galectin-1	0.28	0.48	8.34	1.68	29.33	1E-03
Q9D9V3	Ethylmalonyl-CoA decarboxylase	0.17	0.64	9.36	3.79	55.02	1E-03
P20108	Thioredoxin-dependent peroxide reductase, mitochondrial	0.49	0.65	3.21	1.33	6.60	1E-03
P19157	Glutathione S-transferase P 1	0.31	0.58	6.65	1.90	21.63	1E-03
P26883	Peptidyl-prolyl cis-trans isomerase FKBP1A	0.20	0.55	7.69	2.77	38.97	1E-03
P08121	Collagen alpha-1(III) chain	0.26	0.39	9.92	1.54	38.75	1E-03
P35700	Peroxiredoxin-1	0.28	0.55	6.96	1.94	24.47	1E-03
Q61171	Peroxiredoxin-2	0.23	0.80	5.90	3.46	25.70	1E-03
Q5SWU9	Acetyl-CoA carboxylase 1	0.52	0.56	2.77	1.06	5.31	1E-03
P97371	Proteasome activator complex subunit 1	0.37	0.22	11.36	0.61	30.76	2E-03
P17182	Alpha-enolase	0.37	0.46	5.76	1.23	15.40	2E-03
O88844	Isocitrate dehydrogenase [NADP] cytoplasmic	0.48	0.56	3.71	1.18	7.74	2E-03
P52480	Pyruvate kinase isozymes M1/M2	0.28	0.53	5.30	1.88	18.98	2E-03
Q80X81	Acetyl-CoA acetyltransferase, cytosolic	0.43	0.43	5.70	1.01	13.40	2E-03
Q3UBS3	Haptoglobin	0.20	0.80	4.60	4.06	23.46	2E-03
P10126	Elongation factor 1-alpha 1	0.23	0.88	4.24	3.81	18.45	2E-03
Q9WTP6	Adenylate kinase 2, mitochondrial	0.40	0.49	3.76	1.24	9.50	2E-03
Q01149	Collagen alpha-2(I) chain	0.38	0.48	4.13	1.28	10.98	2E-03
P62897	Cytochrome c, somatic	0.49	0.70	3.23	1.43	6.60	3E-03
A0A0R4J1E2	Elongation factor 1-delta	0.37	0.71	3.94	1.94	10.77	3E-03
P56395	Cytochrome b5	0.30	0.35	9.65	1.16	32.15	3E-03

Q8BPB5	EGF-containing fibulin-like extracellular matrix protein 1	0.28	0.36	9.62	1.28	33.78	3E-03
P45952	Medium-chain specific acyl-CoA dehydrogenase, mitochondrial	0.53	0.63	4.78	1.18	8.95	3E-03
G3UYJ7	D-dopachrome decarboxylase	0.38	0.23	7.99	0.59	20.78	4E-03
P97290	Plasma protease C1 inhibitor	0.24	0.56	7.12	2.35	29.76	4E-03
Q5BMX4	Resistin	0.75	0.52	3.55	0.69	4.76	4E-03
P10493	Nidogen-1	0.29	0.47	6.51	1.60	22.10	4E-03
Q07797	Galectin-3-binding protein	0.40	0.42	6.98	1.06	17.60	4E-03
A0A087WR50	Fibronectin	0.87	0.74	3.16	0.86	3.65	4E-03
Q8R0Y6	Cytosolic 10-formyltetrahydrofolate dehydrogenase	0.31	0.20	8.76	0.64	28.42	5E-03
P07901	Heat shock protein HSP 90-alpha	0.71	0.70	3.31	0.99	4.68	5E-03
P63028	Translationally-controlled tumor protein	0.56	0.46	3.44	0.83	6.14	5E-03
Q9JLI2		0.55	0.56	4.36	1.01	7.96	5E-03
P21460	Cystatin-C	0.31	0.45	8.19	1.44	26.47	5E-03
O54724	Polymerase I and transcript release factor	0.18	0.28	12.70	1.53	68.72	5E-03
P20152	Vimentin	0.42	0.44	6.09	1.06	14.50	5E-03
Q6GT24	Peroxiredoxin-6	0.24	0.45	12.25	1.87	51.45	7E-03
P00493	Hypoxanthine-guanine phosphoribosyltransferase	0.46	0.53	3.97	1.15	8.63	7E-03
P02463	Collagen alpha-1(IV) chain	0.34	0.54	7.45	1.60	22.15	7E-03
Q3UKW2	Calmodulin	0.20	0.48	10.33	2.40	51.91	7E-03
P68372	Tubulin beta-4B chain	0.46	0.42	4.69	0.91	10.11	1E-02

Table 6.3.2 illustrates proteins secreted by adipocytes that displayed significantly increased abundance with respect to vehicle upon rotenone treatment with less than 1% chance of false discovery. Rows of the table are displayed by adjusted pvalue from lowest to highest. Uniprot ID, protein name are provided along with median abundance of replicates with abundance calculated by LFQ Intensity algorithm using MaxQuant Software. “Low ROT” and “High ROT” refers to low and high dose treatments of rotenone respectively with “Low vs. Veh” and “High vs. Veh” representing fold changes respect to vehicle control of low and high doses of antimycin A treatment

respectively. FDR value refers to the adjusted pvalue following a Benjamini-Hochberg correction analysis to estimate the change of a significant pvalue in ANOVA analysis being a false discovery

Table 6.3.3 Secreted Proteins Decreased in Abundance upon Rotenone Treatment in Adipocytes

Protein ID	Protein Name	Median Abundance			Fold Change		FDR
		DMSO	Low ROT	High ROT	Low vs. Veh	High vs. Veh	
P42125	Enoyl-CoA delta isomerase 1, mitochondrial	1.47	1.72	0.49	1.17	0.33	0.000
P14152	Malate dehydrogenase, cytoplasmic	1.44	1.57	0.46	1.09	0.32	0.000
P16015	Carbonic anhydrase 3	1.20	1.37	0.59	1.14	0.49	0.000
Q9CZU6	Citrate synthase, mitochondrial	1.82	1.60	0.35	0.88	0.19	0.000
P11087	Collagen alpha-1(I) chain	1.52	1.58	0.44	1.04	0.29	0.000
Q00612	Glucose-6-phosphate 1-dehydrogenase X	1.38	1.48	0.37	1.08	0.27	0.000
Q8BH64	EH domain-containing protein 2	1.39	1.57	0.45	1.13	0.32	0.001
P31786	Acyl-CoA-binding protein	1.52	1.58	0.46	1.04	0.30	0.001
P13707	Glycerol-3-phosphate dehydrogenase [NAD(+)], cytoplasmic	1.19	1.57	0.54	1.32	0.45	0.001
Q4FK49	Inorganic pyrophosphatase	1.61	1.82	0.32	1.13	0.20	0.001
Q4KL76	10 kDa heat shock protein, mitochondrial	1.34	1.40	0.53	1.05	0.39	0.001
B2RTL5	Aldehyde dehydrogenase, cytosolic 1	1.45	1.88	0.52	1.29	0.36	0.003
P07214	SPARC	1.49	1.85	0.39	1.24	0.26	0.003
P11499	Heat shock protein HSP 90-beta	1.16	1.69	0.47	1.45	0.40	0.003
D3Z041	Long-chain-fatty-acid--CoA ligase 1	1.37	1.62	0.48	1.19	0.35	0.003
P11152	Lipoprotein lipase	1.52	1.76	0.37	1.16	0.25	0.004
Q4FZK2	Elongation factor 1-gamma	1.46	1.45	0.49	1.00	0.33	0.005
A2CEK3	Phosphoglucomutase-1	1.39	1.39	0.58	1.00	0.42	0.005
O88492	Perilipin-4	1.31	1.88	0.49	1.44	0.37	0.005
O08749	Dihydrolipoyl dehydrogenase, mitochondrial	2.02	1.41	0.38	0.70	0.19	0.008

Table 6.3.3 illustrates proteins secreted by adipocytes that displayed significantly decreased abundance with respect to vehicle upon rotenone treatment with less than 1% chance of false discovery. Rows of the table are displayed by adjusted pvalue from lowest to highest. Uniprot ID, protein name are provided along with median abundance

of replicates with abundance calculated by LFQ Intensity algorithm using MaxQuant Software. “Low ROT” and “High ROT” refers to low and high dose treatments of rotenone respectively with “Low vs. Veh” and “High vs. Veh” representing fold changes respect to vehicle control of low and high doses of antimycin A treatment respectively. FDR value refers to the adjusted pvalue following a Benjamini-Hochberg correction analysis to estimate the change of a significant pvalue in ANOVA analysis being a false discovery

Table 6.3.4 Proteins Downregulated by Low Dose but Upregulated by High Dose Rotenone

Protein ID	Protein Name	Median Abundance			Fold Change		FDR
		DMSO	Low ROT	High ROT	Low vs. Veh	High vs. Veh	
Q05816	Fatty acid-binding protein, epidermal	0.83	0.20	4.73	0.23	5.68	0.000
P17751	Triosephosphate isomerase	0.80	0.29	6.38	0.37	7.97	0.000
Q4FJK0	2,4-dienoyl-CoA reductase, mitochondrial	1.20	0.39	2.75	0.32	2.28	0.001
Q540D7	Alcohol dehydrogenase [NADP(+)]	0.88	0.29	4.21	0.33	4.79	0.002
Q62356	Follistatin-related protein 1	0.67	0.13	10.53	0.19	15.60	0.002
O35206	Collagen alpha-1(XV) chain	0.76	0.34	3.46	0.44	4.53	0.002
Q63918	Serum deprivation-response protein	0.70	0.35	7.39	0.50	10.54	0.002
Q99LX0	Protein DJ-1	0.90	0.39	4.19	0.43	4.66	0.002
H3BJQ7	Peroxiredoxin-5, mitochondrial	0.97	0.19	3.82	0.20	3.93	0.003
B2RQQ8	Collagen alpha-2(IV) chain	0.67	0.30	5.10	0.44	7.60	0.004
P10639	Thioredoxin	1.04	0.14	6.03	0.13	5.81	0.005
Q5SXR6	Clathrin heavy chain 1	0.92	0.32	4.53	0.35	4.89	0.005
Q3U7Z6	Phosphoglycerate mutase	0.53	0.19	10.96	0.36	20.70	0.005
P63101	14-3-3 protein zeta/delta	0.75	0.29	5.55	0.39	7.41	0.006
P13020	Gelsolin	0.79	0.24	5.45	0.30	6.92	0.006
Q9D1A2	Cytosolic non-specific dipeptidase	0.72	0.13	10.82	0.18	14.95	0.006
P17742	Peptidyl-prolyl cis-trans isomerase A	0.76	0.23	6.12	0.30	8.07	0.007

Table 6.3.4 illustrates proteins secreted by adipocytes that displayed significantly decreased abundance with a low dose of rotenone and a increase in abundance with a high dose of rotenone. Rows of the table are displayed by adjusted pvalue from lowest to highest. Uniprot ID, protein name are provided along with median abundance of replicates with abundance calculated by LFQ Intensity algorithm using MaxQuant Software. “Low ROT” and “High ROT” refers to low and high dose treatments of rotenone respectively with “Low vs. Veh” and “High vs. Veh” representing fold changes respect to vehicle control of low and high doses of antimycin A treatment respectively. FDR value refers to the adjusted pvalue following a Benjamini-Hochberg

correction analysis to estimate the change of a significant pvalue in ANOVA analysis being a false discovery

Table 6.3.5 Secreted Proteins Increased in Abundance upon Antimycin A Treatment in Adipocytes

Protein ID	Protein name	Median Abundance			Fold Change		FDR
		Vehicle	Low AMA	High AMA	Low vs. Veh	High vs. Veh	
E9Q4M2	Hormone-sensitive lipase	0.08	3.66	3.23	47.20	41.63	0.000
D3Z041	Long-chain-fatty-acid--CoA ligase 1	0.08	4.39	7.76	58.02	102.56	0.000
Q540D7	Alcohol dehydrogenase [NADP(+)]	0.08	3.78	4.27	48.42	54.73	0.000
A0A0R4J093	UMP-CMP kinase	0.10	2.71	4.08	26.36	39.61	0.000
O54724	Polymerase I and transcript release factor	0.22	2.33	2.73	10.74	12.56	0.000
Q9D6R2	Isocitrate dehydrogenase [NAD] subunit alpha, mitochondrial	0.11	3.82	3.57	34.75	32.49	0.000
Q61425	Hydroxyacyl-coenzyme A dehydrogenase, mitochondrial	0.65	1.33	1.54	2.06	2.39	0.000
P17182	Alpha-enolase	0.06	6.53	4.64	103.23	73.37	0.000
Q9D9V3	Ethylmalonyl-CoA decarboxylase	0.11	3.61	4.37	31.46	38.11	0.000
P09411	Phosphoglycerate kinase 1	0.03	4.66	5.78	174.02	215.96	0.000
P45376	Aldose reductase	0.09	3.30	3.72	35.29	39.87	0.000
P62827	GTP-binding nuclear protein Ran	0.07	2.90	4.03	39.72	55.19	0.000
P38647	Stress-70 protein, mitochondrial	0.22	2.04	2.34	9.11	10.45	0.000
Q9QUM9	Proteasome subunit alpha type-6	0.10	4.78	3.80	48.11	38.19	0.000
P17751	Triosephosphate isomerase	0.51	1.63	1.78	3.18	3.46	0.000
Q8CAY6	Acetyl-CoA acetyltransferase, cytosolic	0.27	2.10	2.57	7.92	9.69	0.000
Q4FK49	Inorganic pyrophosphatase	0.06	2.92	3.92	45.97	61.69	0.000
P14901	Heme oxygenase 1	0.09	3.62	4.20	38.17	44.21	0.000
G5E8N5	L-lactate dehydrogenase	0.26	2.17	1.84	8.37	7.09	0.000

Q99L13	3-hydroxyisobutyrate dehydrogenase, mitochondrial	0.27	2.62	1.71	9.84	6.42	0.000
Q8R0Y6	Cytosolic 10-formyltetrahydrofolate dehydrogenase	0.10	2.72	3.09	27.16	30.87	0.000
F8WGL3	Cofilin-1	0.13	2.11	4.66	16.58	36.64	0.000
P26041	Moesin	0.04	4.47	4.83	102.10	110.28	0.000
E9PZC3	Flavin reductase (NADPH)	0.39	1.39	2.01	3.58	5.18	0.000
Q9CZU6	Citrate synthase, mitochondrial	0.24	1.91	2.91	8.02	12.21	0.000
Q543J4	Thyroid hormone-inducible hepatic protein	0.14	1.76	4.05	12.77	29.43	0.000
P63017	Heat shock cognate 71 kDa protein	0.14	2.56	2.68	18.53	19.38	0.000
P10126	Elongation factor 1-alpha 1	0.11	2.56	2.55	23.05	22.98	0.000
Q61171	Peroxiredoxin-2	0.10	3.53	2.10	35.13	20.87	0.000
P34914	Epoxide hydrolase 2	0.07	4.60	3.29	66.66	47.59	0.000
P60843	Eukaryotic initiation factor 4A-I	0.06	4.12	5.17	71.06	89.11	0.000
Q9CQV8	14-3-3 protein beta/alpha	0.07	4.81	3.51	73.70	53.72	0.000
B9EHN0	Ubiquitin-like modifier-activating enzyme 1	0.04	4.27	5.57	106.86	139.50	0.000
P09671	Superoxide dismutase [Mn], mitochondrial	0.05	5.68	5.36	108.81	102.79	0.000
Q8QZS1	3-hydroxyisobutyryl-CoA hydrolase, mitochondrial	0.04	4.19	4.26	112.71	114.59	0.000
P07901	Heat shock protein HSP 90-alpha	0.04	4.55	3.38	122.61	91.12	0.000
Q9D1A2	Cytosolic non-specific dipeptidase	0.18	2.64	1.93	14.53	10.61	0.000
P14206	40S ribosomal protein SA	0.17	2.48	2.63	14.28	15.12	0.000
Q3U7Z6	Phosphoglycerate mutase	0.10	3.29	5.16	32.67	51.29	0.000
O08749	Dihydrolipoyl dehydrogenase, mitochondrial	0.02	7.14	7.01	307.08	301.35	0.000
Q61598	Rab GDP dissociation inhibitor beta	0.06	5.41	3.93	87.46	63.63	0.000
Q9WTP6	Adenylate kinase 2, mitochondrial	0.16	2.14	3.40	13.03	20.72	0.000
Q542H2	Proteasome subunit alpha type	0.16	2.60	3.44	16.02	21.18	0.000

B2RTL5	Aldehyde dehydrogenase, cytosolic 1	0.09	3.69	3.03	39.47	32.43	0.000
Q5SXR6	Clathrin heavy chain 1	0.03	4.49	4.54	161.25	163.09	0.000
Q3U2G2	Heat shock 70 kDa protein 4	0.02	6.47	5.16	265.21	211.63	0.000
P17742	Peptidyl-prolyl cis-trans isomerase A	0.24	1.91	1.81	8.01	7.58	0.000
Q4FJK0	2,4-dienoyl-CoA reductase, mitochondrial	0.10	3.73	3.20	38.34	32.88	0.000
A6ZI44	Fructose-bisphosphate aldolase	0.05	3.94	4.52	76.00	87.25	0.000
P16015	Carbonic anhydrase 3	0.04	4.90	4.99	129.51	131.84	0.000
Q05816	Fatty acid-binding protein, epidermal	0.04	3.68	4.58	82.71	102.86	0.000
P31786	Acyl-CoA-binding protein	0.05	4.64	4.87	92.55	97.20	0.000
P09405	Nucleolin	0.03	5.03	3.74	163.88	121.97	0.001
Q91V76	Ester hydrolase C11orf54 homolog	0.19	2.43	2.96	13.02	15.86	0.001
Q5SWU9	Acetyl-CoA carboxylase 1	0.17	2.89	3.09	16.86	18.01	0.001
P35505	Fumarylacetoacetase	0.17	3.87	2.08	23.10	12.41	0.001
A0A0A0MQF6	Glyceraldehyde-3-phosphate dehydrogenase	0.29	1.34	2.93	4.61	10.05	0.001
P99027	60S acidic ribosomal protein P2	0.41	1.40	2.35	3.38	5.68	0.001
Q93092	Transaldolase	0.17	1.78	3.01	10.21	17.29	0.001
P20152	Vimentin	0.06	4.52	3.82	72.68	61.40	0.001
A8IP69	14-3-3 protein gamma	0.03	6.33	6.62	225.11	235.37	0.001
O09131	Glutathione S-transferase omega-1	0.08	3.61	3.04	43.50	36.65	0.001
O88844	Isocitrate dehydrogenase [NADP] cytoplasmic	0.07	4.58	3.97	63.79	55.29	0.001
P20108	Thioredoxin-dependent peroxide reductase, mitochondrial	0.04	5.58	4.18	143.08	107.15	0.001
Q8BH64	EH domain-containing protein 2	0.07	3.27	3.70	48.28	54.65	0.001
P52480	Pyruvate kinase isozymes M1/M2	0.14	2.28	2.74	16.30	19.61	0.001
Q9DCD0	6-phosphogluconate dehydrogenase, decarboxylating	0.08	3.57	4.02	43.00	48.41	0.001

P23492	Purine nucleoside phosphorylase	0.31	1.76	1.83	5.65	5.89	0.001
P40142	Transketolase	0.05	3.08	5.58	62.62	113.32	0.001
P62715	Serine/threonine-protein phosphatase 2A catalytic subunit beta isoform	0.30	1.97	1.96	6.61	6.59	0.001
P13707	Glycerol-3-phosphate dehydrogenase [NAD(+)], cytoplasmic	0.29	2.53	2.40	8.82	8.34	0.001
P35700	Peroxiredoxin-1	0.22	2.29	3.23	10.64	15.02	0.001
Q63918	Serum deprivation-response protein	0.14	2.27	3.10	16.39	22.35	0.001
P04117	Fatty acid-binding protein, adipocyte	0.13	2.03	2.50	15.08	18.51	0.001
Q6GT24	Peroxiredoxin-6	0.14	9.73	1.77	69.47	12.61	0.001
E9PZF0	Nucleoside diphosphate kinase	0.08	2.24	3.14	27.77	38.90	0.001
P08249	Malate dehydrogenase, mitochondrial	0.28	1.90	2.04	6.71	7.20	0.001
P61979	Heterogeneous nuclear ribonucleoprotein K	0.26	2.45	2.17	9.56	8.46	0.001
Q8BH95	Enoyl-CoA hydratase, mitochondrial	0.17	4.54	1.87	27.04	11.11	0.001
Q99KI0	Aconitate hydratase, mitochondrial	0.08	5.77	2.67	71.92	33.28	0.001
P11499	Heat shock protein HSP 90-beta	0.37	0.61	4.51	1.66	12.35	0.001
A2CEK3	Phosphoglucomutase-1	0.09	4.45	3.91	49.36	43.37	0.001
P05202	Aspartate aminotransferase, mitochondrial	0.22	2.15	4.54	9.88	20.92	0.001
Q00612	Glucose-6-phosphate 1-dehydrogenase X	0.28	2.05	1.31	7.20	4.61	0.001
P97371	Proteasome activator complex subunit 1	0.22	2.42	3.32	10.88	14.90	0.001
P62908	40S ribosomal protein S3	0.07	5.01	2.34	73.63	34.32	0.001
P15105	Glutamine synthetase	0.27	0.51	4.51	1.92	16.85	0.001
Q5SQB7	Nucleophosmin	0.19	2.07	2.40	10.60	12.34	0.001
H3BJQ7	Peroxiredoxin-5, mitochondrial	0.65	0.49	2.04	0.75	3.14	0.002
P62075	Mitochondrial import inner membrane translocase subunit Tim13	0.21	2.87	2.20	13.86	10.61	0.002

A2AE89	Glutathione S-transferase Mu 1	0.13	2.39	2.91	18.84	22.97	0.002
Q99LX0	Protein DJ-1	0.03	4.27	4.90	160.45	184.43	0.002
Q4FZK2	Elongation factor 1-gamma	0.15	2.89	3.12	18.67	20.17	0.002
P63101	14-3-3 protein zeta/delta	0.06	4.72	4.69	83.79	83.21	0.002
P06801	NADP-dependent malic enzyme	0.38	1.57	2.43	4.09	6.32	0.002
P62897	Cytochrome c, somatic	0.09	3.66	4.10	42.68	47.81	0.002
P63038	60 kDa heat shock protein, mitochondrial	0.12	2.93	3.82	23.86	31.12	0.002
P31324	cAMP-dependent protein kinase type II-beta regulatory subunit	0.08	3.34	3.37	40.22	40.57	0.002
P45952	Medium-chain specific acyl-CoA dehydrogenase, mitochondrial	0.05	2.68	3.31	56.55	69.72	0.002
P70296	Phosphatidylethanolamine-binding protein 1	0.20	2.51	3.25	12.33	15.96	0.003
P62259	14-3-3 protein epsilon	0.08	3.64	3.90	43.28	46.39	0.003
P80314	T-complex protein 1 subunit beta	0.06	5.01	3.85	83.29	63.98	0.003
Q9Z2I9	Succinyl-CoA ligase [ADP-forming] subunit beta, mitochondrial	0.06	6.42	3.72	99.63	57.76	0.003
Q01149	Collagen alpha-2(I) chain	0.23	1.83	2.52	8.08	11.13	0.003
O55234	Proteasome subunit beta type-5	0.34	1.26	2.15	3.70	6.30	0.003
O35855	Branched-chain-amino-acid aminotransferase, mitochondrial	0.37	1.41	1.62	3.83	4.39	0.003
Q9D2R0	Acetoacetyl-CoA synthetase	0.07	2.22	3.24	30.79	44.96	0.003
P26350	Prothymosin alpha	0.02	4.17	5.84	235.29	329.46	0.003
P16125	L-lactate dehydrogenase B chain	0.13	2.06	3.04	16.41	24.22	0.003
P42125	Enoyl-CoA delta isomerase 1, mitochondrial	0.07	3.84	3.94	53.80	55.29	0.003
O88569	Heterogeneous nuclear ribonucleoproteins A2/B1	0.05	4.36	4.27	86.28	84.56	0.003
P62858	40S ribosomal protein S28	0.12	3.07	3.08	25.79	25.88	0.003

P08121	Collagen alpha-1(III) chain	0.56	0.73	1.57	1.30	2.83	0.003
Q01853	Transitional endoplasmic reticulum ATPase	0.04	3.95	4.27	97.93	105.92	0.004
Q3TRJ1	Vacuolar protein sorting-associated protein 35	0.07	4.75	6.13	70.12	90.49	0.004
P58252	Elongation factor 2	0.47	1.04	2.06	2.21	4.37	0.004
Q9D0K2	Succinyl-CoA:3-ketoacid-coenzyme A transferase 1, mitochondrial	0.07	3.50	3.92	52.68	59.00	0.004
P24270	Catalase	0.19	2.12	2.70	11.07	14.05	0.004
A3KGU9	Spectrin alpha chain, brain	0.07	4.43	3.28	59.41	43.90	0.004
P14152	Malate dehydrogenase, cytoplasmic	0.06	4.40	4.78	72.63	78.99	0.004
Q62261	Spectrin beta chain, brain 1	0.04	3.92	5.33	94.60	128.62	0.004
P28654	Decorin	0.09	3.56	2.85	40.76	32.64	0.005
P0CG50	Polyubiquitin-C	1.07	0.33	4.49	0.31	4.21	0.005
P11087	Collagen alpha-1(I) chain	0.24	2.52	2.57	10.47	10.69	0.005
P08228	Superoxide dismutase [Cu-Zn]	0.20	2.75	1.96	13.70	9.76	0.005
P63028	Translationally-controlled tumor protein	0.11	3.18	2.98	28.65	26.85	0.006
Q9R1P3	Proteasome subunit beta type-2	0.16	1.78	2.57	11.32	16.30	0.006
P56395	Cytochrome b5	0.08	3.27	4.53	41.65	57.79	0.006
P97372	Proteasome activator complex subunit 2	0.49	1.31	1.48	2.68	3.02	0.007
Q9CY58	Plasminogen activator inhibitor 1 RNA-binding protein	0.03	5.84	4.55	177.43	138.32	0.007
O70435	Proteasome subunit alpha type-3	0.37	1.64	1.98	4.46	5.38	0.007
Q76MZ3	Serine/threonine-protein phosphatase 2A 65 kDa regulatory subunit A alpha isoform	0.16	2.26	3.47	14.25	21.89	0.008
P11276	Fibronectin	0.44	1.48	2.87	3.39	6.56	0.008
E9QPD7	Pyruvate carboxylase, mitochondrial	0.03	5.81	7.60	192.24	251.31	0.008

Q3UBS3	Haptoglobin	0.05	4.56	4.27	88.65	82.96	0.008
P56480	ATP synthase subunit beta, mitochondrial	0.06	3.59	4.23	57.35	67.47	0.009
Q91VA7		0.07	3.37	4.58	51.12	69.43	0.009
P10605	Cathepsin B	0.54	1.51	2.73	2.78	5.04	0.009
E9PWQ3		0.08	4.82	2.54	60.03	31.59	0.009
Q62009	Periostin	0.33	2.30	1.79	7.02	5.47	0.010

Table 6.3.5 illustrates proteins secreted by adipocytes that displayed significantly increased abundance with respect to vehicle upon antimycin A treatment with less than 1% chance of false discovery. Rows of the table are displayed by adjusted pvalue from lowest to highest. Uniprot ID, protein name are provided along with median abundance of replicates with abundance calculated by LFQ Intensity algorithm using MaxQuant Software. “Low AMA” and “High AMA” refers to low and high dose treatments of antimycin A respectively with “Low vs. Veh” and “High vs. Veh” representing fold changes respect to vehicle control of low and high doses of antimycin A treatment respectively. FDR value refers to the adjusted pvalue following a Benjamini-Hochberg correction analysis to estimate the change of a significant pvalue in ANOVA analysis being a false discovery

Table 6.3.6 Secreted Proteins Decreased in Abundance with Antimycin A in Adipocytes

Protein ID	Protein name	Median Abundance			Fold Change		FDR
		Vehicle	low AMA	high AMA	Low vs. Veh	High vs. Veh	
A0A0R4J1E2	Elongation factor 1-delta	2.33	0.69	0.76	0.295	0.327	0.000
Q4KL76	10 kDa heat shock protein, mitochondrial	3.70	0.59	0.59	0.160	0.159	0.000
A0A0R4J083	Long-chain specific acyl-CoA dehydrogenase, mitochondrial	4.22	0.74	0.34	0.176	0.080	0.000
P16045	Galectin-1	2.48	0.66	0.60	0.268	0.241	0.000
P97807	Fumarate hydratase, mitochondrial	2.35	0.65	0.71	0.274	0.300	0.000
P19157	Glutathione S-transferase P 1	1.93	0.72	0.86	0.374	0.442	0.001
P19096	Fatty acid synthase	2.95	0.68	0.63	0.232	0.214	0.002
Q3V117	ATP-citrate synthase	3.32	0.66	0.61	0.198	0.182	0.002
Q543K5	Phosphoserine aminotransferase	2.23	0.76	0.61	0.341	0.275	0.003

Table 6.2.6 illustrates proteins secreted by adipocytes that displayed significantly decreased abundance with respect to vehicle upon antimycin A treatment with less than 1% chance of false discovery. Rows of the table are displayed by adjusted pvalue from lowest to highest. Uniprot ID, protein name are provided along with median abundance of replicates with abundance calculated by LFQ Intensity algorithm using MaxQuant Software. “Low AMA” and “High AMA” refers to low and high dose treatments of antimycin A respectively with “Low vs. Veh” and “High vs. Veh” representing fold changes respect to vehicle control of low and high doses of antimycin A treatment respectively. Adj p value refers to the adjusted pvalue following a Benjamini-Hochberg correction analysis to estimate the change of a significant pvalue in ANOVA analysis being a false discovery

Following statistics, network analysis and KEGG analysis were performed on proteins that were significantly altered by rotenone and antimycin A. Protein IDs were exported to string database (www.string-db.org) using “high confidence (0.7) for the minimum required interaction score and only selecting experiments and databases parameters for active interaction sources. This data was subject to KEGG pathway enrichment analysis presented in Table 6.3.6 and 6.3.7.

For rotenone treatment practically all of the pathways identified are involved in the regulation, uptake, processing or synthesis of metabolic fuel substrates. “Microbial metabolism in diverse environments” was the top pathway for both up-regulated and down-regulated proteins. The same pathway was the top hit for up-regulated proteins in the antimycin A-treated adipocytes, with the majority of other up-regulated pathways (and the two down-regulated pathways) primarily representing aspects of intermediary metabolism.

Table 6.2.7 Enriched KEGG Pathways for Proteins Secreted from Adipocytes that Changed in Abundance with Rotenone treatment

Pathway ID	Pathway Description	observed gene count	FDR
Increased with Rotenone			
1120	Microbial metabolism in diverse environments	19	2.48E-23
1200	Carbon metabolism	13	4.16E-16
1100	Metabolic pathways	25	6.74E-14
1230	Biosynthesis of amino acids	10	6.83E-13
20	Citrate cycle (TCA cycle)	5	1.39E-06
620	Pyruvate metabolism	5	5.68E-06
10	Glycolysis / Gluconeogenesis	5	3.55E-05
30	Pentose phosphate pathway	4	5.32E-05
640	Propanoate metabolism	4	5.42E-05
1212	Fatty acid metabolism	4	0.000343
480	Glutathione metabolism	4	0.000402
1210	2-Oxocarboxylic acid metabolism	3	0.000402
630	Glyoxylate and dicarboxylate metabolism	3	0.00101
4151	PI3K-Akt signaling pathway	7	0.00101
4146	Peroxisome	4	0.00155
61	Fatty acid biosynthesis	2	0.00186
4512	ECM-receptor interaction	4	0.00186
4974	Protein digestion and absorption	4	0.00186
4066	HIF-1 signaling pathway	4	0.00358
5146	Amoebiasis	4	0.00495
Decreased with Rotenone			
1120	Microbial metabolism in diverse environments	5	8.73E-05
20	Citrate cycle (TCA cycle)	3	0.000246
1200	Carbon metabolism	4	0.000246
1100	Metabolic pathways	7	0.00297
3320	PPAR signaling pathway	3	0.00297

Table 6.2.7 Displays significantly enriched (FDR<1%) KEGG pathways by gene ontology in response to Complex I inhibition in adipocytes. Secreted proteins that were significantly increased in abundance by dinitrophenol compared with vehicle ("Increased with Rotenone") and decreased by antimycin A ("Decreased with Rotenone") were separately subject to KEGG pathway enrichment analysis by gene ontology. The table provides the KEGG "Pathway ID" and "Pathway Description". The number of proteins that were annotated under a particular pathway was represented as "Observed Gene Count" and the FDR is provided.

Table 6.2.8 Enriched KEGG Pathways for Proteins Secreted from Adipocytes that Changed in Abundance with Antimycin A treatment

Pathway ID	Pathway Description	Observed gene count	FDR
Upregulated			
1120	Microbial metabolism in diverse environments	28	1.51E-33
1200	Carbon metabolism	23	2.97E-30
1100	Metabolic pathways	41	5.52E-23
1230	Biosynthesis of amino acids	15	4.12E-19
10	Glycolysis / Gluconeogenesis	10	1.62E-11
640	Propanoate metabolism	8	5.97E-11
620	Pyruvate metabolism	8	7.34E-10
280	Valine, leucine and isoleucine degradation	8	2.83E-09
20	Citrate cycle (TCA cycle)	7	3.03E-09
1210	2-Oxocarboxylic acid metabolism	6	4.56E-09
30	Pentose phosphate pathway	6	1.27E-07
630	Glyoxylate and dicarboxylate metabolism	5	2.37E-06
1212	Fatty acid metabolism	6	2.66E-06
3320	PPAR signaling pathway	6	3.59E-05
71	Fatty acid degradation	5	3.93E-05
4146	Peroxisome	6	3.93E-05
480	Glutathione metabolism	5	8.95E-05
650	Butanoate metabolism	4	9.84E-05
410	beta-Alanine metabolism	4	0.000193
4612	Antigen processing and presentation	5	0.000315
5169	Epstein-Barr virus infection	7	0.000554
4114	Oocyte meiosis	5	0.00167
4066	HIF-1 signaling pathway	5	0.00175
5134	Legionellosis	4	0.00175
4151	PI3K-Akt signaling pathway	8	0.00235
51	Fructose and mannose metabolism	3	0.00637
270	Cysteine and methionine metabolism	3	0.00667
4390	Hippo signaling pathway	5	0.00692
Downregulated			
20	Citrate cycle (TCA cycle)	2	0.0184
1212	Fatty acid metabolism	2	0.0241

Table 6.2.8 Displays significantly enriched (FDR<1%) KEGG pathways by gene ontology in response to Complex III inhibition in adipocytes. Secreted proteins that were significantly increased in abundance by dinitrophenol compared with vehicle ("Increased with Antimycin A") and decreased by antimycin A ("Decreased with Antimycin A") were separately subject to KEGG pathway enrichment analysis by gene

ontology. The table provides the KEGG “Pathway ID” and “Pathway Description”. The number of proteins that were annotated under a particular pathway was represented as “Observed Gene Count” and the FDR is provided.

6.3 Discussion

In this chapter, I have characterised the secretome of primary murine adipocytes (adipocytes) in response to ETC stressors. The adipocyte secretome was sensitive to Complex I and Complex III inhibition with many significantly changed proteins but did not change with a mitochondrial OXPHOS uncoupler. This was unexpected because adipocytes responded well to dinitrophenol in terms of stimulation of oxygen consumption rate (Figure 6.2.1) compared with HEK293 cells (Figure 4.3.1) and hepatocytes (Figure 5.3.1). Complex I inhibition by rotenone required a higher dose than complex III inhibition by antimycin A to cause remodelling of the secretome (Figure 6.3.7). It is possible that because adipocytes have a large source of lipid, they have a high capacity to oxidise fatty acids to donate electrons at Complex II due to $FADH_2$ generation in the beta oxidation pathway and hence a mild complex I inhibition may be compensated by this whereas, a mild Complex III inhibition may not.

Comparing individual proteins with previous chapters, fibronectin was also increased in secretion with ETC inhibitors in adipocytes which is consistent with hepatocytes in chapter 5. Additionally, Cathepsin B was increased in secretion in response to antimycin A which is consistent with observations of lysosomal contents leaving HEK293 cells in response to antimycin A in chapter 4.

Strikingly, adipocytes had the most number of differentially secreted proteins compared with other cells used in chapters 4 and 5. In all datasets, adipocyte-specific secreted proteins including resistin and fatty acid binding protein 4 were detected. This increases confidence in the validity of proteins that we detected by MS. Further, 40–50% of proteins had a signal peptide for classical secretion (Figure 6.3.2) which is similar to (or slightly greater than) what is seen in other published studies characterising the adipocyte secretome which are reported at ~40% (L. E. Wu et al., 2014) and ~ 36% for (J. Kim et al., 2010). Further, 80-90% of proteins had an extracellular annotation (Figure 6.3.3). These findings together suggest that roughly half of secreted proteins were due to the classical secretion pathway.

In addition to these protein candidates that were expected to be secreted from adipocytes, proteins detected by MS also included protein candidates that were

previously less well characterised to come from the adipocyte secretome. These included many metabolic enzymes. A study that characterised secreted proteins from insulin sensitive and resistant adipocytes found that 'enzymes' and 'other proteins' were the most represented classes of proteins using a ingenuity tools (J. M. Lim, Wollaston-Hayden, Teo, Hausman, & Wells, 2014). Hence the enzymes detected are in line with other secretomic studies of adipocytes. Metabolic enzymes were also reflected in the KEGG pathway analysis whereby most of the top enriched pathways were all related to metabolism (Table 6.2.7 and 6.2.8). This is interesting as metabolic enzymes have well defined intracellular functions and have not been classically considered to be secreted from cells. However, some more recent literature reports suggest that secreted microvesicles contain a range of metabolic enzymes and could potentially be metabolically active (Ronquist, Ek, Morrell, et al., 2013; Ronquist, Ek, Stavreus-Evers, Larsson, & Ronquist, 2013; Royo et al., 2016). Prostastomes contain glycolytic enzymes (Ronquist, Ek, Stavreus-Evers, et al., 2013) and even have capacity for ATP production in the extracellular space (Ronquist, Ek, Morrell, et al., 2013; Ronquist, Ek, Stavreus-Evers, et al., 2013). Hepatocyte microvesicles contain metabolic enzymes that alter the metabolites of serum upon incubation which suggests they are metabolically active (Royo et al., 2016). So while it was initially a seemingly unexpected finding to observe metabolic enzymes exiting the cell, in the context of new literature it is plausible. Hence it is an important, novel observation that perturbing cellular metabolism through inhibition of mitochondrial function results in release of a host of metabolic enzymes. While further characterisation is needed, it is tempting to speculate based on other literature that these proteins are exiting the cell through microvesicles are potentially metabolically active.

After analysing the general patterns of proteins detected, I went on to look for individual proteins. Increased abundance of the protein DJ-1 (encoded by the Park7 gene) with Antimycin A by ~180 fold and a high dose of rotenone ~ 4.5 fold conditioned medium of adipocytes was of great interest. Firstly, it is intriguing that it is secreted from adipose tissue because it is usually studied in the context of neurons or cancer cells (Clements et al., 2006) and for its intracellular functions making it a somewhat novel discovery. Additionally, it is interesting because DJ-1 is a Parkinson's disease related protein and Parkinson's disease is one where evidence for a component

of mitochondrial dysfunction is strong (see section 1.4). A literature search revealed reports of DJ-1 expression in rodent WAT (Joo et al., 2011) where it is involved in the regulation of adipogenesis (J. M. Kim et al., 2014) and protects from high fat diet induced obesity (Joo et al., 2011; Seyfarth et al., 2015) . Other literature also suggests that DJ-1 can be found in the extracellular space of human samples. For example, DJ-1 has been detected in human serum (Maita et al., 2008) and saliva (Masters, Noyce, Warner, Giovannoni, & Proctor, 2015) of both healthy controls and sporadic PD patients as well as the serum and cerebrospinal fluid of healthy controls and multiple sclerosis patients (Hirotani et al., 2008). It is also overexpressed in the pancreatic juice of pancreatic adenoma carcinoma patients (M. Tian et al., 2008) and in serum from cervical cancer (Arnouk et al., 2009) and nipple fluid (Oda et al., 2012) and serum (Le Naour et al., 2001) from breast cancer patients. Collectively this literature indicates that DJ-1is expressed in adipose tissue and secreted into body fluids, but the findings from the present study are the first to show DJ-1 secretion from adipocytes in response to mitochondrial stress. DJ-1 has been demonstrated to be secreted into conditioned medium from other cell culture models including melanoma cells (Pardo et al., 2006) and HepG2 cells (Phark et al., 2012). In a HeLa cell model, DJ-1 was found to be secreted by microdomains and a critical cysteine residue that gets oxidised was required for secretion (Tsuboi et al., 2008) which suggests that the protein may get secreted upon oxidation. This aligns with our model where DJ-1 secretion was elevated with rotenone and antimycin A, which both increase mitochondrial ROS production (Forkink et al., 2015) but not dinitrophenol which would expected to reduce ROS. However, in contrast, another study found less DJ-1 secretion under oxidising conditions (Koide-Yoshida et al., 2007).

For DJ-1 to be an extracellular signaling molecule rather than simply an inert biomarker of ROS, it must be active in the extracellular space or serum and/ or can enter other cells to elicit cell non-autonomous signaling. While it has been shown that wild type DJ-1 is cell impermeable (Tsuboi et al., 2008), there it has also been shown to mediate cell non-autonomous signaling. DJ-1 was recently shown to regulate whole body energy homeostasis in response to ROS (S. Y. Shi et al., 2015). A possible reason that DJ-1 is cell impermeable but elicits signaling in a cell non-autonomous fashion is that it has been shown to be detected in exosomes in a published paper (Ho, Yi, Seo, Son, & Seol,

2014) and in publically available exosome datasets retrieved from exoCarta. As exosomes allow efficient delivery of soluble proteins (Yim et al., 2016) this may be a mechanism enabling their cell non-autonomous functionality. As such, although we were very interested in this candidate, it probably would not be very effective to exogenously administer recombinant protein to cells and explore the function.

In addition to DJ-1, other antioxidant enzymes were increased in abundance with ETC stress including superoxide dismutase enzymes, catalase, and proteins involved in glutathione metabolism which was also reflected in the KEGG enrichment pathways. Hence I speculate a role for a cell non-autonomous antioxidant stress response following mitochondrial stress in adipocytes.

There was also a trend for a change in proteins involved in whole body glucose homeostasis. For example, secretion of Fatty acid binding protein 4 (FABP4) was increased with antimycin A treatment in adipocytes which is an adipokine that regulates insulin secretion from the pancreas (L. E. Wu et al., 2014). Further, the protein resistin which is involved in whole body metabolic health (Smekal & Vaclavik, 2017) was increased with rotenone. Another protein of interest which was upregulated by antimycin A treatment is Decorin, as it is a known tumour suppressor (Hong, Yang, Wang, Wang, & Xu, 2016).

In summary, the ETC sensitive secretome was characterised in primary murine adipocytes and Complex I and III inhibition, but not an OXPHOS uncoupler caused extensive remodelling of the adipocyte secretome. Many of the proteins that were differentially secreted with complex I and III inhibition were metabolic enzymes, which are likely being secreted via microvesicles. Based on other literature, it is possible that these metabolic enzymes may cause metabolic changes in the extracellular space or induce changes in metabolism in distal tissues (Garcia, Moncayo-Arlandi, Sepulveda, & Diez-Juan, 2016) but more work would have to be performed to interrogate this.

CHAPTER 7: GENERAL DISCUSSION

7.1 Mitochondrial Stress Response Pathways in Mammalian Cells vs. Lower Organisms

Mitochondrial stress responses have mostly been demonstrated in lower models including yeast, *C.elegans* and *Drosophila*. The purpose of this thesis was to explore intracellular and extracellular mitochondrial stress responses in mammalian cells. While a number of pathways had been elucidated when this PhD project was commenced, there have been a number of new developments in this field during the tenure of this thesis, many of which suggest differences between stress responses of mammals and lower organisms.

Interestingly, it appears that many stress-related processes may be conserved at a functional level but regulation of these processes are molecularly distinct. For example, in yeast, 2 proteins RTG1 and RTG2 are transcription factors that are required for retrograde signaling (X. Liao & Butow, 1993). These proteins are not evolutionarily conserved but in mammalian cells there are a number of pathways to retrograde communication (Butow & Avadhani, 2004). Further, many of the mitochondrial chaperones involved in eliciting an mtUPR are conserved but the ways in which they are activated are different. In primate cells, mtUPR is activated by transcription factor *c/ebp*β binding to CHOP promoters (Horibe & Hoogenraad, 2007) whereas in other mammals the transcription factor ATF5 plays the same role (Fiorese et al., 2016) and in *C.elegans* bZIP protein, ZC376.7 (C. M. Haynes et al., 2010)

Mitochondria are the site of programmed cell death and the major site for cellular energy production and mitochondrial function and homeostasis are thus involved in the balance of life and death. The motivation to study these pathways in mammalian cells came from evidence that mitochondrial stress responses are supressed with ageing and degenerative complex diseases, particularly neurodegeneration, and that extension of lifespan in lower organisms is observed with improved mitochondrial quality control. Collectively this suggests that maintenance of mitochondrial fidelity is essential for normal cellular homeostasis. Yet there may also be a possible negative side to mitohormetic adaptations.

Mitochondrial mtUPR genes that improve fitness of lower organisms increase resilience of cancer cells. For example, mitochondrial stress gene TRAP1 extends lifespan in *Drosophila* (Baqri et al., 2014) but is required for paclitaxel resistance in human breast carcinoma cells through a mitochondrial quality control dependent pathway (Maddalena et al., 2013). This illustrates how mitochondrial quality control pathways can promote cancer cell survival. Similarly, mtUPR increases stress resistance in *C.elegans* but it is also engaged in human cancer cells and *in vivo* in mouse models of cancer to promote cell survival (Siegelin et al., 2011). Higher expression of human HSP60, a key mitochondrial chaperone that functions in mtUPR is associated with poor clinical outcome of ovarian cancer (Hjerpe et al., 2013). There is also literature to suggest that mitochondrial dynamics may be involved in oncogenic transformation in mammalian cells. K-Ras oncogenic transformation is associated with enhanced mitophagy (J. H. Kim et al., 2011) which may suggest it is involved in the transformation process.

Part of the reason that we endeavoured to interrogate mitochondrial stress signaling in mammalian cells was due to the potential of mitochondrial quality control to be exploited therapeutically. The discussion above suggests that mitochondrial stress responses could promote an oncogenic phenotype in mammals, but there is not enough literature in mammals at present to assess whether boosting mitochondrial quality control is likely to be an effective therapeutic target. It is likely that it may be useful when there is a substantial mitochondrial deficit e.g. mitochondrial disease, rather than as a means of promoting ‘healthy ageing’ or ‘healthspan’ in relatively healthy or obese people, as it may potentially have other consequences.

7.2 Mitochondrial Stress Signaling and the Metabolic-Signaling Nexus

The goal of chapter 3 was to explore mitochondrial stress signaling in a mammalian cell model. The results of chapter 3 have highlighted that perturbation of cellular metabolism can initiate cell signaling events in contrast (and addition to) a large body of literature that has highlighted the reverse. Further, kinase signaling was the most biologically significant induced response to ETC stress to rescue cells in a mammalian cell model and some of the other stress responses like mtUPR were seemingly less important. As highlighted in the discussion of Chapter 3 (Section 3.4), these other responses may be more important in post mitotic cells.

Phosphorylation and Kinase Signaling –

Post-translational modification of proteins, where amino acids are modified by a chemical group, is a major way in which the proteomic complexity and diversity are achieved. Amino acids can be modified by many different chemicals, with a major modification being phosphorylation. Phosphorylation as a post-translational modification has profound conformational effect on proteins because it has a strong negative charge and high free energy. Phosphorylation can trigger complex signaling networks and is particularly utilised in metabolic regulation (Humphrey, James, & Mann, 2015). One of the key findings of this thesis is that phosphoproteomic changes occur when OXPHOS is perturbed (Chapter 3). I found that phosphorylation networks can be triggered by metabolic stimuli. While AMPK being activated by ETC stress is well known (Distelmaier et al., 2015), I made a novel observation that AMPK activation by ETC stress is ATM dependent (Chapter 3). AMPK has been shown to phosphorylate epigenetic factors to lead to increased mitochondrial biogenesis (Marin et al., 2017) potentially making this a negative feedback mechanism. Akt phosphorylation has been reported in other models of mitochondrial stress (Guha, Fang, et al., 2010; Pelicano et al., 2006; T. Zheng et al., 2015) and in the secretome studies in this thesis PI3K-Akt pathways was enriched in response to mitochondrial perturbations. Mitochondrial stress induced Akt phosphorylation leads to activation of heterogeneous ribonucleoprotein A2 (hnRNPA2) (Guha, Fang, et al., 2010; Guha, Tang, Sondheimer, & Avadhani, 2010) which is a histone acetyltransferase that can possibly influence chromatin remodelling and a mitochondrial stress transcriptional program (Guha et al., 2016). Like AMPK, Akt activation was also ATM-dependent, indicating an especially important role for ATM in the regulation of mitochondrial stress signaling. While metabolic adaptations were not all explored, ATM inhibition did attenuate mitochondrial stress-induced glucose uptake. The full involvement of ATM could be elucidated by examining ETC stress responses in cells with loss of function of ATM.

7.3 Analysis of the ETC Sensitive Secretome

Chapters 4-6 interrogated changes in secreted proteins in response to ETC toxins in HEK293 cells, primary murine hepatocytes and primary murine adipocytes. Overall, the major finding was that there was a large remodelling of the secretome with ETC

Complex I and Complex III inhibition of adipocytes and OXPHOS uncoupling of hepatocytes. While there were cell-specific secreted proteins such as complement proteins from hepatocytes and lysosomal proteins from HEK293 cells, I performed overlap analysis to see to see if there was anything commonly secreted with mitochondrial stress. Since it is difficult to compare human with mouse and the datasets that showed the most significant secretome remodelling in response to mitochondrial stress were dinitrophenol treated hepatocytes and rotenone and antimycin A treated adipocytes, they were chosen for overlap analysis. There was no overlap for proteins where secretion was decreased with ETC stress but there were 7 proteins that were commonly represented in cells with secretion that was increased with mitochondrial stress (presented below in Figure 7.5.1).

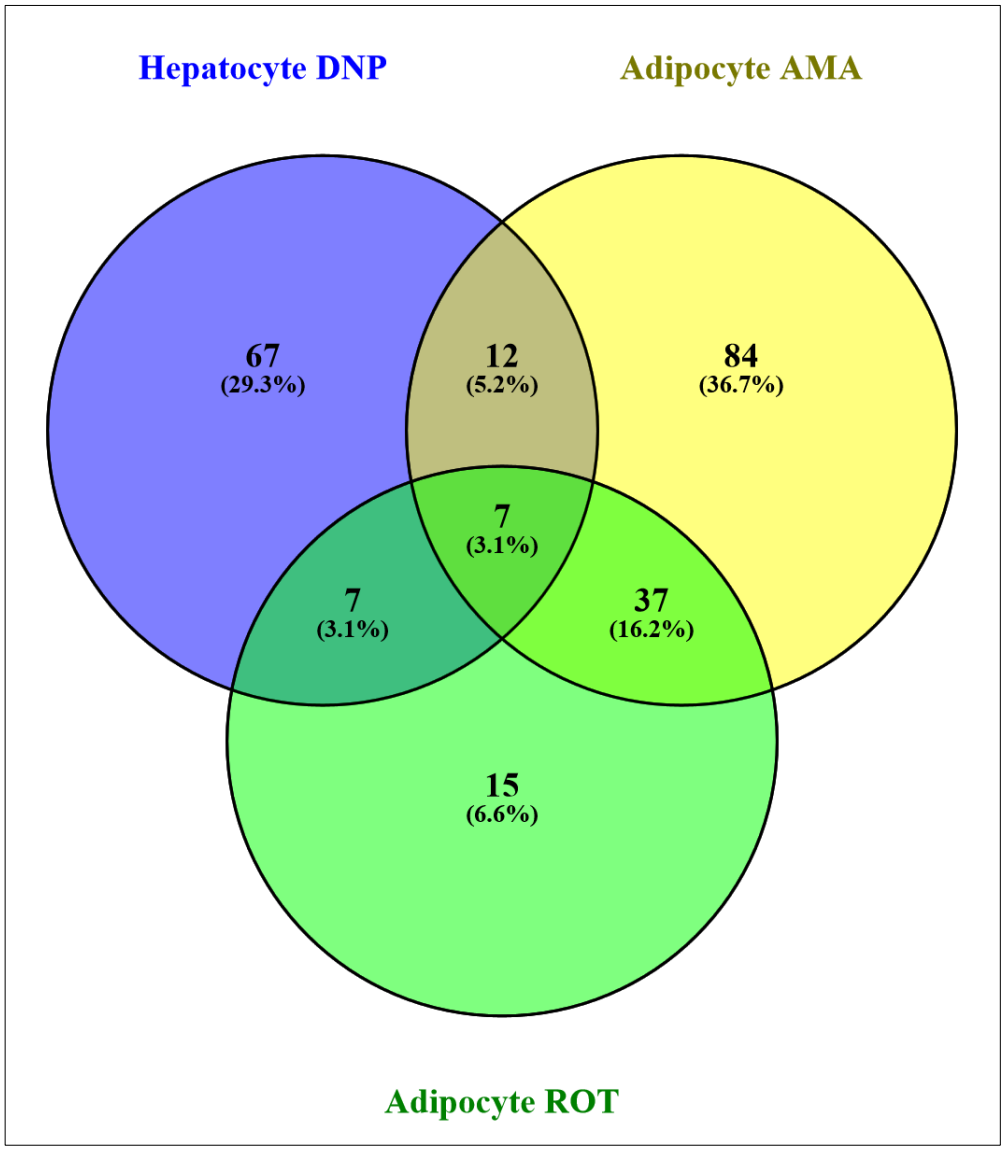

Figure 7.5.1 Overlap Analysis of Upregulated Secreted Protein in Datasets that were substantially changed in response to ETC Stress

Blue represents secreted proteins that were increased in abundance by hepatocytes in response to dinitrophenol, yellow represents secreted proteins that were increased in abundance by antimycin A in adipocytes and green represents secreted proteins that were increased in abundance by rotenone in adipocytes

The 7 proteins commonly increased in response to mitochondrial stress (Figure 7.5.1) were Ethylmalonyl-CoA decarboxylase **(**Echdc1**),** Cytosolic 10-formyltetrahydrofolate dehydrogenase (Aldh1l1), Glyceraldehyde-3-phosphate dehydrogenase (Gapdh), Phosphoglycerate kinase 1 (Pgk1), Alpha-enolase, Fumarylacetoacetase, 14-3-3 protein gamma subtype.

None of these proteins contained a secretion signal peptide but all of them have been reported in ExoCarta database, a database of exosomes which indicates that they are not secreted classically and possibly through extracellular vesicles. Gapdh, Pgk1 and Alpha-enloase are all involved in glycolysis. Further Echdc1, Aldh1l1 and Fumarylacetoacetase are metabolic enzymes. This suggests that ETC stress may lead to secretion of extracellular vesicles containing metabolic enzymes. Consistent with this, KEGG enrichment analysis in chapters 5 and 6 showed metabolic pathways to be enriched.

Previous literature has showed that extracellular vesicles can be metabolically active (Royo et al., 2017; Royo et al., 2016). Further, the extracellular vesicles, prostasomes contain glycolytic enzymes and even have capacity for extracellular ATP synthesis (Ronquist, Ek, Morrell, et al., 2013; Ronquist, Ek, Stavreus-Evers, et al., 2013). Since cells experiencing mitochondrial stress increase glycolysis for ATP synthesis, secretion of vesicles with glycolytic capacity may be a means by which ETC stress is communicated to other cells.

Non-Conventional Protein Secretion in Response to Mitochondrial Stress –

In all datasets, the majority of proteins detected did not have an signal peptide for classical protein secretion despite most proteins being annotated as having an extracellular function. This indicates that the majority of proteins were secreted by non-conventional protein secretion. Components of the classical secretion pathway were identified in the 1970s (Ferro-Novick & Brose, 2013). To summarise, proteins with a signal peptide translocate to the ER lumen where they are glycosylated then subsequently exported from COP-II coated vesicles attaches to the Golgi body where it is trafficked to the plasma membrane (Ferro-Novick & Brose, 2013). However, over the last 15 years it has been increasingly appreciated that most proteins are secreted from

the cell by non-conventional protein secretion (Rabouille, 2016). Pathways of non-conventional protein secretion in the literature include plasma membrane pore formation, golgi bypass and more recently autophagosomes and release through extracellular microvesicles including exosomes. However, the molecular mechanisms of these non-conventional protein secretion pathways are surprisingly not well characterised.

Most of the proteins annotated as extracellular were annotated as being an "Extracellular Exosome" or "Extracellular Vesicle" suggesting that microvesicles including exosomes may have been a key way in which proteins were secreted in he cellular models in this study. Exosomes have recently been appreciated to have high potential as biologically important mediators of intercellular communication in mammalian systems for several reasons. Firstly, all cell types, at least in culture have the capacity to shed exosomes (Charoenviriyakul et al., 2017) and all body fluids *in vivo* contain exosomes (Keller, Ridinger, Rupp, Janssen, & Altevogt, 2011). This ubiquitous expression indicates an important functional role that is conserved. In the mammalian system, exosomes can cross the blood brain barrier (BBB) which enables cell non-autonomous communication from the periphery into the brain and vice versa (Andras & Toborek, 2016). Exosomes contents are protected meaning that their contents are unlikely to be degraded in the extracellular matrix or in plasma (Corrado et al., 2013).

7.4 Future Directions

Exploring the Therapeutic Potential of ATM –

A key finding of this thesis was that ATM kinase is activated in response to mitochondrial stress to promote pro-survival signaling and metabolic adaptations (Chapter 3). It would be valuable to further investigate the therapeutic potential of ATM kinase mitochondrial disease. A pilot study similar in design to that exploring mitochondrial adaptation presence and importance in MELAS cybrids would be useful (Garrido-Maraver et al., 2015) (discussed in section 1.4.1). In this study, mitochondrial quality control adaptations including AMPK activation and mitochondrial biogenesis, were measured in cybrid cells of MELAS from patients with differing degrees of clinical manifestation. It was found that when mitochondrial quality control adaptations

were engaged, the cell phenotype was rescued resulting in a less severe pathology (Garrido-Maraver et al., 2015). Conversely, cells sourced from a more severe pathology did not engage these adaptations and exogenous stimulation of these adaptations improved cell survival (Garrido-Maraver et al., 2015). Similarly, it is possible that ATM kinase activation is important in mitigating mitochondrial disease pathology and exogenous activation could improve the phenotype of cells that do not engage it. This could be studied in mitochondrial disease patient fibroblasts or cybrids with different degrees of heteroplasmy by performing immunoblot for phosphorylated and total ATM. I hypothesise that ATM will be activated in less severe cells where an inhibitor would reduce viability. Chloroquine is known to activate ATM kinase without eliciting DNA damage (Bakkenist & Kastan, 2003). If ATM is not activated in more severe cells, chloroquine could be used to try to rescue them which would validate ATM as a target for mitochondrial disease. There is currently a body of literature concentrated on using ATM inhibitors for cancer (A. M. Weber & Ryan, 2015) but perhaps there is also potential for ATM activators in mitochondrial disease.

Is Mitophagy Coupled with Vesicular Secretion a Pathway of Non-Conventional Protein Secretion in Response to Mitochondrial Stress? –

Given that most proteins being secreted from the cells in response to cellular stress were likely to be secreted via microvesicles including exosomes, it may be valuable to explore general secretion of microvesicles and exosomes from cells in the context of mitochondrial stress. More specifically, given that ‘secreted autophagy’ is a newly discovered mechanism of unconventional protein secretion (Abrahamsen & Stenmark, 2010) and data in chapter 4 found lysosomal contents being secreted with mitochondrial stress in HEK293 cells it may be important to explore whether mitochondrial contents could exit the cell following mitophagy in a process that could be termed ‘exomitophagy’. mtDNA can be amplified from microvesicles (Guescini, Genedani, et al., 2010; Guescini, Guidolin, et al., 2010). Further, rotenone treatment increases autophagy and exosome secretion (A. L. Wang et al., 2009). These data provide evidence that mitochondrial contents are present in exosomes and collectively suggest that mitochondrial stress may indeed by coupled with microvesicular removal of contents.

To confirm this, microscopy could be used to image the process. However, due to the size of exosomes, electron microscopy would need to be used. A more simple approach would be to collect microvesicles and exosomes and see if they contain mitochondrial contents. Overnight ultracentrifugation of FBS can largely deplete exosomes which can then be used to culture cells. Differential centrifugation (including ultracentrifugation) can then be used on culture media to isolate. In addition to measuring mtDNA, western blot could be used to examine if there are any mitochondrial proteins in the microvesicles. Since some literature discussed in chapter 6 highlighted that microvesicles can be metabolically active (Ronquist, Ek, Morrell, et al., 2013; Ronquist, Ek, Stavreus-Evers, et al., 2013; Royo et al., 2016), another question is whether respiration-competent mitochondria are present in microvesicles. If the process is coupled to mitophagy, I speculate that mitochondria are likely to non-function that are selected and then subsquently degraded by lysosomal contents. Further, since exosomes are ≤ 100 nm (Thery, Zitvogel, & Amigorena, 2002), they are probably too small to accommodate functional mitochondria. Although this does not preclude a small number of functional mitochondria being present in larger microvesicles under unstimulated conditions. It may be possible to permeabilise microvesicles with digitonin and measure respiration to assess this.

Mitochondrial Cross–talk with Organelles other than the Nucleus –

The literature of mitochondrial communication is heavily focussed on ‘retrograde’ or “mitochondria-to-nucleus” signaling. Discussion of mitochondrial communication to lysosomes in the context of non-conventional protein secretion has prompted interest in whether mitochondria signal to other organelles rather than the focus on strictly mitochondria-to-nucleus communication. Mitochondrial function affects lysosomal function (Baixauli et al., 2015) indicating that mitochondria-to-lysosome signaling may be an important cellular process. It would be of interest to further study the effect of mitochondrial stress on production of lipofuscin-loaded lysosomes as they are associated with ageing (Terman et al., 2010). In addition to lysosomes, there is some literature implicating interactions between mitochondria and peroxisomes in dynamics and biogenesis of both organelles. (Mohanty & McBride, 2013). It is already appreciated that because of the physical tethering between mitochondria and ER that

cross talk between these organelles is important (Walter & Hajnoczky, 2005). To date, this has most been studied in the context of mitochondrial fusion and fission and calcium signaling. It is possible that there is more scope there for protein translation. To summarise, mitochondrial function may need to be integrated with other organelles besides the nucleus to maintain fitness of the cell and this is a relatively untouched area.

7.5 Conclusion

This thesis explored intracellular and cell non-autonomous communication of mitochondrial stress. From the work presented in this thesis, I can conclude that ATM-Akt-AMPK is a way in which mammalian cells respond to mitochondrial stress. I can also conclude that in response to ETC stress, there is a reprogramming of the complement of proteins being secreted from mammalian cells and many of the proteins are secreted by non-conventional protein secretion. This may be a potential mechanism by which information of mitochondrial stress is communicated to distal tissues. Remodelling of the secretome in response to ETC stress was especially prominent from metabolically relevant cell types and it appears that perturbation of cellular molecular metabolism is associated with secretion of metabolic enzymes, possibly through extracellular vesicles. Overall, it appears that mammalian cells do signal mitochondrial stress in a way that is molecularly very distinct from lower organisms.

REFERENCES

Abrahamsen, H., & Stenmark, H. (2010). Protein secretion: unconventional exit by exophagy. *Curr Biol, 20*(9), R415-418. doi:10.1016/j.cub.2010.03.011

Abu Bakar, M. H., Cheng, K. K., Sarmidi, M. R., Yaakob, H., & Huri, H. Z. (2015). Celastrol Protects against Antimycin A-Induced Insulin Resistance in Human Skeletal Muscle Cells. *Molecules, 20*(5), 8242-8269. doi:10.3390/molecules20058242

Acin-Perez, R., Fernandez-Silva, P., Peleato, M. L., Perez-Martos, A., & Enriquez, J. A. (2008). Respiratory active mitochondrial supercomplexes. *Mol Cell, 32*(4), 529-539. doi:10.1016/j.molcel.2008.10.021

Adam-Vizi, V., & Chinopoulos, C. (2006). Bioenergetics and the formation of mitochondrial reactive oxygen species. *Trends Pharmacol Sci, 27*(12), 639-645. doi:10.1016/j.tips.2006.10.005

Adhihetty, P. J., Uguccioni, G., Leick, L., Hidalgo, J., Pilegaard, H., & Hood, D. A. (2009). The role of PGC-1alpha on mitochondrial function and apoptotic susceptibility in muscle. *Am J Physiol Cell Physiol, 297*(1), C217-225. doi:10.1152/ajpcell.00070.2009

Agarraberes, F. A., & Dice, J. F. (2001). Protein translocation across membranes. *Biochim Biophys Acta, 1513*(1), 1-24.

Aird, K. M., Worth, A. J., Snyder, N. W., Lee, J. V., Sivanand, S., Liu, Q., . . . Zhang, R. (2015). ATM couples replication stress and metabolic reprogramming during cellular senescence. *Cell Rep, 11*(6), 893-901. doi:10.1016/j.celrep.2015.04.014

Aksenov, M. Y., Tucker, H. M., Nair, P., Aksenova, M. V., Butterfield, D. A., Estus, S., & Markesbery, W. R. (1998). The expression of key oxidative stress-handling genes in different brain regions in Alzheimer's disease. *J Mol Neurosci, 11*(2), 151-164. doi:10.1385/jmn:11:2:151

Al-Furoukh, N., Ianni, A., Nolte, H., Holper, S., Kruger, M., Wanrooij, S., & Braun, T. (2015). ClpX stimulates the mitochondrial unfolded protein response (UPRmt) in mammalian cells. *Biochim Biophys Acta, 1853*(10 Pt A), 2580-2591. doi:10.1016/j.bbamcr.2015.06.016

Al-Lahham, R., Deford, J. H., & Papaconstantinou, J. (2016). Mitochondrial-generated ROS down regulates insulin signaling via activation of the p38MAPK stress response pathway. *Mol Cell Endocrinol, 419*, 1-11. doi:10.1016/j.mce.2015.09.013

Al Haj Ahmad, R. M., & Al-Domi, H. A. (2016). Complement 3 serum levels as a pro-inflammatory biomarker for insulin resistance in obesity. *Diabetes Metab Syndr*. doi:10.1016/j.dsx.2016.12.036

Alam, T. I., Kanki, T., Muta, T., Ukaji, K., Abe, Y., Nakayama, H., . . . Kang, D. (2003). Human mitochondrial DNA is packaged with TFAM. *Nucleic Acids Res, 31*(6), 1640-1645.

Alam, Z. I., Jenner, A., Daniel, S. E., Lees, A. J., Cairns, N., Marsden, C. D., . . . Halliwell, B. (1997). Oxidative DNA damage in the parkinsonian brain: an

apparent selective increase in 8-hydroxyguanine levels in substantia nigra. *J Neurochem, 69*(3), 1196-1203.

Alaynick, W. A., Kondo, R. P., Xie, W., He, W., Dufour, C. R., Downes, M., . . . Evans, R. M. (2007). ERRgamma directs and maintains the transition to oxidative metabolism in the postnatal heart. *Cell Metab, 6*(1), 13-24. doi:10.1016/j.cmet.2007.06.007

Aldridge, J. E., Horibe, T., & Hoogenraad, N. J. (2007). Discovery of genes activated by the mitochondrial unfolded protein response (mtUPR) and cognate promoter elements. *PLoS ONE [Electronic Resource], 2*(9), e874.

Allen, G. F., Toth, R., James, J., & Ganley, I. G. (2013). Loss of iron triggers PINK1/Parkin-independent mitophagy. *EMBO Rep, 14*(12), 1127-1135. doi:10.1038/embor.2013.168

Andras, I. E., & Toborek, M. (2016). Extracellular vesicles of the blood-brain barrier. *Tissue Barriers, 4*(1), e1131804. doi:10.1080/21688370.2015.1131804

Andrisse, S., Patel, G. D., Chen, J. E., Webber, A. M., Spears, L. D., Koehler, R. M., . . . Fisher, J. S. (2013). ATM and GLUT1-S490 phosphorylation regulate GLUT1 mediated transport in skeletal muscle. *PLoS One, 8*(6), e66027. doi:10.1371/journal.pone.0066027

Anello, M., Lupi, R., Spampinato, D., Piro, S., Masini, M., Boggi, U., . . . Marchetti, P. (2005). Functional and morphological alterations of mitochondria in pancreatic beta cells from type 2 diabetic patients. *Diabetologia, 48*(2), 282-289. doi:10.1007/s00125-004-1627-9

Anesti, V., & Scorrano, L. (2006). The relationship between mitochondrial shape and function and the cytoskeleton. *Biochim Biophys Acta, 1757*(5-6), 692-699. doi:10.1016/j.bbabio.2006.04.013

Ansari, M. A., & Scheff, S. W. (2010). Oxidative stress in the progression of Alzheimer disease in the frontal cortex. *J Neuropathol Exp Neurol, 69*(2), 155-167. doi:10.1097/NEN.0b013e3181cb5af4

Antonicka, H., & Shoubridge, E. A. (2015). Mitochondrial RNA Granules Are Centers for Posttranscriptional RNA Processing and Ribosome Biogenesis. *Cell Rep*. doi:10.1016/j.celrep.2015.01.030

Arany, Z., Foo, S. Y., Ma, Y., Ruas, J. L., Bommi-Reddy, A., Girnun, G., . . . Spiegelman, B. M. (2008). HIF-independent regulation of VEGF and angiogenesis by the transcriptional coactivator PGC-1alpha. *Nature, 451*(7181), 1008-1012. doi:10.1038/nature06613

Arany, Z., He, H., Lin, J., Hoyer, K., Handschin, C., Toka, O., . . . Spiegelman, B. M. (2005). Transcriptional coactivator PGC-1 alpha controls the energy state and contractile function of cardiac muscle. *Cell Metab, 1*(4), 259-271. doi:10.1016/j.cmet.2005.03.002

Ardail, D., Privat, J. P., Egret-Charlier, M., Levrat, C., Lerme, F., & Louisot, P. (1990). Mitochondrial contact sites. Lipid composition and dynamics. *J Biol Chem, 265*(31), 18797-18802.

Arnold, I., Wagner-Ecker, M., Ansorge, W., & Langer, T. (2006). Evidence for a novel mitochondria-to-nucleus signalling pathway in respiring cells lacking i-AAA protease and the ABC-transporter Mdl1. *Gene, 367*, 74-88. doi:10.1016/j.gene.2005.09.044

Arnouk, H., Merkley, M. A., Podolsky, R. H., Stoppler, H., Santos, C., Alvarez, M., . . . Dynan, W. S. (2009). Characterization of Molecular Markers Indicative of Cervical Cancer Progression. *Proteomics Clin Appl, 3*(5), 516-527. doi:10.1002/prca.200800068

Arnould, T., Michel, S., & Renard, P. (2015). Mitochondria Retrograde Signaling and the UPR mt: Where Are We in Mammals? *Int J Mol Sci, 16*(8), 18224-18251. doi:10.3390/ijms160818224

Ashrafian, H., Frenneaux, M. P., & Opie, L. H. (2007). Metabolic mechanisms in heart failure. *Circulation, 116*(4), 434-448. doi:10.1161/circulationaha.107.702795

Asin-Cayuela, J., & Gustafsson, C. M. (2007). Mitochondrial transcription and its regulation in mammalian cells. *Trends Biochem Sci, 32*(3), 111-117. doi:10.1016/j.tibs.2007.01.003

Attwell, D., & Laughlin, S. B. (2001). An energy budget for signaling in the grey matter of the brain. *J Cereb Blood Flow Metab, 21*(10), 1133-1145. doi:10.1097/00004647-200110000-00001

Augustin, S., Nolden, M., Muller, S., Hardt, O., Arnold, I., & Langer, T. (2005). Characterization of peptides released from mitochondria: evidence for constant proteolysis and peptide efflux. *J Biol Chem, 280*(4), 2691-2699. doi:10.1074/jbc.M410609200

Awasthi, P., Foiani, M., & Kumar, A. (2015). ATM and ATR signaling at a glance. *J Cell Sci, 128*(23), 4255-4262. doi:10.1242/jcs.169730

Backer, J. M., & Weinstein, I. B. (1982). Interaction of benzo(a)pyrene and its dihydrodiol-epoxide derivative with nuclear and mitochondrial DNA in C3H10T 1/2 cell cultures. *Cancer Res, 42*(7), 2764-2769.

Baixauli, F., Acin-Perez, R., Villarroya-Beltri, C., Mazzeo, C., Nunez-Andrade, N., Gabande-Rodriguez, E., . . . Mittelbrunn, M. (2015). Mitochondrial Respiration Controls Lysosomal Function during Inflammatory T Cell Responses. *Cell Metab, 22*(3), 485-498. doi:10.1016/j.cmet.2015.07.020

Baixauli, F., Lopez-Otin, C., & Mittelbrunn, M. (2014). Exosomes and autophagy: coordinated mechanisms for the maintenance of cellular fitness. *Front Immunol, 5*, 403. doi:10.3389/fimmu.2014.00403

Bakkenist, C. J., & Kastan, M. B. (2003). DNA damage activates ATM through intermolecular autophosphorylation and dimer dissociation. *Nature, 421*(6922), 499-506. doi:10.1038/nature01368

Bakthavatchalu, V., Dey, S., Xu, Y., Noel, T., Jungsuwadee, P., Holley, A. K., . . . St Clair, D. K. (2012). Manganese superoxide dismutase is a mitochondrial fidelity protein that protects Pol against UV-induced inactivation. *Oncogene, 31*(17), 2129-2139. doi:http://dx.doi.org/10.1038/onc.2011.407

Ball, E. H., & Singer, S. J. (1982). Mitochondria are associated with microtubules and not with intermediate filaments in cultured fibroblasts. *Proc Natl Acad Sci U S A, 79*(1), 123-126.

Ban-Ishihara, R., Ishihara, T., Sasaki, N., Mihara, K., & Ishihara, N. (2013). Dynamics of nucleoid structure regulated by mitochondrial fission contributes to cristae reformation and release of cytochrome c. *Proc Natl Acad Sci U S A, 110*(29), 11863-11868. doi:10.1073/pnas.1301951110

Baqri, R. M., Pietron, A. V., Gokhale, R. H., Turner, B. A., Kaguni, L. S., Shingleton, A. W., . . . Miller, K. E. (2014). Mitochondrial chaperone TRAP1 activates the mitochondrial UPR and extends healthspan in Drosophila. *Mech Ageing Dev, 141-142*, 35-45. doi:10.1016/j.mad.2014.09.002

Barbour, J. A., & Turner, N. (2014). Mitochondrial stress signaling promotes cellular adaptations. *Int J Cell Biol, 2014*, 156020. doi:10.1155/2014/156020

Barone, M. C., Sykiotis, G. P., & Bohmann, D. (2011). Genetic activation of Nrf2 signaling is sufficient to ameliorate neurodegenerative phenotypes in a Drosophila model of Parkinson's disease. *Dis Model Mech, 4*(5), 701-707. doi:10.1242/dmm.007575

Batlevi, Y., & La Spada, A. R. (2011). Mitochondrial autophagy in neural function, neurodegenerative disease, neuron cell death, and aging. *Neurobiology of Disease, 43*(1), 46-51. doi:http://dx.doi.org/10.1016/j.nbd.2010.09.009

Beal, M. F. (2004). Mitochondrial dysfunction and oxidative damage in Alzheimer's and Parkinson's diseases and coenzyme Q10 as a potential treatment. *J Bioenerg Biomembr, 36*(4), 381-386. doi:10.1023/b:jobb.0000041772.74810.92

Beck, J. S., Mufson, E. J., & Counts, S. E. (2016). Evidence for Mitochondrial UPR Gene Activation in Familial and Sporadic Alzheimer's Disease. *Curr Alzheimer Res, 13*(6), 610-614.

Befroy, D. E., Petersen, K. F., Dufour, S., Mason, G. F., de Graaf, R. A., Rothman, D. L., & Shulman, G. I. (2007). Impaired mitochondrial substrate oxidation in muscle of insulin-resistant offspring of type 2 diabetic patients. *Diabetes, 56*(5), 1376-1381. doi:10.2337/db06-0783

Belkacemi, A., & Ramassamy, C. (2012). Time sequence of oxidative stress in the brain from transgenic mouse models of Alzheimer's disease related to the amyloid-beta cascade. *Free Radic Biol Med, 52*(3), 593-600. doi:10.1016/j.freeradbiomed.2011.11.020

Bellacosa, A., Kumar, C. C., Di Cristofano, A., & Testa, J. R. (2005). Activation of AKT kinases in cancer: implications for therapeutic targeting. *Adv Cancer Res, 94*, 29-86. doi:10.1016/s0065-230x(05)94002-5

Benedetti, C., Haynes, C. M., Yang, Y., Harding, H. P., & Ron, D. (2006). Ubiquitin-like protein 5 positively regulates chaperone gene expression in the mitochondrial unfolded protein response. *Genetics, 174*(1), 229-239. doi:10.1534/genetics.106.061580

Bennett, C. F., Vander Wende, H., Simko, M., Klum, S., Barfield, S., Choi, H., . . . Kaeberlein, M. (2014). Activation of the mitochondrial unfolded protein

response does not predict longevity in Caenorhabditis elegans. *Nat Commun, 5*, 3483. doi:10.1038/ncomms4483

Berendzen, K. M., Durieux, J., Shao, L. W., Tian, Y., Kim, H. E., Wolff, S., . . . Dillin, A. (2016). Neuroendocrine Coordination of Mitochondrial Stress Signaling and Proteostasis. *Cell, 166*(6), 1553-1563 e1510. doi:10.1016/j.cell.2016.08.042

Bhat, K. S., Avdalovic, N., & Avadhani, N. G. (1989). Characterization of primary transcripts and identification of transcription initiation sites on the heavy and light strands of mouse mitochondrial DNA. *Biochemistry, 28*(2), 763-769.

Bhatt, M. P., Lim, Y.-C., Kim, Y.-M., & Ha, K.-S. (2013). C-peptide activates AMPKα and prevents ROS-mediated mitochondrial fission and endothelial apoptosis in diabetes mellitus. *Diabetes*. doi:10.2337/db13-0039

Bironaite, D., Westberg, J. A., Andersson, L. C., & Venalis, A. (2013). A variety of mild stresses upregulate stanniocalcin-1 (STC-1) and induce mitohormesis in neural crest-derived cells. *Journal of the Neurological Sciences, 329*(1–2), 38-44. doi:http://dx.doi.org/10.1016/j.jns.2013.03.011

Bironaite, D., Westberg, J. A., Andersson, L. C., & Venalis, A. (2013). A variety of mild stresses upregulate stanniocalcin-1 (STC-1) and induce mitohormesis in neural crest-derived cells. *J Neurol Sci, 329*(1-2), 38-44. doi:10.1016/j.jns.2013.03.011

Bogenhagen, D. F., Yoza, B. K., & Cairns, S. S. (1986). Identification of initiation sites for transcription of Xenopus laevis mitochondrial DNA. *J Biol Chem, 261*(18), 8488-8494.

Bolten, C. W., Blanner, P. M., McDonald, W. G., Staten, N. R., Mazzarella, R. A., Arhancet, G. B., . . . Colca, J. R. (2007). Insulin sensitizing pharmacology of thiazolidinediones correlates with mitochondrial gene expression rather than activation of PPAR gamma. *Gene Regul Syst Bio, 1*, 73-82.

Bonello, S., Zahringer, C., BelAiba, R. S., Djordjevic, T., Hess, J., Michiels, C., . . . Gorlach, A. (2007). Reactive oxygen species activate the HIF-1alpha promoter via a functional NFkappaB site. *Arteriosclerosis, Thrombosis & Vascular Biology, 27*(4), 755-761.

Booth, A., Magnuson, A., Fouts, J., & Foster, M. (2015). Adipose tissue, obesity and adipokines: role in cancer promotion. *Horm Mol Biol Clin Investig, 21*(1), 57-74. doi:10.1515/hmbci-2014-0037

Bortolami, S., Comelato, E., Zoccarato, F., Alexandre, A., & Cavallini, L. (2008). Long chain fatty acyl-CoA modulation of H(2)O (2) release at mitochondrial complex I. *J Bioenerg Biomembr, 40*(1), 9-18. doi:10.1007/s10863-008-9126-1

Bottani, E., Giordano, C., Civiletto, G., Di Meo, I., Auricchio, A., Ciusani, E., . . . Zeviani, M. (2014). AAV-mediated liver-specific MPV17 expression restores mtDNA levels and prevents diet-induced liver failure. *Mol Ther, 22*(1), 10-17. doi:10.1038/mt.2013.230

Brandstadt, S., Schmeisser, K., Zarse, K., & Ristow, M. (2013). Lipid-lowering fibrates extend C. elegans lifespan in a NHR-49/PPARalpha-dependent manner. *Aging (Albany NY), 5*(4), 270-275.

Bratic, A., & Larsson, N. G. (2013). The role of mitochondria in aging. *J Clin Invest, 123*(3), 951-957. doi:10.1172/jci64125

Braun, H. P., Sunderhaus, S., Boekema, E. J., & Kouril, R. (2009). Chapter 10 Purification of the cytochrome C reductase/cytochrome C oxidase super complex of yeast mitochondria. *Methods Enzymol, 456*, 183-190. doi:10.1016/s0076-6879(08)04410-8

Brownlee, M. (2005). The pathobiology of diabetic complications: a unifying mechanism. *Diabetes, 54*(6), 1615-1625.

Bucio, L., Garcia, C., Souza, V., Hernandez, E., Gonzalez, C., Betancourt, M., & Gutierrez-Ruiz, M. C. (1999). Uptake, cellular distribution and DNA damage produced by mercuric chloride in a human fetal hepatic cell line. *Mutat Res, 423*(1-2), 65-72.

Buhmann, C., Arlt, S., Kontush, A., Moller-Bertram, T., Sperber, S., Oechsner, M., . . . Beisiegel, U. (2004). Plasma and CSF markers of oxidative stress are increased in Parkinson's disease and influenced by antiparkinsonian medication. *Neurobiol Dis, 15*(1), 160-170.

Bulteau, A. L., Szweda, L. I., & Friguet, B. (2006). Mitochondrial protein oxidation and degradation in response to oxidative stress and aging. *Exp Gerontol, 41*(7), 653-657. doi:10.1016/j.exger.2006.03.013

Burton, N. C., Kensler, T. W., & Guilarte, T. R. (2006). In vivo modulation of the Parkinsonian phenotype by Nrf2. *Neurotoxicology, 27*(6), 1094-1100. doi:10.1016/j.neuro.2006.07.019

Bustamante, C. J., Kaiser, C. M., Maillard, R. A., Goldman, D. H., & Wilson, C. A. (2014). Mechanisms of cellular proteostasis: insights from single-molecule approaches. *Annu Rev Biophys, 43*, 119-140. doi:10.1146/annurev-biophys-051013-022811

Butow, R. A., & Avadhani, N. G. (2004). Mitochondrial signaling: the retrograde response. *Mol Cell, 14*(1), 1-15.

Cairns, R. A., Harris, I. S., & Mak, T. W. (2011). Regulation of cancer cell metabolism. *Nat Rev Cancer, 11*(2), 85-95. doi:10.1038/nrc2981

Calligaris, R., Banica, M., Roncaglia, P., Robotti, E., Finaurini, S., Vlachouli, C., . . . Gustincich, S. (2015). Blood transcriptomics of drug-naive sporadic Parkinson's disease patients. *BMC Genomics, 16*(1), 876. doi:10.1186/s12864-015-2058-3

Cam, H., Easton, J. B., High, A., & Houghton, P. J. (2010). mTORC1 signaling under hypoxic conditions is controlled by ATM-dependent phosphorylation of HIF-1alpha. *Mol Cell, 40*(4), 509-520. doi:10.1016/j.molcel.2010.10.030

Canto, C., Gerhart-Hines, Z., Feige, J. N., Lagouge, M., Noriega, L., Milne, J. C., . . . Auwerx, J. (2009). AMPK regulates energy expenditure by modulating NAD+ metabolism and SIRT1 activity. *Nature, 458*(7241), 1056-1060. doi:10.1038/nature07813

Canto, C., Houtkooper, R. H., Pirinen, E., Youn, D. Y., Oosterveer, M. H., Cen, Y., . . . Auwerx, J. (2012). The NAD(+) precursor nicotinamide riboside enhances

oxidative metabolism and protects against high-fat diet-induced obesity. *Cell Metab, 15*(6), 838-847. doi:10.1016/j.cmet.2012.04.022

Casadei, N., Sood, P., Ulrich, T., Fallier-Becker, P., Kieper, N., Helling, S., . . . Fitzgerald, J. C. (2016). Mitochondrial defects and neurodegeneration in mice overexpressing wild-type or G399S mutant HtrA2. *Hum Mol Genet, 25*(3), 459-471. doi:10.1093/hmg/ddv485

Castellino, N., & Aloj, S. (1969). Intracellular distribution of lead in the liver and kidney of the rat. *Br J Ind Med, 26*(2), 139-143.

Castro Mdel, R., Suarez, E., Kraiselburd, E., Isidro, A., Paz, J., Ferder, L., & Ayala-Torres, S. (2012). Aging increases mitochondrial DNA damage and oxidative stress in liver of rhesus monkeys. *Exp Gerontol, 47*(1), 29-37. doi:10.1016/j.exger.2011.10.002

Cerutti, R., Pirinen, E., Lamperti, C., Marchet, S., Sauve, A. A., Li, W., . . . Zeviani, M. (2014). NAD(+)-dependent activation of Sirt1 corrects the phenotype in a mouse model of mitochondrial disease. *Cell Metab, 19*(6), 1042-1049. doi:10.1016/j.cmet.2014.04.001

Chambers, K. T., Chen, Z., Crawford, P. A., Fu, X., Burgess, S. C., Lai, L., . . . Finck, B. N. (2012). Liver-specific PGC-1beta deficiency leads to impaired mitochondrial function and lipogenic response to fasting-refeeding. *PLoS One, 7*(12), e52645. doi:10.1371/journal.pone.0052645

Chance, B., Sies, H., & Boveris, A. (1979). Hydroperoxide metabolism in mammalian organs. *Physiol Rev, 59*(3), 527-605.

Chandel, N. S. (2015). Evolution of Mitochondria as Signaling Organelles. *Cell Metab, 22*(2), 204-206. doi:10.1016/j.cmet.2015.05.013

Chang, J. Y., & Chang, N. S. (2015). WWOX dysfunction induces sequential aggregation of TRAPPC6ADelta, TIAF1, tau and amyloid beta, and causes apoptosis. *Cell Death Discov, 1*, 15003. doi:10.1038/cddiscovery.2015.3

Charoenviriyakul, C., Takahashi, Y., Morishita, M., Matsumoto, A., Nishikawa, M., & Takakura, Y. (2017). Cell type-specific and common characteristics of exosomes derived from mouse cell lines: Yield, physicochemical properties, and pharmacokinetics. *Eur J Pharm Sci, 96*, 316-322. doi:10.1016/j.ejps.2016.10.009

Chaudhary, K. R., El-Sikhry, H., & Seubert, J. M. (2011). Mitochondria and the aging heart. *J Geriatr Cardiol, 8*(3), 159-167. doi:10.3724/sp.j.1263.2011.00159

Chen, X., Hunt, D., Cushman, S. W., & Hess, S. (2009). Proteomic characterization of thiazolidinedione regulation of obese adipose secretome in Zucker obese rats. *Proteomics Clin Appl, 3*(9), 1099-1111. doi:10.1002/prca.200900026

Chen, Y. C., Wu, Y. T., & Wei, Y. H. (2015). Depletion of mitoferrins leads to mitochondrial dysfunction and impairment of adipogenic differentiation in 3T3-L1 preadipocytes. *Free Radic Res, 49*(11), 1285-1295. doi:10.3109/10715762.2015.1067695

Choudhary, V., Kaddour-Djebbar, I., Alaisami, R., Kumar, M. V., & Bollag, W. B. (2014). Mitofusin 1 degradation is induced by a disruptor of mitochondrial

calcium homeostasis, CGP37157: a role in apoptosis in prostate cancer cells. *Int J Oncol, 44*(5), 1767-1773. doi:10.3892/ijo.2014.2343

Chung, H. K., Ryu, D., Kim, K. S., Chang, J. Y., Kim, Y. K., Yi, H. S., . . . Shong, M. (2017). Growth differentiation factor 15 is a myomitokine governing systemic energy homeostasis. *J Cell Biol, 216*(1), 149-165. doi:10.1083/jcb.201607110

Ciapaite, J., van den Broek, N. M., Te Brinke, H., Nicolay, K., Jeneson, J. A., Houten, S. M., & Prompers, J. J. (2011). Differential effects of short- and long-term high-fat diet feeding on hepatic fatty acid metabolism in rats. *Biochim Biophys Acta, 1811*(7-8), 441-451. doi:10.1016/j.bbalip.2011.05.005

Ciesielski, G. L., Bermek, O., Rosado-Ruiz, F. A., Hovde, S. L., Neitzke, O. J., Griffith, J. D., & Kaguni, L. S. (2015). Mitochondrial Single-stranded DNA-binding Proteins Stimulate the Activity of DNA Polymerase gamma by Organization of the Template DNA. *J Biol Chem, 290*(48), 28697-28707. doi:10.1074/jbc.M115.673707

Cinti, S. (2005). The adipose organ. *Prostaglandins Leukot Essent Fatty Acids, 73*(1), 9-15. doi:10.1016/j.plefa.2005.04.010

Cipolat, S., Martins de Brito, O., Dal Zilio, B., & Scorrano, L. (2004). OPA1 requires mitofusin 1 to promote mitochondrial fusion. *Proc Natl Acad Sci U S A, 101*(45), 15927-15932. doi:10.1073/pnas.0407043101

Clapham, D. E. (2007). Calcium signaling. *Cell, 131*(6), 1047-1058. doi:10.1016/j.cell.2007.11.028

Clayton, D. A., Doda, J. N., & Friedberg, E. C. (1974). The absence of a pyrimidine dimer repair mechanism in mammalian mitochondria. *Proc Natl Acad Sci U S A, 71*(7), 2777-2781.

Clements, C. M., McNally, R. S., Conti, B. J., Mak, T. W., & Ting, J. P. (2006). DJ-1, a cancer- and Parkinson's disease-associated protein, stabilizes the antioxidant transcriptional master regulator Nrf2. *Proc Natl Acad Sci U S A, 103*(41), 15091-15096. doi:10.1073/pnas.0607260103

Cline, S. D. (2012). Mitochondrial DNA damage and its consequences for mitochondrial gene expression. *Biochim Biophys Acta, 1819*(9-10), 979-991. doi:10.1016/j.bbagrm.2012.06.002

Coelho, M., Oliveira, T., & Fernandes, R. (2013). Biochemistry of adipose tissue: an endocrine organ. *Arch Med Sci, 9*(2), 191-200. doi:10.5114/aoms.2013.33181

Cogliati, S., Enriquez, J. A., & Scorrano, L. (2016). Mitochondrial Cristae: Where Beauty Meets Functionality. *Trends Biochem Sci, 41*(3), 261-273. doi:10.1016/j.tibs.2016.01.001

Cogliati, S., Frezza, C., Soriano, M. E., Varanita, T., Quintana-Cabrera, R., Corrado, M., . . . Scorrano, L. (2013). Mitochondrial cristae shape determines respiratory chain supercomplexes assembly and respiratory efficiency. *Cell, 155*(1), 160-171. doi:10.1016/j.cell.2013.08.032

Coleman, R. (1987). Biochemistry of bile secretion. *Biochem J, 244*(2), 249-261.

Connor, K. M., Subbaram, S., Regan, K. J., Nelson, K. K., Mazurkiewicz, J. E., Bartholomew, P. J., . . . Melendez, J. A. (2005). Mitochondrial H2O2 regulates

the angiogenic phenotype via PTEN oxidation. *J Biol Chem, 280*(17), 16916-16924. doi:10.1074/jbc.M410690200

Cooper, J. M., Mann, V. M., & Schapira, A. H. (1992). Analyses of mitochondrial respiratory chain function and mitochondrial DNA deletion in human skeletal muscle: effect of ageing. *J Neurol Sci, 113*(1), 91-98.

Corrado, C., Raimondo, S., Chiesi, A., Ciccia, F., De Leo, G., & Alessandro, R. (2013). Exosomes as intercellular signaling organelles involved in health and disease: basic science and clinical applications. *Int J Mol Sci, 14*(3), 5338-5366. doi:10.3390/ijms14035338

Cosentino, C., Grieco, D., & Costanzo, V. (2011). ATM activates the pentose phosphate pathway promoting anti-oxidant defence and DNA repair. *EMBO J, 30*(3), 546-555. doi:10.1038/emboj.2010.330

Cotan, D., Cordero, M. D., Garrido-Maraver, J., Oropesa-Avila, M., Rodriguez-Hernandez, A., Gomez Izquierdo, L., . . . Sanchez-Alcazar, J. A. (2011). Secondary coenzyme Q10 deficiency triggers mitochondria degradation by mitophagy in MELAS fibroblasts. *FASEB J, 25*(8), 2669-2687. doi:10.1096/fj.10-165340

Courtois, G., Morgan, J. G., Campbell, L. A., Fourel, G., & Crabtree, G. R. (1987). Interaction of a liver-specific nuclear factor with the fibrinogen and alpha 1-antitrypsin promoters. *Science, 238*(4827), 688-692.

Coxhead, J., Kurzawa-Akanbi, M., Hussain, R., Pyle, A., Chinnery, P., & Hudson, G. (2016). Somatic mtDNA variation is an important component of Parkinson's disease. *Neurobiol Aging, 38*, 217 e211-216. doi:10.1016/j.neurobiolaging.2015.10.036

Cree, L. M., Samuels, D. C., & Chinnery, P. F. (2009). The inheritance of pathogenic mitochondrial DNA mutations. *Biochim Biophys Acta, 1792*(12), 1097-1102. doi:10.1016/j.bbadis.2009.03.002

Cunningham, J. T., Rodgers, J. T., Arlow, D. H., Vazquez, F., Mootha, V. K., & Puigserver, P. (2007). mTOR controls mitochondrial oxidative function through a YY1-PGC-1alpha transcriptional complex. *Nature, 450*(7170), 736-740. doi:10.1038/nature06322

Davis, R. L., Liang, C., Edema-Hildebrand, F., Riley, C., Needham, M., & Sue, C. M. (2013). Fibroblast growth factor 21 is a sensitive biomarker of mitochondrial disease. *Neurology, 81*(21), 1819-1826. doi:10.1212/01.wnl.0000436068.43384.ef

De Haes, W., Frooninckx, L., Van Assche, R., Smolders, A., Depuydt, G., Billen, J., . . . Temmerman, L. (2014). Metformin promotes lifespan through mitohormesis via the peroxiredoxin PRDX-2. *Proc Natl Acad Sci U S A, 111*(24), E2501-2509. doi:10.1073/pnas.1321776111

Dean, M., Hamon, Y., & Chimini, G. (2001). The human ATP-binding cassette (ABC) transporter superfamily. *Journal of Lipid Research, 42*(7), 1007-1017.

Demaurex, N., Poburko, D., & Frieden, M. (2009). Regulation of plasma membrane calcium fluxes by mitochondria. *Biochim Biophys Acta, 1787*(11), 1383-1394. doi:10.1016/j.bbabio.2008.12.012

Demel, H. R., Feuerecker, B., Piontek, G., Seidl, C., Blechert, B., Pickhard, A., & Essler, M. (2015). Effects of topoisomerase inhibitors that induce DNA damage response on glucose metabolism and PI3K/Akt/mTOR signaling in multiple myeloma cells. *Am J Cancer Res, 5*(5), 1649-1664.

Dexter, D. T., Carter, C. J., Wells, F. R., Javoy-Agid, F., Agid, Y., Lees, A., . . . Marsden, C. D. (1989). Basal lipid peroxidation in substantia nigra is increased in Parkinson's disease. *J Neurochem, 52*(2), 381-389.

Dhar, S. S., Johar, K., & Wong-Riley, M. T. (2013). Bigenomic transcriptional regulation of all thirteen cytochrome c oxidase subunit genes by specificity protein 1. *Open Biol, 3*(3), 120176. doi:10.1098/rsob.120176

Di Domenico, F., Pupo, G., Giraldo, E., Badia, M. C., Monllor, P., Lloret, A., . . . Perluigi, M. (2016). Oxidative signature of cerebrospinal fluid from mild cognitive impairment and Alzheimer disease patients. *Free Radic Biol Med, 91*, 1-9. doi:10.1016/j.freeradbiomed.2015.12.004

Diaz, F., Garcia, S., Hernandez, D., Regev, A., Rebelo, A., Oca-Cossio, J., & Moraes, C. T. (2008). Pathophysiology and fate of hepatocytes in a mouse model of mitochondrial hepatopathies. *Gut, 57*(2), 232-242. doi:10.1136/gut.2006.119180

Dietzel, E., Wessling, J., Floehr, J., Schafer, C., Ensslen, S., Denecke, B., . . . Jahnen-Dechent, W. (2013). Fetuin-B, a liver-derived plasma protein is essential for fertilization. *Dev Cell, 25*(1), 106-112. doi:10.1016/j.devcel.2013.03.001

Dinardo, M. M., Musicco, C., Fracasso, F., Milella, F., Gadaleta, M. N., Gadaleta, G., & Cantatore, P. (2003). Acetylation and level of mitochondrial transcription factor A in several organs of young and old rats. *Biochem Biophys Res Commun, 301*(1), 187-191.

Ding, H., Zhang, Z. Y., Zhang, J. W., & Zhang, Y. (2013). Role of mitochondrial quality control in exercise-induced health adaptation. *Zhongguo Ying Yong Sheng Li Xue Za Zhi, 29*(6), 543-553.

Diot, A., Morten, K., & Poulton, J. (2016). Mitophagy plays a central role in mitochondrial ageing. *Mamm Genome, 27*(7-8), 381-395. doi:10.1007/s00335-016-9651-x

Distefano, G., Standley, R. A., Dube, J. J., Carnero, E. A., Ritov, V. B., Stefanovic-Racic, M., . . . Coen, P. M. (2016). Chronological Age Does not Influence Ex-vivo Mitochondrial Respiration and Quality Control in Skeletal Muscle. *J Gerontol A Biol Sci Med Sci*. doi:10.1093/gerona/glw102

Distelmaier, F., Valsecchi, F., Liemburg-Apers, D. C., Lebiedzinska, M., Rodenburg, R. J., Heil, S., . . . Koopman, W. J. (2015). Mitochondrial dysfunction in primary human fibroblasts triggers an adaptive cell survival program that requires AMPK-alpha. *Biochim Biophys Acta, 1852*(3), 529-540. doi:10.1016/j.bbadis.2014.12.012

Dominy, J. E., & Puigserver, P. (2013). Mitochondrial biogenesis through activation of nuclear signaling proteins. *Cold Spring Harb Perspect Biol, 5*(7). doi:10.1101/cshperspect.a015008

Dudek, J., Rehling, P., & van der Laan, M. (2013). Mitochondrial protein import: common principles and physiological networks. *Biochim Biophys Acta, 1833*(2), 274-285. doi:10.1016/j.bbamcr.2012.05.028

Dufour, C. R., Wilson, B. J., Huss, J. M., Kelly, D. P., Alaynick, W. A., Downes, M., . . . Giguere, V. (2007). Genome-wide orchestration of cardiac functions by the orphan nuclear receptors ERRalpha and gamma. *Cell Metab, 5*(5), 345-356. doi:10.1016/j.cmet.2007.03.007

Durieux, J., Wolff, S., & Dillin, A. (2011). The cell-non-autonomous nature of electron transport chain-mediated longevity. *Cell, 144*(1), 79-91. doi:10.1016/j.cell.2010.12.016

Dyrks, T., Monning, U., Beyreuther, K., & Turner, J. (1994). Amyloid precursor protein secretion and beta A4 amyloid generation are not mutually exclusive. *FEBS Lett, 349*(2), 210-214.

Egan, D. F., Shackelford, D. B., Mihaylova, M. M., Gelino, S., Kohnz, R. A., Mair, W., . . . Shaw, R. J. (2011). Phosphorylation of ULK1 (hATG1) by AMP-activated protein kinase connects energy sensing to mitophagy. *Science, 331*(6016), 456-461. doi:http://dx.doi.org/10.1126/science.1196371

Endo, T., Mitsui, S., & Roise, D. (1995). Mitochondrial presequences can induce aggregation of unfolded proteins. *FEBS Lett, 359*(1), 93-96.

Fajas, L. (2013). Re-thinking cell cycle regulators: the cross-talk with metabolism. *Front Oncol, 3*, 4. doi:10.3389/fonc.2013.00004

Fantuzzi, G. (2005). Adipose tissue, adipokines, and inflammation. *J Allergy Clin Immunol, 115*(5), 911-919; quiz 920. doi:10.1016/j.jaci.2005.02.023

Faulk, E. A., McCully, J. D., Tsukube, T., Hadlow, N. C., Krukenkamp, I. B., & Levitsky, S. (1995). Myocardial mitochondrial calcium accumulation modulates nuclear calcium accumulation and DNA fragmentation. *Ann Thorac Surg, 60*(2), 338-344.

Fealy, C. E., Mulya, A., Lai, N., & Kirwan, J. P. (2014). Exercise training decreases activation of the mitochondrial fission protein dynamin-related protein-1 in insulin-resistant human skeletal muscle. *J Appl Physiol (1985), 117*(3), 239-245. doi:10.1152/japplphysiol.01064.2013

Ferro-Novick, S., & Brose, N. (2013). Nobel 2013 Physiology or medicine: Traffic control system within cells. *Nature, 504*(7478), 98. doi:10.1038/504098a

Fillmore, N., Jacobs, D. L., Mills, D. B., Winder, W. W., & Hancock, C. R. (2010). Chronic AMP-activated protein kinase activation and a high-fat diet have an additive effect on mitochondria in rat skeletal muscle. *Journal of Applied Physiology, 109*(2), 511-520. doi:10.1152/japplphysiol.00126.2010

Fiorese, C. J., Schulz, A. M., Lin, Y. F., Rosin, N., Pellegrino, M. W., & Haynes, C. M. (2016). The Transcription Factor ATF5 Mediates a Mammalian Mitochondrial UPR. *Curr Biol, 26*(15), 2037-2043. doi:10.1016/j.cub.2016.06.002

Floor, E., & Wetzel, M. G. (1998). Increased protein oxidation in human substantia nigra pars compacta in comparison with basal ganglia and prefrontal cortex

measured with an improved dinitrophenylhydrazine assay. *J Neurochem, 70*(1), 268-275.

Forkink, M., Basit, F., Teixeira, J., Swarts, H. G., Koopman, W. J., & Willems, P. H. (2015). Complex I and complex III inhibition specifically increase cytosolic hydrogen peroxide levels without inducing oxidative stress in HEK293 cells. *Redox Biol, 6*, 607-616. doi:10.1016/j.redox.2015.09.003

Forman, H. J., & Azzi, A. (1997). On the virtual existence of superoxide anions in mitochondria: thoughts regarding its role in pathophysiology. *FASEB J, 11*(5), 374-375.

Frazier, T. P., Gimble, J. M., Kheterpal, I., & Rowan, B. G. (2013). Impact of low oxygen on the secretome of human adipose-derived stromal/stem cell primary cultures. *Biochimie, 95*(12), 2286-2296. doi:10.1016/j.biochi.2013.07.011

Friedman, J. R., Lackner, L. L., West, M., DiBenedetto, J. R., Nunnari, J., & Voeltz, G. K. (2011). ER tubules mark sites of mitochondrial division. *Science, 334*(6054), 358-362. doi:10.1126/science.1207385

Fujisawa, K., Nishikawa, T., Kukidome, D., Imoto, K., Yamashiro, T., Motoshima, H., . . . Araki, E. (2009). TZDs reduce mitochondrial ROS production and enhance mitochondrial biogenesis. *Biochem Biophys Res Commun, 379*(1), 43-48. doi:10.1016/j.bbrc.2008.11.141

Fukui, H., & Moraes, C. T. (2008). The mitochondrial impairment, oxidative stress and neurodegeneration connection: reality or just an attractive hypothesis? *Trends Neurosci, 31*(5), 251-256. doi:10.1016/j.tins.2008.02.008

Furler, S. M., Cooney, G. J., Hegarty, B. D., Lim-Fraser, M. Y., Kraegen, E. W., & Oakes, N. D. (2000). Local factors modulate tissue-specific NEFA utilization: assessment in rats using 3H-(R)-2-bromopalmitate. *Diabetes, 49*(9), 1427-1433.

Gakh, O., Cavadini, P., & Isaya, G. (2002). Mitochondrial processing peptidases. *Biochim Biophys Acta, 1592*(1), 63-77.

Garcia-Perez, C., Hajnoczky, G., & Csordas, G. (2008). Physical coupling supports the local Ca2+ transfer between sarcoplasmic reticulum subdomains and the mitochondria in heart muscle. *J Biol Chem, 283*(47), 32771-32780. doi:10.1074/jbc.M803385200

Garcia-Roves, P. M., Osler, M. E., Holmström, M. H., & Zierath, J. R. (2008). Gain-of-function R225Q Mutation in AMP-activated Protein Kinase γ3 Subunit Increases Mitochondrial Biogenesis in Glycolytic Skeletal Muscle. *Journal of Biological Chemistry, 283*(51), 35724-35734. doi:10.1074/jbc.M805078200

Garcia, N. A., Moncayo-Arlandi, J., Sepulveda, P., & Diez-Juan, A. (2016). Cardiomyocyte exosomes regulate glycolytic flux in endothelium by direct transfer of GLUT transporters and glycolytic enzymes. *Cardiovasc Res, 109*(3), 397-408. doi:10.1093/cvr/cvv260

Garg, S. G., & Martin, W. F. (2016). Mitochondria, the Cell Cycle, and the Origin of Sex via a Syncytial Eukaryote Common Ancestor. *Genome Biol Evol, 8*(6), 1950-1970. doi:10.1093/gbe/evw136

Garrido-Maraver, J., Paz, M. V., Cordero, M. D., Bautista-Lorite, J., Oropesa-Avila, M., de la Mata, M., . . . Sanchez-Alcazar, J. A. (2015). Critical role of AMP-activated protein kinase in the balance between mitophagy and mitochondrial biogenesis in MELAS disease. *Biochim Biophys Acta, 1852*(11), 2535-2553. doi:10.1016/j.bbadis.2015.08.027

Gavin, C. E., Gunter, K. K., & Gunter, T. E. (1992). Mn2+ sequestration by mitochondria and inhibition of oxidative phosphorylation. *Toxicol Appl Pharmacol, 115*(1), 1-5.

Geisler, S., Holmstrom, K. M., Skujat, D., Fiesel, F. C., Rothfuss, O. C., Kahle, P. J., & Springer, W. (2010). PINK1/Parkin-mediated mitophagy is dependent on VDAC1 and p62/SQSTM1. *Nat Cell Biol, 12*(2), 119-131. doi:10.1038/ncb2012

Gelfand, R., & Attardi, G. (1981). Synthesis and turnover of mitochondrial ribonucleic acid in HeLa cells: the mature ribosomal and messenger ribonucleic acid species are metabolically unstable. *Mol Cell Biol, 1*(6), 497-511.

Genereux, J. C., & Wiseman, R. L. (2015). Regulating extracellular proteostasis capacity through the unfolded protein response. *Prion, 9*(1), 10-21. doi:10.1080/19336896.2015.1011887

Gerhart-Hines, Z., Rodgers, J. T., Bare, O., Lerin, C., Kim, S. H., Mostoslavsky, R., . . . Puigserver, P. (2007). Metabolic control of muscle mitochondrial function and fatty acid oxidation through SIRT1/PGC-1alpha. *EMBO J, 26*(7), 1913-1923. doi:10.1038/sj.emboj.7601633

Ghebrehiwet, B. (2016). The complement system: an evolution in progress. *F1000Res, 5*, 2840. doi:10.12688/f1000research.10065.1

Ghosh, A., Langley, M. R., Harischandra, D. S., Neal, M. L., Jin, H., Anantharam, V., . . . Kanthasamy, A. G. (2016). Mitoapocynin Treatment Protects Against Neuroinflammation and Dopaminergic Neurodegeneration in a Preclinical Animal Model of Parkinson's Disease. *J Neuroimmune Pharmacol, 11*(2), 259-278. doi:10.1007/s11481-016-9650-4

Giordano, C., Iommarini, L., Giordano, L., Maresca, A., Pisano, A., Valentino, M. L., . . . Carelli, V. (2014). Efficient mitochondrial biogenesis drives incomplete penetrance in Leber's hereditary optic neuropathy. *Brain, 137*(Pt 2), 335-353. doi:10.1093/brain/awt343

Glater, E. E., Megeath, L. J., Stowers, R. S., & Schwarz, T. L. (2006). Axonal transport of mitochondria requires milton to recruit kinesin heavy chain and is light chain independent. *J Cell Biol, 173*(4), 545-557. doi:10.1083/jcb.200601067

Gleyzer, N., Vercauteren, K., & Scarpulla, R. C. (2005). Control of mitochondrial transcription specificity factors (TFB1M and TFB2M) by nuclear respiratory factors (NRF-1 and NRF-2) and PGC-1 family coactivators. *Mol Cell Biol, 25*(4), 1354-1366. doi:10.1128/mcb.25.4.1354-1366.2005

Glunde, K., Guggino, S. E., Solaiyappan, M., Pathak, A. P., Ichikawa, Y., & Bhujwalla, Z. M. (2003). Extracellular acidification alters lysosomal trafficking in human breast cancer cells. *Neoplasia, 5*(6), 533-545.

Goldstein, J. C., Munoz-Pinedo, C., Ricci, J. E., Adams, S. R., Kelekar, A., Schuler, M., . . . Green, D. R. (2005). Cytochrome c is released in a single step during apoptosis. *Cell Death Differ, 12*(5), 453-462. doi:10.1038/sj.cdd.4401596

Golpich, M., Amini, E., Mohamed, Z., Azman Ali, R., Mohamed Ibrahim, N., & Ahmadiani, A. (2017). Mitochondrial Dysfunction and Biogenesis in Neurodegenerative diseases: Pathogenesis and Treatment. *CNS Neurosci Ther, 23*(1), 5-22. doi:10.1111/cns.12655

Goncalves, I. O., Passos, E., Diogo, C. V., Rocha-Rodrigues, S., Santos-Alves, E., Oliveira, P. J., . . . Magalhaes, J. (2016). Exercise mitigates mitochondrial permeability transition pore and quality control mechanisms alterations in nonalcoholic steatohepatitis. *Appl Physiol Nutr Metab, 41*(3), 298-306. doi:10.1139/apnm-2015-0470

Goncalves, R. L., Rothschild, D. E., Quinlan, C. L., Scott, G. K., Benz, C. C., & Brand, M. D. (2014). Sources of superoxide/H2O2 during mitochondrial proline oxidation. *Redox Biol, 2*, 901-909. doi:10.1016/j.redox.2014.07.003

Gopalakrishnan, L., & Scarpulla, R. C. (1994). Differential regulation of respiratory chain subunits by a CREB-dependent signal transduction pathway. Role of cyclic AMP in cytochrome c and COXIV gene expression. *J Biol Chem, 269*(1), 105-113.

Gorman, G. S., Chinnery, P. F., DiMauro, S., Hirano, M., Koga, Y., McFarland, R., . . . Turnbull, D. M. (2016). Mitochondrial diseases. *Nat Rev Dis Primers, 2*, 16080. doi:10.1038/nrdp.2016.80

Gottlieb, R. A., Mentzer, R. M., Jr., & Linton, P. J. (2011). Impaired mitophagy at the heart of injury. *Autophagy, 7*(12), 1573-1574.

Grant, D. M. (1991). Detoxification pathways in the liver. *J Inherit Metab Dis, 14*(4), 421-430.

Gray, M. W., Burger, G., & Lang, B. F. (2001). The origin and early evolution of mitochondria. *Genome Biol, 2*(6), REVIEWS1018.

Greenamyre, J. T., Sherer, T. B., Betarbet, R., & Panov, A. V. (2001). Complex I and Parkinson's disease. *IUBMB Life, 52*(3-5), 135-141. doi:10.1080/15216540152845939

Greene, N. P., Lee, D. E., Brown, J. L., Rosa, M. E., Brown, L. A., Perry, R. A., . . . Washington, T. A. (2015). Mitochondrial quality control, promoted by PGC-1alpha, is dysregulated by Western diet-induced obesity and partially restored by moderate physical activity in mice. *Physiol Rep, 3*(7). doi:10.14814/phy2.12470

Griffiths, G. M. (2016). Secretion from Myeloid Cells: Secretory Lysosomes. *Microbiol Spectr, 4*(4). doi:10.1128/microbiolspec.MCHD-0030-2016

Grunewald, A., Rygiel, K. A., Hepplewhite, P. D., Morris, C. M., Picard, M., & Turnbull, D. M. (2016). Mitochondrial DNA Depletion in Respiratory Chain-Deficient Parkinson Disease Neurons. *Ann Neurol, 79*(3), 366-378. doi:10.1002/ana.24571

Guaita-Esteruelas, S., Bosquet, A., Saavedra, P., Guma, J., Girona, J., Lam, E. W., . . . Masana, L. (2017). Exogenous FABP4 increases breast cancer cell proliferation

and activates the expression of fatty acid transport proteins. *Mol Carcinog, 56*(1), 208-217. doi:10.1002/mc.22485

Guescini, M., Genedani, S., Stocchi, V., & Agnati, L. F. (2010). Astrocytes and Glioblastoma cells release exosomes carrying mtDNA. *J Neural Transm (Vienna), 117*(1), 1-4. doi:10.1007/s00702-009-0288-8

Guescini, M., Guidolin, D., Vallorani, L., Casadei, L., Gioacchini, A. M., Tibollo, P., . . . Stocchi, V. (2010). C2C12 myoblasts release micro-vesicles containing mtDNA and proteins involved in signal transduction. *Exp Cell Res, 316*(12), 1977-1984. doi:10.1016/j.yexcr.2010.04.006

Guha, M., Fang, J. K., Monks, R., Birnbaum, M. J., & Avadhani, N. G. (2010). Activation of Akt is essential for the propagation of mitochondrial respiratory stress signaling and activation of the transcriptional coactivator heterogeneous ribonucleoprotein A2. *Mol Biol Cell, 21*(20), 3578-3589. doi:10.1091/mbc.E10-03-0192

Guha, M., Srinivasan, S., Guja, K., Mejia, E., Garcia-Diaz, M., Johnson, F. B., . . . Avadhani, N. G. (2016). HnRNPA2 is a novel histone acetyltransferase that mediates mitochondrial stress-induced nuclear gene expression. *Cell Discov, 2*, 16045. doi:10.1038/celldisc.2016.45

Guha, M., Tang, W., Sondheimer, N., & Avadhani, N. G. (2010). Role of calcineurin, hnRNPA2 and Akt in mitochondrial respiratory stress-mediated transcription activation of nuclear gene targets. *Biochim Biophys Acta, 1797*(6-7), 1055-1065. doi:10.1016/j.bbabio.2010.02.008

Gulick, T., Cresci, S., Caira, T., Moore, D. D., & Kelly, D. P. (1994). The peroxisome proliferator-activated receptor regulates mitochondrial fatty acid oxidative enzyme gene expression. *Proc Natl Acad Sci U S A, 91*(23), 11012-11016.

Guo, J. L., & Lee, V. M. (2014). Cell-to-cell transmission of pathogenic proteins in neurodegenerative diseases. *Nat Med, 20*(2), 130-138. doi:10.1038/nm.3457

Guo, Z., Kozlov, S., Lavin, M. F., Person, M. D., & Paull, T. T. (2010). ATM activation by oxidative stress. *Science, 330*(6003), 517-521. doi:10.1126/science.1192912

Gustafson, B., & Smith, U. (2015). Regulation of white adipogenesis and its relation to ectopic fat accumulation and cardiovascular risk. *Atherosclerosis, 241*(1), 27-35. doi:10.1016/j.atherosclerosis.2015.04.812

Halaby, M. J., Hibma, J. C., He, J., & Yang, D. Q. (2008). ATM protein kinase mediates full activation of Akt and regulates glucose transporter 4 translocation by insulin in muscle cells. *Cell Signal, 20*(8), 1555-1563. doi:10.1016/j.cellsig.2008.04.011

Hambrecht, R., Fiehn, E., Yu, J., Niebauer, J., Weigl, C., Hilbrich, L., . . . Schuler, G. (1997). Effects of endurance training on mitochondrial ultrastructure and fiber type distribution in skeletal muscle of patients with stable chronic heart failure. *J Am Coll Cardiol, 29*(5), 1067-1073.

Harmon, J. L., Wills, L. P., McOmish, C. E., Demireva, E. Y., Gingrich, J. A., Beeson, C. C., & Schnellmann, R. G. (2016). 5-HT2 Receptor Regulation of Mitochondrial Genes: Unexpected Pharmacological Effects of Agonists and Antagonists. *J Pharmacol Exp Ther, 357*(1), 1-9. doi:10.1124/jpet.115.228395

Harris, D. A., & Das, A. M. (1991). Control of mitochondrial ATP synthesis in the heart. *Biochem J, 280 (Pt 3)*, 561-573.

Haynes, C. M., Petrova, K., Benedetti, C., Yang, Y., & Ron, D. (2007). ClpP mediates activation of a mitochondrial unfolded protein response in C. elegans. *Dev Cell, 13*(4), 467-480. doi:10.1016/j.devcel.2007.07.016

Haynes, C. M., Yang, Y., Blais, S. P., Neubert, T. A., & Ron, D. (2010). The matrix peptide exporter HAF-1 signals a mitochondrial UPR by activating the transcription factor ZC376.7 in C. elegans. *Molecular Cell, 37*(4), 529-540. doi:http://dx.doi.org/10.1016/j.molcel.2010.01.015

Haynes, C. M., Yang, Y., Blais, S. P., Neubert, T. A., & Ron, D. (2010). The matrix peptide exporter HAF-1 signals a mitochondrial UPR by activating the transcription factor ZC376.7 in C. elegans. *Mol Cell, 37*(4), 529-540. doi:10.1016/j.molcel.2010.01.015

Hayyan, M., Hashim, M. A., & AlNashef, I. M. (2016). Superoxide Ion: Generation and Chemical Implications. *Chem Rev, 116*(5), 3029-3085. doi:10.1021/acs.chemrev.5b00407

He, J., Cooper, H. M., Reyes, A., Di Re, M., Sembongi, H., Litwin, T. R., . . . Holt, I. J. (2012). Mitochondrial nucleoid interacting proteins support mitochondrial protein synthesis. *Nucleic Acids Res, 40*(13), 6109-6121. doi:10.1093/nar/gks266

Hebert, A. S., Dittenhafer-Reed, K. E., Yu, W., Bailey, D. J., Selen, E. S., Boersma, M. D., . . . Coon, J. J. (2013). Calorie restriction and SIRT3 trigger global reprogramming of the mitochondrial protein acetylome. *Mol Cell, 49*(1), 186-199. doi:10.1016/j.molcel.2012.10.024

Hegarty, B. D., Cooney, G. J., Kraegen, E. W., & Furler, S. M. (2002). Increased efficiency of fatty acid uptake contributes to lipid accumulation in skeletal muscle of high fat-fed insulin-resistant rats. *Diabetes, 51*(5), 1477-1484.

Heinonen, S., Buzkova, J., Muniandy, M., Kaksonen, R., Ollikainen, M., Ismail, K., . . . Pietilainen, K. H. (2015). Impaired Mitochondrial Biogenesis in Adipose Tissue in Acquired Obesity. *Diabetes, 64*(9), 3135-3145. doi:10.2337/db14-1937

Hernandez-Mijares, A., Banuls, C., Bellod, L., Jover, A., Sola, E., Morillas, C., . . . Rocha, M. (2012). Effect of weight loss on C3 and C4 components of complement in obese patients. *Eur J Clin Invest, 42*(5), 503-509. doi:10.1111/j.1365-2362.2011.02606.x

Herst, P. M., & Berridge, M. V. (2007). Cell surface oxygen consumption: a major contributor to cellular oxygen consumption in glycolytic cancer cell lines. *Biochim Biophys Acta, 1767*(2), 170-177. doi:10.1016/j.bbabio.2006.11.018

Hertzberg, K. M., Pindyck, J., Mosesson, M. W., & Grieninger, G. (1981). Thyroid hormone stimulation of plasma protein synthesis in cultured hepatocytes. *J Biol Chem, 256*(2), 563-566.

Higa, L. M., Caruso, M. B., Canellas, F., Soares, M. R., Oliveira-Carvalho, A. L., Chapeaurouge, D. A., . . . Da Poian, A. T. (2008). Secretome of HepG2 cells infected with dengue virus: implications for pathogenesis. *Biochim Biophys Acta, 1784*(11), 1607-1616. doi:10.1016/j.bbapap.2008.06.015

Hirotani, M., Maita, C., Niino, M., Iguchi-Ariga, S., Hamada, S., Ariga, H., & Sasaki, H. (2008). Correlation between DJ-1 levels in the cerebrospinal fluid and the progression of disabilities in multiple sclerosis patients. *Mult Scler, 14*(8), 1056-1060. doi:10.1177/1352458508093616

Hjerpe, E., Egyhazi, S., Carlson, J., Stolt, M. F., Schedvins, K., Johansson, H., . . . Avall-Lundqvist, E. (2013). HSP60 predicts survival in advanced serous ovarian cancer. *Int J Gynecol Cancer, 23*(3), 448-455. doi:10.1097/IGC.0b013e318284308b

Ho, D. H., Yi, S., Seo, H., Son, I., & Seol, W. (2014). Increased DJ-1 in urine exosome of Korean males with Parkinson's disease. *Biomed Res Int, 2014*, 704678. doi:10.1155/2014/704678

Hokari, Y., Seki, T., Nakano, H., Matsuo, Y., Fukamizu, A., Munekata, E., . . . Mukai, H. (2012). Isolation and identification of novel neutrophil-activating cryptides hidden in mitochondrial cytochrome C. *Protein Pept Lett, 19*(6), 680-687.

Holmbeck, M. A., Donner, J. R., Villa-Cuesta, E., & Rand, D. M. (2015). A Drosophila model for mito-nuclear diseases generated by an incompatible interaction between tRNA and tRNA synthetase. *Dis Model Mech, 8*(8), 843-854. doi:10.1242/dmm.019323

Hong, X., Yang, Z., Wang, M., Wang, L., & Xu, Q. (2016). Reduced decorin expression in the tumor stroma correlates with tumor proliferation and predicts poor prognosis in patients with I-IIIA non-small cell lung cancer. *Tumour Biol*. doi:10.1007/s13277-016-5431-1

Hood, D. A. (2009). Mechanisms of exercise-induced mitochondrial biogenesis in skeletal muscle. *Appl Physiol Nutr Metab, 34*(3), 465-472. doi:10.1139/h09-045

Horard, B., & Vanacker, J. M. (2003). Estrogen receptor-related receptors: orphan receptors desperately seeking a ligand. *J Mol Endocrinol, 31*(3), 349-357.

Horibe, T., & Hoogenraad, N. J. (2007). The chop gene contains an element for the positive regulation of the mitochondrial unfolded protein response. *PLoS One, 2*(9), e835. doi:10.1371/journal.pone.0000835

Hornig-Do, H. T., Tatsuta, T., Buckermann, A., Bust, M., Kollberg, G., Rotig, A., . . . Wiesner, R. J. (2012). Nonsense mutations in the COX1 subunit impair the stability of respiratory chain complexes rather than their assembly. *EMBO J, 31*(5), 1293-1307. doi:10.1038/emboj.2011.477

Houtkooper, R. H., Mouchiroud, L., Ryu, D., Moullan, N., Katsyuba, E., Knott, G., . . . Auwerx, J. (2013). Mitonuclear protein imbalance as a conserved longevity mechanism. *Nature, 497*(7450), 451-457. doi:10.1038/nature12188

Hu, Q., & Wang, G. (2016). Mitochondrial dysfunction in Parkinson's disease. *Transl Neurodegener, 5*, 14. doi:10.1186/s40035-016-0060-6

Huang, J. H., & Hood, D. A. (2009). Age-associated mitochondrial dysfunction in skeletal muscle: Contributing factors and suggestions for long-term interventions. *IUBMB Life, 61*(3), 201-214. doi:10.1002/iub.164

Huang, Y., Li, W., & Kong, A.-N. (2012). Anti-oxidative stress regulator NF-E2-related factor 2 mediates the adaptive induction of antioxidant and detoxifying enzymes by lipid peroxidation metabolite 4-hydroxynonenal. *Cell & Bioscience, 2*(1), 40.

Huckriede, A., & Agsteribbe, E. (1994). Decreased synthesis and inefficient mitochondrial import of hsp60 in a patient with a mitochondrial encephalomyopathy. *Biochim Biophys Acta, 1227*(3), 200-206.

Humphrey, S. J., James, D. E., & Mann, M. (2015). Protein Phosphorylation: A Major Switch Mechanism for Metabolic Regulation. *Trends Endocrinol Metab, 26*(12), 676-687. doi:10.1016/j.tem.2015.09.013

Hunter, W. G., Kelly, J. P., McGarrah, R. W., 3rd, Kraus, W. E., & Shah, S. H. (2016). Metabolic Dysfunction in Heart Failure: Diagnostic, Prognostic, and Pathophysiologic Insights From Metabolomic Profiling. *Curr Heart Fail Rep, 13*(3), 119-131. doi:10.1007/s11897-016-0289-5

Huo, L., Shaw, J. E., Wong, E., Harding, J. L., Peeters, A., & Magliano, D. J. (2016). Burden of diabetes in Australia: life expectancy and disability-free life expectancy in adults with diabetes. *Diabetologia, 59*(7), 1437-1445. doi:10.1007/s00125-016-3948-x

Hwang, H. H., Moon, P. G., Lee, J. E., Kim, J. G., Lee, W., Ryu, S. H., & Baek, M. C. (2011). Identification of the target proteins of rosiglitazone in 3T3-L1 adipocytes through proteomic analysis of cytosolic and secreted proteins. *Mol Cells, 31*(3), 239-246. doi:10.1007/s10059-011-0026-6

Indo, H. P., Davidson, M., Yen, H. C., Suenaga, S., Tomita, K., Nishii, T., . . . Majima, H. J. (2007). Evidence of ROS generation by mitochondria in cells with impaired electron transport chain and mitochondrial DNA damage. *Mitochondrion, 7*(1-2), 106-118. doi:10.1016/j.mito.2006.11.026

Indo, H. P., Hawkins, C. L., Nakanishi, I., Matsumoto, K. I., Matsui, H., Suenaga, S., . . . Majima, H. J. (2017). Role of Mitochondrial Reactive Oxygen Species in the Activation of Cellular Signals, Molecules, and Function. *Handb Exp Pharmacol*. doi:10.1007/164_2016_117

Iroz, A., Couty, J. P., & Postic, C. (2015). Hepatokines: unlocking the multi-organ network in metabolic diseases. *Diabetologia, 58*(8), 1699-1703. doi:10.1007/s00125-015-3634-4

Irrcher, I., Adhihetty, P. J., Joseph, A. M., Ljubicic, V., & Hood, D. A. (2003). Regulation of mitochondrial biogenesis in muscle by endurance exercise. *Sports Med, 33*(11), 783-793.

Irrcher, I., Adhihetty, P. J., Sheehan, T., Joseph, A. M., & Hood, D. A. (2003). PPARgamma coactivator-1alpha expression during thyroid hormone- and contractile activity-induced mitochondrial adaptations. *Am J Physiol Cell Physiol, 284*(6), C1669-1677. doi:10.1152/ajpcell.00409.2002

Irvine, K. M., Skoien, R., Bokil, N. J., Melino, M., Thomas, G. P., Loo, D., . . . Powell, E. E. (2014). Senescent human hepatocytes express a unique secretory phenotype and promote macrophage migration. *World J Gastroenterol, 20*(47), 17851-17862. doi:10.3748/wjg.v20.i47.17851

Itakura, E., Kishi-Itakura, C., Koyama-Honda, I., & Mizushima, N. (2012). Structures containing Atg9A and the ULK1 complex independently target depolarized mitochondria at initial stages of Parkin-mediated mitophagy. *J Cell Sci, 125*(Pt 6), 1488-1499. doi:10.1242/jcs.094110

Jacobi, D., Liu, S., Burkewitz, K., Kory, N., Knudsen, N. H., Alexander, R. K., . . . Lee, C. H. (2015). Hepatic Bmal1 Regulates Rhythmic Mitochondrial Dynamics and Promotes Metabolic Fitness. *Cell Metab, 22*(4), 709-720. doi:10.1016/j.cmet.2015.08.006

Jahng, J. W., Song, E., & Sweeney, G. (2016). Crosstalk between the heart and peripheral organs in heart failure. *Exp Mol Med, 48*, e217. doi:10.1038/emm.2016.20

James, A. M., Wei, Y. H., Pang, C. Y., & Murphy, M. P. (1996). Altered mitochondrial function in fibroblasts containing MELAS or MERRF mitochondrial DNA mutations. *Biochem J, 318 (Pt 2)*, 401-407.

Janero, D. R., Siuta-Mangano, P., Miller, K. W., & Lane, M. D. (1984). Synthesis, processing, and secretion of hepatic very low density lipoprotein. *J Cell Biochem, 24*(2), 131-152. doi:10.1002/jcb.240240205

Jemt, E., Farge, G., Backstrom, S., Holmlund, T., Gustafsson, C. M., & Falkenberg, M. (2011). The mitochondrial DNA helicase TWINKLE can assemble on a closed circular template and support initiation of DNA synthesis. *Nucleic Acids Res, 39*(21), 9238-9249. doi:10.1093/nar/gkr653

Jeong, H. J., Jeong, H. W., Song, S. S., Kang, J. W., Seo, J. H., Lee, Y. H., . . . Kim, D. W. (2011). Upregulation of peroxiredeoxin III in the hippocampus of acute immobilization stress model rats and the Foxo3a-dependent expression in PC12 cells. *Cellular & Molecular Neurobiology, 31*(7), 1041-1046. doi:http://dx.doi.org/10.1007/s10571-011-9703-4

Ji, X., Zhao, L., Ji, K., Zhao, Y., Li, W., Zhang, R., . . . Yan, C. (2016). Growth Differentiation Factor 15 Is a Novel Diagnostic Biomarker of Mitochondrial Diseases. *Mol Neurobiol*. doi:10.1007/s12035-016-0283-7

Jiang, L., Xiao, L., Sugiura, H., Huang, X., Ali, A., Kuro-o, M., . . . Boothman, D. A. (2015). Metabolic reprogramming during TGFbeta1-induced epithelial-to-mesenchymal transition. *Oncogene, 34*(30), 3908-3916. doi:10.1038/onc.2014.321

Jin, S. M., & Youle, R. J. (2013). The accumulation of misfolded proteins in the mitochondrial matrix is sensed by PINK1 to induce PARK2/Parkin-mediated mitophagy of polarized mitochondria. *Autophagy, 9*(11), 1750-1757. doi:10.4161/auto.26122

Johansen, T., & Lamark, T. (2011). Selective autophagy mediated by autophagic adapter proteins. *Autophagy, 7*(3), 279-296.

Johansson, A. C., Nandakumar, K. S., Persson, A. M., Olsson, I., & Hansson, M. (2009). Secretory lysosome targeting and induced secretion of human soluble TNF-alpha receptor in murine hematopoietic cells in vivo as a principle for immunoregulation in inflammation and malignancy. *Exp Hematol, 37*(8), 969-978. doi:10.1016/j.exphem.2009.05.009

Joo, J. I., Oh, T. S., Kim, D. H., Choi, D. K., Wang, X., Choi, J. W., & Yun, J. W. (2011). Differential expression of adipose tissue proteins between obesity-susceptible and -resistant rats fed a high-fat diet. *Proteomics, 11*(8), 1429-1448. doi:10.1002/pmic.201000515

Joseph, A. M., Rungi, A. A., Robinson, B. H., & Hood, D. A. (2004). Compensatory responses of protein import and transcription factor expression in mitochondrial DNA defects. *Am J Physiol Cell Physiol, 286*(4), C867-875. doi:10.1152/ajpcell.00191.2003

Jourdain, A. A., Koppen, M., Wydro, M., Rodley, C. D., Lightowlers, R. N., Chrzanowska-Lightowlers, Z. M., & Martinou, J. C. (2013). GRSF1 regulates RNA processing in mitochondrial RNA granules. *Cell Metab, 17*(3), 399-410. doi:10.1016/j.cmet.2013.02.005

Kageyama, Y., Hoshijima, M., Seo, K., Bedja, D., Sysa-Shah, P., Andrabi, S. A., . . . Sesaki, H. (2014). Parkin-independent mitophagy requires Drp1 and maintains the integrity of mammalian heart and brain. *EMBO J, 33*(23), 2798-2813. doi:10.15252/embj.201488658

Kaguni, L. S. (2004). DNA polymerase gamma, the mitochondrial replicase. *Annu Rev Biochem, 73*, 293-320. doi:10.1146/annurev.biochem.72.121801.161455

Kanninen, K., Malm, T. M., Jyrkkanen, H. K., Goldsteins, G., Keksa-Goldsteine, V., Tanila, H., . . . Koistinaho, J. (2008). Nuclear factor erythroid 2-related factor 2 protects against beta amyloid. *Mol Cell Neurosci, 39*(3), 302-313. doi:10.1016/j.mcn.2008.07.010

Kawajiri, S., Saiki, S., Sato, S., Sato, F., Hatano, T., Eguchi, H., & Hattori, N. (2010). PINK1 is recruited to mitochondria with parkin and associates with LC3 in mitophagy. *FEBS Lett, 584*(6), 1073-1079. doi:10.1016/j.febslet.2010.02.016

Keller, S., Ridinger, J., Rupp, A. K., Janssen, J. W., & Altevogt, P. (2011). Body fluid derived exosomes as a novel template for clinical diagnostics. *J Transl Med, 9*, 86. doi:10.1186/1479-5876-9-86

Kelley, D. E., Goodpaster, B., Wing, R. R., & Simoneau, J. A. (1999). Skeletal muscle fatty acid metabolism in association with insulin resistance, obesity, and weight loss. *Am J Physiol, 277*(6 Pt 1), E1130-1141.

Kemp, B. E., Mitchelhill, K. I., Stapleton, D., Michell, B. J., Chen, Z. P., & Witters, L. A. (1999). Dealing with energy demand: the AMP-activated protein kinase. *Trends Biochem Sci, 24*(1), 22-25.

Kent-Braun, J. A., & Ng, A. V. (2000). Skeletal muscle oxidative capacity in young and older women and men. *J Appl Physiol (1985), 89*(3), 1072-1078.

Khan, N. A., Auranen, M., Paetau, I., Pirinen, E., Euro, L., Forsstrom, S., . . . Suomalainen, A. (2014). Effective treatment of mitochondrial myopathy by nicotinamide riboside, a vitamin B3. *EMBO Mol Med, 6*(6), 721-731. doi:10.1002/emmm.201403943

Khan, N. A., Govindaraj, P., Meena, A. K., & Thangaraj, K. (2015). Mitochondrial disorders: challenges in diagnosis & treatment. *Indian J Med Res, 141*(1), 13-26.

Khandelwal, P. J., Herman, A. M., Hoe, H.-S., Rebeck, G. W., & Moussa, C. E.-H. (2011). Parkin mediates beclin-dependent autophagic clearance of defective mitochondria and ubiquitinated Aβ in AD models. *Human Molecular Genetics, 20*(11), 2091-2102. doi:10.1093/hmg/ddr091

Kim, H. E., Du, F., Fang, M., & Wang, X. (2005). Formation of apoptosome is initiated by cytochrome c-induced dATP hydrolysis and subsequent nucleotide exchange on Apaf-1. *Proc Natl Acad Sci U S A, 102*(49), 17545-17550. doi:10.1073/pnas.0507900102

Kim, I., & Lemasters, J. J. (2011). Mitochondrial degradation by autophagy (mitophagy) in GFP-LC3 transgenic hepatocytes during nutrient deprivation. *Am J Physiol Cell Physiol, 300*(2), C308-317. doi:10.1152/ajpcell.00056.2010

Kim, J., Choi, Y. S., Lim, S., Yea, K., Yoon, J. H., Jun, D. J., . . . Lee, T. G. (2010). Comparative analysis of the secretory proteome of human adipose stromal vascular fraction cells during adipogenesis. *Proteomics, 10*(3), 394-405. doi:10.1002/pmic.200900218

Kim, J. H., Kim, H. Y., Lee, Y. K., Yoon, Y. S., Xu, W. G., Yoon, J. K., . . . Yoon, G. (2011). Involvement of mitophagy in oncogenic K-Ras-induced transformation: overcoming a cellular energy deficit from glucose deficiency. *Autophagy, 7*(10), 1187-1198. doi:10.4161/auto.7.10.16643

Kim, J. M., Jang, H. J., Choi, S. Y., Park, S. A., Kim, I. S., Yang, Y. R., . . . Suh, P. G. (2014). DJ-1 contributes to adipogenesis and obesity-induced inflammation. *Sci Rep, 4*, 4805. doi:10.1038/srep04805

Kim, K. H., Jeong, Y. T., Oh, H., Kim, S. H., Cho, J. M., Kim, Y. N., . . . Lee, M. S. (2013). Autophagy deficiency leads to protection from obesity and insulin resistance by inducing Fgf21 as a mitokine. *Nat Med, 19*(1), 83-92. doi:10.1038/nm.3014

King, B. C., & Blom, A. M. (2016). Non-traditional roles of complement in type 2 diabetes: Metabolism, insulin secretion and homeostasis. *Mol Immunol*. doi:10.1016/j.molimm.2016.12.009

Kissova, I., Deffieu, M., Manon, S., & Camougrand, N. (2004). Uth1p is involved in the autophagic degradation of mitochondria. *J Biol Chem, 279*(37), 39068-39074. doi:10.1074/jbc.M406960200

Kitaoka, Y., Nakazato, K., & Ogasawara, R. (2016). Combined effects of resistance training and calorie restriction on mitochondrial fusion and fission proteins in rat skeletal muscle. *J Appl Physiol (1985), 121*(3), 806-810. doi:10.1152/japplphysiol.00465.2016

Klimcakova, E., Moro, C., Mazzucotelli, A., Lolmede, K., Viguerie, N., Galitzky, J., . . . Langin, D. (2007). Profiling of adipokines secreted from human subcutaneous adipose tissue in response to PPAR agonists. *Biochem Biophys Res Commun, 358*(3), 897-902. doi:10.1016/j.bbrc.2007.05.012

Knebel, B., Lehr, S., Hartwig, S., Haas, J., Kaber, G., Dicken, H. D., . . . Kotzka, J. (2014). Phosphorylation of sterol regulatory element-binding protein (SREBP)-1c by p38 kinases, ERK and JNK influences lipid metabolism and the secretome

of human liver cell line HepG2. *Arch Physiol Biochem, 120*(5), 216-227. doi:10.3109/13813455.2014.973418

Kohler, F., Muller-Rischart, A. K., Conradt, B., & Rolland, S. G. (2015). The loss of LRPPRC function induces the mitochondrial unfolded protein response. *Aging (Albany NY), 7*(9), 701-717.

Koide-Yoshida, S., Niki, T., Ueda, M., Himeno, S., Taira, T., Iguchi-Ariga, S. M., . . . Ariga, H. (2007). DJ-1 degrades transthyretin and an inactive form of DJ-1 is secreted in familial amyloidotic polyneuropathy. *Int J Mol Med, 19*(6), 885-893.

Koliaki, C., & Roden, M. (2016). Alterations of Mitochondrial Function and Insulin Sensitivity in Human Obesity and Diabetes Mellitus. *Annu Rev Nutr, 36*, 337-367. doi:10.1146/annurev-nutr-071715-050656

Kops, G. J. P. L., Dansen, T. B., Polderman, P. E., Saarloos, I., Wirtz, K. W. A., Coffer, P. J., . . . Burgering, B. M. T. (2002). Forkhead transcription factor FOXO3a protects quiescent cells from oxidative stress. *Nature, 419*(6904), 316-321.

Koutsopoulos, O. S., Laine, D., Osellame, L., Chudakov, D. M., Parton, R. G., Frazier, A. E., & Ryan, M. T. (2010). Human Miltons associate with mitochondria and induce microtubule-dependent remodeling of mitochondrial networks. *Biochim Biophys Acta, 1803*(5), 564-574. doi:10.1016/j.bbamcr.2010.03.006

Krebiehl, G., Ruckerbauer, S., Burbulla, L. F., Kieper, N., Maurer, B., Waak, J., . . . Kruger, R. (2010). Reduced basal autophagy and impaired mitochondrial dynamics due to loss of Parkinson's disease-associated protein DJ-1. *PLoS ONE [Electronic Resource], 5*(2), e9367. doi:http://dx.doi.org/10.1371/journal.pone.0009367

Krishnan, K. J., Reeve, A. K., Samuels, D. C., Chinnery, P. F., Blackwood, J. K., Taylor, R. W., . . . Turnbull, D. M. (2008). What causes mitochondrial DNA deletions in human cells? *Nat Genet, 40*(3), 275-279. doi:10.1038/ng.f.94

Kroemer, G., Dallaporta, B., & Resche-Rigon, M. (1998). The mitochondrial death/life regulator in apoptosis and necrosis. *Annu Rev Physiol, 60*, 619-642. doi:10.1146/annurev.physiol.60.1.619

Kucej, M., Kucejova, B., Subramanian, R., Chen, X. J., & Butow, R. A. (2008). Mitochondrial nucleoids undergo remodeling in response to metabolic cues. *J Cell Sci, 121*(11), 1861-1868. doi:10.1242/jcs.028605

Kudin, A. P., Bimpong-Buta, N. Y., Vielhaber, S., Elger, C. E., & Kunz, W. S. (2004). Characterization of superoxide-producing sites in isolated brain mitochondria. *J Biol Chem, 279*(6), 4127-4135. doi:10.1074/jbc.M310341200

Kukat, C., Davies, K. M., Wurm, C. A., Spahr, H., Bonekamp, N. A., Kuhl, I., . . . Larsson, N. G. (2015). Cross-strand binding of TFAM to a single mtDNA molecule forms the mitochondrial nucleoid. *Proc Natl Acad Sci U S A, 112*(36), 11288-11293. doi:10.1073/pnas.1512131112

Kukat, C., Wurm, C. A., Spahr, H., Falkenberg, M., Larsson, N. G., & Jakobs, S. (2011). Super-resolution microscopy reveals that mammalian mitochondrial nucleoids have a uniform size and frequently contain a single copy of mtDNA. *Proc Natl Acad Sci U S A, 108*(33), 13534-13539. doi:10.1073/pnas.1109263108

Kurtz, A., & Oh, S. J. (2012). Age related changes of the extracellular matrix and stem cell maintenance. *Prev Med, 54 Suppl*, S50-56. doi:10.1016/j.ypmed.2012.01.003

Kusminski, C. M., Holland, W. L., Sun, K., Park, J., Spurgin, S. B., Lin, Y., . . . Scherer, P. E. (2012). MitoNEET-driven alterations in adipocyte mitochondrial activity reveal a crucial adaptive process that preserves insulin sensitivity in obesity. *Nat Med, 18*(10), 1539-1549. doi:10.1038/nm.2899

Kusminski, C. M., & Scherer, P. E. (2012). Mitochondrial dysfunction in white adipose tissue. *Trends Endocrinol Metab, 23*(9), 435-443. doi:10.1016/j.tem.2012.06.004

Kussmaul, L., & Hirst, J. (2006). The mechanism of superoxide production by NADH:ubiquinone oxidoreductase (complex I) from bovine heart mitochondria. *Proc Natl Acad Sci U S A, 103*(20), 7607-7612. doi:10.1073/pnas.0510977103

Lakshmipathy, U., & Campbell, C. (1999). Double strand break rejoining by mammalian mitochondrial extracts. *Nucleic Acids Res, 27*(4), 1198-1204.

Lane, N. (2014). Bioenergetic constraints on the evolution of complex life. *Cold Spring Harb Perspect Biol, 6*(5), a015982. doi:10.1101/cshperspect.a015982

Lane, N., & Martin, W. (2010). The energetics of genome complexity. *Nature, 467*(7318), 929-934. doi:10.1038/nature09486

Lanza, I. R., Befroy, D. E., & Kent-Braun, J. A. (2005). Age-related changes in ATP-producing pathways in human skeletal muscle in vivo. *J Appl Physiol (1985), 99*(5), 1736-1744. doi:10.1152/japplphysiol.00566.2005

Lapuente-Brun, E., Moreno-Loshuertos, R., Acin-Perez, R., Latorre-Pellicer, A., Colas, C., Balsa, E., . . . Enriquez, J. A. (2013). Supercomplex assembly determines electron flux in the mitochondrial electron transport chain. *Science, 340*(6140), 1567-1570. doi:10.1126/science.1230381

Latorre-Pellicer, A., Moreno-Loshuertos, R., Lechuga-Vieco, A. V., Sánchez-Cabo, F., Torroja, C., Acín-Pérez, R., . . . Enríquez, J. A. (2016). Mitochondrial and nuclear DNA matching shapes metabolism and healthy ageing. *Nature, advance online publication*. doi:10.1038/nature18618

http://www.nature.com/nature/journal/vaop/ncurrent/abs/nature18618.html#supplementary-information

Lazarou, M., Jin, S. M., Kane, L. A., & Youle, R. J. (2012). Role of PINK1 binding to the TOM complex and alternate intracellular membranes in recruitment and activation of the E3 ligase Parkin. *Dev Cell, 22*(2), 320-333. doi:10.1016/j.devcel.2011.12.014

Lazarou, M., Sliter, D. A., Kane, L. A., Sarraf, S. A., Wang, C., Burman, J. L., . . . Youle, R. J. (2015). The ubiquitin kinase PINK1 recruits autophagy receptors to induce mitophagy. *Nature, 524*(7565), 309-314. doi:10.1038/nature14893

Le Naour, F., Misek, D. E., Krause, M. C., Deneux, L., Giordano, T. J., Scholl, S., & Hanash, S. M. (2001). Proteomics-based identification of RS/DJ-1 as a novel circulating tumor antigen in breast cancer. *Clin Cancer Res, 7*(11), 3328-3335.

Lebensztejn, D. M., Flisiak-Jackiewicz, M., Bialokoz-Kalinowska, I., Bobrus-Chociej, A., & Kowalska, I. (2016). Hepatokines and non-alcoholic fatty liver disease. *Acta Biochim Pol*. doi:10.18388/abp.2016_1252

LeDoux, S. P., Wilson, G. L., Beecham, E. J., Stevnsner, T., Wassermann, K., & Bohr, V. A. (1992). Repair of mitochondrial DNA after various types of DNA damage in Chinese hamster ovary cells. *Carcinogenesis, 13*(11), 1967-1973.

Lee, C., Yen, K., & Cohen, P. (2013). Humanin: a harbinger of mitochondrial-derived peptides? *Trends Endocrinol Metab, 24*(5), 222-228. doi:10.1016/j.tem.2013.01.005

Lee, C., Zeng, J., Drew, B. G., Sallam, T., Martin-Montalvo, A., Wan, J., . . . Cohen, P. (2015). The mitochondrial-derived peptide MOTS-c promotes metabolic homeostasis and reduces obesity and insulin resistance. *Cell Metab, 21*(3), 443-454. doi:10.1016/j.cmet.2015.02.009

Lee, H.-C., Yin, P.-H., Chi, C.-W., & Wei, Y.-H. (2002). Increase in mitochondrial mass in human fibroblasts under oxidative stress and during replicative cell senescence. *Journal of Biomedical Science, 9*(6 Pt 1), 517-526.

Lee, H. C., Yin, P. H., Lu, C. Y., Chi, C. W., & Wei, Y. H. (2000). Increase of mitochondria and mitochondrial DNA in response to oxidative stress in human cells. *Biochemical Journal, 348 Pt 2*, 425-432.

Lee, I. H., & Finkel, T. (2013). Metabolic regulation of the cell cycle. *Curr Opin Cell Biol, 25*(6), 724-729. doi:10.1016/j.ceb.2013.07.002

Lee, S. Y., Jeon, H. M., Ju, M. K., Jeong, E. K., Kim, C. H., Yoo, M. A., . . . Kang, H. S. (2015). Dlx-2 is implicated in TGF-beta- and Wnt-induced epithelial-mesenchymal, glycolytic switch, and mitochondrial repression by Snail activation. *Int J Oncol, 46*(4), 1768-1780. doi:10.3892/ijo.2015.2874

Lee, W. J., Kim, M., Park, H.-S., Kim, H. S., Jeon, M. J., Oh, K. S., . . . Park, J.-Y. (2006). AMPK activation increases fatty acid oxidation in skeletal muscle by activating PPARα and PGC-1. *Biochemical and Biophysical Research Communications, 340*(1), 291-295. doi:http://dx.doi.org/10.1016/j.bbrc.2005.12.011

Lemasters, J. J. (2005). Selective mitochondrial autophagy, or mitophagy, as a targeted defense against oxidative stress, mitochondrial dysfunction, and aging. *Rejuvenation Res, 8*(1), 3-5. doi:10.1089/rej.2005.8.3

Lesmana, R., Sinha, R. A., Singh, B. K., Zhou, J., Ohba, K., Wu, Y., . . . Yen, P. M. (2016). Thyroid Hormone Stimulation of Autophagy Is Essential for Mitochondrial Biogenesis and Activity in Skeletal Muscle. *Endocrinology, 157*(1), 23-38. doi:10.1210/en.2015-1632

Leuner, K., Schutt, T., Kurz, C., Eckert, S. H., Schiller, C., Occhipinti, A., . . . Muller, W. E. (2012). Mitochondrion-derived reactive oxygen species lead to enhanced amyloid beta formation. *Antioxidants & Redox Signaling, 16*(12), 1421-1433. doi:10.1089/ars.2011.4173

Li, N., Frigerio, F., & Maechler, P. (2008). The sensitivity of pancreatic beta-cells to mitochondrial injuries triggered by lipotoxicity and oxidative stress. *Biochem Soc Trans, 36*(Pt 5), 930-934. doi:10.1042/bst0360930

Liao, C., Ashley, N., Diot, A., Morten, K., Phadwal, K., Williams, A., . . . Poulton, J. (2017). Dysregulated mitophagy and mitochondrial organization in optic atrophy due to OPA1 mutations. *Neurology, 88*(2), 131-142. doi:10.1212/wnl.0000000000003491

Liao, X., & Butow, R. A. (1993). RTG1 and RTG2: two yeast genes required for a novel path of communication from mitochondria to the nucleus. *Cell, 72*(1), 61-71.

Lim, C. Y., & Zoncu, R. (2016). The lysosome as a command-and-control center for cellular metabolism. *J Cell Biol, 214*(6), 653-664. doi:10.1083/jcb.201607005

Lim, J. M., Wollaston-Hayden, E. E., Teo, C. F., Hausman, D., & Wells, L. (2014). Quantitative secretome and glycome of primary human adipocytes during insulin resistance. *Clin Proteomics, 11*(1), 20. doi:10.1186/1559-0275-11-20

Lim, S. E., Longley, M. J., & Copeland, W. C. (1999). The mitochondrial p55 accessory subunit of human DNA polymerase gamma enhances DNA binding, promotes processive DNA synthesis, and confers N-ethylmaleimide resistance. *J Biol Chem, 274*(53), 38197-38203.

Lin, Y. F., Schulz, A. M., Pellegrino, M. W., Lu, Y., Shaham, S., & Haynes, C. M. (2016). Maintenance and propagation of a deleterious mitochondrial genome by the mitochondrial unfolded protein response. *Nature, 533*(7603), 416-419. doi:10.1038/nature17989

Liu, Z., Xu, J., He, J., Liu, H., Lin, P., Wan, X., . . . Yang, J. (2015). Mature adipocytes in bone marrow protect myeloma cells against chemotherapy through autophagy activation. *Oncotarget, 6*(33), 34329-34341. doi:10.18632/oncotarget.6020

Lo, M. C., Chen, M. H., Lee, W. S., Lu, C. I., Chang, C. R., Kao, S. H., & Lee, H. M. (2015). Nepsilon-(carboxymethyl) lysine-induced mitochondrial fission and mitophagy cause decreased insulin secretion from beta-cells. *Am J Physiol Endocrinol Metab, 309*(10), E829-839. doi:10.1152/ajpendo.00151.2015

Longley, M. J., Prasad, R., Srivastava, D. K., Wilson, S. H., & Copeland, W. C. (1998). Identification of 5'-deoxyribose phosphate lyase activity in human DNA polymerase gamma and its role in mitochondrial base excision repair in vitro. *Proc Natl Acad Sci U S A, 95*(21), 12244-12248.

Longley, M. J., Ropp, P. A., Lim, S. E., & Copeland, W. C. (1998). Characterization of the native and recombinant catalytic subunit of human DNA polymerase gamma: identification of residues critical for exonuclease activity and dideoxynucleotide sensitivity. *Biochemistry, 37*(29), 10529-10539. doi:10.1021/bi980772w

Lopez, L. C., Akman, H. O., Garcia-Cazorla, A., Dorado, B., Marti, R., Nishino, I., . . . Hirano, M. (2009). Unbalanced deoxynucleotide pools cause mitochondrial DNA instability in thymidine phosphorylase-deficient mice. *Hum Mol Genet, 18*(4), 714-722. doi:10.1093/hmg/ddn401

Lord, C., Ferro-Novick, S., & Miller, E. A. (2013). The highly conserved COPII coat complex sorts cargo from the endoplasmic reticulum and targets it to the golgi. *Cold Spring Harb Perspect Biol, 5*(2). doi:10.1101/cshperspect.a013367

Lorenzo, C., Okoloise, M., Williams, K., Stern, M. P., & Haffner, S. M. (2003). The metabolic syndrome as predictor of type 2 diabetes: the San Antonio heart study. *Diabetes Care, 26*(11), 3153-3159.

Lu, B., Lee, J., Nie, X., Li, M., Morozov, Y. I., Venkatesh, S., . . . Suzuki, C. K. (2013). Phosphorylation of human TFAM in mitochondria impairs DNA binding and promotes degradation by the AAA+ Lon protease. *Mol Cell, 49*(1), 121-132. doi:10.1016/j.molcel.2012.10.023

Lu, W., Chen, Z., Zhang, H., Wang, Y., Luo, Y., & Huang, P. (2012). ZNF143 transcription factor mediates cell survival through upregulation of the GPX1 activity in the mitochondrial respiratory dysfunction. *Cell Death & Disease, 3*, e422. doi:http://dx.doi.org/10.1038/cddis.2012.156

Luo, D. X., Huang, M. C., Ma, J., Gao, Z., Liao, D. F., & Cao, D. (2011). Aldo-keto reductase family 1, member B10 is secreted through a lysosome-mediated non-classical pathway. *Biochem J, 438*(1), 71-80. doi:10.1042/bj20110111

Lusis, A. J., Attie, A. D., & Reue, K. (2008). Metabolic syndrome: from epidemiology to systems biology. *Nat Rev Genet, 9*(11), 819-830. doi:10.1038/nrg2468

Macao, B., Uhler, J. P., Siibak, T., Zhu, X., Shi, Y., Sheng, W., . . . Falkenberg, M. (2015). The exonuclease activity of DNA polymerase gamma is required for ligation during mitochondrial DNA replication. *Nat Commun, 6*, 7303. doi:10.1038/ncomms8303

Maddalena, F., Sisinni, L., Lettini, G., Condelli, V., Matassa, D. S., Piscazzi, A., . . . Landriscina, M. (2013). Resistance to paclitxel in breast carcinoma cells requires a quality control of mitochondrial antiapoptotic proteins by TRAP1. *Mol Oncol, 7*(5), 895-906. doi:10.1016/j.molonc.2013.04.009

Magliarelli, H. F., Matondo, M., Meszaros, G., Goginashvili, A., Erbs, E., Zhang, Z., . . . Ricci, R. (2016). Liver ubiquitome uncovers nutrient-stress-mediated trafficking and secretion of complement C3. *Cell Death Dis, 7*(10), e2411. doi:10.1038/cddis.2016.312

Maita, C., Tsuji, S., Yabe, I., Hamada, S., Ogata, A., Maita, H., . . . Ariga, H. (2008). Secretion of DJ-1 into the serum of patients with Parkinson's disease. *Neurosci Lett, 431*(1), 86-89. doi:10.1016/j.neulet.2007.11.027

Manini, T. M., Patel, K. V., Bauer, D. C., Ziv, E., Schoeller, D. A., Mackey, D. C., . . . Harris, T. B. (2011). European ancestry and resting metabolic rate in older African Americans. *Eur J Clin Nutr, 65*(6), 663-667. doi:10.1038/ejcn.2011.22

Manjithaya, R., & Subramani, S. (2011). Autophagy: a broad role in unconventional protein secretion? *Trends Cell Biol, 21*(2), 67-73. doi:10.1016/j.tcb.2010.09.009

Mao, C., Kim, S. H., Almenoff, J. S., Rudner, X. L., Kearney, D. M., & Kindman, L. A. (1996). Molecular cloning and characterization of SCaMPER, a sphingolipid Ca2+ release-mediating protein from endoplasmic reticulum. *Proc Natl Acad Sci U S A, 93*(5), 1993-1996.

Marcelino, L. A., & Thilly, W. G. (1999). Mitochondrial mutagenesis in human cells and tissues. *Mutat Res, 434*(3), 177-203.

Marin-Garcia, J. (2016). Mitochondrial DNA repair: a novel therapeutic target for heart failure. *Heart Fail Rev, 21*(5), 475-487. doi:10.1007/s10741-016-9543-x

Marin, T. L., Gongol, B., Zhang, F., Martin, M., Johnson, D. A., Xiao, H., . . . Shyy, J. Y. (2017). AMPK promotes mitochondrial biogenesis and function by phosphorylating the epigenetic factors DNMT1, RBBP7, and HAT1. *Sci Signal, 10*(464). doi:10.1126/scisignal.aaf7478

Marques, I., Dencher, N. A., Videira, A., & Krause, F. (2007). Supramolecular organization of the respiratory chain in Neurospora crassa mitochondria. *Eukaryot Cell, 6*(12), 2391-2405. doi:10.1128/ec.00149-07

Marroquin, L. D., Hynes, J., Dykens, J. A., Jamieson, J. D., & Will, Y. (2007). Circumventing the Crabtree effect: replacing media glucose with galactose increases susceptibility of HepG2 cells to mitochondrial toxicants. *Toxicol Sci, 97*(2), 539-547. doi:10.1093/toxsci/kfm052

Martina, J. A., Diab, H. I., Lishu, L., Jeong, A. L., Patange, S., Raben, N., & Puertollano, R. (2014). The nutrient-responsive transcription factor TFE3 promotes autophagy, lysosomal biogenesis, and clearance of cellular debris. *Sci Signal, 7*(309), ra9. doi:10.1126/scisignal.2004754

Martinez-Reyes, I., Diebold, L. P., Kong, H., Schieber, M., Huang, H., Hensley, C. T., . . . Chandel, N. S. (2016). TCA Cycle and Mitochondrial Membrane Potential Are Necessary for Diverse Biological Functions. *Mol Cell, 61*(2), 199-209. doi:10.1016/j.molcel.2015.12.002

Martinus, R. D., Garth, G. P., Webster, T. L., Cartwright, P., Naylor, D. J., Hoj, P. B., & Hoogenraad, N. J. (1996). Selective induction of mitochondrial chaperones in response to loss of the mitochondrial genome. *Eur J Biochem, 240*(1), 98-103.

Marutani, T., Hattori, T., Tsutsumi, K., Koike, Y., Harada, A., Noguchi, K., . . . Mukai, H. (2015). Mitochondrial protein-derived cryptides: Are endogenous N-formylated peptides including mitocryptide-2 components of mitochondrial damage-associated molecular patterns? *Biopolymers*. doi:10.1002/bip.22788

Masters, J. M., Noyce, A. J., Warner, T. T., Giovannoni, G., & Proctor, G. B. (2015). Elevated salivary protein in Parkinson's disease and salivary DJ-1 as a potential marker of disease severity. *Parkinsonism Relat Disord, 21*(10), 1251-1255. doi:10.1016/j.parkreldis.2015.07.021

Matsuda, N., Sato, S., Shiba, K., Okatsu, K., Saisho, K., Gautier, C. A., . . . Tanaka, K. (2010). PINK1 stabilized by mitochondrial depolarization recruits Parkin to damaged mitochondria and activates latent Parkin for mitophagy. *J Cell Biol, 189*(2), 211-221. doi:10.1083/jcb.200910140

McKenzie, M., Chiotis, M., Pinkert, C. A., & Trounce, I. A. (2003). Functional respiratory chain analyses in murid xenomitochondrial cybrids expose coevolutionary constraints of cytochrome b and nuclear subunits of complex III. *Mol Biol Evol, 20*(7), 1117-1124. doi:10.1093/molbev/msg132

Meakin, P. J., Chowdhry, S., Sharma, R. S., Ashford, F. B., Walsh, S. V., McCrimmon, R. J., . . . Ashford, M. L. (2014). Susceptibility of Nrf2-null mice to steatohepatitis and cirrhosis upon consumption of a high-fat diet is associated with oxidative stress, perturbation of the unfolded protein response, and

disturbance in the expression of metabolic enzymes but not with insulin resistance. *Mol Cell Biol, 34*(17), 3305-3320. doi:10.1128/mcb.00677-14

Meex, R. C., Hoy, A. J., Morris, A., Brown, R. D., Lo, J. C., Burke, M., . . . Watt, M. J. (2015). Fetuin B Is a Secreted Hepatocyte Factor Linking Steatosis to Impaired Glucose Metabolism. *Cell Metab, 22*(6), 1078-1089. doi:10.1016/j.cmet.2015.09.023

Meiklejohn, C. D., Holmbeck, M. A., Siddiq, M. A., Abt, D. N., Rand, D. M., & Montooth, K. L. (2013). An Incompatibility between a mitochondrial tRNA and its nuclear-encoded tRNA synthetase compromises development and fitness in Drosophila. *PLoS Genet, 9*(1), e1003238. doi:10.1371/journal.pgen.1003238

Meissner, C., Lorenz, H., Weihofen, A., Selkoe, D. J., & Lemberg, M. K. (2011). The mitochondrial intramembrane protease PARL cleaves human Pink1 to regulate Pink1 trafficking. *J Neurochem, 117*(5), 856-867. doi:10.1111/j.1471-4159.2011.07253.x

Mena, N. P., Garcia-Beltran, O., Lourido, F., Urrutia, P. J., Mena, R., Castro-Castillo, V., . . . Nunez, M. T. (2015). The novel mitochondrial iron chelator 5-((methylamino)methyl)-8-hydroxyquinoline protects against mitochondrial-induced oxidative damage and neuronal death. *Biochem Biophys Res Commun, 463*(4), 787-792. doi:10.1016/j.bbrc.2015.06.014

Mercer, T. R., Neph, S., Dinger, M. E., Crawford, J., Smith, M. A., Shearwood, A. M., . . . Mattick, J. S. (2011). The human mitochondrial transcriptome. *Cell, 146*(4), 645-658. doi:10.1016/j.cell.2011.06.051

Meyer, J. N., Leung, M. C., Rooney, J. P., Sendoel, A., Hengartner, M. O., Kisby, G. E., & Bess, A. S. (2013). Mitochondria as a target of environmental toxicants. *Toxicol Sci, 134*(1), 1-17. doi:10.1093/toxsci/kft102

Michel, S., Canonne, M., Arnould, T., & Renard, P. (2015). Inhibition of mitochondrial genome expression triggers the activation of CHOP-10 by a cell signaling dependent on the integrated stress response but not the mitochondrial unfolded protein response. *Mitochondrion, 21*, 58-68. doi:10.1016/j.mito.2015.01.005

Miller, L. L., Bly, C. G., Watson, M. L., & Bale, W. F. (1951). The dominant role of the liver in plasma protein synthesis; a direct study of the isolated perfused rat liver with the aid of lysine-epsilon-C14. *J Exp Med, 94*(5), 431-453.

Mimaki, M., Wang, X., McKenzie, M., Thorburn, D. R., & Ryan, M. T. (2012). Understanding mitochondrial complex I assembly in health and disease. *Biochim Biophys Acta, 1817*(6), 851-862. doi:10.1016/j.bbabio.2011.08.010

Mishra, P., Varuzhanyan, G., Pham, A. H., & Chan, D. C. (2015). Mitochondrial Dynamics is a Distinguishing Feature of Skeletal Muscle Fiber Types and Regulates Organellar Compartmentalization. *Cell Metab, 22*(6), 1033-1044. doi:10.1016/j.cmet.2015.09.027

Mitchell, T., Johnson, M. S., Ouyang, X., Chacko, B. K., Mitra, K., Lei, X., . . . Darley-Usmar, V. M. (2013). Dysfunctional mitochondrial bioenergetics and oxidative stress in Akita+/Ins2-derived β-cells. *American Journal of Physiology - Endocrinology And Metabolism*. doi:10.1152/ajpendo.00093.2013

Mizuno, Y., Ohta, S., Tanaka, M., Takamiya, S., Suzuki, K., Sato, T., . . . Kagawa, Y. (1989). Deficiencies in complex I subunits of the respiratory chain in Parkinson's disease. *Biochem Biophys Res Commun, 163*(3), 1450-1455.

Modica-Napolitano, J. S., & Aprille, J. R. (2001). Delocalized lipophilic cations selectively target the mitochondria of carcinoma cells. *Adv Drug Deliv Rev, 49*(1-2), 63-70.

Mogilenko, D. A., Kudriavtsev, I. V., Shavva, V. S., Dizhe, E. B., Vilenskaya, E. G., Efremov, A. M., . . . Orlov, S. V. (2013). Peroxisome proliferator-activated receptor alpha positively regulates complement C3 expression but inhibits tumor necrosis factor alpha-mediated activation of C3 gene in mammalian hepatic-derived cells. *J Biol Chem, 288*(3), 1726-1738. doi:10.1074/jbc.M112.437525

Mohanty, A., & McBride, H. M. (2013). Emerging roles of mitochondria in the evolution, biogenesis, and function of peroxisomes. *Front Physiol, 4*, 268. doi:10.3389/fphys.2013.00268

Moisoi, N., Klupsch, K., Fedele, V., East, P., Sharma, S., Renton, A., . . . Martins, L. M. (2009). Mitochondrial dysfunction triggered by loss of HtrA2 results in the activation of a brain-specific transcriptional stress response. *Cell Death Differ, 16*(3), 449-464. doi:10.1038/cdd.2008.166

Moller, A. B., Vendelbo, M. H., Christensen, B., Clasen, B. F., Bak, A. M., Jorgensen, J. O., . . . Jessen, N. (2015). Physical exercise increases autophagic signaling through ULK1 in human skeletal muscle. *J Appl Physiol (1985), 118*(8), 971-979. doi:10.1152/japplphysiol.01116.2014

Montgomery, M. K., Fiveash, C. E., Braude, J. P., Osborne, B., Brown, S. H., Mitchell, T. W., & Turner, N. (2015). Disparate metabolic response to fructose feeding between different mouse strains. *Sci Rep, 5*, 18474. doi:10.1038/srep18474

Mony, V. K., Benjamin, S., & O'Rourke, E. J. (2016). A lysosome-centered view of nutrient homeostasis. *Autophagy, 12*(4), 619-631. doi:10.1080/15548627.2016.1147671

Mori, K., Emoto, M., Araki, T., Yokoyama, H., Lee, E., Teramura, M., . . . Nishizawa, Y. (2008). Effects of pioglitazone on serum fetuin-A levels in patients with type 2 diabetes mellitus. *Metabolism, 57*(9), 1248-1252. doi:10.1016/j.metabol.2008.04.019

Morita, A., Tanimoto, K., Murakami, T., Morinaga, T., & Hosoi, Y. (2014). Mitochondria are required for ATM activation by extranuclear oxidative stress in cultured human hepatoblastoma cell line Hep G2 cells. *Biochem Biophys Res Commun, 443*(4), 1286-1290. doi:10.1016/j.bbrc.2013.12.139

Morlino, G., Barreiro, O., Baixauli, F., Robles-Valero, J., Gonzalez-Granado, J. M., Villa-Bellosta, R., . . . Sanchez-Madrid, F. (2014). Miro-1 links mitochondria and microtubule Dynein motors to control lymphocyte migration and polarity. *Mol Cell Biol, 34*(8), 1412-1426. doi:10.1128/mcb.01177-13

Moullan, N., Mouchiroud, L., Wang, X., Ryu, D., Williams, E. G., Mottis, A., . . . Auwerx, J. (2015). Tetracyclines Disturb Mitochondrial Function across Eukaryotic Models: A Call for Caution in Biomedical Research. *Cell Rep*. doi:10.1016/j.celrep.2015.02.034

Mourier, A., Matic, S., Ruzzenente, B., Larsson, N. G., & Milenkovic, D. (2014). The respiratory chain supercomplex organization is independent of COX7a2l isoforms. *Cell Metab, 20*(6), 1069-1075. doi:10.1016/j.cmet.2014.11.005

Mukai, H., Hokari, Y., Seki, T., Takao, T., Kubota, M., Matsuo, Y., . . . Munekata, E. (2008). Discovery of mitocryptide-1, a neutrophil-activating cryptide from healthy porcine heart. *J Biol Chem, 283*(45), 30596-30605. doi:10.1074/jbc.M803913200

Mukai, H., Seki, T., Nakano, H., Hokari, Y., Takao, T., Kawanami, M., . . . Munekata, E. (2009). Mitocryptide-2: purification, identification, and characterization of a novel cryptide that activates neutrophils. *J Immunol, 182*(8), 5072-5080. doi:10.4049/jimmunol.0802965

Murphy, M. P. (2009). How mitochondria produce reactive oxygen species. *Biochem J, 417*(1), 1-13. doi:10.1042/bj20081386

Nakamura, M., Ohsawa, S., & Igaki, T. (2014). Mitochondrial defects trigger proliferation of neighbouring cells via a senescence-associated secretory phenotype in Drosophila. *Nat Commun, 5*, 5264. doi:10.1038/ncomms6264

Nakata, K., Saitoh, R., Amano, J., Ichibangase, T., Ishigai, M., & Imai, K. (2014). Comprehensive and temporal analysis of secreted proteins in the medium from IL-6 exposed human hepatocyte. *Biomed Chromatogr, 28*(6), 742-750. doi:10.1002/bmc.3103

Namioka, N., Hanyu, H., Hirose, D., Hatanaka, H., Sato, T., & Shimizu, S. (2016). Oxidative stress and inflammation are associated with physical frailty in patients with Alzheimer's disease. *Geriatr Gerontol Int*. doi:10.1111/ggi.12804

Narendra, D. P., Jin, S. M., Tanaka, A., Suen, D. F., Gautier, C. A., Shen, J., . . . Youle, R. J. (2010). PINK1 is selectively stabilized on impaired mitochondria to activate Parkin. *PLoS Biol, 8*(1), e1000298. doi:10.1371/journal.pbio.1000298

Nargund, A. M., Fiorese, C. J., Pellegrino, M. W., Deng, P., & Haynes, C. M. (2015). Mitochondrial and nuclear accumulation of the transcription factor ATFS-1 promotes OXPHOS recovery during the UPR(mt). *Mol Cell, 58*(1), 123-133. doi:10.1016/j.molcel.2015.02.008

Nargund, A. M., Pellegrino, M. W., Fiorese, C. J., Baker, B. M., & Haynes, C. M. (2012). Mitochondrial import efficiency of ATFS-1 regulates mitochondrial UPR activation. *Science, 337*(6094), 587-590. doi:http://dx.doi.org/10.1126/science.1223560

Nemoto, S., Fergusson, M. M., & Finkel, T. (2005). SIRT1 functionally interacts with the metabolic regulator and transcriptional coactivator PGC-1{alpha}. *J Biol Chem, 280*(16), 16456-16460. doi:10.1074/jbc.M501485200

Ngo, H. B., Kaiser, J. T., & Chan, D. C. (2011). The mitochondrial transcription and packaging factor Tfam imposes a U-turn on mitochondrial DNA. *Nat Struct Mol Biol, 18*(11), 1290-1296. doi:10.1038/nsmb.2159

Nguyen, T., Nioi, P., & Pickett, C. B. (2009). The Nrf2-antioxidant response element signaling pathway and its activation by oxidative stress. *Journal of Biological Chemistry, 284*(20), 13291-13295. doi:http://dx.doi.org/10.1074/jbc.R900010200

Nichols, B. J., & Denton, R. M. (1995). Towards the molecular basis for the regulation of mitochondrial dehydrogenases by calcium ions. *Mol Cell Biochem, 149-150*, 203-212.

Nickel, W. (2003). The mystery of nonclassical protein secretion. A current view on cargo proteins and potential export routes. *Eur J Biochem, 270*(10), 2109-2119.

Nilsson, P., & Saido, T. C. (2014). Dual roles for autophagy: degradation and secretion of Alzheimer's disease Abeta peptide. *Bioessays, 36*(6), 570-578. doi:10.1002/bies.201400002

Oakhill, J. S., Steel, R., Chen, Z. P., Scott, J. W., Ling, N., Tam, S., & Kemp, B. E. (2011). AMPK is a direct adenylate charge-regulated protein kinase. *Science, 332*(6036), 1433-1435. doi:10.1126/science.1200094

Oda, M., Makita, M., Iwaya, K., Akiyama, F., Kohno, N., Tsuchiya, B., . . . Matsubara, O. (2012). High levels of DJ-1 protein in nipple fluid of patients with breast cancer. *Cancer Sci, 103*(6), 1172-1176. doi:10.1111/j.1349-7006.2012.02267.x

Oh, K. J., Lee, D. S., Kim, W. K., Han, B. S., Lee, S. C., & Bae, K. H. (2016). Metabolic Adaptation in Obesity and Type II Diabetes: Myokines, Adipokines and Hepatokines. *Int J Mol Sci, 18*(1). doi:10.3390/ijms18010008

Ojala, D., Montoya, J., & Attardi, G. (1981). tRNA punctuation model of RNA processing in human mitochondria. *Nature, 290*(5806), 470-474.

Osborne, B., Cooney, G. J., & Turner, N. (2014). Are sirtuin deacylase enzymes important modulators of mitochondrial energy metabolism? *Biochim Biophys Acta, 1840*(4), 1295-1302. doi:10.1016/j.bbagen.2013.08.016

Ost, M., Keipert, S., van Schothorst, E. M., Donner, V., van der Stelt, I., Kipp, A. P., . . . Klaus, S. (2015). Muscle mitohormesis promotes cellular survival via serine/glycine pathway flux. *FASEB J, 29*(4), 1314-1328. doi:10.1096/fj.14-261503

Otera, H., Ishihara, N., & Mihara, K. (2013). New insights into the function and regulation of mitochondrial fission. *Biochim Biophys Acta, 1833*(5), 1256-1268. doi:10.1016/j.bbamcr.2013.02.002

Owusu-Ansah, E., Song, W., & Perrimon, N. (2013). Muscle mitohormesis promotes longevity via systemic repression of insulin signaling. *Cell, 155*(3), 699-712. doi:10.1016/j.cell.2013.09.021

Pal, D., Dasgupta, S., Kundu, R., Maitra, S., Das, G., Mukhopadhyay, S., . . . Bhattacharya, S. (2012). Fetuin-A acts as an endogenous ligand of TLR4 to promote lipid-induced insulin resistance. *Nat Med, 18*(8), 1279-1285. doi:10.1038/nm.2851

Palade, G. E. (1953). An electron microscope study of the mitochondrial structure. *J Histochem Cytochem, 1*(4), 188-211.

Palmer, C. S., Osellame, L. D., Stojanovski, D., & Ryan, M. T. (2011). The regulation of mitochondrial morphology: intricate mechanisms and dynamic machinery. *Cell Signal, 23*(10), 1534-1545. doi:10.1016/j.cellsig.2011.05.021

Palmieri, F., Rieder, B., Ventrella, A., Blanco, E., Do, P. T., Nunes-Nesi, A., . . . Neuhaus, H. E. (2009). Molecular identification and functional characterization

of Arabidopsis thaliana mitochondrial and chloroplastic NAD+ carrier proteins. *J Biol Chem, 284*(45), 31249-31259. doi:10.1074/jbc.M109.041830

Pandey, P., Sliker, B., Peters, H. L., Tuli, A., Herskovitz, J., Smits, K., . . . Solheim, J. C. (2016). Amyloid precursor protein and amyloid precursor-like protein 2 in cancer. *Oncotarget, 7*(15), 19430-19444. doi:10.18632/oncotarget.7103

Pardini, R. S., Heidker, J. C., Baker, T. A., & Payne, B. (1980). Toxicology of various pesticides and their decomposition products on mitochondrial electron transport. *Arch Environ Contam Toxicol, 9*(1), 87-97.

Pardo, M., Garcia, A., Thomas, B., Pineiro, A., Akoulitchev, A., Dwek, R. A., & Zitzmann, N. (2006). The characterization of the invasion phenotype of uveal melanoma tumour cells shows the presence of MUC18 and HMG-1 metastasis markers and leads to the identification of DJ-1 as a potential serum biomarker. *Int J Cancer, 119*(5), 1014-1022. doi:10.1002/ijc.21942

Pavlova, N. N., & Thompson, C. B. (2016). The Emerging Hallmarks of Cancer Metabolism. *Cell Metab, 23*(1), 27-47. doi:10.1016/j.cmet.2015.12.006

Pelicano, H., Xu, R. H., Du, M., Feng, L., Sasaki, R., Carew, J. S., . . . Huang, P. (2006). Mitochondrial respiration defects in cancer cells cause activation of Akt survival pathway through a redox-mediated mechanism. *J Cell Biol, 175*(6), 913-923. doi:10.1083/jcb.200512100

Pellegrini, M., Asin-Cayuela, J., Erdjument-Bromage, H., Tempst, P., Larsson, N. G., & Gustafsson, C. M. (2009). MTERF2 is a nucleoid component in mammalian mitochondria. *Biochim Biophys Acta, 1787*(5), 296-302. doi:10.1016/j.bbabio.2009.01.018

Pereira, G. C., Silva, A. M., Diogo, C. V., Carvalho, F. S., Monteiro, P., & Oliveira, P. J. (2011). Drug-induced cardiac mitochondrial toxicity and protection: from doxorubicin to carvedilol. *Curr Pharm Des, 17*(20), 2113-2129.

Perez-Pinzon, M. A., Dave, K. R., & Raval, A. P. (2005). Role of reactive oxygen species and protein kinase C in ischemic tolerance in the brain. *Antioxidants & Redox Signaling, 7*(9-10), 1150-1157.

Pernas, L., & Scorrano, L. (2016). Mito-Morphosis: Mitochondrial Fusion, Fission, and Cristae Remodeling as Key Mediators of Cellular Function. *Annu Rev Physiol, 78*, 505-531. doi:10.1146/annurev-physiol-021115-105011

Pettepher, C. C., LeDoux, S. P., Bohr, V. A., & Wilson, G. L. (1991). Repair of alkali-labile sites within the mitochondrial DNA of RINr 38 cells after exposure to the nitrosourea streptozotocin. *J Biol Chem, 266*(5), 3113-3117.

Pharaoh, G., Pulliam, D., Hill, S., Sataranatarajan, K., & Van Remmen, H. (2016). Ablation of the mitochondrial complex IV assembly protein Surf1 leads to increased expression of the UPR(MT) and increased resistance to oxidative stress in primary cultures of fibroblasts. *Redox Biol, 8*, 430-438. doi:10.1016/j.redox.2016.05.001

Phark, S., Park, S. Y., Choi, S., Zheng, Z., Cho, E., Lee, M., . . . Sul, D. (2012). Toxicological biomarkers of 2,3,4,7,8-pentachlorodibenzofuran in proteins secreted by HepG2 cells. *Biochim Biophys Acta, 1824*(4), 656-666. doi:10.1016/j.bbapap.2012.01.013

Phieler, J., Garcia-Martin, R., Lambris, J. D., & Chavakis, T. (2013). The role of the complement system in metabolic organs and metabolic diseases. *Semin Immunol, 25*(1), 47-53. doi:10.1016/j.smim.2013.04.003

Piantadosi, C. A., & Suliman, H. B. (2006). Mitochondrial transcription factor A induction by redox activation of nuclear respiratory factor 1. *Journal of Biological Chemistry, 281*(1), 324-333.

Picard, M., Ritchie, D., Thomas, M. M., Wright, K. J., & Hepple, R. T. (2011). Alterations in intrinsic mitochondrial function with aging are fiber type-specific and do not explain differential atrophy between muscles. *Aging Cell, 10*(6), 1047-1055. doi:10.1111/j.1474-9726.2011.00745.x

Pinto, M., & Moraes, C. T. (2015). Mechanisms linking mtDNA damage and aging. *Free Radic Biol Med, 85*, 250-258. doi:10.1016/j.freeradbiomed.2015.05.005

Pirinen, E., Canto, C., Jo, Y. S., Morato, L., Zhang, H., Menzies, K. J., . . . Auwerx, J. (2014). Pharmacological Inhibition of poly(ADP-ribose) polymerases improves fitness and mitochondrial function in skeletal muscle. *Cell Metab, 19*(6), 1034-1041. doi:10.1016/j.cmet.2014.04.002

Pittelli, M., Formentini, L., Faraco, G., Lapucci, A., Rapizzi, E., Cialdai, F., . . . Chiarugi, A. (2010). Inhibition of nicotinamide phosphoribosyltransferase: cellular bioenergetics reveals a mitochondrial insensitive NAD pool. *J Biol Chem, 285*(44), 34106-34114. doi:10.1074/jbc.M110.136739

Ponpuak, M., Mandell, M. A., Kimura, T., Chauhan, S., Cleyrat, C., & Deretic, V. (2015). Secretory autophagy. *Curr Opin Cell Biol, 35*, 106-116. doi:10.1016/j.ceb.2015.04.016

Pontoglio, M. (2000). Hepatocyte nuclear factor 1, a transcription factor at the crossroads of glucose homeostasis. *J Am Soc Nephrol, 11 Suppl 16*, S140-143.

Pontoglio, M., Pausa, M., Doyen, A., Viollet, B., Yaniv, M., & Tedesco, F. (2001). Hepatocyte nuclear factor 1alpha controls the expression of terminal complement genes. *J Exp Med, 194*(11), 1683-1689.

Prigione, A., Begni, B., Galbussera, A., Beretta, S., Brighina, L., Garofalo, R., . . . Ferrarese, C. (2006). Oxidative stress in peripheral blood mononuclear cells from patients with Parkinson's disease: negative correlation with levodopa dosage. *Neurobiol Dis, 23*(1), 36-43. doi:10.1016/j.nbd.2006.01.013

Qin, X., & Gao, B. (2006). The complement system in liver diseases. *Cell Mol Immunol, 3*(5), 333-340.

Quinlan, C. L., Goncalves, R. L., Hey-Mogensen, M., Yadava, N., Bunik, V. I., & Brand, M. D. (2014). The 2-oxoacid dehydrogenase complexes in mitochondria can produce superoxide/hydrogen peroxide at much higher rates than complex I. *J Biol Chem, 289*(12), 8312-8325. doi:10.1074/jbc.M113.545301

Quinlan, C. L., Orr, A. L., Perevoshchikova, I. V., Treberg, J. R., Ackrell, B. A., & Brand, M. D. (2012). Mitochondrial complex II can generate reactive oxygen species at high rates in both the forward and reverse reactions. *J Biol Chem, 287*(32), 27255-27264. doi:10.1074/jbc.M112.374629

Quiros, P. M., Mottis, A., & Auwerx, J. (2016). Mitonuclear communication in homeostasis and stress. *Nat Rev Mol Cell Biol, 17*(4), 213-226. doi:10.1038/nrm.2016.23

Rabouille, C. (2016). Pathways of Unconventional Protein Secretion. *Trends Cell Biol*. doi:10.1016/j.tcb.2016.11.007

Rackham, O., Shearwood, A. M., Mercer, T. R., Davies, S. M., Mattick, J. S., & Filipovska, A. (2011). Long noncoding RNAs are generated from the mitochondrial genome and regulated by nuclear-encoded proteins. *RNA, 17*(12), 2085-2093. doi:10.1261/rna.029405.111

Radak, Z., Atalay, M., Jakus, J., Boldogh, I., Davies, K., & Goto, S. (2009). Exercise improves import of 8-oxoguanine DNA glycosylase into the mitochondrial matrix of skeletal muscle and enhances the relative activity. *Free Radical Biology & Medicine, 46*(2), 238-243. doi:http://dx.doi.org/10.1016/j.freeradbiomed.2008.10.022

Raichle, M. E., & Gusnard, D. A. (2002). Appraising the brain's energy budget. *Proc Natl Acad Sci U S A, 99*(16), 10237-10239. doi:10.1073/pnas.172399499

Raimundo, N., Fernandez-Mosquera, L., Yambire, K. F., & Diogo, C. V. (2016). Mechanisms of communication between mitochondria and lysosomes. *Int J Biochem Cell Biol, 79*, 345-349. doi:10.1016/j.biocel.2016.08.020

Rasmussen, U. F., Krustrup, P., Kjaer, M., & Rasmussen, H. N. (2003). Human skeletal muscle mitochondrial metabolism in youth and senescence: no signs of functional changes in ATP formation and mitochondrial oxidative capacity. *Pflugers Arch, 446*(2), 270-278. doi:10.1007/s00424-003-1022-2

Raukas, M., Rebane, R., Mahlapuu, R., Jefremov, V., Zilmer, K., Karelson, E., . . . Zilmer, M. (2012). Mitochondrial oxidative stress index, activity of redox-sensitive aconitase and effects of endogenous anti- and pro-oxidants on its activity in control, Alzheimer's disease and Swedish Familial Alzheimer's disease brain. *Free Radic Res, 46*(12), 1490-1495. doi:10.3109/10715762.2012.728286

Reifschneider, N. H., Goto, S., Nakamoto, H., Takahashi, R., Sugawa, M., Dencher, N. A., & Krause, F. (2006). Defining the mitochondrial proteomes from five rat organs in a physiologically significant context using 2D blue-native/SDS-PAGE. *J Proteome Res, 5*(5), 1117-1132. doi:10.1021/pr0504440

Renes, J., Rosenow, A., Roumans, N., Noben, J. P., & Mariman, E. C. (2014). Calorie restriction-induced changes in the secretome of human adipocytes, comparison with resveratrol-induced secretome effects. *Biochim Biophys Acta, 1844*(9), 1511-1522. doi:10.1016/j.bbapap.2014.04.023

Richter, C., Park, J. W., & Ames, B. N. (1988). Normal oxidative damage to mitochondrial and nuclear DNA is extensive. *Proc Natl Acad Sci U S A, 85*(17), 6465-6467.

Riedl, S. J., & Salvesen, G. S. (2007). The apoptosome: signalling platform of cell death. *Nat Rev Mol Cell Biol, 8*(5), 405-413. doi:10.1038/nrm2153

Riis, S., Stensballe, A., Emmersen, J., Pennisi, C. P., Birkelund, S., Zachar, V., & Fink, T. (2016). Mass spectrometry analysis of adipose-derived stem cells reveals a

significant effect of hypoxia on pathways regulating extracellular matrix. *Stem Cell Res Ther, 7*(1), 52. doi:10.1186/s13287-016-0310-7

Ristow, M., & Schmeisser, K. (2014). Mitohormesis: Promoting Health and Lifespan by Increased Levels of Reactive Oxygen Species (ROS). *Dose Response, 12*(2), 288-341. doi:10.2203/dose-response.13-035.Ristow

Ristow, M., & Zarse, K. (2010). How increased oxidative stress promotes longevity and metabolic health: The concept of mitochondrial hormesis (mitohormesis). *Exp Gerontol, 45*(6), 410-418. doi:10.1016/j.exger.2010.03.014

Ristow, M., Zarse, K., Oberbach, A., Kloting, N., Birringer, M., Kiehntopf, M., . . . Bluher, M. (2009). Antioxidants prevent health-promoting effects of physical exercise in humans. *Proc Natl Acad Sci U S A, 106*(21), 8665-8670. doi:10.1073/pnas.0903485106

Rizzuto, R., De Stefani, D., Raffaello, A., & Mammucari, C. (2012). Mitochondria as sensors and regulators of calcium signalling. *Nat Rev Mol Cell Biol, 13*(9), 566-578. doi:10.1038/nrm3412

Ro, S. H., Semple, I., Ho, A., Park, H. W., & Lee, J. H. (2015). Sestrin2, a Regulator of Thermogenesis and Mitohormesis in Brown Adipose Tissue. *Front Endocrinol (Lausanne), 6*, 114. doi:10.3389/fendo.2015.00114

Robberson, D. L., Kasamatsu, H., & Vinograd, J. (1972). Replication of mitochondrial DNA. Circular replicative intermediates in mouse L cells. *Proc Natl Acad Sci U S A, 69*(3), 737-741.

Robey, R. B., & Hay, N. (2009). Is Akt the "Warburg kinase"?-Akt-energy metabolism interactions and oncogenesis. *Semin Cancer Biol, 19*(1), 25-31. doi:10.1016/j.semcancer.2008.11.010

Robinson, M. W., Harmon, C., & O'Farrelly, C. (2016). Liver immunology and its role in inflammation and homeostasis. *Cell Mol Immunol, 13*(3), 267-276. doi:10.1038/cmi.2016.3

Robson-Doucette, C. A., Sultan, S., Allister, E. M., Wikstrom, J. D., Koshkin, V., Bhattacharjee, A., . . . Wheeler, M. B. (2011). Beta-cell uncoupling protein 2 regulates reactive oxygen species production, which influences both insulin and glucagon secretion. *Diabetes, 60*(11), 2710-2719. doi:10.2337/db11-0132

Rodriguez-Pena, A., Escriva, H., Handler, A. C., & Vallejo, C. G. (2002). Thyroid hormone increases transcription of GA-binding protein/nuclear respiratory factor-2 alpha-subunit in rat liver. *FEBS Lett, 514*(2-3), 309-314.

Rolfe, D. F., & Brown, G. C. (1997). Cellular energy utilization and molecular origin of standard metabolic rate in mammals. *Physiol Rev, 77*(3), 731-758.

Ronquist, K. G., Ek, B., Morrell, J., Stavreus-Evers, A., Strom Holst, B., Humblot, P., . . . Larsson, A. (2013). Prostasomes from four different species are able to produce extracellular adenosine triphosphate (ATP). *Biochim Biophys Acta, 1830*(10), 4604-4610. doi:10.1016/j.bbagen.2013.05.019

Ronquist, K. G., Ek, B., Stavreus-Evers, A., Larsson, A., & Ronquist, G. (2013). Human prostasomes express glycolytic enzymes with capacity for ATP

production. *Am J Physiol Endocrinol Metab, 304*(6), E576-582. doi:10.1152/ajpendo.00511.2012

Rose, G., Santoro, A., & Salvioli, S. (2016). Mitochondria and mitochondria-induced signalling molecules as longevity determinants. *Mech Ageing Dev*. doi:10.1016/j.mad.2016.12.002

Rosenow, A., Noben, J. P., Bouwman, F. G., Mariman, E. C., & Renes, J. (2013). Hypoxia-mimetic effects in the secretome of human preadipocytes and adipocytes. *Biochim Biophys Acta, 1834*(12), 2761-2771. doi:10.1016/j.bbapap.2013.10.003

Ross, J. M., Stewart, J. B., Hagstrom, E., Brene, S., Mourier, A., Coppotelli, G., . . . Larsson, N. G. (2013). Germline mitochondrial DNA mutations aggravate ageing and can impair brain development. *Nature, 501*(7467), 412-415. doi:10.1038/nature12474

Rossi, M. N., Carbone, M., Mostocotto, C., Mancone, C., Tripodi, M., Maione, R., & Amati, P. (2009). Mitochondrial localization of PARP-1 requires interaction with mitofilin and is involved in the maintenance of mitochondrial DNA integrity. *J Biol Chem, 284*(46), 31616-31624. doi:10.1074/jbc.M109.025882

Rothfuss, O., Gasser, T., & Patenge, N. (2010). Analysis of differential DNA damage in the mitochondrial genome employing a semi-long run real-time PCR approach. *Nucleic Acids Res, 38*(4), e24. doi:10.1093/nar/gkp1082

Roy, M., Kageyama, Y., Iijima, M., & Sesaki, H. (2015). PARK2/Parkin becomes critical when DNM1L/Drp1 is absent. *Autophagy, 11*(3), 573-574. doi:10.1080/15548627.2015.1017193

Royo, F., Moreno, L., Mleczko, J., Palomo, L., Gonzalez, E., Cabrera, D., . . . Falcon-Perez, J. M. (2017). Hepatocyte-secreted extracellular vesicles modify blood metabolome and endothelial function by an arginase-dependent mechanism. *Sci Rep, 7*, 42798. doi:10.1038/srep42798

Royo, F., Palomo, L., Mleczko, J., Gonzalez, E., Alonso, C., Martinez, I., . . . Falcon-Perez, J. M. (2016). Metabolically active extracellular vesicles released from hepatocytes under drug-induced liver-damaging conditions modify serum metabolome and might affect different pathophysiological processes. *Eur J Pharm Sci*. doi:10.1016/j.ejps.2016.10.020

Rusinol, A. E., Cui, Z., Chen, M. H., & Vance, J. E. (1994). A unique mitochondria-associated membrane fraction from rat liver has a high capacity for lipid synthesis and contains pre-Golgi secretory proteins including nascent lipoproteins. *J Biol Chem, 269*(44), 27494-27502.

Ryu, D., Jo, Y. S., Lo Sasso, G., Stein, S., Zhang, H., Perino, A., . . . Auwerx, J. (2014). A SIRT7-dependent acetylation switch of GABPbeta1 controls mitochondrial function. *Cell Metab, 20*(5), 856-869. doi:10.1016/j.cmet.2014.08.001

Sabbah, H. N. (2016). Targeting mitochondrial dysfunction in the treatment of heart failure. *Expert Rev Cardiovasc Ther, 14*(12), 1305-1313. doi:10.1080/14779072.2016.1249466

Sakai, K., Matsumoto, K., Nishikawa, T., Suefuji, M., Nakamaru, K., Hirashima, Y., . . . Araki, E. (2003). Mitochondrial reactive oxygen species reduce insulin secretion by pancreatic beta-cells. *Biochem Biophys Res Commun, 300*(1), 216-222.

Sanchez, M. I., Mercer, T. R., Davies, S. M., Shearwood, A. M., Nygard, K. K., Richman, T. R., . . . Filipovska, A. (2011). RNA processing in human mitochondria. *Cell Cycle, 10*(17), 2904-2916. doi:10.4161/cc.10.17.17060

Sanders, L. H., & Greenamyre, J. T. (2013). Oxidative damage to macromolecules in human Parkinson disease and the rotenone model. *Free Radic Biol Med, 62*, 111-120. doi:10.1016/j.freeradbiomed.2013.01.003

Santo-Domingo, J., & Demaurex, N. (2012). Perspectives on: SGP symposium on mitochondrial physiology and medicine: the renaissance of mitochondrial pH. *J Gen Physiol, 139*(6), 415-423. doi:10.1085/jgp.201110767

Sarma, J. V., & Ward, P. A. (2011). The complement system. *Cell Tissue Res, 343*(1), 227-235. doi:10.1007/s00441-010-1034-0

Sarzi, E., Angebault, C., Seveno, M., Gueguen, N., Chaix, B., Bielicki, G., . . . Lenaers, G. (2012). The human OPA1delTTAG mutation induces premature age-related systemic neurodegeneration in mouse. *Brain, 135*(Pt 12), 3599-3613. doi:10.1093/brain/aws303

Schafer, E., Dencher, N. A., Vonck, J., & Parcej, D. N. (2007). Three-dimensional structure of the respiratory chain supercomplex I1III2IV1 from bovine heart mitochondria. *Biochemistry, 46*(44), 12579-12585. doi:10.1021/bi700983h

Schapira, A. H., Cooper, J. M., Dexter, D., Clark, J. B., Jenner, P., & Marsden, C. D. (1990). Mitochondrial complex I deficiency in Parkinson's disease. *J Neurochem, 54*(3), 823-827.

Scherz-Shouval, R., Shvets, E., Fass, E., Shorer, H., Gil, L., & Elazar, Z. (2007). Reactive oxygen species are essential for autophagy and specifically regulate the activity of Atg4. *EMBO Journal, 26*(7), 1749-1760.

Schieber, M., & Chandel, N. S. (2014). ROS function in redox signaling and oxidative stress. *Curr Biol, 24*(10), R453-462. doi:10.1016/j.cub.2014.03.034

Schmeisser, S., Priebe, S., Groth, M., Monajembashi, S., Hemmerich, P., Guthke, R., . . . Ristow, M. (2013). Neuronal ROS signaling rather than AMPK/sirtuin-mediated energy sensing links dietary restriction to lifespan extension. *Mol Metab, 2*(2), 92-102. doi:10.1016/j.molmet.2013.02.002

Schmeisser, S., Schmeisser, K., Weimer, S., Groth, M., Priebe, S., Fazius, E., . . . Ristow, M. (2013). Mitochondrial hormesis links low-dose arsenite exposure to lifespan extension. *Aging Cell, 12*(3), 508-517. doi:10.1111/acel.12076

Schmeisser, S., Zarse, K., & Ristow, M. (2011). Lonidamine extends lifespan of adult Caenorhabditis elegans by increasing the formation of mitochondrial reactive oxygen species. *Horm Metab Res, 43*(10), 687-692. doi:10.1055/s-0031-1286308

Schmidt, O., Pfanner, N., & Meisinger, C. (2010). Mitochondrial protein import: from proteomics to functional mechanisms. *Nat Rev Mol Cell Biol, 11*(9), 655-667. doi:10.1038/nrm2959

Schreiber, S. N., Emter, R., Hock, M. B., Knutti, D., Cardenas, J., Podvinec, M., . . . Kralli, A. (2004). The estrogen-related receptor alpha (ERRalpha) functions in PPARgamma coactivator 1alpha (PGC-1alpha)-induced mitochondrial biogenesis. *Proc Natl Acad Sci U S A, 101*(17), 6472-6477. doi:10.1073/pnas.0308686101

Schulz, T. J., Zarse, K., Voigt, A., Urban, N., Birringer, M., & Ristow, M. (2007). Glucose restriction extends Caenorhabditis elegans life span by inducing mitochondrial respiration and increasing oxidative stress. *Cell Metab, 6*(4), 280-293. doi:10.1016/j.cmet.2007.08.011

Searcy, D. G. (2003). Metabolic integration during the evolutionary origin of mitochondria. *Cell Res, 13*(4), 229-238. doi:10.1038/sj.cr.7290168

Seillier, M., Pouyet, L., N'Guessan, P., Nollet, M., Capo, F., Guillaumond, F., . . . Carrier, A. (2015). Defects in mitophagy promote redox-driven metabolic syndrome in the absence of TP53INP1. *EMBO Mol Med, 7*(6), 802-818. doi:10.15252/emmm.201404318

Seki, T., Fukamizu, A., Kiso, Y., & Mukai, H. (2011). Mitocryptide-2, a neutrophil-activating cryptide, is a specific endogenous agonist for formyl-peptide receptor-like 1. *Biochem Biophys Res Commun, 404*(1), 482-487. doi:10.1016/j.bbrc.2010.12.007

Selak, M. A., Duran, R. V., & Gottlieb, E. (2006). Redox stress is not essential for the pseudo-hypoxic phenotype of succinate dehydrogenase deficient cells. *Biochim Biophys Acta, 1757*(5-6), 567-572. doi:10.1016/j.bbabio.2006.05.015

Settembre, C., Fraldi, A., Medina, D. L., & Ballabio, A. (2013). Signals from the lysosome: a control centre for cellular clearance and energy metabolism. *Nat Rev Mol Cell Biol, 14*(5), 283-296. doi:10.1038/nrm3565

Seyfarth, K., Poschmann, G., Rozman, J., Fromme, T., Rink, N., Hofmann, A., . . . Klingenspor, M. (2015). The development of diet-induced obesity and associated metabolic impairments in Dj-1 deficient mice. *J Nutr Biochem, 26*(1), 75-81. doi:10.1016/j.jnutbio.2014.09.002

Shao, L. W., Niu, R., & Liu, Y. (2016). Neuropeptide signals cell non-autonomous mitochondrial unfolded protein response. *Cell Res, 26*(11), 1182-1196. doi:10.1038/cr.2016.118

Shi, S. Y., Lu, S. Y., Sivasubramaniyam, T., Revelo, X. S., Cai, E. P., Luk, C. T., . . . Woo, M. (2015). DJ-1 links muscle ROS production with metabolic reprogramming and systemic energy homeostasis in mice. *Nat Commun, 6*, 7415. doi:10.1038/ncomms8415

Shi, X., Burkart, A., Nicoloro, S. M., Czech, M. P., Straubhaar, J., & Corvera, S. (2008). Paradoxical effect of mitochondrial respiratory chain impairment on insulin signaling and glucose transport in adipose cells. *J Biol Chem, 283*(45), 30658-30667. doi:10.1074/jbc.M800510200

Shiba-Fukushima, K., Imai, Y., Yoshida, S., Ishihama, Y., Kanao, T., Sato, S., & Hattori, N. (2012). PINK1-mediated phosphorylation of the Parkin ubiquitin-like domain primes mitochondrial translocation of Parkin and regulates mitophagy. *Sci Rep, 2*, 1002. doi:10.1038/srep01002

Shibata, Y., & Morimoto, R. I. (2014). How the nucleus copes with proteotoxic stress. *Curr Biol, 24*(10), R463-474. doi:10.1016/j.cub.2014.03.033

Shirwany, N. A., & Zou, M. H. (2014). AMPK: a cellular metabolic and redox sensor. A minireview. *Front Biosci (Landmark Ed), 19*, 447-474.

Shoubridge, E. A. (2002). The ABCs of mitochondrial transcription. *Nat Genet, 31*(3), 227-228. doi:10.1038/ng0702-227

Siegelin, M. D., Dohi, T., Raskett, C. M., Orlowski, G. M., Powers, C. M., Gilbert, C. A., . . . Altieri, D. C. (2011). Exploiting the mitochondrial unfolded protein response for cancer therapy in mice and human cells. *J Clin Invest, 121*(4), 1349-1360. doi:10.1172/jci44855

Silva, B. A., Einarsdottir, O., Fink, A. L., & Uversky, V. N. (2013). Biophysical Characterization of alpha-Synuclein and Rotenone Interaction. *Biomolecules, 3*(3), 703-732. doi:10.3390/biom3030703

Silva, J. P., Kohler, M., Graff, C., Oldfors, A., Magnuson, M. A., Berggren, P. O., & Larsson, N. G. (2000). Impaired insulin secretion and beta-cell loss in tissue-specific knockout mice with mitochondrial diabetes. *Nat Genet, 26*(3), 336-340. doi:10.1038/81649

Simoneau, J. A., Veerkamp, J. H., Turcotte, L. P., & Kelley, D. E. (1999). Markers of capacity to utilize fatty acids in human skeletal muscle: relation to insulin resistance and obesity and effects of weight loss. *FASEB J, 13*(14), 2051-2060.

Singh, B., Chatterjee, A., Ronghe, A., Bhat, N., & Bhat, H. (2013). Antioxidant-mediated up-regulation of OGG1 via NRF2 induction is associated with inhibition of oxidative DNA damage in estrogen-induced breast cancer. *BMC Cancer, 13*(1), 253.

Singh, R., & Cuervo, A. M. (2011). Autophagy in the cellular energetic balance. *Cell Metab, 13*(5), 495-504. doi:10.1016/j.cmet.2011.04.004

Sjostrand, F. S. (1953). Electron microscopy of mitochondria and cytoplasmic double membranes. *Nature, 171*(4340), 30-32.

Slany, A., Haudek, V. J., Zwickl, H., Gundacker, N. C., Grusch, M., Weiss, T. S., . . . Gerner, C. (2010). Cell characterization by proteome profiling applied to primary hepatocytes and hepatocyte cell lines Hep-G2 and Hep-3B. *J Proteome Res, 9*(1), 6-21. doi:10.1021/pr900057t

Smekal, A., & Vaclavik, J. (2017). Adipokines and cardiovascular disease: a comprehensive review. *Biomed Pap Med Fac Univ Palacky Olomouc Czech Repub*. doi:10.5507/bp.2017.002

Smith, S. A., Young, P., & Cawthorne, M. A. (1986). Quantification in vivo of the effects of insulin on glucose utilization in individual tissues of warm- and cold-acclimated rats. *Biochem J, 237*(3), 789-795.

Sokolova, I. M., Ringwood, A. H., & Johnson, C. (2005). Tissue-specific accumulation of cadmium in subcellular compartments of eastern oysters Crassostrea virginica Gmelin (Bivalvia: Ostreidae). *Aquat Toxicol, 74*(3), 218-228. doi:10.1016/j.aquatox.2005.05.012

Song, S. W., Kim, K. E., Choi, J. W., Lee, C. Y., Lee, J., Seo, H. H., . . . Hwang, K. C. (2016). Proteomic Analysis and Identification of Paracrine Factors in Mesenchymal Stem Cell-Conditioned Media under Hypoxia. *Cell Physiol Biochem, 40*(1-2), 400-410. doi:10.1159/000452555

Song, Z., Ghochani, M., McCaffery, J. M., Frey, T. G., & Chan, D. C. (2009). Mitofusins and OPA1 mediate sequential steps in mitochondrial membrane fusion. *Mol Biol Cell, 20*(15), 3525-3532. doi:10.1091/mbc.E09-03-0252

Sparks, L. M., Xie, H., Koza, R. A., Mynatt, R., Hulver, M. W., Bray, G. A., & Smith, S. R. (2005). A high-fat diet coordinately downregulates genes required for mitochondrial oxidative phosphorylation in skeletal muscle. *Diabetes, 54*(7), 1926-1933.

St-Pierre, J., Drori, S., Uldry, M., Silvaggi, J. M., Rhee, J., Jager, S., . . . Spiegelman, B. M. (2006). Suppression of reactive oxygen species and neurodegeneration by the PGC-1 transcriptional coactivators. *Cell, 127*(2), 397-408.

Starkov, A. A., Fiskum, G., Chinopoulos, C., Lorenzo, B. J., Browne, S. E., Patel, M. S., & Beal, M. F. (2004). Mitochondrial alpha-ketoglutarate dehydrogenase complex generates reactive oxygen species. *J Neurosci, 24*(36), 7779-7788. doi:10.1523/jneurosci.1899-04.2004

Starkov, A. A., & Wallace, K. B. (2002). Structural determinants of fluorochemical-induced mitochondrial dysfunction. *Toxicol Sci, 66*(2), 244-252.

Stefan, N., & Haring, H. U. (2013). The role of hepatokines in metabolism. *Nat Rev Endocrinol, 9*(3), 144-152. doi:10.1038/nrendo.2012.258

Stefan, N., Sun, Q., Fritsche, A., Machann, J., Schick, F., Gerst, F., . . . Schulze, M. B. (2014). Impact of the adipokine adiponectin and the hepatokine fetuin-A on the development of type 2 diabetes: prospective cohort- and cross-sectional phenotyping studies. *PLoS One, 9*(3), e92238. doi:10.1371/journal.pone.0092238

Stein, L. R., & Imai, S. (2012). The dynamic regulation of NAD metabolism in mitochondria. *Trends Endocrinol Metab, 23*(9), 420-428. doi:10.1016/j.tem.2012.06.005

Stojanovski, D., Muller, J. M., Milenkovic, D., Guiard, B., Pfanner, N., & Chacinska, A. (2008). The MIA system for protein import into the mitochondrial intermembrane space. *Biochim Biophys Acta, 1783*(4), 610-617. doi:10.1016/j.bbamcr.2007.10.004

Stojkovic, G., Makarova, A. V., Wanrooij, P. H., Forslund, J., Burgers, P. M., & Wanrooij, S. (2016). Oxidative DNA damage stalls the human mitochondrial replisome. *Sci Rep, 6*, 28942. doi:10.1038/srep28942

Stone, S. J., Levin, M. C., Zhou, P., Han, J., Walther, T. C., & Farese, R. V., Jr. (2009). The endoplasmic reticulum enzyme DGAT2 is found in mitochondria-associated membranes and has a mitochondrial targeting signal that promotes its association with mitochondria. *J Biol Chem, 284*(8), 5352-5361. doi:10.1074/jbc.M805768200

Strappazzon, F., Nazio, F., Corrado, M., Cianfanelli, V., Romagnoli, A., Fimia, G. M., . . . Cecconi, F. (2015). AMBRA1 is able to induce mitophagy via LC3 binding,

regardless of PARKIN and p62/SQSTM1. *Cell Death Differ, 22*(3), 419-432. doi:10.1038/cdd.2014.139

Stride, N., Larsen, S., Treebak, J. T., Hansen, C. N., Hey-Mogensen, M., Speerschneider, T., . . . Dela, F. (2012). 5'-AMP Activated Protein Kinase is involved in the regulation of myocardial ß-oxidative capacity in mice. *Frontiers in Physiology, 3*. doi:10.3389/fphys.2012.00033

Sun, Y., Connors, K. E., & Yang, D. Q. (2007). AICAR induces phosphorylation of AMPK in an ATM-dependent, LKB1-independent manner. *Mol Cell Biochem, 306*(1-2), 239-245. doi:10.1007/s11010-007-9575-6

Sun, Y., Vashisht, A. A., Tchieu, J., Wohlschlegel, J. A., & Dreier, L. (2012). Voltage-dependent anion channels (VDACs) recruit Parkin to defective mitochondria to promote mitochondrial autophagy. *Journal of Biological Chemistry, 287*(48), 40652-40660. doi:http://dx.doi.org/10.1074/jbc.M112.419721

Sunny, N. E., Bril, F., & Cusi, K. (2016). Mitochondrial Adaptation in Nonalcoholic Fatty Liver Disease: Novel Mechanisms and Treatment Strategies. *Trends Endocrinol Metab*. doi:10.1016/j.tem.2016.11.006

Suthammarak, W., Somerlot, B. H., Opheim, E., Sedensky, M., & Morgan, P. G. (2013). Novel interactions between mitochondrial superoxide dismutases and the electron transport chain. *Aging Cell, 12*(6), 1132-1140. doi:10.1111/acel.12144

Swerdlow, R. H., & Khan, S. M. (2004). A "mitochondrial cascade hypothesis" for sporadic Alzheimer's disease. *Med Hypotheses, 63*(1), 8-20. doi:10.1016/j.mehy.2003.12.045

Szabadkai, G., Bianchi, K., Varnai, P., De Stefani, D., Wieckowski, M. R., Cavagna, D., . . . Rizzuto, R. (2006). Chaperone-mediated coupling of endoplasmic reticulum and mitochondrial Ca2+ channels. *J Cell Biol, 175*(6), 901-911. doi:10.1083/jcb.200608073

Szczepanowska, K., & Trifunovic, A. (2015). Different faces of mitochondrial DNA mutators. *Biochim Biophys Acta, 1847*(11), 1362-1372. doi:10.1016/j.bbabio.2015.05.016

Taanman, J. W. (1999). The mitochondrial genome: structure, transcription, translation and replication. *Biochim Biophys Acta, 1410*(2), 103-123.

Takagi, M., Uno, H., Nishi, R., Sugimoto, M., Hasegawa, S., Piao, J., . . . Mizutani, S. (2015). ATM Regulates Adipocyte Differentiation and Contributes to Glucose Homeostasis. *Cell Rep*. doi:10.1016/j.celrep.2015.01.027

Tan, A. S., Baty, J. W., Dong, L. F., Bezawork-Geleta, A., Endaya, B., Goodwin, J., . . . Berridge, M. V. (2015). Mitochondrial genome acquisition restores respiratory function and tumorigenic potential of cancer cells without mitochondrial DNA. *Cell Metab, 21*(1), 81-94. doi:10.1016/j.cmet.2014.12.003

Tan, W.-Q., Wang, K., Lv, D.-Y., & Li, P.-F. (2008). Foxo3a inhibits cardiomyocyte hypertrophy through transactivating catalase. *Journal of Biological Chemistry, 283*(44), 29730-29739. doi:http://dx.doi.org/10.1074/jbc.M805514200

Tanaka, A., Cleland, M. M., Xu, S., Narendra, D. P., Suen, D. F., Karbowski, M., & Youle, R. J. (2010). Proteasome and p97 mediate mitophagy and degradation of

mitofusins induced by Parkin. *J Cell Biol, 191*(7), 1367-1380. doi:10.1083/jcb.201007013

Tanaka, T., Kurose, A., Halicka, H. D., Traganos, F., & Darzynkiewicz, Z. (2006). 2-deoxy-D-glucose reduces the level of constitutive activation of ATM and phosphorylation of histone H2AX. *Cell Cycle, 5*(8), 878-882. doi:10.4161/cc.5.8.2681

Tang, B. L. (2016). Sirt1 and the Mitochondria. *Mol Cells, 39*(2), 87-95. doi:10.14348/molcells.2016.2318

Tang, S., Hou, Y., Zhang, H., Tu, G., Yang, L., Sun, Y., . . . Liu, M. (2015). Oxidized ATM promotes abnormal proliferation of breast CAFs through maintaining intracellular redox homeostasis and activating the PI3K-AKT, MEK-ERK, and Wnt-beta-catenin signaling pathways. *Cell Cycle, 14*(12), 1908-1924. doi:10.1080/15384101.2015.1041685

Tapia, P. C. (2006). Sublethal mitochondrial stress with an attendant stoichiometric augmentation of reactive oxygen species may precipitate many of the beneficial alterations in cellular physiology produced by caloric restriction, intermittent fasting, exercise and dietary phytonutrients: "Mitohormesis" for health and vitality. *Med Hypotheses, 66*(4), 832-843. doi:10.1016/j.mehy.2005.09.009

Tarnopolsky, M. A., Rennie, C. D., Robertshaw, H. A., Fedak-Tarnopolsky, S. N., Devries, M. C., & Hamadeh, M. J. (2007). Influence of endurance exercise training and sex on intramyocellular lipid and mitochondrial ultrastructure, substrate use, and mitochondrial enzyme activity. *Am J Physiol Regul Integr Comp Physiol, 292*(3), R1271-1278. doi:10.1152/ajpregu.00472.2006

Terman, A., Gustafsson, B., & Brunk, U. T. (2006). Mitochondrial damage and intralysosomal degradation in cellular aging. *Mol Aspects Med, 27*(5-6), 471-482. doi:10.1016/j.mam.2006.08.006

Terman, A., Kurz, T., Navratil, M., Arriaga, E. A., & Brunk, U. T. (2010). Mitochondrial turnover and aging of long-lived postmitotic cells: the mitochondrial-lysosomal axis theory of aging. *Antioxid Redox Signal, 12*(4), 503-535. doi:10.1089/ars.2009.2598

Thery, C., Zitvogel, L., & Amigorena, S. (2002). Exosomes: composition, biogenesis and function. *Nat Rev Immunol, 2*(8), 569-579. doi:10.1038/nri855

Tian, L., Ma, L., Kaarela, T., & Li, Z. (2012). Neuroimmune crosstalk in the central nervous system and its significance for neurological diseases. *J Neuroinflammation, 9*, 155. doi:10.1186/1742-2094-9-155

Tian, M., Cui, Y. Z., Song, G. H., Zong, M. J., Zhou, X. Y., Chen, Y., & Han, J. X. (2008). Proteomic analysis identifies MMP-9, DJ-1 and A1BG as overexpressed proteins in pancreatic juice from pancreatic ductal adenocarcinoma patients. *BMC Cancer, 8*, 241. doi:10.1186/1471-2407-8-241

Ting, L., Cowley, M. J., Hoon, S. L., Guilhaus, M., Raftery, M. J., & Cavicchioli, R. (2009). Normalization and statistical analysis of quantitative proteomics data generated by metabolic labeling. *Mol Cell Proteomics, 8*(10), 2227-2242. doi:10.1074/mcp.M800462-MCP200

Todisco, S., Agrimi, G., Castegna, A., & Palmieri, F. (2006). Identification of the mitochondrial NAD+ transporter in Saccharomyces cerevisiae. *J Biol Chem, 281*(3), 1524-1531. doi:10.1074/jbc.M510425200

Tong, M., & Sadoshima, J. (2016). Mitochondrial autophagy in cardiomyopathy. *Curr Opin Genet Dev, 38*, 8-15. doi:10.1016/j.gde.2016.02.006

Toyama, E. Q., Herzig, S., Courchet, J., Lewis, T. L., Jr., Loson, O. C., Hellberg, K., . . . Shaw, R. J. (2016). Metabolism. AMP-activated protein kinase mediates mitochondrial fission in response to energy stress. *Science, 351*(6270), 275-281. doi:10.1126/science.aab4138

Trayhurn, P., & Beattie, J. H. (2001). Physiological role of adipose tissue: white adipose tissue as an endocrine and secretory organ. *Proc Nutr Soc, 60*(3), 329-339.

Trefely, S., Khoo, P. S., Krycer, J. R., Chaudhuri, R., Fazakerley, D. J., Parker, B. L., . . . Stockli, J. (2015). Kinome Screen Identifies PFKFB3 and Glucose Metabolism as Important Regulators of the Insulin/Insulin-like Growth Factor (IGF)-1 Signaling Pathway. *J Biol Chem, 290*(43), 25834-25846. doi:10.1074/jbc.M115.658815

Tretter, L., & Adam-Vizi, V. (2004). Generation of reactive oxygen species in the reaction catalyzed by alpha-ketoglutarate dehydrogenase. *J Neurosci, 24*(36), 7771-7778. doi:10.1523/jneurosci.1842-04.2004

Trifunovic, A., Wredenberg, A., Falkenberg, M., Spelbrink, J. N., Rovio, A. T., Bruder, C. E., . . . Larsson, N. G. (2004). Premature ageing in mice expressing defective mitochondrial DNA polymerase. *Nature, 429*(6990), 417-423. doi:10.1038/nature02517

Tripathi, D. N., Chowdhury, R., Trudel, L. J., Tee, A. R., Slack, R. S., Walker, C. L., & Wogan, G. N. (2013). Reactive nitrogen species regulate autophagy through ATM-AMPK-TSC2-mediated suppression of mTORC1. *Proc Natl Acad Sci U S A, 110*(32), E2950-2957. doi:10.1073/pnas.1307736110

Trounce, I., Byrne, E., & Marzuki, S. (1989). Decline in skeletal muscle mitochondrial respiratory chain function: possible factor in ageing. *Lancet, 1*(8639), 637-639.

Trounce, I. A., Crouch, P. J., Carey, K. T., & McKenzie, M. (2013). Modulation of ceramide-induced cell death and superoxide production by mitochondrial DNA-encoded respiratory chain defects in Rattus xenocybrid mouse cells. *Biochim Biophys Acta, 1827*(7), 817-825. doi:10.1016/j.bbabio.2013.03.012

Tsuboi, Y., Munemoto, H., Ishikawa, S., Matsumoto, K., Iguchi-Ariga, S. M., & Ariga, H. (2008). DJ-1, a causative gene product of a familial form of Parkinson's disease, is secreted through microdomains. *FEBS Lett, 582*(17), 2643-2649. doi:10.1016/j.febslet.2008.06.043

Tuppen, H. A., Blakely, E. L., Turnbull, D. M., & Taylor, R. W. (2010). Mitochondrial DNA mutations and human disease. *Biochim Biophys Acta, 1797*(2), 113-128. doi:10.1016/j.bbabio.2009.09.005

Turrens, J. F., Alexandre, A., & Lehninger, A. L. (1985). Ubisemiquinone is the electron donor for superoxide formation by complex III of heart mitochondria. *Arch Biochem Biophys, 237*(2), 408-414.

Tyurina, Y. Y., Winnica, D. E., Kapralova, V. I., Kapralov, A. A., Tyurin, V. A., & Kagan, V. E. (2013). LC/MS characterization of rotenone induced cardiolipin oxidation in human lymphocytes: Implications for mitochondrial dysfunction associated with Parkinson's disease. *Mol Nutr Food Res, 57*(8), 1410-1422. doi:10.1002/mnfr.201200801

Tyynismaa, H., Carroll, C. J., Raimundo, N., Ahola-Erkkila, S., Wenz, T., Ruhanen, H., . . . Suomalainen, A. (2010). Mitochondrial myopathy induces a starvation-like response. *Hum Mol Genet, 19*(20), 3948-3958. doi:10.1093/hmg/ddq310

Vainshtein, A., Tryon, L. D., Pauly, M., & Hood, D. A. (2015). Role of PGC-1alpha during acute exercise-induced autophagy and mitophagy in skeletal muscle. *Am J Physiol Cell Physiol, 308*(9), C710-719. doi:10.1152/ajpcell.00380.2014

Valero, R. A., Senovilla, L., Nunez, L., & Villalobos, C. (2008). The role of mitochondrial potential in control of calcium signals involved in cell proliferation. *Cell Calcium, 44*(3), 259-269. doi:10.1016/j.ceca.2007.12.002

Valle, I., Alvarez-Barrientos, A., Arza, E., Lamas, S., & Monsalve, M. (2005). PGC-1alpha regulates the mitochondrial antioxidant defense system in vascular endothelial cells. *Cardiovascular Research, 66*(3), 562-573.

van den Ouweland, J. M., Lemkes, H. H., Ruitenbeek, W., Sandkuijl, L. A., de Vijlder, M. F., Struyvenberg, P. A., . . . Maassen, J. A. (1992). Mutation in mitochondrial tRNA(Leu)(UUR) gene in a large pedigree with maternally transmitted type II diabetes mellitus and deafness. *Nat Genet, 1*(5), 368-371. doi:10.1038/ng0892-368

van der Bliek, A. M., Shen, Q., & Kawajiri, S. (2013). Mechanisms of mitochondrial fission and fusion. *Cold Spring Harb Perspect Biol, 5*(6). doi:10.1101/cshperspect.a011072

Vance, J. E. (1990). Phospholipid synthesis in a membrane fraction associated with mitochondria. *J Biol Chem, 265*(13), 7248-7256.

Vance, J. E. (2008). Phosphatidylserine and phosphatidylethanolamine in mammalian cells: two metabolically related aminophospholipids. *J Lipid Res, 49*(7), 1377-1387. doi:10.1194/jlr.R700020-JLR200

Vance, J. E., & Vance, D. E. (1986). Specific pools of phospholipids are used for lipoprotein secretion by cultured rat hepatocytes. *J Biol Chem, 261*(10), 4486-4491.

Vanden Hoek, T. L., Becker, L. B., Shao, Z., Li, C., & Schumacker, P. T. (1998). Reactive oxygen species released from mitochondria during brief hypoxia induce preconditioning in cardiomyocytes. *Journal of Biological Chemistry, 273*(29), 18092-18098.

VanLinden, M. R., Dolle, C., Pettersen, I. K., Kulikova, V. A., Niere, M., Agrimi, G., . . . Ziegler, M. (2015). Subcellular Distribution of NAD+ between Cytosol and Mitochondria Determines the Metabolic Profile of Human Cells. *J Biol Chem, 290*(46), 27644-27659. doi:10.1074/jbc.M115.654129

Vazquez-Vela, M. E., Torres, N., & Tovar, A. R. (2008). White adipose tissue as endocrine organ and its role in obesity. *Arch Med Res, 39*(8), 715-728. doi:10.1016/j.arcmed.2008.09.005

Vermulst, M., Wanagat, J., Kujoth, G. C., Bielas, J. H., Rabinovitch, P. S., Prolla, T. A., & Loeb, L. A. (2008). DNA deletions and clonal mutations drive premature aging in mitochondrial mutator mice. *Nat Genet, 40*(4), 392-394. doi:10.1038/ng.95

Vernochet, C., Mourier, A., Bezy, O., Macotela, Y., Boucher, J., Rardin, M. J., . . . Kahn, C. R. (2012). Adipose-specific deletion of TFAM increases mitochondrial oxidation and protects mice against obesity and insulin resistance. *Cell Metab, 16*(6), 765-776. doi:10.1016/j.cmet.2012.10.016

Vidali, S., Cheret, J., Giesen, M., Haeger, S., Alam, M., Watson, R. E., . . . Paus, R. (2016). Thyroid Hormones Enhance Mitochondrial Function in Human Epidermis. *J Invest Dermatol*. doi:10.1016/j.jid.2016.05.118

Viniegra, J. G., Martinez, N., Modirassari, P., Hernandez Losa, J., Parada Cobo, C., Sanchez-Arevalo Lobo, V. J., . . . Sanchez-Prieto, R. (2005). Full activation of PKB/Akt in response to insulin or ionizing radiation is mediated through ATM. *J Biol Chem, 280*(6), 4029-4036. doi:10.1074/jbc.M410344200

Virbasius, J. V., & Scarpulla, R. C. (1994). Activation of the human mitochondrial transcription factor A gene by nuclear respiratory factors: a potential regulatory link between nuclear and mitochondrial gene expression in organelle biogenesis. *Proc Natl Acad Sci U S A, 91*(4), 1309-1313.

Vitzel, K. F., Bikopoulos, G., Hung, S., Pistor, K. E., Patterson, J. D., Curi, R., & Ceddia, R. B. (2013). Chronic Treatment with the AMP-Kinase Activator AICAR Increases Glycogen Storage and Fatty Acid Oxidation in Skeletal Muscles but Does Not Reduce Hyperglucagonemia and Hyperglycemia in Insulin Deficient Rats. *PLoS ONE [Electronic Resource], 8*(4), e62190. doi:10.1371/journal.pone.0062190

Vives-Bauza, C., Zhou, C., Huang, Y., Cui, M., de Vries, R. L., Kim, J., . . . Przedborski, S. (2010). PINK1-dependent recruitment of Parkin to mitochondria in mitophagy. *Proc Natl Acad Sci U S A, 107*(1), 378-383. doi:10.1073/pnas.0911187107

Volden, P. A., Skor, M. N., Johnson, M. B., Singh, P., Patel, F. N., McClintock, M. K., . . . Conzen, S. D. (2016). Mammary Adipose Tissue-Derived Lysophospholipids Promote Estrogen Receptor-Negative Mammary Epithelial Cell Proliferation. *Cancer Prev Res (Phila), 9*(5), 367-378. doi:10.1158/1940-6207.capr-15-0107

Votyakova, T. V., & Reynolds, I. J. (2001). DeltaPsi(m)-Dependent and -independent production of reactive oxygen species by rat brain mitochondria. *J Neurochem, 79*(2), 266-277.

Wai, T., Garcia-Prieto, J., Baker, M. J., Merkwirth, C., Benit, P., Rustin, P., . . . Langer, T. (2015). Imbalanced OPA1 processing and mitochondrial fragmentation cause heart failure in mice. *Science, 350*(6265), aad0116. doi:10.1126/science.aad0116

Walter, L., & Hajnoczky, G. (2005). Mitochondria and endoplasmic reticulum: the lethal interorganelle cross-talk. *J Bioenerg Biomembr, 37*(3), 191-206. doi:10.1007/s10863-005-6600-x

Wang, A. L., Lukas, T. J., Yuan, M., Du, N., Tso, M. O., & Neufeld, A. H. (2009). Autophagy and exosomes in the aged retinal pigment epithelium: possible

relevance to drusen formation and age-related macular degeneration. *PLoS One, 4*(1), e4160. doi:10.1371/journal.pone.0004160

Wang, L., Liu, X., Nie, J., Zhang, J., Kimball, S. R., Zhang, H., . . . Shi, Y. (2015). ALCAT1 controls mitochondrial etiology of fatty liver diseases, linking defective mitophagy to steatosis. *Hepatology, 61*(2), 486-496. doi:10.1002/hep.27420

Wang, R., Meschia, J. F., Cotter, R. J., & Sisodia, S. S. (1991). Secretion of the beta/A4 amyloid precursor protein. Identification of a cleavage site in cultured mammalian cells. *J Biol Chem, 266*(25), 16960-16964.

Wang, X., Feng, Z., Wang, X., Yang, L., Han, S., Cao, K., . . . Liu, J. (2016). O-GlcNAcase deficiency suppresses skeletal myogenesis and insulin sensitivity in mice through the modulation of mitochondrial homeostasis. *Diabetologia, 59*(6), 1287-1296. doi:10.1007/s00125-016-3919-2

Weber, A. M., & Ryan, A. J. (2015). ATM and ATR as therapeutic targets in cancer. *Pharmacol Ther, 149*, 124-138. doi:10.1016/j.pharmthera.2014.12.001

Weber, K., Bruck, P., Mikes, Z., Kupper, J. H., Klingenspor, M., & Wiesner, R. J. (2002). Glucocorticoid hormone stimulates mitochondrial biogenesis specifically in skeletal muscle. *Endocrinology, 143*(1), 177-184. doi:10.1210/endo.143.1.8600

Webster, M. T., Groome, N., Francis, P. T., Pearce, B. R., Sherriff, F. E., Thinakaran, G., . . . Bowen, D. M. (1995). A novel protein, amyloid precursor-like protein 2, is present in human brain, cerebrospinal fluid and conditioned media. *Biochem J, 310 (Pt 1)*, 95-99.

Weitzel, J. M., Radtke, C., & Seitz, H. J. (2001). Two thyroid hormone-mediated gene expression patterns in vivo identified by cDNA expression arrays in rat. *Nucleic Acids Res, 29*(24), 5148-5155.

Westermann, B. (2012). Bioenergetic role of mitochondrial fusion and fission. *Biochim Biophys Acta, 1817*(10), 1833-1838. doi:10.1016/j.bbabio.2012.02.033

Whittington, H., Hall, A., McLaughlin, C., Hausenloy, D., Yellon, D., & Mocanu, M. (2013). Chronic Metformin Associated Cardioprotection Against Infarction: Not Just a Glucose Lowering Phenomenon. *Cardiovascular Drugs and Therapy, 27*(1), 5-16. doi:10.1007/s10557-012-6425-x

Wiedemann, N., Frazier, A. E., & Pfanner, N. (2004). The protein import machinery of mitochondria. *J Biol Chem, 279*(15), 14473-14476. doi:10.1074/jbc.R400003200

Wilkins, H. M., Carl, S. M., & Swerdlow, R. H. (2014). Cytoplasmic hybrid (cybrid) cell lines as a practical model for mitochondriopathies. *Redox Biol, 2*, 619-631. doi:10.1016/j.redox.2014.03.006

Williams, G. S., Boyman, L., & Lederer, W. J. (2015). Mitochondrial calcium and the regulation of metabolism in the heart. *J Mol Cell Cardiol, 78*, 35-45. doi:10.1016/j.yjmcc.2014.10.019

Wilson-Fritch, L., Nicoloro, S., Chouinard, M., Lazar, M. A., Chui, P. C., Leszyk, J., . . . Corvera, S. (2004). Mitochondrial remodeling in adipose tissue associated with

obesity and treatment with rosiglitazone. *J Clin Invest, 114*(9), 1281-1289. doi:10.1172/jci21752

Woods, A., Dickerson, K., Heath, R., Hong, S. P., Momcilovic, M., Johnstone, S. R., . . . Carling, D. (2005). Ca2+/calmodulin-dependent protein kinase kinase-beta acts upstream of AMP-activated protein kinase in mammalian cells. *Cell Metab, 2*(1), 21-33. doi:10.1016/j.cmet.2005.06.005

Wu, H., Kanatous, S. B., Thurmond, F. A., Gallardo, T., Isotani, E., Bassel-Duby, R., & Williams, R. S. (2002). Regulation of mitochondrial biogenesis in skeletal muscle by CaMK. *Science, 296*(5566), 349-352. doi:10.1126/science.1071163

Wu, L. E., Samocha-Bonet, D., Whitworth, P. T., Fazakerley, D. J., Turner, N., Biden, T. J., . . . Cantley, J. (2014). Identification of fatty acid binding protein 4 as an adipokine that regulates insulin secretion during obesity. *Mol Metab, 3*(4), 465-473. doi:10.1016/j.molmet.2014.02.005

Wu, S. B., Wu, Y. T., Wu, T. P., & Wei, Y. H. (2014). Role of AMPK-mediated adaptive responses in human cells with mitochondrial dysfunction to oxidative stress. *Biochim Biophys Acta, 1840*(4), 1331-1344. doi:10.1016/j.bbagen.2013.10.034

Wunderlich, V., Tetzlaff, I., & Graffi, A. (1972). Studies on nitrosodimethylamine: preferential methylation of mitochondrial DNA in rats and hamsters. *Chem Biol Interact, 4*(2), 81-89.

Xu, C., Chen, Y., Xu, L., Miao, M., Li, Y., & Yu, C. (2016). Serum complement C3 levels are associated with nonalcoholic fatty liver disease independently of metabolic features in Chinese population. *Sci Rep, 6*, 23279. doi:10.1038/srep23279

Yakes, F. M., & Van Houten, B. (1997). Mitochondrial DNA damage is more extensive and persists longer than nuclear DNA damage in human cells following oxidative stress. *Proc Natl Acad Sci U S A, 94*(2), 514-519.

Yamamoto, M., Hikosaka, K., Mahmood, A., Tobe, K., Shojaku, H., Inohara, H., & Nakagawa, T. (2016). Nmnat3 Is Dispensable in Mitochondrial NAD Level Maintenance In Vivo. *PLoS One, 11*(1), e0147037. doi:10.1371/journal.pone.0147037

Yamano, K., & Youle, R. J. (2013). PINK1 is degraded through the N-end rule pathway. *Autophagy, 9*(11), 1758-1769. doi:10.4161/auto.24633

Yang, D., Oyaizu, Y., Oyaizu, H., Olsen, G. J., & Woese, C. R. (1985). Mitochondrial origins. *Proc Natl Acad Sci U S A, 82*(13), 4443-4447.

Yang, W. H., Aziz, P. V., Heithoff, D. M., Mahan, M. J., Smith, J. W., & Marth, J. D. (2015). An intrinsic mechanism of secreted protein aging and turnover. *Proc Natl Acad Sci U S A, 112*(44), 13657-13662. doi:10.1073/pnas.1515464112

Yang, Z. F., Drumea, K., Mott, S., Wang, J., & Rosmarin, A. G. (2014). GABP transcription factor (nuclear respiratory factor 2) is required for mitochondrial biogenesis. *Mol Cell Biol, 34*(17), 3194-3201. doi:10.1128/mcb.00492-12

Yao, Y., Chinnici, C., Tang, H., Trojanowski, J. Q., Lee, V. M., & Pratico, D. (2004). Brain inflammation and oxidative stress in a transgenic mouse model of

Alzheimer-like brain amyloidosis. *J Neuroinflammation, 1*(1), 21. doi:10.1186/1742-2094-1-21

Yatsuga, S., Fujita, Y., Ishii, A., Fukumoto, Y., Arahata, H., Kakuma, T., . . . Koga, Y. (2015). Growth differentiation factor 15 as a useful biomarker for mitochondrial disorders. *Ann Neurol, 78*(5), 814-823. doi:10.1002/ana.24506

Yen, H. C., Chen, F. Y., Chen, S. W., Huang, Y. H., Chen, Y. R., & Chen, C. W. (2011). Effect of mitochondrial dysfunction and oxidative stress on endogenous levels of coenzyme Q(10) in human cells. *J Biochem Mol Toxicol, 25*(5), 280-289. doi:10.1002/jbt.20387

Yim, N., Ryu, S. W., Choi, K., Lee, K. R., Lee, S., Choi, H., . . . Choi, C. (2016). Exosome engineering for efficient intracellular delivery of soluble proteins using optically reversible protein-protein interaction module. *Nat Commun, 7*, 12277. doi:10.1038/ncomms12277

Yoritaka, A., Hattori, N., Uchida, K., Tanaka, M., Stadtman, E. R., & Mizuno, Y. (1996). Immunohistochemical detection of 4-hydroxynonenal protein adducts in Parkinson disease. *Proc Natl Acad Sci U S A, 93*(7), 2696-2701.

Yoshii, S. R., Kishi, C., Ishihara, N., & Mizushima, N. (2011). Parkin mediates proteasome-dependent protein degradation and rupture of the outer mitochondrial membrane. *J Biol Chem, 286*(22), 19630-19640. doi:10.1074/jbc.M110.209338

Youle, R. J., & van der Bliek, A. M. (2012). Mitochondrial fission, fusion, and stress. *Science, 337*(6098), 1062-1065. doi:10.1126/science.1219855

Yuyun, X., Jinjun, Q., Minfang, X., Jing, Q., Juan, X., Rui, M., . . . Jing, G. (2013). Effects of Low Concentrations of Rotenone upon Mitohormesis in SH-SY5Y Cells. *Dose Response, 11*(2), 270-280. doi:10.2203/dose-response.12-005.Gao

Zarse, K., Schmeisser, S., Groth, M., Priebe, S., Beuster, G., Kuhlow, D., . . . Ristow, M. (2012). Impaired insulin/IGF1 signaling extends life span by promoting mitochondrial L-proline catabolism to induce a transient ROS signal. *Cell Metab, 15*(4), 451-465. doi:10.1016/j.cmet.2012.02.013

Zelenka, J., Dvorak, A., & Alan, L. (2015). L-Lactate Protects Skin Fibroblasts against Aging-Associated Mitochondrial Dysfunction via Mitohormesis. *Oxid Med Cell Longev, 2015*, 351698. doi:10.1155/2015/351698

Zhang, B., Asadi, S., Weng, Z., Sismanopoulos, N., & Theoharides, T. C. (2012). Stimulated human mast cells secrete mitochondrial components that have autocrine and paracrine inflammatory actions. *PLoS One, 7*(12), e49767. doi:10.1371/journal.pone.0049767

Zhang, L., Yu, L., & Yu, C. A. (1998). Generation of superoxide anion by succinate-cytochrome c reductase from bovine heart mitochondria. *J Biol Chem, 273*(51), 33972-33976.

Zhang, Z., Wakabayashi, N., Wakabayashi, J., Tamura, Y., Song, W. J., Sereda, S., . . . Sesaki, H. (2011). The dynamin-related GTPase Opa1 is required for glucose-stimulated ATP production in pancreatic beta cells. *Mol Biol Cell, 22*(13), 2235-2245. doi:10.1091/mbc.E10-12-0933

Zhao, Q., Wang, J., Levichkin, I. V., Stasinopoulos, S., Ryan, M. T., & Hoogenraad, N. J. (2002). A mitochondrial specific stress response in mammalian cells. *EMBO J, 21*(17), 4411-4419.

Zhao, Q., Wang, J., Levichkin, I. V., Stasinopoulos, S., Ryan, M. T., & Hoogenraad, N. J. (2002). A mitochondrial specific stress response in mammalian cells. *EMBO Journal, 21*(17), 4411-4419.

Zhao, X., Dong, Y., Zhang, J., Li, D., Hu, G., Yao, J., . . . Li, H. (2016). Leptin changes differentiation fate and induces senescence in chondrogenic progenitor cells. *Cell Death Dis, 7*, e2188. doi:10.1038/cddis.2016.68

Zheng, T., Yang, X., Wu, D., Xing, S., Bian, F., Li, W., . . . Jin, S. (2015). Salidroside ameliorates insulin resistance through activation of a mitochondria-associated AMPK/PI3K/Akt/GSK3beta pathway. *Br J Pharmacol, 172*(13), 3284-3301. doi:10.1111/bph.13120

Zheng, W., Khrapko, K., Coller, H. A., Thilly, W. G., & Copeland, W. C. (2006). Origins of human mitochondrial point mutations as DNA polymerase gamma-mediated errors. *Mutat Res, 599*(1-2), 11-20. doi:10.1016/j.mrfmmm.2005.12.012

Zielonka, J., Hardy, M., & Kalyanaraman, B. (2009). HPLC study of oxidation products of hydroethidine in chemical and biological systems: ramifications in superoxide measurements. *Free Radic Biol Med, 46*(3), 329-338. doi:10.1016/j.freeradbiomed.2008.10.031